CYBERNETIC DIAGNOSTICS OF MECHANICAL SYSTEMS
WITH VIBRO-ACOUSTIC PHENOMENA

$, \vec{v} \, \iota'$

Translation of "Kiberneticheskaya diagnostika
mekhanicheskikh sistem po vibroakusticheskim protsessam,"
Kaunas, "KPI" Press, 1972, 292 pages

NATIONAL AERONAUTICS AND SPACE ADMINISTRATION
WASHINGTON, D.C. 20546   MAY 1973

1. Report No. NASA TT F-14,	2. Government Accession No.	3. Recipient's Catalog No.
4. Title and Subtitle CYBERNETIC DIAGNOSTICS OF MECHANICAL SYSTEMS WITH VIBRO-ACOUSTIC PHENOMENA (Materials, All-UnionSymposium, 1972)		5. Report Date June 1973
		6. Performing Organization Code
7. Author(s) K. M. Ragul'skis (Ed.)		8. Performing Organization Report No.
		10. Work Unit No.
9. Performing Organization Name and Address Leo Kanner Associates, PO Box 5187, Redwood City, CA 94063		11. Contract or Grant No. NASw 2481
		13. Type of Report and Period Covered
12. Sponsoring Agency Name and Address National Aeronautics and Space Administration, Washington, D.C. 20546		
		14. Sponsoring Agency Code

15. Supplementary Notes

Translation of "Kiberneticheskaya diagnostika mekhanicheskikh sistem po vibroakusticheskim protsessam," Kaunas, "KPI" Press, 1972, 292 pages.

16. Abstract   The 86 articles and abstracts include 23 on measurement and analysis of vibroacoustic phenomena to diagnose condition of gear transmissions of mining machinery, excavators, tractors and other equipment (pp. 28, 150-165, 232, 241), bearings (p. 91), aircraft skin panels (p. 41), tape, wire and electrostatic recorder feed mechanisms (pp. 103-114, 279), textile machinery (p. 239), automotive engines (p. 243), aircraft jet engines (p. 317), stressing data analysis by computer, band filters and reference spectra. Measuring systems and equipment (pp. 1-6, 10-20, 25, 35, 83, 118, 171, 229, 235), laboratory studies of vibroacoustics of equipment and structures (pp. 30, 44-49, 61, 81, 87, 271, 285-291, 306-310), measuring equipment accuracy (pp. 21, 36) and damping (pp. 78, 260) are discussed. Theoretical studies are presented in detail, or are summarized, including computer programs (pp. 53, 57), algorithms for determination and analysis of vibroacoustic phenomena (pp. 134, 166, 301), mathematical modeling of processes, systems and phenomena (pp. 34, 38, 51, 74, 123-130), theoretical calculations of optimum systems, units and measurement (pp. 7, 115, 119, 131, 139-149, 181-189, 193, 197, 204, 275, 283) and vibration and noise damping (pp. 209-228, 264-270, 314)

17. Key Words (Selected by Author(s))	18. Distribution Statement
	Unclassified -- Unlimited

19. Security Classif. (of this report)	20. Security Classif. (of this page)	21. No. of Pages	22. Price
Unclassifed	Unclassified	319	

TABLE OF CONTENTS

MULTIPLE-POINT UNIT FOR REMOTE AUTOMATIC SPECTRAL ANALYSIS

O.A. Aleksandrov, V.A. Ivanov, V.N. Karovetskiy, A.N. Lapenko, and
B.N. Masharskiy
(Leningrad)

One of the algorithms of diagnostics of machines and mechan- /5*
isms can be a comparison of the 1/3 octave vibration characteristics
of a mechanism, measured by a spectrometer, with records obtained
with precise knowledge of its condition.

Such measurements must be carried out at many points and during
different modes of operation of the machine, which is connected
with a large number of like operations, recordings and laborious
processing of the data. Moreover, because of the random nature of
the vibration signals, the needles of the measuring instrument lead
to errors in reading.

An experimental model of an automatic spectrometer has now
been produced. The automatic spectrometer permits measurement of
vibrations at 297 points, in the 5-20,000 Hz frequency range and
in a range of change in vibration level from 36 to 134 dB. The
dynamic range of the 1/3 octave analysis is 50 dB, with informa-
tion delivery to an automatic recorder and digital-printout.

The unit consists of three main parts: input devices, intended
for switching and preliminary amplification of the converter sig-
nals; measurement and analysis devices; and control devices.

During automatic operation, the input signal level can change
in a dynamic range of 100 dB, with a dynamic spectrometer range
of 50 dB. Therefore, the signal from the switching output is
attenuated by an automatic voltage divider (AVD) in 10 dB steps,
so that the analyzer can operate in the linear dynamic range of
the spectrometer.

If the measured signal fluctuates close to the limit of the
"window," the AVD step, instability can arise in its operation.
To attenuate this phenomenon, it is possible to extend the limits /6
of the "window" by 2 or 4 dB, simultaneously on the high and low
sides.

After finishing the necessary attenuation of the signal by
the automatic divider, sequential measurement of the signal levels
and the 1/3 octave filter bands and the integral level is begun.

---

*Numbers in the margin indicate pagination in the foreign text.

To reduce the analysis time, the interrogation is begun with the high frequency filter integrators. Subsequently, the total level integrator is questioned. The interrogation rate is selected with consideration of the duration of the transition processes in the integrators of the lowest frequency filters, for "white" and "pink" type signal noises. If the signal level from the sensor changes during the time of the automatic interrogation and goes beyond the limits of the AVD step "window," further automatic measurement is stopped, with appropriate signals.

Experience in operation of the unit has demonstrated that, by use of it, the reliability of the data obtained is increased and the time for measurement and processing the results is decreased.

SYSTEM FOR AUTOMATED MEASUREMENT
OF FULL-SCALE NOISES AND VIBRATIONS

G.S. Lyubashevskiy, B.D. Tartakovskiy, and V.E. Frishberg
(Moscow)

Devices for measurement of the electrical spectrum of a signal, full-scale noises and vibrations include a set of parallel filters, with detectors at the filtration channel outlet [1]. However, knowledge of the ener. spectrum is insufficient for plotting an equivalent diagram of the active sources of noises and vibrations and for disclosing the interconnections between signals at various points in an object. More complete information is given by a reciprocal spectral density matrix $G^{(\omega_n)}$ [2], the elements of which are written in the form

$$G_{j\xi}^{(\omega_n)} = C_{j\xi}^{(\omega_n)} - i \, Q_{j\xi}^{(\omega_n)} \, . \tag{1}$$

where

$$C_{j\xi}^{(\omega_n)} = \lim_{T \to \infty} \frac{1}{T} \int_{0}^{T} F_{\xi}^{(\omega_n)}(t) \cdot F_{j}^{(\omega_n)}(t) \cdot dt$$

and

$$Q_{j\xi}^{(\omega_n)} = \lim_{T \to \infty} \frac{1}{T} \int_{0}^{T} F_{j}^{(\omega_n)}(t) \cdot F_{j}^{\cdot(\omega_n)}(t) \cdot dt$$

$\xi = 1, 2, \ldots, m$; $j = 1, 2, \ldots, m$; m is the number of measurement points and $F_{j}^{(\omega_n)}(t)$ is the signal, integrally coupled with signal $F_{j}^{(\omega_n)}(t)$ at the j-th measurement point, passing through the band filter with a frequency ω_n, $n = 1, 2, \ldots, N$. The symmetry of the matrix $G^{(\omega_n)}$ permits the measurement of elements $G_{\xi j}^{(\omega_n)}$ to be limited to $\xi \le j$ and, in this manner, the experiment time to be cut approximately in half. Then, the number of measurements reaches $\sim 30 \, m^2$ in the third octave analysis in the sound range of frequencies.

A functional diagram of the processing arrangement included in the automated measurement system is presented in Fig. 1. The signal from the measurement point, after amplification $F_1(t)$, $F_2(t)$, ... $F_m(t)$, enters the two switches of channels KK_1 and KK_2. By control commands U_1 and U_2, the channel switches connect signals $F_j(t)$ and $F\xi(t)$ to the inlets of two identical filters Φ_1 and Φ_2. Filters Φ_1 and Φ_2 are sets of band filters, with frequencies ω_1, ω_2, ..., ω_N, having a common inlet and separate outlets. By control command U_3, the switches of filters $k\Phi_1$ and $k\Phi_2$ connect signals $F_j^{(\omega_n)}(t)$ and $F_\xi^{(\omega_n)}(t)$, passing through the band filters with frequency ω_n, to the amplifier inlets, with automatic

discrete gain control devices AGC_1 and AGC_2 [3]. Signal $k_2 F_\xi^{(\omega n)}(t)$ is transmitted to both multiplier inlets. Signals $K_1 F_j^{(\omega n)}(t)$ and $K_1 F_j^{*(\omega n)}(t)$, shifted by 90° relative to one another, enter the second multiplier inlets. The direct current voltages from the averager outlets, equal to within the proportionality coefficient to the values $c_{j\xi}^{(\omega n)}$ and $Q_{j\xi}^{(\omega n)}$, are transformed, in succession, into digital form by analog-digital converter ADC. Further, all the information ($c_{j\xi}^{(\omega n)}$ and $Q_{j\xi}^{(\omega n)}$, gain factors K_1 and K_2, band filter frequencies ω_n) is transmitted to the digital computer core memory or is recorded in the memory buffer register.
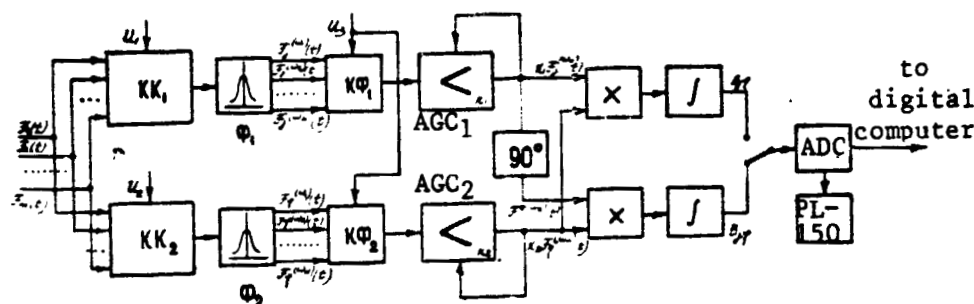
Fig. 1.

After each change-over of switches KK_1 and KK_2, a definite /8 time is required for a search for the necessary gain factor, which increases the total measurement time. However, use of the automatic gain control permits the range of change in measured values $c_{j\xi}^{(\omega n)}$ and $Q_{j\xi}^{(\omega n)}$ to be reduced to 40 dB, with a range in change in effective values of the signals $F_j^{(\omega n)}(t)$ and $F_\xi^{(\omega n)}(t)$ within 80 dB each.

A simplified functional diagram of the control system arrangement is presented in Fig. 2. The control device includes three series-connected shift registers $T_1' - T_m'$, $T_1'' - T_m''$, $T_1''' - T_N'''$. At the start-up command, the system is brought to the state of calculation of elements of the first row of matrix $G^{(\omega 1)}$ (beginning with $G_{11}^{(\omega n)}$). Then, the pulse timing generator PTG, entering shift register T', by command U_1, connects signal $F_j^{(\omega n)}(t)$ in sequence, for calculation of $G_{1j}^{(\omega 1)}$. After calculation of

4

$G_{1m}^{(\omega_1)}$, a pulse from T_m' is transmitted to shift register T'' and, by commands U_1 and U_2, the system is brought to the state for calculation of elements of the second row of the matrix (beginning with $G_{22}^{(\omega_1)}$).   The cycle is repeated until the completion of calculation of all elements of the matrix at frequency ω_1. Further, the pulse from T_m'' is transmitted to shift register T''' and, by /9 commands U_1, U_2 and U_3, the system is brought to the state for calculation of elements of the following matrix $G^{(\omega_2)}$. After cal- culation of the elements of all matrices $G^{(\omega_1)}$, $G^{(\omega_2)}$, ..., $G^{(\omega_N)}$, the system is stopped by a pulse from T_N''' , entering the control flip-flop T.
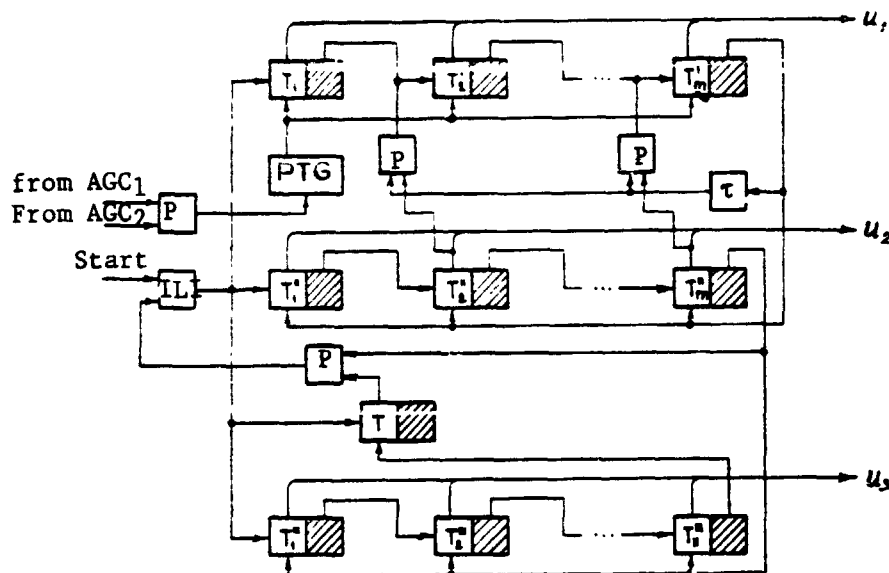
Fig. 2.

In this manner, the automated measurement system permits a matrix $G^{(\omega_n)}$ to be obtained for each of the frequencies ω_1, ω_2, ..., ω_n, ..., ω_N:

$$G^{(\omega_n)} = \begin{vmatrix} G_{11}^{(\omega_n)} & G_{12}^{(\omega_n)} & \dots & G_{1m}^{(\omega_n)} \\ & G_{22}^{(\omega_n)} & & G_{2m}^{(\omega_n)} \\ & & \dots & \dots \\ & & & G_{mm}^{(\omega_n)} \end{vmatrix}$$

The information obtained on the interaction of signals from various sources can be used in sound diagnostics problems and in control of noises and vibrations.

REFERENCES

1. Zaveri, K., M. Phil, "Conventional On-Line Methods of Sound Power Measurements," Tech. Rev. Bruel and Kjaer (3), 1971.

2. Bendat, G. and A. Pearson, Izmereniye i analiz sluchaynykh protsessov [Measurement and Analysis of Random Processes] Mir Press, Moscow, 1971.

3. Lyubashevskiy, G.S., A.A. Petrov, I.V. Sanayev and V.E. Frishberg, "Discrete Gain Control in Systems for Automatic Collection and Processing of Experimental Data," (in this collection).

METHOD FOR EXPERIMENTAL DETERMINATION OF THE CONTRIBUTION OF INDIVIDUAL SOURCES TO TOTAL NOISE

N.A. Rubichev
(Moscow)

Let there be n noise sources in an object being studied (various mills, mechanisms, individual assemblies of one mechanism, etc.), each of which generates its signal $x_i(t)$ $(i=1,1,...,n)$. We will consider that the medium transmitting the sound is linear. Then, the noise formed $z(t)$ at the observation point can be presented in the form of a block-diagram (Fig. 1).
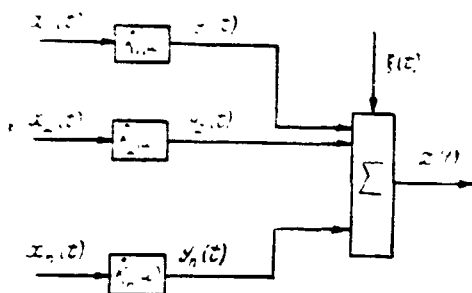
Fig. 1. $K_i(\omega)$ is a complex coefficient of signal transfer from a source to the observation point and $\xi(t)$ is the additive noise of the medium.

In direct proximity to /10 the i-th source, let us locate a receiver, at the outlet of which the signal will have the form $\hat{x}_i(t)=x_i(t)*Ki(\omega)$, where $\hat{K}_i(\omega)$ is a complex coefficient of transfer of the noise of the i-th source to i-th receiver. We disregard the penetration of signals from other sources.

A method is proposed below, which is similar to synchronous detection by quadrature components, which permits determination of the component N_{iv} of the total power N_v, caused by the i-th source, in a quite narrow frequency band $[\Omega_{v-1}; \Omega_v]$. The signal $\hat{x}_i(t)$, passing through the band filter with pass band $[\Omega_{v-}; \Omega_v]$, is used as the reference signal. The subscript v covers all values insuring full coverage of the spectrum of signal $x_i(T)$.

We introduce the following designations:

$z_v(t)$ — is the result of transformation of signals $z(t)$ by a band filter with pass band $[\Omega_{v-1};\Omega_v]$,

$x_{iv}(t)$ — is the same, in conversion of signal $x_i(t)$,

$\hat{x}_{iv}(t)$ — is the same for signal $\hat{x}_i(t)$, and

$z_{iv}(t)$ — is the same for signal $z_i(t)=z(t)-y_i(t)$.

7

We analyze the quantity

$$q_{i\nu} = \left[\frac{1}{2T} \int_{T} z_i(t)\, \tilde{x}_{i\iota}(t)\, dt \right]^2 + \left[\frac{1}{2T} \int_{-T}^{T} z_i(t)\, \hat{\tilde{x}}_{i\iota}(t)\, dt \right]_2 , \tag{1}$$

where

$$\hat{\tilde{x}}_{i\iota}(t) = \frac{1}{\pi} \int_{-\infty}^{\infty} \frac{\tilde{x}_{i\iota}(\tau)}{t-\tau}\, d\tau -$$

is the Gilbert conversion of   signal $\tilde{x}_{i\nu}(\tau)$.

Having made certain transformations, considering the small-/11 ness of the frequency band $[\Omega_{\nu-1}; \Omega_\nu]$ and disregarding higher order smallness terms, we can write

$$q_{i\nu} \approx K_i^2(\omega_\nu)\, \tilde{K}_i^2(\omega_\nu)\, \overline{[x_{i\iota}^2(t)]_2} + \tag{2}$$

$$+ \frac{2K_i(\omega_\nu)\, \tilde{K}_i(\omega_\nu)}{T} \int_{-T}^{T} A_{i\nu}^2(t)\, A_{2i\iota}^2(t)\, \cos{[\varphi_{2i\iota}(t) - \varphi_{i\nu}(t)]}\, dt,$$

where $A_{i\nu}(t)$ and $\phi_{i\nu}(t)$ are the envelope and phase of signal $x_{i\nu}(t)$, and $A_{2i\nu}(t)$ and $\phi_{2i\nu}(t)$ are the same for the signal $Z_{i\nu}(t)$. (The line above the quantity indicates its average.)

Since the mean value $q_{i\nu}$ equals $K_i^2(\omega_\nu)\tilde{K}_i^2(\omega_\nu)\overline{[x_{i\nu}^2(t)]}^2$, and its dispersion tends toward zero with an unbounded increase T, $q_{i\nu}$ can be considered unskewed and an effective estimate of

the value $K_i^2(\omega_\nu)\tilde{K}_i^2(\omega_\nu)\overline{[x_{i\nu}^2(t)]}^2$.

Considering that the power

$$N_{i\iota} = K_i^2(\omega_\nu)\, \overline{x_{i\nu}^2(t)}, \quad a \quad \overline{\tilde{x}_{i\iota}^2(t)} = \tilde{K}_i^2(\omega_\nu)\, \overline{x_{i\nu}^2(t)},$$

we can write

$$N_{i\nu} \approx N_{i\nu}^* = q_{i\nu} / \overline{\tilde{x}_{i\nu}^2(t)}. \tag{3}$$

A block diagram of the arrangement for measurement of $N_{i\nu}$ is shown in Fig. 2.

Fig. 2. BΦv, band filter with
pass band; GC, Gilbert converter
(wide-band phase-shifter with
90° phase shift); PM, power meter;
Q,quadrator; D,divider.

Having determined N_{ip},
it is easy to determine the
total power of the signal at
the observation point, which
is caused by the i-th source,

$$N_i = \sum_r N_{ir}. \qquad (4)$$

USE OF THE MATHEMATICAL MODELLING METHOD FOR THE INVESTIGATION OF DYNAMIC CHARACTERISTICS OF ACOUSTICAL MEASURING INSTRUMENTS

Yu. M. Vasil'yev and L.F. Lagunov
(Moscow)

The dynamic parameters of measuring devices with needle in-/12
dicators completely determines the errors in measurement of sig-
nals of complex shapes. To carry out detailed studies of the
errors of such instruments, it is proposed that the mathematical
modelling method be used.

The error in measurement of the peak value of pulses of var-
ious shapes, depending on their duration and repetition rate,
was studied on models, by means of a type MN-7M analog computer.
As a consequence of the diversity of real signals, the minimum
and maximum errors obtained in measurement of square and sawtooth
pulses, accordingly, were determined. Triangular-shaped and
exponentially decreasing pulses, which are idealized sound shapes,
were used as intermediates. It was shown that the dependence of
error on pulse shape and duration is quite considerable, and that
it is difficult to take account of it during measurement of real
signals.

Therefore, it was proposed to introduce a device into the
measurement circuit which expands the signal, according to the
peak or any other measured value, to such a length that it can
be measured with the necessary accuracy.

The results of measurement by the model instruments, with
expanded exponential pulses, single ones and series of them, are
presented in Fig. 1. The error in measurement is defined here by
the difference between deflection angle $\alpha_o=0.8$ rad, correspond-
ing to the peak signal value, and actual deflection angle α.
The lower curves on the graphs are the   readings   of the
instrument without pulse expansion (the amplitude of the needle
fluctuations is shown in Fig. 1b), and the remaining ones, with
expansion to a duration of 500 $msec$, with different time constants
in the expander charge storage capacitance circuit τ_{ch}.

Similar relationships were obtained for pulses of different
shapes. It was shown that, by appropriate selection of values of
τ_{ch}, practically complete independence of the instrument readings
from pulse shape and duration can be acheived in the specified
range.   The error, within an angle of 0.01-0.05 rad,   /14
does not exceed 1-2 dB in level, even in the left part of the
logarithmic scale of the instrument, where the divisions are
closest. The necessary duration of the expansion depends on the
specific parameters of the instrument, and it can be determined
experimentally.
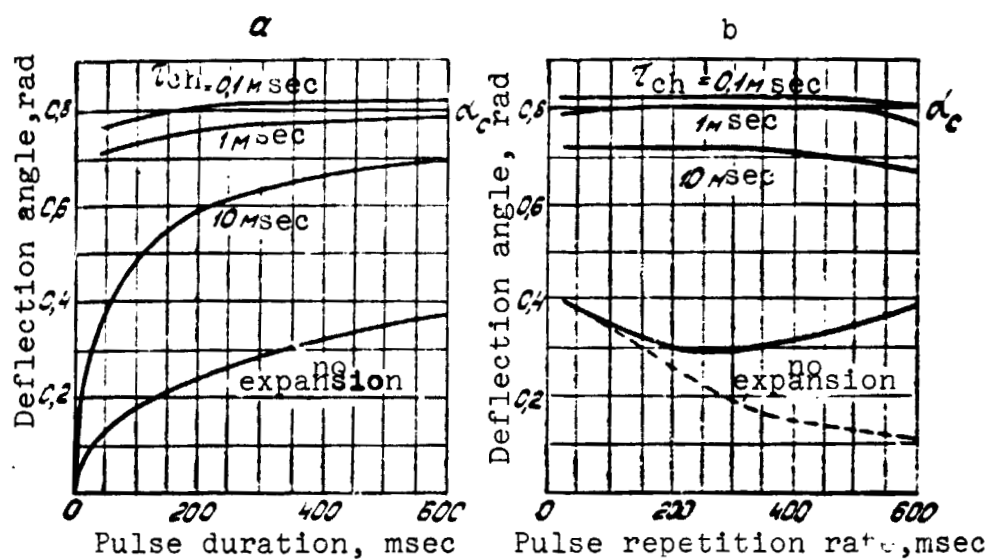
Fig. 1.   Readings   of instrument with expander, in measure- <u>/13</u>
ment of single (*a*) and a series (*b*) of exponentially decreasing
pulses.
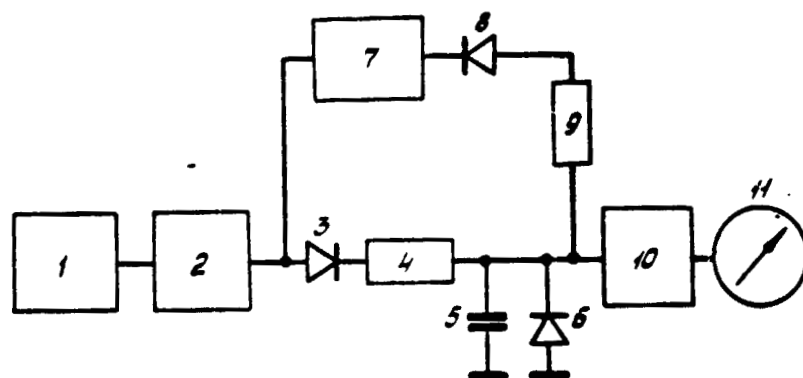
Fig. 2.   Schematic diagram of measuring device with pulse expander.

A schematic diagram of a measuring device with signal pulse
expander is presented in Fig. 2. It consists of sensor 1, ampli-
fier 2, detector 3, connecting resistor 4, low-loss capacitor 5,
diode 6, delay multivibrator 7, discharge circuit 8 and 9, emitter
repeater 10 and needle indicator 11. Upon transmission of a sig-
nal pulse to the inlet, capacitor 5 is charged, through the detec-
tor and resistor, to a voltage close to the peak value of the
input signal.

The charge circuit parameters are calculated in such a man-
ner that a low dependence of the readings   on signal shape
is provided, within a given range of signal duration. The multi-
vibrator closes the discharge circuit for a time which is suf-
ficient for a positive reading,   and it then
quickly discharges the capacitor.

INDUSTRIAL REALIZATION OF A DIRECT FOURIER TRANSFORM IN AUTOMATED EXPERIMENTAL DATA PROCESSING SYSTEMS

G.S. Lyubashevskiy
(Moscow)

Industrial realization of a direct Fourier transform comes down to calculation of the value

$$R = \lim_{T \to \infty} \frac{1}{T} \int_{-\frac{T}{2}}^{\frac{T}{2}} F_1(t) \cdot F_2(t)\, dt. \tag{1}$$

where $F_2(t) = U_2 \cdot e^{-i\omega t}$. This is equivalent to the nonresonator method of filtration of signal $F_1(t)$, with a pass band determined by the electrical circuit parameters. The calculation result, in the form of a direct current voltage, is easily transformed into numerical form. Thanks to the indicated advantages, algorithm (1) is used in automated experimental data processing systems [1,2].

Time-pulse multiplying devices [3,6] are widely used for /15 calculation of the product $F_1(t) \cdot F_2(t)$; they have advantages over other analog methods of multiplication [7], since an additive interference, reducing the resolving power of the device, is inherent in this method of multiplication.

Let us estimate the value of the ratio of the interference energy to the signal energy.

It is known that the total energy is determined with complex coefficients of expansion of the signal at the outlet of the device in a Fourier series. With pulse-width modulation of a high-frequency signal of amplitude A and period T*, a pulse-width sequence of pulses is produced by the first factor $F_1(t) = U_1 \sin 2\pi \frac{t}{T}$ [6]. Then, this pulse sequence is used for amplitude modulation of the second factor $F_2(t) = U_2 \sin(2\pi \frac{t}{T} + \phi)$, as a result of which

$$F_1(t) F_2(t) = f(t) = \sum_{n=1}^{r \cdot r} f_n(t). \tag{2}$$

where

$$f_n(t) = \begin{cases} u_2 \sin 2\pi \left(\frac{t}{T} + \phi \right) & \text{at } nT^* - \frac{a_n}{2} \leqslant t \leqslant nT^* + \frac{a_n}{2} \\ 0 & \text{at } nT^* - \frac{a_n}{2} < t < nT^* - \frac{a_n}{2}, \end{cases} \tag{3}$$

$$a_n = \frac{T^*}{2} \left[1 + \alpha \cdot \sin \left(2\pi n \frac{T^*}{T} \right) \right]. \tag{4}$$

13

$\alpha = \dfrac{U_1}{A}$ **is** the depth of the width modulation and $n = 1, 2, \ldots \dfrac{T}{T^*}$.

Then, the complex coefficients of expansion of the function $f(t)$

$$(5)$$

$$C_k = \frac{u_1}{T} \sum_{n=1}^{T/T^*} \int_{nT^* - \frac{a_n}{2}}^{nT^* - \frac{a_n}{2}} \sin\left(2\pi \frac{t}{T} + \varphi\right) \cdot e^{-2\pi i k \frac{t}{T}} \cdot dt.$$

After integration and summation of (5), we obtain a final expression for the coefficient C_k:

/16

$$C_k = \frac{U_1}{A} \cdot \frac{T^*}{T} \left\{ \alpha \cdot \cos\varphi \cdot e^{-2\pi i k \frac{T^*}{T}} \frac{1 - e^{2\pi i k}}{1 - e^{2\pi i k T^*/T}} + \right.$$

$$+ \frac{1}{i}\left[e^{i\varphi - 2\pi i \frac{T^*}{T}(1-k)} \frac{1 - e^{-2\pi i(1-k)}}{1 - e^{-2\pi i(1-k)}} - \right.$$

$$\left. - e^{-i\varphi - 2\pi i \frac{T^*}{T}(1-k)} \frac{1 - e^{2\pi i(1+k)}}{1 - e^{2\pi i \frac{T^*}{T}(1-k)}} \right] -$$

$$(6)$$

$$- \frac{\alpha}{2}\left[e^{i\varphi - 2\pi i \frac{T^*}{T}(2-k)} \frac{1 - e^{-2\pi i(1-k)}}{1 - e^{-2\pi i \frac{T^*}{T}(2-k)}} - \right.$$

$$\left.\left. - e^{-i\varphi - 2\pi i \frac{T^*}{T}(2-k)} \frac{1 - e^{2\pi i(1+k)}}{1 - e^{2\pi i \frac{T^*}{T}(2-k)}} \right]\right\}.$$

After averaging function $p(t)$ with transfer function $W(j\omega) = 1/(1 - i\omega\tau)$, where τ is the averaging time constant, in the device, the signal expansion coefficient at the output of the device will be expressed as

$$C_k' = \frac{C_k}{1 + 2\pi i k \frac{\tau}{T}}.$$

$$(7)$$

From this, for $K = 0$

$$C_0' = \frac{u_1 u_2}{4A} \cos\varphi.$$

$$(8)$$

i.e., the direct current voltage at the outlet of the device, correct within the proportionality coefficient, equals the value sought R. Components of the spectrum C_k' for $K \gg 1$ are the additive interference. Then, the ratio of the interference energy to the

14

useful signal energy is

$$\tau_i = \frac{\sum\limits^{\tau} c_k{}^i}{(c_o')^2} - 1 \simeq \frac{2\sum\limits_{k=0}^{2} c_k'{}^i}{(c_o')^2} - 1 = \frac{1+\left(\frac{x}{4}\right)^2}{\left(\sqrt{2}\,\pi x\,\frac{\tau}{T}\,\cos\varphi\right)^2}. \tag{9}$$

At $\left(\frac{\alpha}{4}\right)^2 \ll 1$, which is always satisfied,

$$\tau_i = \left(\sqrt{2}\,\pi x\,\frac{\tau}{T}\,\cos\varphi\right)^2. \tag{10,}$$

It is clear from the solution obtained (10) that the ratio
of the interference to the useful signal energy is inversely pro-
portional to the square of the product of the depth of the width
modulation and the ratio of the time constant averaging to the
cross-multiplied signals.

REFERENCES

1. Lyubashevskiy, G.S., B.D. Tartakovskiy and V.E. Frishberg, "Multichannel Method of Study of Distributed Vibrational Structures," in the collection Vibratsii i shumy [Vibrations and Noise], Moscow, Nauka Press, 1969.

2. Genkin, M.D. and V.V. Yablonskiy, "New Methods of Measurement of the Parameters of Multidimensional Oscillations of Linear Mechanical Systems," in the collection Dinamiki i akustike mashin [Machine Dynamics and Acoustics], Nauka Press, Moscow, 1971.

3. Latenko, I.V., Analogovyye mnozhitel'nyye ustroystv: [Analog Multipliers], Ukrainian SSR Technical Litera' : Press, Kiev, 1963.

4. Petrov, V.K., V.B. Smolov, et al, "Transistorizt ecision Time-Pulse Multiplier-Divider," Avtomatika i telemekhanika, (10), 1965.

5. Smolov, V.B. and Ye. R. Ugryumov, Vremya-impul'snyye vychislitel'nyye ustroystva [Time-Pulse Computing Devices], Energiya Press, Moscow, 1968.

6. Lyubashevskiy, G.S., A.I. Orlov, et al, "Device for Computer Input of Data and Signals with a Wide Frequency Spectrum," Otbor i peredacha informatsii, (19), 1969.

7. Maslov, A.A., "Survey and Classification of Multiplication Devices," Avtomatika i telemekhanika, (10), 1965.

16

DISCRETE REGULATION OF TRANSFER FUNCTION OF A CIRCUIT
IN EXPERIMENTAL DATA AUTOMATIC COLLECTION AND PROCESSING SYSTEMS

G.S. Lyubashevskiy, A.A. Petrov,   I.A. Sanayev and
V.E. Frishberg
(Moscow)

In systems for automatic collection and processing of experi-
mental data in analog form [1-3], the dynamic range of input
signals of the processing devices does not exceed 50-60 dB in
the best case, which is significantly less than the actual dynamic
range of change in vibration levels, which reaches 80-100 dB.
Therefore, it is advisable to use discrete control of the trans-
fer function   of the circuit, for coordination of the
dynamic range of the vibration level change, on the one hand,
and the signal range at the processing device output, on the
other har l. Autonomous amplication systems with automatic dis-
crete gain control, connected after each filter and permitting /18
the rated effective signal value to be maintained, is useful in
narrow band   noise analysis.

Statistical characteristics $K=K(U_{in})$ and $u_{out}=u_{out}(u_{in})$, ex-
plaining the principle of operation of the device by the example
of a 4-stage automatic control system, are presented in Fig. 1.
It is clear from the qualitative relationships presented that,
by change in u_{in}, within the limits of a dynamic range of D dB,
due to automatic selection of the transfer function K,
the value of the u_{out}, changes within a dynamic range of 4 dB. In
principle, the selection of the value of D, like the number of
control steps, is determined by a compromise between the require-
ments of dynamic input signal range and maximum control time
placed on the processing device.

Fig. 1.

Let us examine the functional diagram of the device developed
for discrete control of the circuit transfer function (Fig. 2).
The input signal u_{in}, in the dynamic range of 80 dB ($10^{-5} \div 10^{-1}$V)

passes through attenuator AT, having one of the transfer functions within the series 1, 10^{-1}, 10^{-2}, 10^{-3} (D=20dB). The attenuator transfer function is set in accordance with the state of double break counter T_1-T_2 in such a manner that the output of the next amplifier is within dynamic range D=20dB. After detection of the signal, u_{out} enters the inlet of the minimum CC_{min}-maximum CC_{max} comparator . The response levels of the comparator correspond to the lower and upper levels of the signal u_{out}, within the selected limits of the range of change $u_{out\ min}$- $u_{out\ max}$.
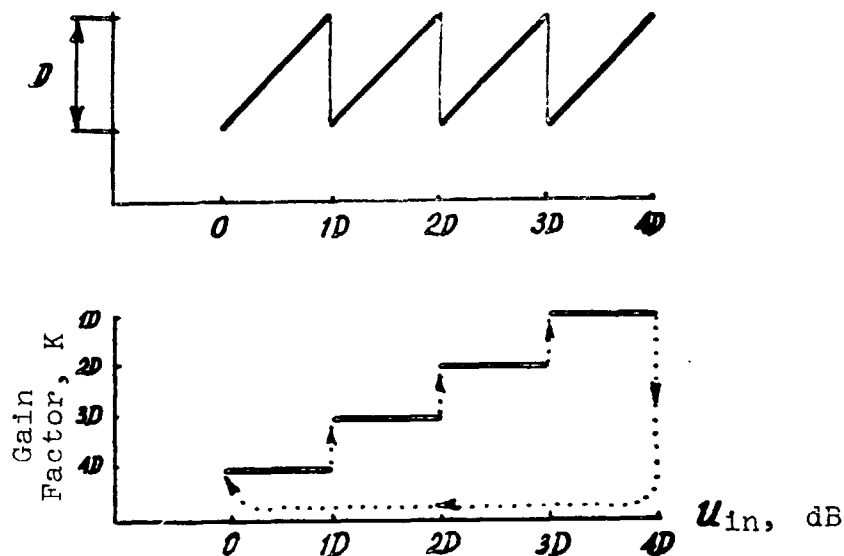
Fig. 2.

At a u_{out} signal level within the selected range ($u_{out\ min}$ <u_{out}$ <u_{out\ max}$), the CC_{min} system trips, there is no potential across the HE and CC_{max} systems, the I system is closed and pulse timing generator PTG is cut off from the counting inlet of counter T_1-T_2. This condition of the device corresponds to a correctly established attenuator transfer function. At a u_{out} signal level beyond the selected range (u_{out}< u_{min} or u_{out}> u_{max}), system I opens, generator G is switched on to the counter inlet and a sequential sorting of the attenuator transfer function begins, until the condition $u_{out\,min}$<u_{out}<$u_{out\,max}$ is satisfied.

To increase the control speed, the detector capacitor is periodically discharged, with a delay τ with respect to the main sequence of cyclic pulses. This permits the frequency

To increase the control speed, the detector capacitor is periodically discharged, with a delay τ with respect to the main sequence of cyclic pulses. This permits the frequency

/19

18

nonuniformity of the detector to be reduced, while maintaining the required dynamic control.

Experimental verification of the device has demonstrated that, in the 20-20 kHz signal range, with a frequency nonuniformity of approximately 10%, the maximum control speed does not exceed 0.5 *sec.*

REFERENCES

1. Lyubashevskiy, G.S., B.D.Tartakovsky and V.E. Frishberg, /20
   "Multichannel Method of Study of Distributed Vibrational
   Structures," in the collection Vibratsii i shumy [Vibration
   and Noise], Nauka Press, Moscow, 1969.

2. Bazhenov, D.V. L.A. Bazhenova and A.V. Rimskiy-Korsakov,
   "Measurement of Statistical Characteristics of Oscillations
   of Complex Mechanical Systems," Dokl. VI Vsesoyuznoy Akusti-
   cheskoy konf. [Reports, VIth All-Union Acoustical Conference],
   Moscow, 1968.

3. Morozov, K.D. and V.V. Yablonskiy, "Reciprocal Spectrum and
   Frequency Characteristic Analyzer," in the collection Dinamika
   i akustika mashin [Machine Dynamics and Acoustics], Nauka
   Press, Moscow, 1971.

ESTIMATION OF ERRORS IN MEASUREMENT OF STATIONARY SIGNALS FROM A CONTINUOUS FREQUENCY BAND SPECTRUM

V.A. Ivanov
(Leningrad)

Errors arise in the measurement of signals in a frequency band, which are caused by passage of part of the energy through lateral branches and through regions of delay in the filter characteristics. Therefore, it is advisable to estimate the measurement error of filters with transconductance drops in the branches of the frequency characteristics $a \neq \infty$ and dynamic range $D \neq \infty$. It is assumed that, on the logarithmic scale, filter frequency characteristics are represented in the form of an isosceles trapezoid and that the input signal has a continuous spectrum in the frequency range from Ω_1 to Ω_h.

The measurement error is determined in the form of a ratio of power P_ϕ and P_{1-2}, at the outlets of a real and an ideal filter:

$$\delta = \frac{P_\phi}{P_{1-2}} \qquad (1)$$

If the mean normalized geometrical filter frequency (Fig. 1) is designated by Ω_m, the limiting frequencies Ω_1 and Ω_2 and the cutoff frequencies Ω_c and Ω_d can be presented in the form [1]

$$\Omega_1 = \Omega_m K, \quad \Omega_2 = K \Omega_m; \quad \Omega_c = \Omega_m \cdot \alpha K \text{ и } \Omega_d = \Omega_m \cdot K \alpha;$$

where $\alpha = 2^{N/a}$, K is a proportionality coefficient equal to $\sqrt[6]{2}$, $\sqrt[4]{2}$ and $\sqrt{2}$ for the 1/3, 1/2 and 1/1 octave filters, respectively, N is the level of decrease of the filter characteristics at frequencies Ω_1 and Ω_2, in dB, and a is the transconductance drop of the branches of the filter frequency characteristics, in dB/octave.

In accordance with Fig. 1, power P_ϕ can be determined in the /21 form

$$P_\phi = P_c + P_d + P_{c-d} + P_{H-3} - P_c' - P_d' - P_{c-d}'$$

The powers of the spectral components P_c and P_d, which would filter through the left and right branches of the filter characteristics as $D \to \infty$, can be obtained in the form
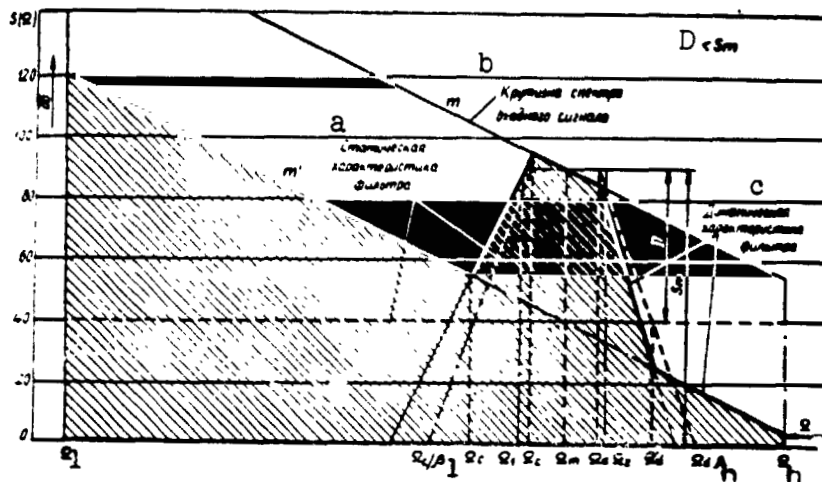
Fig. 1.

Key: a. Filter statistical characteristics
     b. Input signal spectrum slope
     c. Filter dynamic characteristics

$$P_c = S_m \int\limits_{\Omega_c/\beta_1}^{\Omega h} \left(\frac{\Omega}{\Omega_m}\right)^{\tau_s} \left(\frac{\Omega}{\Omega_c}\right)^{\tau_s} d\Omega =$$

$$= \frac{S_m \cdot \Omega_m}{\tau_s + \gamma + 1} \left(\frac{\alpha}{K}\right)^{\tau_s - 1} \left[1 - 2^{-\frac{S_m}{a-m}\left(\frac{\alpha}{K}\right)^{\tau_s} \cdot (\tau_s - \gamma + 1)}\right] ; \qquad (2)$$

$$P_d = S_m \int\limits_{\Omega_d}^{\Omega_d \cdot b_b} \left(\frac{\Omega}{\Omega_m}\right) \left(\frac{\Omega}{\Omega_d}\right)^{-\gamma} d\Omega =$$

$$= \frac{S_m \cdot \Omega_m}{\gamma - \tau_s - 1} \left(\frac{K}{\alpha}\right)^{\tau_s - 1} \left[1 - 2^{\frac{S_m}{a-m}\left(\frac{K}{\alpha}\right)^{\tau_s} \cdot (\tau_s - \gamma + 1)}\right] ;$$

where

$$\tau_s = \frac{m}{3,0103} ; \qquad \gamma = \frac{a}{3,0103} ;$$

$$\beta_1 = 2^{\frac{S_m}{a-m}} \left(\frac{\alpha}{K}\right)^{\tau_s} ; \qquad \beta_h = 2^{\frac{S_m}{a-m}} \left(\frac{K}{\alpha}\right)^{\tau_s} ;$$

m is the input signal spectrum slope in dB/octave; and S_m is the /22
spectral density at frequency Ω_m, in dB. The powers of the spectral
components in the $\Omega_c - \Omega_d$ and $\Omega_1 - \Omega_2$ bands equal

22

$$P_{c-d} = S_m \int_{\Omega_c}^{\Omega_d} \left(\frac{\Omega}{\Omega_m}\right)^{\gamma} d\Omega = \frac{S_m \cdot \Omega_m [K^{\alpha(\gamma+1)} - \alpha^{\alpha(\gamma+1)}]}{n^{\gamma+1} \cdot \alpha^{\gamma+1} \cdot (\gamma+1)} \; ;$$

$$P_{1-c} = S_m \int_{\Omega_1}^{\Omega_c} \left(\frac{\Omega}{\Omega_m}\right)^{\gamma} \cdot d\Omega = \frac{S_m \cdot \Omega_m [K^{\alpha(\gamma+1)} - 1]}{K^{\gamma+1} \cdot (\gamma+1)} \; . \tag{3}$$

Expression (2) has physical meaning only at $|\gamma| > |\eta + 1|$, and expression (3), at $\ln K \geq \ln \alpha$, from which the limits of the slope of the frequency characteristic branches are obtained. For the 1/3, 1/2 and 1/1, we have $a_{1/3} \geq 6N$, $a_{1/2} \geq 4N$ and $a_{1/1} \geq 2N$, respectively. The power P_{1-h} of the spectral components in the frequency range $\Omega_1 - \Omega_h$, bounded above by the straight line m', equals

$$P_{1-h} = (S_m - D) \int_{\Omega_1}^{\Omega_h} \left(\frac{\Omega}{\Omega_m}\right)^{\gamma} d\Omega = \frac{S_m - D}{(\gamma+1) \cdot \Omega_m^{\gamma}} (\Omega_h^{\gamma-1} - \Omega_1^{\gamma-1}).$$

In a similar manner, powers P_c', P_d' and P_{c-d}', in accordance with Fig. 1, equal

$$P_c' = (S_m - D) \int_{\Omega_c/2}^{\Omega_c'} \left(\frac{\Omega}{\Omega_m}\right)^{\gamma} \left(\frac{\Omega}{\Omega_c'}\right)^{\gamma} \cdot d\Omega = 2^{-\frac{D}{a}(\gamma+1)} \cdot \frac{P_c}{C} \; ;$$

$$P_d' = (S_m - D) \int_{\Omega_d'}^{\Omega_c' \cdot \delta_b} \left(\frac{\Omega}{\Omega_m}\right)^{\gamma} \left(\frac{\Omega}{\Omega_d'}\right)^{-\gamma} \cdot d\Omega = 2^{\frac{D}{a}(\gamma-1)} \cdot \frac{P_d}{D} \; ;$$

$$P_{c-d}' = \frac{(S_m - D) \cdot \Omega_m}{(\gamma+1) \cdot 2^{\frac{D}{a}(\gamma-1)}} \left[2^{2\frac{D}{a}(\gamma-1)} \left(\frac{K}{\alpha}\right)^{\gamma-1} - \left(\frac{\alpha}{K}\right)^{\gamma-1} \right] \; ;$$

where

$$\Omega_c' = \Omega_c \cdot 2^{\frac{D}{a}} \; ; \quad \Omega_d' = 2^{\frac{D}{a}} \cdot \Omega_d.$$

Analysis of formula (1), for 1/3-1/2 and 1/1 octave filters and the values m = 12-6 dB/octave, Ω_h/Ω_1 = 500, a = 20 dB/octave and a = 100 dB/octave, shows that the measurement error δ, at small values D = 30-50 dB, for signals with a steep slope m, can reach tens of decibels. At small values of the dynamic ranges of the filters, the measurement error δ quickly decreases with increase in D. In this section, δ is practically independent of a.

However, with further increase in D to 50-70 dB, the error,
although it decreases, does not do so as rapidly, since its
dependence on a begins to appear gradually. With still greater
increase in D (to 70-90 dB), the error depends only on a, and,
for filters with a = 20 dB/octave, does not exceed 2.4 dB, and
for filters with a = 100 dB/octave, does not exceed 0.4 dB.

Conclusions

In design of apparatus for frequency analysis of signals with
a continuous spectrum, to decrease the errors, the dynamic range
of the filters must be expanded to 80 dB and more or the input
signal spectra must be limited beforehand, with the aid of range
filters. A series connection of several band filters can give the
most effective results.

REFERENCES

1. Sepmeyer, L.W., IASA 30(10) (1962).

AUTOMATIC MEASURING DEVICE FOR OCTAVE ANALYSIS OF NOISE

D.L. Memnonov and A.M. Nikitin
(Moscow)

The instrument consists of a recorder, serial tape recorder and decoder, with pulse counters. The noise levels are recorded on the tape recorder in coded form. They are counted by the pulse counters in the decoder.

The recorder measurement system forms audio signals, each of which is proportional in duration to the total or one of the octave noise levels. These signals are recorded on the tape recorder.

The measurement cycle of the recorder consists of four parts. First, the tens, then units of decibels of the total noise level are recorded; then the tens of decibels of the octave levels are recorded and, finally, the units of decibels of the octave noise levels.

The octave levels are counted relative to the total noise level. All octave levels are recorded simultaneously.

Besides the audio signals, square pulses are continually /24 recorded on one of the frequencies, at a constant carrier frequency.

A block-diagram of the recorder is shown in Fig. 1.

The recorder consists of an overall equalizing channel, eight octave level channels, with parallel operating octave filters, square pulse channel and programmer. All ten channels have audio generators, with noncoincident frequencies, at the outlets.

The attenuators are switched by the programmer, in accordance with the square pulses entering it. Audio generators 1-9 are switched on at the initial moment of operation of the channel, and they are switched off by the comparators. In changing from recording of the tens of decibels to recording the units of decibels, the reference voltages on the comparators are increased by 10 dB. At the initial moment of time, the attenuators are set at maximum attenuation.

To obtain more reliable data, an automatic ten-fold repe- /25 tition of the measurement cycle is provided at each measurement point, and, only after this, is the transition to a new point made.

The programmer switches off the tape recorder after completion of the planned measurement program.
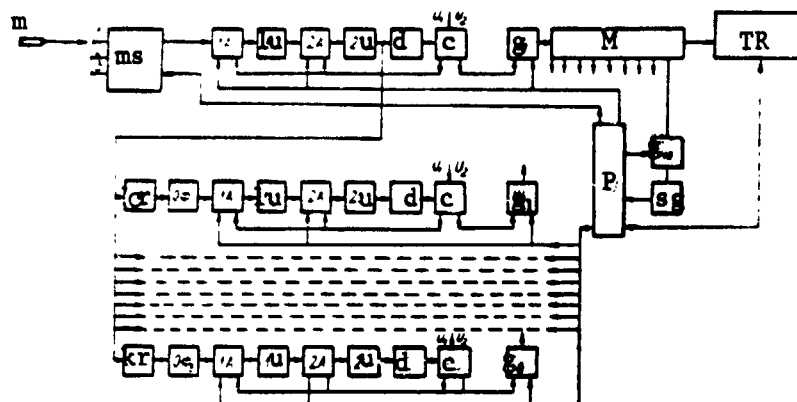
Fig. 1. Recorder block diagram:

m	Microphone
ms	Microphone switch
1a,2a	Attenuators
1u,2u	Amplifiers
d	Detector
c	Comparator
cr	Cathode repeater
$o\Phi_1 \ldots o\Phi_8$	Octave filters
$g_1 \ldots g_{10}$	Sinusoidal voltage generators
sg	Square pulse generator
M	Mixer
P	Programmer
TR	Tape recorder

In carrying out deciphering, the magnetic tape record is reproduced by the tape recorder, connected to the decoder (2).

The decoder consists of a set of filters, with detectors at the outlets. Each of the filters is tuned to one of the audio signal frequencies recorded by the tape recorder. One of these filters is tuned to passage of the square pulses. In addition, the decoder includes a control device, pulse converter and pulse counters. Pulses go to all nine counters through the square pulse channel and through the control device. /26

Each counter counts pulses only in the presence of a control voltage in the control device. In this manner, the number of pulses counted proves to be proportional to the duration of the control voltage and, consequently, to the noise level. In order that each pulse is perceived by the counters as tenths of a pulse in the measurement cycle period when tenths of decibels should be counted, the pulse converter divides each pulse entering it during these periods into ten shorter pulses. During those periods when the count of units of decibels is carried out, the incoming pulses pass through the converter without change.
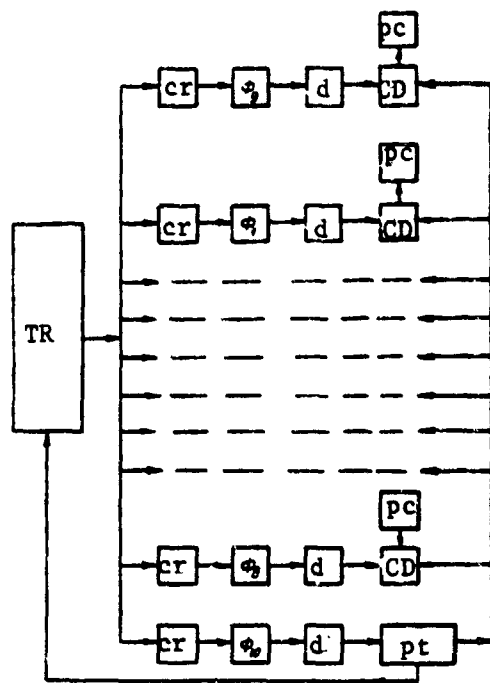
Fig. 2. Decoder block diagram:

TR	Tape recorder
cr	Cathode repeater
$\Phi_1 \ldots \Phi_{10}$	Filters
CD	Control device
pc	Pulse counter
pt	Pulse converter
d	Detector

In view of the fact that, in order to obtain more reliable data, an automatic ten-fold repetition of the measurement cycle is provided for during the recording period, the mean noise level is obtained by dividing the pulse counter readings by ten.

In addition to the basic purpose of the pulse converter, after reproduction of the noise record is completed at each measurement point, it switches off the tape recorder.

The recorder programmer and attenuators, as well as the control devices and pulse converters, are based on a relay system, using electromagnetic relays or devices replacing them as elements.

In the absence of a sufficient number of pulse counters, decoding of the record can be carried out sequentially, by connecting one counter with one control device to all nine filters.

APPARATUS FOR MONITORING THE CONDITION OF MINING MACHINERY TRANSMISSIONS

I.A. Levites and I.G. Fiks
(Donetsk)

A series of correspondences between the signal parameters and transmission conditions have been revealed in study of the vibro-acoustic signals of operating mining machinery transmissions.

In particular, the spectrum width and the amplitudes of its /27 components characterize the degree of wear of the transmissions and abrasion in kinematic pairs, the presence of periodic components in the signal are evidence of the presence of transmission damage, and the frequency sequence of these components depend on which pair is damaged.

Proceeding from this, a portable apparatus was developed for monitoring the technical condition of mining machinery transmissions (Fig. 1). The apparatus consists of channels for measurement of vibration levels and for detecting damage.
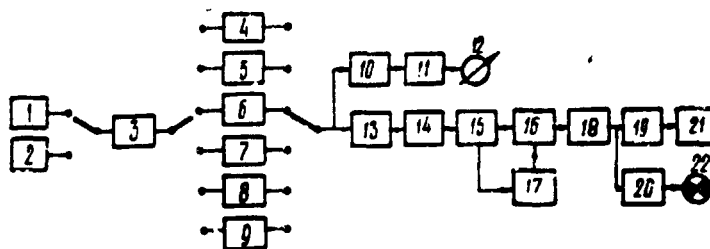
Fig. 1. Block diagram of apparatus for monitoring condition of mining machinery transmissions.

A vibro-acoustic signal, taken from piezoelectric sensors 1 and 2, is first amplified by preamplifier 3, with high input resistance (about 50 Mohm). The amplified signal enters measuring amplifier 10, either directly or through octave band filters (4-9), encompassing the frequency range from 175 to 11,200 Hz.

Needle 12 or, in case of necessity, an automatic recording instrument, is connected to the measuring amplifier through peak or quadratic detector 11.

The apparatus permits measurement of the overall level of vibroacceleration of the transmission being tested and the level of the vibroacceleration in octave bands.

For evaluation of the condition of the transmission, the results of the measurements are compared with standard data.

The detection channel operates in the following manner. The vibro-acoustic signal of a mechanism in good working order is a

complex vibration with random amplitudes, phases and frequencies. In the presence of defects, for example, caused by considerable wear of kinematic pairs or damage to contact surfaces of the teeth of individual gear pairs, a periodic component appears in the signal, the repetition rate of which is determined by the frequency of impact of elements of the damaged pair.

During operation of the apparatus in the damage detection /28 mode, after preliminary amplification and filtration by detector 13, with threshold selector, the signal envelope, which is a sequence of pulses of different durations and repetition rates, is extracted. These pulses are amplified by pulse amplifier 14, shaped by shaper 15 and enter one inlet of coincidence system 16, and the same sequence of pulses enters the second inlet through delay control unit 17.

The delay time is established for each kinematic pair by an equal impact period of elements of the same kind. During the search for damage, the delay time changes as many times as there are kinematic pairs in the mechanism. By adjusting the delay unit to the frequency of impact of damaged elements, a signal appears at its outlet, in the form of a series of equally spaced pulses, with the tuned frequency. After division by frequency divider 18 and amplification by output power amplifiers 19 and 20, these pulses enter pulse counter 21 and signal lamp 22.

A periodically blinking lamp signals the presence of damage. The number of pulses, determined by the counter, depends on a control pair and is known previously. The absence of pulses or a small number of them is evidence that the pair monitored is in good working order.

An experimental test specimen of the apparatus was checked under laboratory conditions.

MEASUREMENT OF VIBRATION RATE OF
MANUALLY OPERATED PERCUSSION MACHINES

Ye.V. Aleksandrov and Yu.V. Flavitskiy
(Moscow)

A quanti,ative evaluation of vibroshock pulses was carried
out, the extent of their effect on the efficiency of apparatus
used at the present time was determined and appropriate technical
requirements were developed:

1. A method was developed for calibrating apparatus with
test acceleration pulses, consisting of the following: the shape
and magnitude of stress pulses is determined, by calculation or
experimentally, on an intermediate section of a loaded rod (L =
= 1400 mm, D = 35 mm); the rod is loaded by dropping blocks with /29
different contact rigidities (L = 100 mm, D = 35 mm, radius r =
= 17.5 mm - 400 mm) from various heights; the strain gauges and
cathode oscillographs used in this case, as well as the methods
of calculation developed in the laboratory, guaruntee sufficient
measurement accuracy.

The test acceleration pulses are determined according to the
resulting function $\sigma(t)$ and they are compared with the readings
of the apparatus being tested (an accelercmeter sensor is installed
on the free end of the rod).

2. A special apparatus for measurement of accelerations of
between 1 and 5000 g and shock stress pulses from 20 kg/cm^2 up,
with durations of $50 \cdot 10^6$ sec and higher was designed and built.
By means of it, the amplitudes and shapes of the peak vibroshock
pulses, arising during operation of a hammer, were obtained; the
recording time of the continuous process (with electrical scanning
disconnected) is determined by the time of one revolution of the
drum of a specially made mechanical photo attachment, allowing
a film 2000 mm long to be pulled through at a speed of from 2 to
100 m/sec.

3. The nature and magnitude of acceleration pulses and the
speed of the hammer shaft during its operation were determined
experimentally. The curves obtained, as analysis of the experi-
mental data demonstrates, are far from correspondence with the
acceleration curves, which should deviate, because of filtration
in the shock acceleration integrator during operation of the
percussion machine; this, in turn, shows up in a significant
manner in the composition of the vibration spectrum, especially
in the higher portion of it.

30

Conclusions

1. Existing vibrometric apparatus, in principle, eliminates the possibility of using it for measurements of vibration rates of percussion machines, for the following reasons:

    a. Overloads, setting in as a consequence of superimposition on the overall vibration of vibroshock accelerations on the order of 50-100 g (calibration of the apparatus is carried out under conditions of measurement of the acceleration of the total vibrations, not exceeding 3-5 g);

    b. Partial filtration of the shock accelerations in the integrator.

2. Analysis carried out of the actual loads arising during operation of percussion machines can serve as a basis for development of technical problems in planning appropriate vibrometric apparatus, as well as for development of means of modeling shock vibrations under test-stand conditions.

SYNTHESIS OF PARAMETERS OF A MACHINE SET, ACCORDING TO AMPLITUDES OF VIBRATION, IN THE CASE OF COAXIAL MISALIGNMENT OF SHAFTS

M.S. Rondomanskas, K.M. Ragul'skis, Rem.A. Ionushas, and R.Yu. Bansevichyus
(Kaunas)

In practice, the problem frequently arises in assembly of machine sets of the basis for selection of requirements for c axial alignment of connected machines, depending on permissible le· .ls of vibration of the set. Together with this, it is important to correctly select certain set parameters, with fixed, permissible coaxial nonalignment parameters of the connected machines.

A system and dynamic model of a set, widely used in practice, is shown in Fig. 1a and b, consisting of two machines, connected by a flexible coupling, one of which is installed on shock absorbers. Let us consider that the machine on shock absorbers has four degrees of freedom. In the general case, coaxial nonalignment of the machine shafts is determined by three coaxial nonalignment parameters (Fig. 1c): radial dispacement e, angular displacement γ and angle β, determined by the phase shift between e and γ.

The amplitudes of the vibrations of the machine on shock absorbers have the following form:

$$\eta_{qi} = \sqrt{K_{q1}^2 e^2 - K_{q2}^2 \cdots - 2K_{q1} K_{q12} e \gamma \cos \beta.} \tag{1}$$

where $\qquad q = y,\ z;\ i = 1,\ 2;$

$$K_{q_{11}} = \frac{k_{mp} \lambda_q^{-2} (k_{mo} s_3^2 - k_q s_2)}{\Delta q} \ ;$$

$$K_{q_{12}} = \frac{k_{mo} d s_1 \lambda_q^{-2} (k_q - k_{mo} s_1)}{\Delta q} \ ;$$

$$\Delta q = (k_{mp} s_1^2 - k_{mo} s_3^2 - k_q)(k_{mp} s_1^2 + k_{mo} s_2^2 + k_q) \lambda_{2q}^{-2} \lambda_{3q}^{-2} - [(k_{mp} s_1 s_2 - k_{mo} s_3) \lambda_{4q}^{-2}]^2;$$

k_{mp} and k_{mo} are the radial and axial rigidity of the coupling, respectively; k_q is the rigidity cf the shock absorbers in the directions of the corresponding degrees of freedom; λ_{1q}, λ'_{1q}, λ_{2q}, λ_{3q}, λ_{4q} are dynamic response factors;

32

Fig. 1. Movement leveling synthesis. a. Set diagram; b. dynamic model of set; c. coaxial nonalignment parameters in the general case of shaft arrangement.
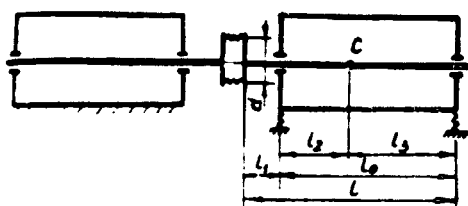
$$s_1 = \frac{l_1}{l_0} \; ; \quad s_2 = \frac{l}{l_0} \; ; \quad s_3 = \frac{d}{l_0} \, .$$

The amplitudes of the vibra- /31 tions of the machine on shock absorbers are functions depending on the axial nonalignment parameters. Therefore, there is interest in determining the conditions under which the amplitude n_{qi} is at a minimum:

$$K_{q_{i1}} e \pm K_{q_{i3}} \gamma \cos \beta = 0,$$
$$K_{q_{i1}} e \cos \beta \pm K_{q_{i3}} \gamma = 0. \tag{2}$$

It is easy to ascertain that, /32 even at $e \neq 0$ and $\gamma \neq 0$, the amplitude $n_{qi} = 0$, if the following condition is satisfied:

$$\tag{3}$$

Condition (3) is of practical interest, since, for specified e and γ (which cannot be avoided during alignment or which is economically inadvisable), system parameters can be selected, at which n_{qi} tends toward zero.

In a similar manner, we determine the optimum coupling rigidity, at which the amplitude n_{qi} will be at a minimum. In this case, we consider that $k_{mo} \leq k_{mp}$. Then,

$$k_{mp} = \frac{k_q}{s_1 s_2} \left[\sqrt{\frac{l_{sq}^2 - l_{3q}^2}{l_{sq}^2 \, l_{3q}^2 - l_{sq}^4}} \right] . \tag{4}$$

What has been presented above permits a dynamic synthesis of certain parameters of the set overall and of the coupling parameters in particular. This makes it possible to build couplings with very small disturbing forces, in the event the shafts are out of alignment.

SOME QUESTIONS OF AN OPTIMUM PROBABILITY SYNTHESIS OF DYNAMIC METALWORKING MACHINE SYSTEMS

S.A. Dobrynin and G.I. Firsov
(Moscow)

It is advisable to present the problem of an optimum probability design of a dynamic machine tool system in the form of a determination of the optimum values of the system parameters, on the basis of probability information on external factors and independent disturbances of the parameters.

It is very difficult to create a complete mathematical model of a dynamic machine tool system, considering the probability nature of the disturbing influences, at the existing level of development of computer technology.

It is proposed to carry out the solution of the problem of optimization by two stages:

a. Creation of mathematical models, under conditions of determinacy of the input influences; and b. processing the results of the calculations obtained on such models, using optimum condition criteria, and taking into account the proba- /33 bility nature of the parameter values and disturbing input influences, with given distribution patterns.

As basic simplifications, the normal law of distribution of external influences and independent disturbance of the parameters can be assumed.

It is proposed to obtain the patterns of distribution of the dynamic quality characteristics of the machine tool, vibration frequencies and amplitudes, attenuation coefficient, duration of a transition process, etc., by digital computer, using the statistical test method or by means of logical possibility trees.

34

IDENTIFICATION OF A MECHANICAL VIBRATION SYSTEM

S.S. Korablev, Yu.Ye. Filatov, and V.I. Shapin
(Ivanovo)

The actual values of the parameters of a precision instrument assembly vibration system are determined according to experimental amplitude-frequency characteristics.

The assembly is considered as a complex mechanical vibrating system, consisting of elements with concentrated and distributed parameters (see figure).

A calculation procedure has been compiled. A system of equations of vibrational motion for elements with concentrated parameters, converted to quasinormal coordinates [1]:

$$\ddot{\Theta}_i + \omega_i^2 \Theta_i = \varepsilon \Theta_i \qquad (1)$$

where

$$x_j = \sum_{i=1}^n \Delta_i(\lambda_i^2)\Theta_i;$$

$$\omega_i^2 = \frac{c_i}{a_i};$$

$$c_i = \sum_l \sum_k c_{lk} \Delta_l(\lambda_i^2) \Delta_k(\lambda_i^2);$$

$$a_i = \sum_l \sum_k a_{lk} \Delta_l(\lambda_i^2) \Delta_k(\lambda_i^2);$$

$$Q_i = Q_i \left\{ \sum_i \Delta_k(\lambda_i^2)\Theta_i; \quad \sum_i \Delta_k(\lambda_i^2)\dot{\Theta}_i; \quad t \right\};$$

$$i, l, k = 1, 2, \dots, 18,$$

$\lambda_i = \omega_i$ are the natural frequencies of a uniform system, c_{lk} are /35 the rigidity coefficients, a_{lk} are the coefficients of inertia, $\Delta(\lambda_i^2)$ are the algebraic supplements of elements of the specified row of the determinant.

The system indicated is a set of elementary oscillators, the interactions of which are described by small terms on the right sides. The system with parameters distributed by the Galerkin method is reduced to a series of linear mechanical oscillators, which are excited kinematically.
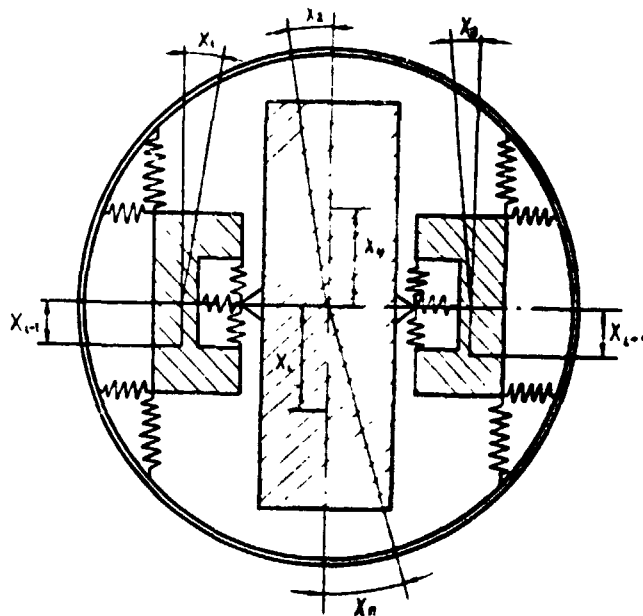
Fig. 1.

An analysis of the effect of compliance coefficients on the change in the frequency spectrum of the system was carried out on an analog computer. The values of the compliances of the flexible elements were calculated from the experimental amplitude-frequency characteristics, using the criterion of finding the discrepancy function minimum. [2].

The damping coefficients were determined on a digital computer, by the method of successive approximations of the calculated amplitude-frequency characteristics to the experimental and control points of resonance and non-resonance bands.

Determination of the numerical values of the coefficients permits analysis of the instrument quality to be carried out.

REFERENCES

1. Kononenko, V.O., Kolebatel'nyye sistemy s ogranichennym /36 vozbuzhdeniyem [Vibrating Systems with Limited Excitation], Nauka Press, Moscow, 1964.

2. Genkin, I.D., V.I. Sergeyev, L.V. Sukhorukov, "Calculation-Experimental Investigation of the Dynamics of Reducing Gears Using Computers," Vibroakusticheskaya aktivnost' mekhanizmov s zubchatymi peredachami [Vibro-Acoustic Activity of Mechanisms with Gear Transmissions], Nauka Press, Moscow, 1971.

CONSTRUCTION OF A MATHEMATICAL MODEL OF THE HUMAN BODY, TAKING THE NONLINEAR RIGIDITY OF THE SPINE INTO ACCOUNT

K.K. Glukharev, N.I. Morozova, B.A. Potemkin, V.S. Solov'yev,
and K.V. Frolov
(Moscow)

In study of vibrational processes in "man-machine" systems, it frequently is necessary to consider the dynamic nature of the body of the human operator. A mathematical model of the human body has been constructed, under the action of harmonic vibrations on it, in the 2.5-7 Hz frequency range.

In this frequency range, it is permissible to consider the model of the human body as a vibrating system, with concentrated parameters [1]. Vertical movements of the seat and vertical components of vibrations of the human body are investigated. A mathematical model is considered found, if the functional connection between the input (vibrations of the seat) and output (vibrations of the human head) signals is determined.

The method of the investigation consisted of experimental production of amplitude-frequency characteristics of the human body and subsequent determination of the numerical values of the coefficients of the differential equations, solutions of which correspond to results obtained during the experiment.

The averaged amplitude-frequency relations, obtained by carrying out experiments with ten subjects, are shown by solid lines in Fig. 1. Each of the relations presented corresponds to a constant level of seat vibration amplitudes. The lower level (0.3 mm) was determined by the possibilities of the experimental setup and the upper leve⁻ (3 mm) was restricted by sanitary standards.

A downward shift in the resonance frequency with increase in vibration stimulation level is evidence of the nonlinear properties /37 of the system being studied. The rigidity characteristics, determined by the properties of the human spinal column [2], correspond to a "soft" type of nonlinear characteristic.

A mathematical model was proposed on the basis of analysis of the experimental data, which describes the vibrations of the human body by a Duffing type equation, with "soft" nonlinearity:

$$m\ddot{x} + \delta(\dot{x} - \dot{u}) + c(x - u) - \gamma(x - u)^3 = 0,$$

$$u(t) = a_0 \sin \omega t,$$

here

$$\dot{u}(t) = a_0 \omega \cos \omega t.$$

(1)

38

X,мм

3 мм

1 мм

0,5мм

0,3мм

2   4   6 ω, Hz

———— Experiment

------ Analog computer calculation
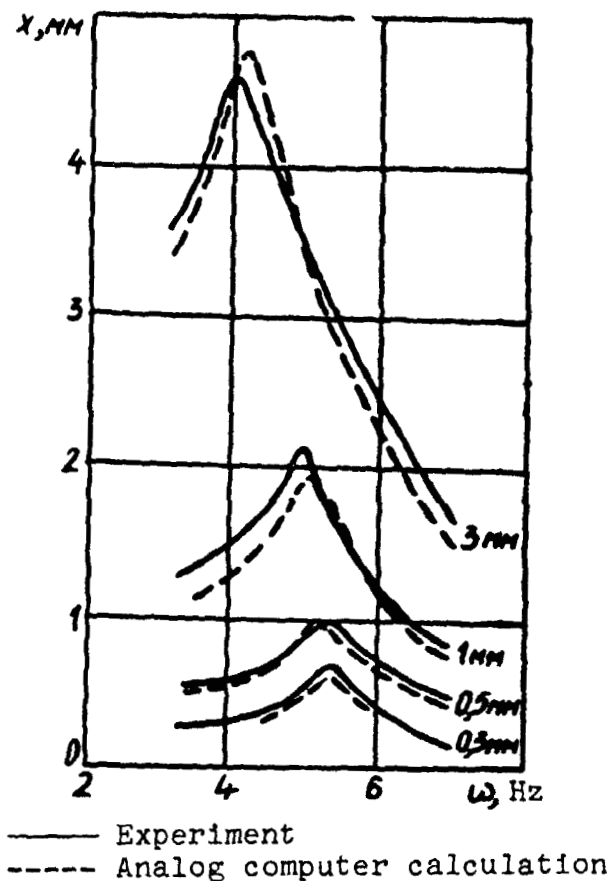
Fig. 1.

The equation obtained was analyzed on a MN-7 analog computer.

To facilitate creation /38 of a structural modeling scheme, Eq. (1) should be presented in Cauchey form:

$$\tag{2}$$

As a result of the modeling, it proved possible to determine the numerical values of the parameters of the system, ensuring satisfactory concordance between experimental and calculation data, which confirms the correctness of the selected mathematical model.

Amplitude-frequency characteristics, with one and the same nonlinearity paramter γ, were plotted from the results of processing of the modeling data, for levels of harmonic action of 3 mm, 1 mm, 0.5 mm and 0.3 mm.

The following values of the coefficients sought were found by analysis of Eq. (1) on an analog computer:

$$m = 0.085 \ \frac{kg \cdot sec^2}{cm}; \quad \delta = 1.0 \ \frac{kg \cdot sec}{cm}$$

$$c = 78 \ kg/cm;$$

$$\gamma = 240 \ kg/cm^3; \quad \omega = 2.5\text{-}7 \ Hz;$$

$$a_0 = 0.03\text{-}0.3 \ cm$$

The amplitude-frequency characteristics of the vibration of the human body, at various levels of harmonic action, obtained as a result of modeling of Eq. (1), are shown by dashed lines in Fig. 1.

REFERENCES

1. Potemkin, B.A. and K.V. Frolov,"Model Presentations of 'Human Operator' Biomechanical System, with Random Influences," Doklady AN SSSR 197(6) (1971).

2. Glukharev, K.K., B.A. Potemkin and K.V. Frolov, "Construction of the Simplest Nonlinear Mechanical Model of the Human Body, with Harmonic Vibrating Actions," Tezisy dokladov Konferentsii po kolebaniyam mekhanicheskikh sistem [Summaries of Reports, Conference on Vibrations of Mechanical Systems], Naukova dumka Press, Kiev, 1971.

INVESTIGATION OF THE REACTIONS OF SKIN PANELS
IN RELATION TO DURATION OF ACOUSTICAL LOADING

V.Ye. Kvitka and G.I. Kernes
(Moscow)

The skin of modern passenger aircraft is most intensively loaded by acou_tical pressure, created by the exhaust jets of jet engines.

Certain characteristics of the reactions of typical skin panels of a passenger aircraft to acoustical loading are being investigated, for development of an objective method of diagnostics of the technical condition of the skin, under the conditions of operations and maintenance sections of civil aviation. There are a number of difficulties connected with the solution of this problem. They depend on the complexity of construction, the loading characteristics of the panels and their reactions. The reactions of skin panels exposed to the noises of the exhaust jets depend on the aircraft operating conditions, the geometric parameters and limiting conditions of the panels. Among the geometric parameters are the linear dimensions of the cells, the radius of curvature and thickness of the skin sheets and limiting conditions or nature of the skin sheet attachment to the rigid elements, determined by the pliability of the panels. For determination of these parameters, measurements were carried out on jet engine passenger aircraft, having accrued operating times from 0 to 6000-73,000 hours. The pliability (elasticity) and curvature of the panels were measured with a special instrument for measuring the stress and deflection of the aircraft skins. In this case, the pliability is characterized by the value of the force P, which is necessary to create a fixed deflection of the panels. As a result, the statistical values of the geometric dimensions and panel pliability were determined. It turned out that, for panels of a given type of passenger aircraft, the ratios of the sides = 2/2 where 2 and 2 are the long and short sides of the panels, have the greatest potential at =2 and =4. The mean statistical value of the radius of curvature of the panels, in different sections, is P = 175 cm, at a root mean deflection of 58 cm. The limiting conditions, for which panel pliability is a criterion, change significantly during prolonged operation of the aircraft. The nature of the change in pliability is shown in Fig. la. The operating time is plotted on the abscissa and the ratio of the force P for aircraft panels with different hours of operation to the mean statistical value P_{mean} for aircraft panels which have flown 7300 hours, is plotted on the ordinate. During the 3000-hour preventive technical maintenance, as a result of replacement of defective rivets or skin sheets, the pliability is restored practically to the initial values.
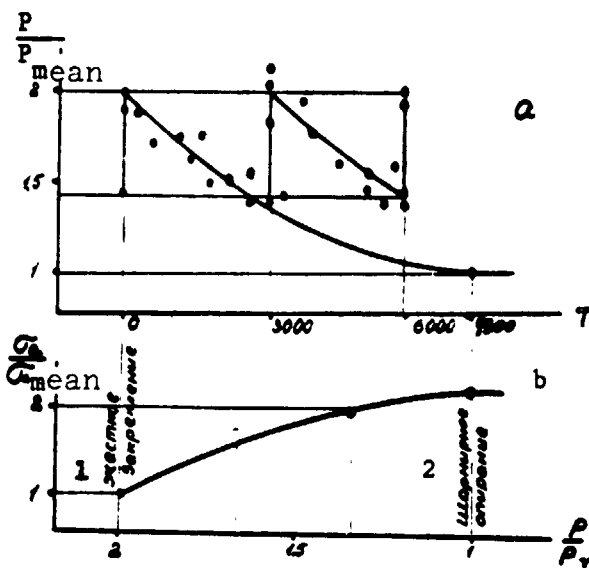
Fig. 1.

Key: 1. Rigid fastening
     2. Hinged support

Flight tests have shown that the root mean value of the amplitude of vibrational displacement and vibrational stress of the skin panels is greater in aircraft, after the prolonged action of acoustical pressure during their operation, than in new aircraft. On the basis of the statistical data obtained, the geometric parameters and limiting conditions of the skin panels were determined, and laboratory studies of their reactions were carried out on a special acoustical test stand. Flat and cylindrical panels were loaded with a pure tone sound pressure, at a constant level and smooth change in frequency from a few to 800 Hz. At every resonance excitation of the panels, deformation signals coming from the wire strain gauges, glued to the surfaces in the transverse and longitudinal directions, were recorded. As a result, the change in amplitude of the vibrational stress was determined, during different forms of natural vibrations of the panels, for given dimensions and limiting conditions. The nature of the change in stress for the flat panels vs. limiting conditions (pliability) is shown in Fig. 1b. The change in stress amplitude, with dif-   /41 ferent forms of vibration of the cylindrical panels, rigidly fastened around the periphery, vs. its radius of curvature P is shown in Fig. 2 (where the solid lines are the concave and the dashed lines are the convex surfaces of the panels: 1 and 2 are the change in stress in the longitudinal and transverse directions of the panels).

Laboratory studies showed that, in proportion to the weakness of the fastenings around the peripheries of the flat panels and increase in radius of curvature of the cylindrical skin panels, their pliability is increased (elasticity is decreased), and the stress on their surfaces under sound pressure loading increases significantly. In this case, the stresses on the convex surfaces are greater than on the concave ones, but this difference disappears in proportion to the increase in radius of curvature. The limiting conditions noticeably affect the tension of the panels in the first four forms of their vibrations, and the maximum stress amplitude values are reached in elongated flat and cylindrical panels at certain higher vibration forms.
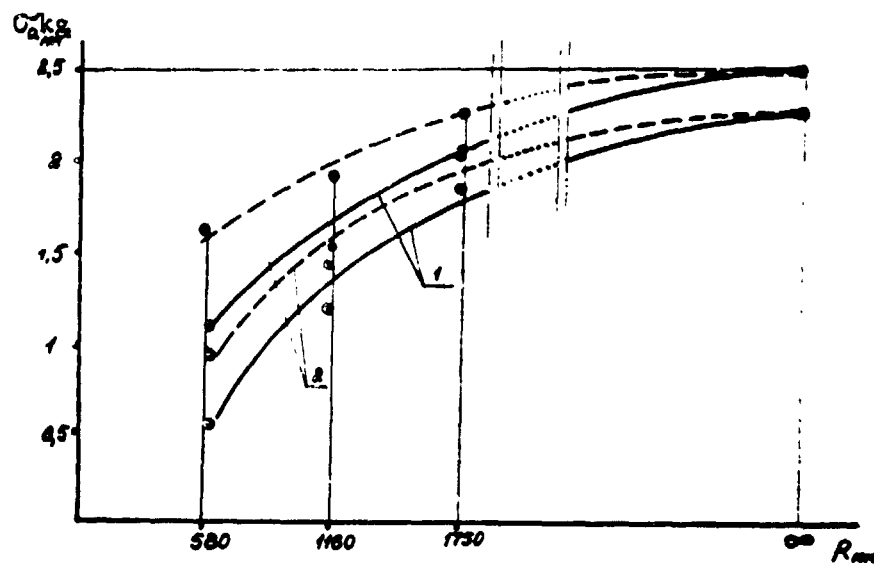
Fig. 2.

In this manner, the panel pliability or a parameter depending on it, for example, the attenuation decrement or the relative deformation of the surfaces of the panel sheets with specific forms of vibration, can be used as diagnostic parameters of the technical condition of the skins of passenger aircraft.

INVESTIGATION OF VIBROSHOCK STABILITY OF A
MECHANICAL CONTACT BY MEASUREMENT OF ITS RESISTANCE

S.G. Butsevichyus and V.-S.S. Zaretskas
(Kaunas)

The results of experimental investigation of the vibration and impact strength of a contact junction, by the method of measurement of the contact resistance, as a function of the contact pressure, condition and cleanliness of surfaces in contact, as well as of the type and intensity of mechanical action, are presented.

Fig. 1. Experimental unit block diagram.

The experimental unit (Fig. 1) permits study of contact junctions of any construction, which can be installed on the board of a vibration or shock test stand. In this case, the investigations were carried out on console-type loop contacts used in television channel pre-selectors (TCP). The TCP housing was fastened to the board of the test stand, whereupon the contact (or group of contacts) being studied is disconnected from the TCP system and connected in parallel to resistor R_2 of the constant voltage E divider R_1/R_2. The resistor ratings were selected according to the formulas

$$R_1 = \frac{E}{I_{max}} \sim 300 \text{ ohm}$$

$$R_2 = \frac{E U_{max}}{I_{max}(E-U_{max})} \sim \frac{U_{max}}{I_{max}} \sim 1 \text{ ohm}$$

where $U_{max} \leq 20$ mV is the voltage on the disconnected contact and $I_{max} \leq 20$ mA is the current passing through the closed contact at $R_c = 0$.

This allowed [1] the dynamic range of change in voltage of the signal presenting information to be narrowed down approximately 100 fold, and the resistance of contact R_c to be measured in the "dry circuit" mode. At the values of R_1 and R_2 indicated above, the unit permits the resistance R_c to be measured in the 0.02- 50 ohm range, during which the error $\leq 15\%$ in the 0.1-10 ohm range.

With observation of the signal on the Cl-15/4 oscilloscope, the time resolving power of the unit $\tau \leq 2 \cdot 10^{-6}$ sec. The static value of the contact resistance R_{cs} was determined with a E6-12 instrument, and it was approximately 10-15 mohm between the contact leads.

Vibration strength was investigated in the 30-3000 Hz range, with a sinusoidal acceleration up to 10 g, during which the VU-5/5000 vibration test stand was powered from generator G3-18, for reduction of distortion. The shape of the shock half-wave curves, of 1.4-3 msec duration and 1-60 g amplitude was selected so that the succeeding half wave of opposite polarity had an amplitude $\leq 25\%$. Damping pads were specially selected for this. Acceleration of the TCP housing was monitored by a set, consisting of piezoelectric sensor KD-12, acceleration meter SDM-132 and oscillograph Cl-29 (or Cl-19). As a result of the investigation, it was found that, in the frequency range studied, at quite high accelerations, some comparatively narrow "dangerous" frequency bands are observed, in which the contact junction loses vibration strength. For each contact, at any "dangerous" frequency, there is a specific critical acceleration value for loss of vibration strength by the contact, which is highly reproducible by multiple measurements (in the case of a smooth increase in acceleration). Upon exceeding this value, the spread of the stochastic change (instability) of R_c increases sharply, during which R_c sometimes "breathes," with a period of 15-30 sec. Therefore, only the maximum $(R_{c\,max})$ and minimum $(R_{c\,min})$ values of R_c are recorded in a time interval of about 30 sec, during measurements. Upon loss of vibration strength, the resistance variation $\dfrac{R_{c\,max}}{R_{c\,min}} \leq 10\text{-}20$, while $\dfrac{R_{c\,min}}{R_{cs}} \leq \leq 10$.

It was found that there is an optimum contact pressure (0.7-1.7 N) for the contact system studied, at which vibration strength over the entire frequency range is greater than 10-100 msec^{-2}. A decrease in pressure to 0.1 N (7-17 fold) leads to a sharp reduction (up to 0.08-2 msec^{-2}) in vibration strength of the contact, while, at the resonance frequency of the pressed-down contact blade $f_p =$ 600-900 Hz, it reaches 500 times (in comparison with the vibration strength at a pressure of 0.7 N). The pressed-down contact junction dynamic response factor has a significant value at low pressures. In the contact investigated, depending on the pressure, it changed over a range of $\lambda_p = 5\text{-}20$ (for a free blade $\lambda_0 = 50\text{-}70$ and $f_0 = = 320\text{-}450$ Hz). Reduction in vibration strength (up to 20 fold) with increase in contact pressure to 2-2.2 N appears in a few very narrow excitation frequency bands.
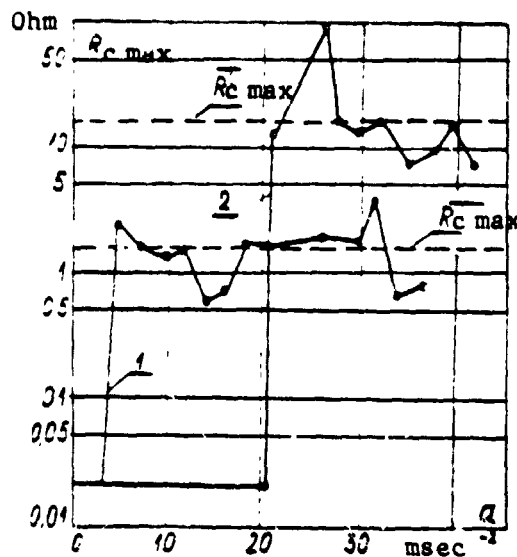
Fig. 2. Maximum value of contact surface resistances $r_{c\ max}$ vs. vibration acceleration a: 1. with unlubricated contact surfaces; 2. with contact surfaces lubricated with 12-153-9 lubricant.

The vibration strength of the contact depends on the condition (cleanliness) of the surfaces in contact, especially with a considerable contact area. With a contact pressure of 0.1 N and lubrication of the contact surface investigated with electrically conducting 12-153-5 lubricant, the "cementing" effect of the contact increased its vibration stability by approximately 300 times at the resonance frequency indicated above. On the average, a lubricant, depending on its type, increases vibration strength of a contact up to 2-5 times.

Investigation of the impact strength of this mechanical contact shows that it always is higher than the vibration strength, if the repetition rate of the impacts is not a multiple of the resonance frequency of the system investigated (Fig. 3), when it is slightly damped. In this case, the direct proportionality between impact strength and contact pressure is maintained well. It was found that use of a lubricant has a /45 favorable effect, principally at pressures of 0.2-0.5 N, with impact strength increasing up to two times, on the average. In the case of use of 12-153-5 lubricant, traces of lubricant (an adhesion film) are completely sufficient to increase the impact strength of the contact investigated; however, certain types of contamination of the surfaces in contact (for example, with 12-131-6 lubricant) can somewhat impair the impact strength of the contact.

In this manner, the method of determination of vibration and impact strength of a mechanical contact, by measurement of the contact resistance, allows the condition (cleanliness) of surfaces in contact to be evaluated and monitored to a certain extent.

Conclusions

1. Vibration strength of a mechanical contact, in a real, slightly damped system, with several natural frequencies, is not in direct proportion to the contact pressure.
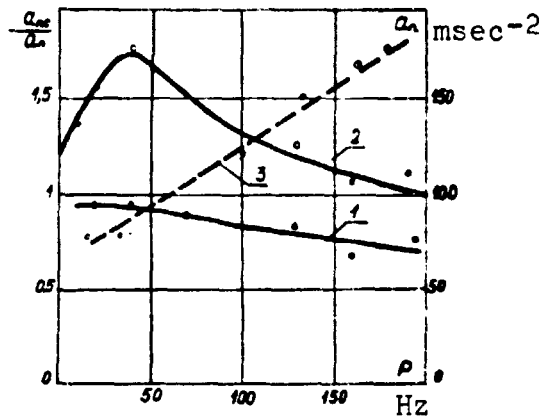
Fig. 3. Impact strength a of a lubricated contact surface vs. pressure P: 1,2. lubricated with 12-131-6 and 12-153-9 lubricant, respectively; 3. absolute impact strength a of unlubricated contact surface.

2. For such systems, there is an optimum contact pressure, within a selected excitation frequency range, in which the "cementing" effect in a contact with contaminated surfaces in contact can be disregarded only at quite high pressures.

3. The method of determination of vibration and impact strength, by measurement of contact resistance, is characterized by simplicity and high sensitivity, and it requires a smooth increase in acceleration.

INVESTIGATION OF VIBRATIONS
IN ELECTRIC POWER TRANSMISSION LINES

I.I. Vitkus, T.P. Matekonis, K.M. Ragul'skis
(Kaunas)

Vibrations of the wires in electric power transmission lines, caused by the wind, lead to fatigue failure of the wires, which brings on great economic losses. In connection with this, extensive research has begun into the dynamic characteristics of wires, including the self-damping properties of wires, and a series of new types of wire-insulator fastenings, with and without dampers, has been developed. The research was carried out under laboratory conditions, on test stands and in a test field, specially constructed for this purpose.
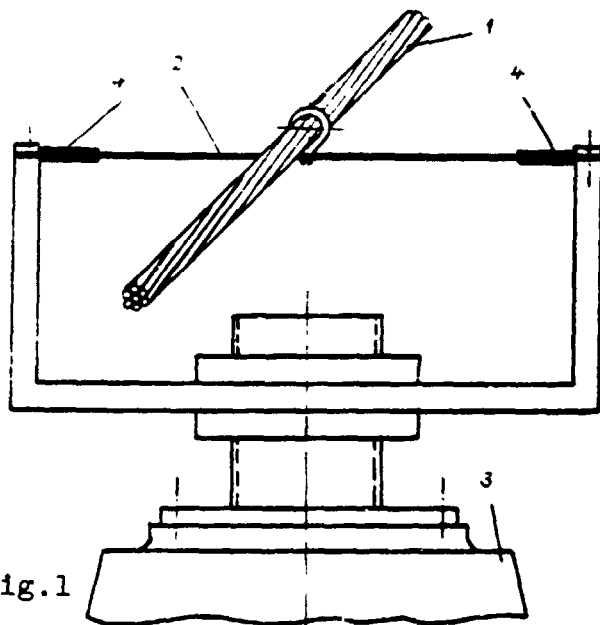
Fig.1

A method for determination of the self-damping properties of aluminum and steel-aluminum wires of electric power transmission lines was put into practice under laboratory conditions. The research was carried out by two parallel methods: the dynamic hysteresis loop method, in the steady vibration mode, and the vibration damping method.

A rigid connection between the stretched wire being studied and the vibrator is not permissible, since the moving mass of the latter becomes part of the system /47 and, thereby, distorts the shape of the sinusoidal standing waves and the resonance frequencies of the wire. For a solution of this problem, a special drive from the vibrator to the wire was developed (Fig. 1). Wire 1 is rigidly connected to flat spring 2, the ends of which are rigidly connected to vibrator 3. Four strain gauge sensors 4 are cemented to the spring. During operation of the unit, the variable force applied to the actuator is proportional to the difference between displacement of the attachment point of the wire and displacement of the vibrator. When the vibrator is shut off, the energy dissipated by the spring is small in comparison with the energy dissipated by the wire, and there is no mutual exchange of energy. Two no-contact, inductive sensors, connected according to a differential system, for measurement of displacement of the wire, are installed next to the point of

attachment of the wire to spring 2. Two more analog sensors were used for transmission of the displacement signal to the El'kar automatic recording instrument.

A signal, proportional to the exciting force, is transmitted to one axis of an oscillograph, and a signal, proportional to displacement of the wire, to the other axis. In order to obtain high accuracy in the measurement of the energy diffused per cycle, the wire is put into one of the resonance modes.

The vibration damping method permits the value of the logarithmic damping coefficient to be obtained immediately, for a wide range of amplitudes.

Overall, the method described permitted two basic self-damping characteristics of the wires to be obtained, i.e., the energy dissipated per cycle and the logarithmic damping coefficient vs. vibration frequency and amplitude, at various tensions of the wires investigated.

LOAD PULSE DISSEMINATION IN NONLINEAR-HEREDITARY MATERIAL

Yu.N. Rabotnov and Yu.V. Suvorova
(Moscow)

A nonlinear-hereditary type equation of state is proposed
for description of the behavior of metals under uniaxial loading,
in particular, those which disclose delayed flow (low carbon steel).
Basically, the model assumes the hypothesis of the existence of
a dynamic diagram, corresponding to an infinitely great deformation
rate. It was shown that the magnitude of the yield point and the
load-elongation curve in the plastic region depend essentially
on processes taking place at a time when the material is still   /48
elastic, and that the effect of the deformation rate in the plastic
region turns out to be not so significant as usually is thought.

The problem of load pulse propagation in a semi-infinite rod,
of material with a nonlinear-hereditary equation of state, was
examined. The Laplace transform   was used in integration of
the equation of motion. The solution was obtained in the form of
asymptotic   expansions   around the wave front.

A general picture of propagation of elastic-plastic waves in
materials with selected equations of state was presented.

ANALYTIC DESCRIPTION OF VIBRATIONS IN A PIPING SYSTEM WITH PULSATING FLOW

G.P. Bosnyatskiy, R.I. Grossman, A.A. Kozobkov, and A.I. Koppel'
(Moscow)

The problem of describing vibrations of complex piping systems includes a description of vibrations of piping under the influence of a pulsating flow of liquid or gas in them, with consideration of the effect of the method of fastening the piping system.

The equations describing the dynamics of liquids and gases in pipelines, as well as equations describing the vibrations of pipelines with uniform boundary conditions, have been studied sufficiently well. Questions connected with the effect of flows in a pipeline system have been examined less. The methods of accounting for the effect of pipeline supports on their vibrations and, in particular, of accounting for friction in the supports, are still more vague.

During movement of a pulsating flow of a gas (liquid) through a pipeline with irregularities, the energy of the flow changes to mechanical vibration energy in the latter. An estimation of the forces generated in this case is necessary for a description of the behavior of a vibrating pipeline system.

Classical conceptions of the effect of steady state flow in a pipeline element (for example, at the outlet) cannot automatically be transferred to pulsating flows. Since the lengths of the waves generated by a compressor may prove to be comparable to the lengths of pipeline elements, the magnitudes of the forces acting on these elements can be considerably different from the magnitudes calcula- /49 ted from the equations for steady state flow. The forces generated in the irregularities are calculated with the aid of an equation for the pulse energy balance.

Various calculation schemes have been proposed, depending on the type of irregularity: concentrated ones, extended ones and complex ones. The choice of a calculation scheme depends on comparability of the extent of the irregularities with the pressure wavelengths and velocity in the flow. The limits of applicability of the formulas derived have been obtained.

Relations have been found which permit a description of the interaction of a pulsating flow with any irregularity in the system and then solution of problems on the resulting forces in complex systems.

For complex systems with varying temperatures ~~along the length~~ and some irregularities, relations have been obtained, which reflect the varying phase displacement of the forces in these irregularities.

No less important than determination of the forces acting on a pipeline system with a pulsating flow is determination of the reactions of the supports. Accounting for friction in the supports presents special complexities. The effect of the frictional torque on pipeline supports, in the presence of flexural and torsional vibrations was investigated, on the assumption that the frictional torque depends linearly on the angular velocity.

A relation was obtained between the impedances in the pipeline supports, from which frequency equations can be obtained for different cases of limiting condition recordings, corresponding to different cases of pipeline fastenings. This relation can be used when the impedances of the support are obtained by measurement. In this case, the frequency equation gives a frequency value which is closest to the actual one.

The frequency equations were investigated, with account taken of the frictional torque in the supports, which are linearly dependent on velocity. It was shown that, if the friction is considered in one of the pipeline supports, the frequency equation is split into two, corresponding to the limiting cases, i.e., possible vibrations of the pipeline with two different frequency groups, in which the transition from one group to another takes place by jumps.

It was shown that, under such conditions, the frictional torque in the supports can be considered proportional to the first power of the angular velocity. This concerns flexural vibrations of shafts, as well as vibrations of pipelines taking place in two mutually perpendicular planes, under conditions when a specific ratio between the velocity components at points on the pipeline are satisfied in cross sections drawn through the support.

The effect of damping pads in pipeline supports on its vibra- /50
tions was investigated.

The possibility in principle was shown of substituting the distributed friction and analytical relations obtained between the coefficients of concentrated and distributed friction for friction concentrated in the supports. The former can be used in electrical modeling of pipelines.

52

THE USE OF A DIGITAL COMPUTER FOR CALCULATION OF ACOUSTIC FIELDS OF COMPLEX VIBRATING STRUCTURES BY THE RECIPROCITY PRINCIPLE

A.V. Rimskiy-Korsakov, Yu.I. Belousov
(Moscow)

A program was compiled for calculation of acoustical pressure levels, which might be created by vibrations of complex structures (an assembly of shells and rods), under the influence of a given force, for cases when these fields cannot be measured directly. The acoustical field is determined according to transition frequency and pulse characteristics of the structure in the projection mode. The projection characteristics are equal to the reception characteristics, for vibrating systems in which the recipricity principle holds true [1, 2]. The characteristics in the receiving mode are calculated on the basis of experimental data on a point pulse space velocity source (input signal) and vibration response of the structure $a_n(t)$ (output signal). The space velocity of a pulse source, set at a point in space r, where it is necessary to calculate the sound field of the structure $p(r,t)$, is determined by measurements of acoustic pressure p_R, created by a point source at a distance R. The vibration response is measured at the point where the forces F and f exciting the system should act. The acoustic pressure created by the structure is calculated by the formulas:

-- spectral presentation

$$p(r,\omega) = \frac{\rho}{4\pi R} \frac{a_n^{(1)}(r,\omega)}{p_R(\omega)} F^{(2)}(\omega). \tag{1}$$

-- for determinative relationships to time t

$$p(r,t) = \frac{\rho}{4\pi R} \int\limits_{t'}^{t'} \int\limits_{t''}^{t''} a_n(t-\tau_1) \frac{1}{2\pi} \int\limits_{-\infty}^{\infty} \frac{e^{j\omega\tau_1}}{p_R(\omega)} \, d\omega \, d\tau_1 f(t-\tau_2) \, d\tau_2. \tag{2}$$

where ρ is the density of the medium and ω is the cyclic frequency.

A program was compiled in Algol language, intended for calculation by a BESM-6 computer. Basically, the program set a procedure for rapid Fourier transform [3], permitting the forward and reverse transforms to be calculated. There is a procedure in the program for calculation of the Fourier coefficients, power spectra and amplitude and phase spectra of processes. A procedure for averaging spectra in constant bands is used for smoothing the spectra by frequencies and for decreasing dispersion. The signals in fixed relative-constant frequency bands are filtered by a procedure for

synthesis of z, the parameters of a recursive digital filter [4].
A procedure for statistical processing of input signals permits
the mean signal amplitude values, as well as the mean and root
mean deviations from these values, to be calculated.

The program can operate in two modes: generation of a diagram
of the sound projection directions in relative-constant frequency
bands and determination of the time dependence of the amplitude of
an acoustic projection pressure field of a vibrating structure.
In the first mode of operation, the input signals are subjected to
statistical processing, as a result of which an averaged time area
of the input signal is generated. After calculation of the spectral
characteristics of the input and output signals and exciting forces,
in relative-constant bands, by formula (1), the acoustic pressure
spectrum at a given point in space is determined. Such calculations
are carried out for all assigned points in space, and the areas of
acoustic pressure values are then formulated in fixed frequency
bands, but for different points in space. If the acoustic
pressures are determined at a uniform distance from the structure,
but at different angles to it, the areas generated, developed in
the form of a graph, are the directional diagrams sought. In the
second mode of operation, the transitional pulse characteristics
of the projection of the system (internal integral by $d\tau_1$ in
formula (2)) are calculated initially. Then, the sound pressure,
as the integral of the spectra of the exciting forces and the transi-
tion characteristics, are determined by formula (2). As an illus-
tration of the program operation, a sound field of a cylindrical
shell, stimulated by point forces, was determined. A starting
pistol, creating a sound pulse over the spectrum (Fig. 1), was   /53
used as a pulse source. The spectrum, in 1/3 octave bands of
the vibration pulse, is shown in Fig. 2.

The calculated d.rec-
tional diagrams (Fig. 3)
coincide with the direct
measurements, with an error
not exceeding ±2 dB.

f — Hertz
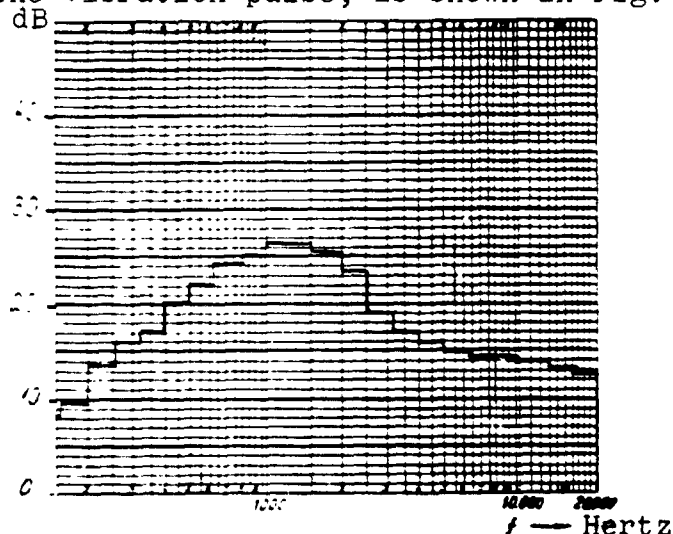
Fig. 1. Spectrum of a starting
pistol sound pulse (0 dB cor-
responds to 10 μVAh).

54
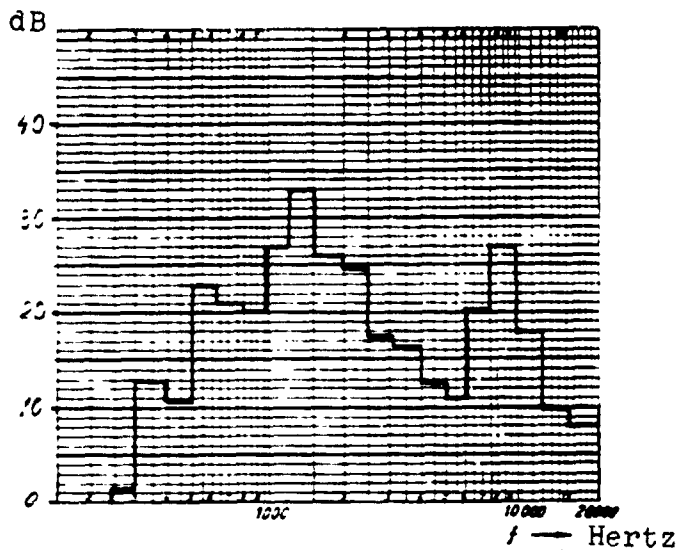
Fig. 2. Spectrogram of vibration
pulse of a shell, at a sound wave
angle of incidence of 10° (0 dB
corresponds to 0.03 d).
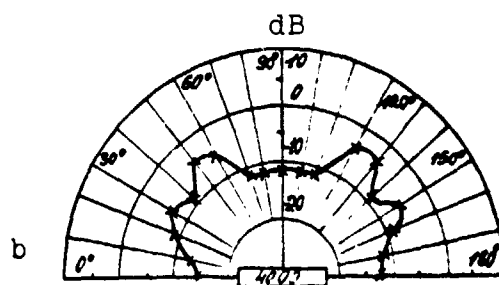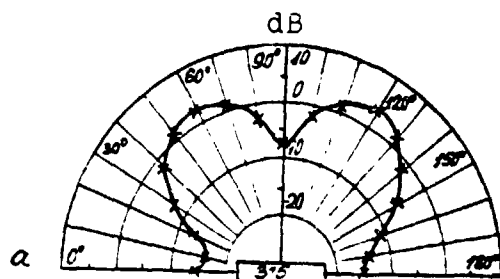
Fig. 3. Diagram of sound projection
directions of a shell, in 1/3 octave
bands, with mean frequencies: a. 315 Hz;
b. 4000 Hz (0 dB corresponds to 0.18
μVAh).

REFERENCES

1. Lyamshev, L.M., "The Problem of the Reciprocity Principle in Acoustics," DAN SSSR 125 (1959).

2. Belousov, Yu.I. and A.V. Rimskiy-Korsakov, "The Reciprocity Principle in Acoustics for Nonequilibrium Processes," Akusticheskiy zhurnal 17, 1 (1971).

3. Kur'yanov, B.F. and L.Ye.Medvedeva, Garmonicheskiy analiz statsionarnykh sluchaynykh protsessov [Harmonic Analysis of Random Steady State Processes], Issue 8, Moscow State University Press, 1970.

4. Lozovskiy, V.S., "Programs for Spectral Analysis in Frequency and Time Fields," in the collection Vychislitel'nyye sistemy [Computer Systems], Issue 45, Novosibirsk, 1971.

STATISTICAL PARAMETERS OF REVERBERATING FIELDS, CALCULATED BY COMPUTER

I.V. Lebedeva and L.G. Rubanova
(Moscow)

The development of a statistical theory of sound fields in closed spaces [1, 2, 3] has permitted development of a method for measurements in reverberation chambers, in the steady state mode.

The spatial distribution patterns of the square of the sound pressure vs. type of exciting signal were produced theoretically. Thus, in excitation of a field in the chamber by a pure tone, the density probability function of the square of the sound pressure $p^2(\omega)$, normalized to the mean value $<p^2(\omega)>$, is exponential:

$P(x) = e^{-x}$, where $x = p^2(\omega)/<p^2(\omega)>$. This means that the appearance of small values of x is more likely than large values. The standardized dispersion in this case equals unity.

The normal is gradually approached by averaging the squares of the pressure by frequency or by spatial distribution. In general form, the distribution pattern is described by the γ distribution:

Here, the parameter M is the product of the numbers of statistically independent frequencies and statistically independent points over which the averaging takes place. The standardized dispersion of this frequency ν^2 is inversely proportional to M: $\nu^2 = 1/M$.

An equivalent value of M is introduced for the white noise band, showing how much the statistically independent components contribute to a given band: $M \sim 1 + BT_0/6,9$, where B is the filter pass bandwidth and T_0 is the reverberation time in the chamber at the average frequency of the band.

The theoretical relations were checked experimentally in the Moscow State University Reverberation Chamber [4], with a volume of 217 m^3, and with good acoustical quality, and the measurements were continued in other reverberation chambers in Moscow.

The data obtained in the Moscow State University chamber and in the chamber of the All-Union State Planning Institute for the Planning of Aircraft Industry Scientific Research Institutes, with a volume of 118 m^3 and with worse acoustical properties, are compared. The results of measurements of the spatial irregularities

of the field with pure tones and with noise bands in the 200-
2000 Hz frequency range were used for calculation of the statis-
tical parameters of the reverberation fields by computer.

Values selected from 100 statistically independent values
of the sound pressure level, measured in the space of the rever-
beration chamber and recorded on automatic recorder tape (in dB),
were processed by the small Mir digital computer. The calcula-
tion program included determination of the density probability
function, integral distribution pattern, mathematical expectation
and normalized dispersion of the mean square of the pressure.

The values of the experimentally normalized dispersion by
pure tones and at different frequencies are shown for both chambers
in Fig. 1. The excess of the experimental values of ν^2 over the
theoretical values, equal to one, is an indication of inadequate dif-
fusivity   of the field at low frequencies (200 Hz). This
divergence is especially noticeable in the comparatively small
volume of the All-Union State Planning Institute for the Planning
of Aircraft Industry Scientific Research Institutes chamber.
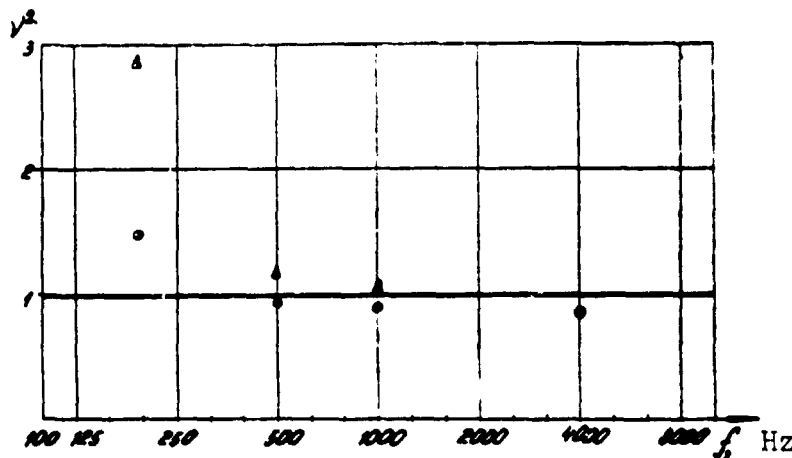
Fig. 1. Normalized dispersion values,
measured with pure tones, vs. frequency:
• Moscow State University chamber
Δ All-Union State Planning Institute
   for the Planning of Aircraft Indus-
   try Scientific Research Institutes
   chamber

Experimental values
of ν^2, obtained during
excitation of the field
by 3% noise bands (Moscow
State University) and 1/3
octave noise bands (All-
Union State Planning
Institute for the Plan-
ning of Aircraft Industry
Scientific Research Insti-
tutes) are shown in Fig.
2. They all are located
above the theoretical
curve, calculated with
certain simplifying
assumptions. However,
the experimental values
of ν^2, obtained in both
chambers, with identical
values of the parameter
M, but at different excit-
ing frequencies, proved
to be close together.
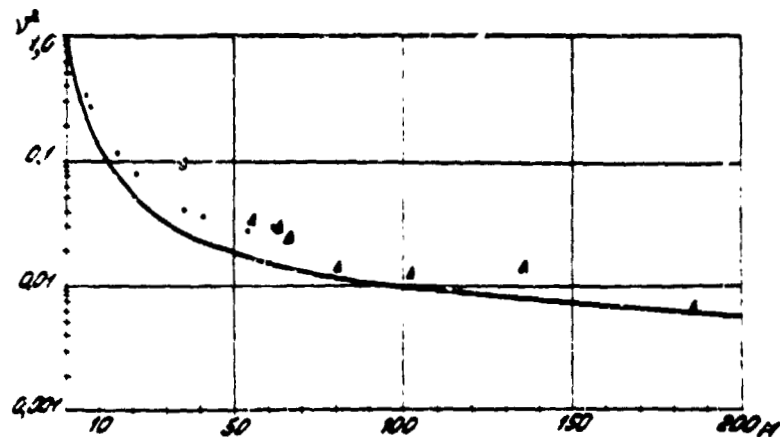
Fig. 2. Normalized dispersion values,
measured with white noise bands, vs.
parameter M:

• 3% bands, Moscow State University chamber;
△ 1/3 octave bands, All-Union State Planning
   Institute for the Planning of Aircraft
   Industry Scientific Research Institutes chamber;
—— Theory

REFERENCES

1. Schroeder, M.R., "Effect of Frequency and Space Averaging on the Transmission Responses of Multimode Media," <u>JASA</u> <u>46</u>(2) 277-283 (1969).

2. Baron, S.B. and A.A. Yanpol'skiy, "Analysis of the Frequency Characteristics of Acoustic   Pressure in a Closed Space," <u>Akusticheskiy zhurnal</u> <u>XVI</u>(2) (1970).

3. Zubman, D., "Spatial Averaging in Sound Power Measurements," <u>J. Sound and Vibr</u>. <u>66</u>(1), 43-58 (1971).

4. Lebedeva, I.V. and A.A. Shkol'nikova, "Investigation of a Reverberation Field in the Steady State Mode," <u>Vestnik MGU, Fizika Astronomiya</u> <u>6</u> (1971).

EXPERIMENTAL ESTIMATION OF THE STATISTICAL PARAMETERS /57
OF VIBRATIONS OF A SHELL
(USING A DIGITAL COMPUTER) I.

B.A. Kanayev, G.S. Lyubashevskiy, and B. D. Tartakovskiy
(Moscow)

The distribution pattern of the amplitudes of vibrations,
measured at various points on the surface of a shell, stimulated
by a point source of harmonic force in the sound frequency range
is being studied experimentally. This pattern permits a valid
spacing estimate to be carried out of the average structural char-
acteristics of the vibrations, which are used for both estimation
of the vibration excitability of the structure and for estimation
of the effectiveness of use of a vibration-absorbing covering.
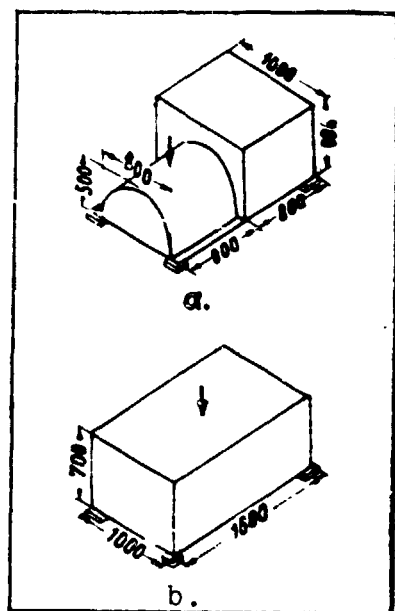
Fig. 1.

Steel shells (8 mm thick)
were used for the research, in
two configurations: combined
(Fig. 1a) and rectangular (Fig.
1b). For an estimate of the
effect of internal losses on the
nature of the amplitude distribu-
tion, vibration damping shells,
with a high loss coefficient,
also were investigated. The
amplitudes of the vibration rates
at points, uniformly distributed
over the surface of the shell,
were measured with an automatic
unit [1], which records the results /58
of the measurements on punched tape,
which is fed directly to a digital
computer. The empirical density
probability function was calculated
by the digital computer, from the
totality of the normalized ampli-
tudes $x_i = A_i/\overline{A}$, where

$$\overline{A} = \frac{1}{n} \sum A_i$$

is the mean of the vibration amplitude at n points, for each excit-
ing frequency.

For the rectangular shells, 150, 280 a. 350 points were
chosen at all exciting fre   encies (the mean distance between
neighboring points was   15 .; 9.7 and 8.6 cm, respectively). Histo-
grams of the normalized amplitude x_i distribution, corresponding to
different values of n, are represented in Figs. 2 and 3. Normalized
amplitude is plotted on the abscissa and the probability density on

the ordinate. Since, during change in volume of the sample, the
shape of the histogram is essentially unchanged, the distribution
found is characteristic of a given shell and exciting frequency.
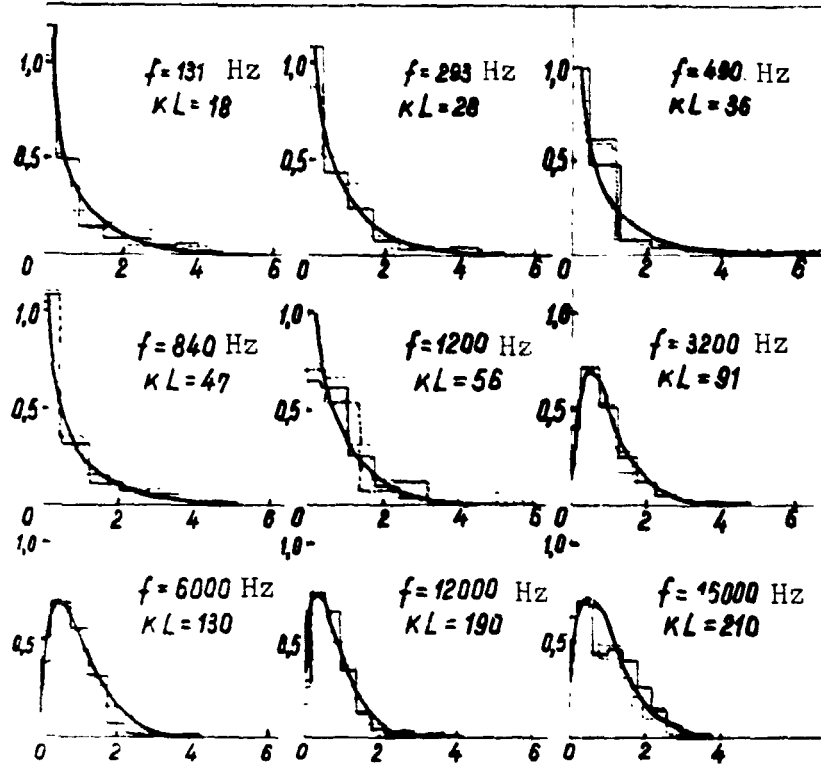
Fig. 2.

The gamma distribution function was selected as approximating <u>/59</u>
the analytical curve:

$$G(x\, p.\, x) = \frac{x^p}{\Gamma_{(p)}}\ x^{p-1} e^{-xx},$$

where x > 0, α > 0, p > 0 and Γ(p) is the gamma function of p [2].
The shape of the distribution curve G(x/p, α) is determined by
the parameter p; the parameter α is a scale factor. At p = 1, the
gamma distribution changes to exponential; at p >> 1, the distribu-
tion is close to normal. The mathematical expectation of the
random value ξ, subordinated to the gamma distribution, is deter-
mined by the ratio E(ξ) = p/α, and the dispersion is D = p/α².
Consequently,

$$\hat{p} = \bar{x}^2 s^2 \text{ and } \hat{\alpha} = \bar{x}/s^2,$$

62
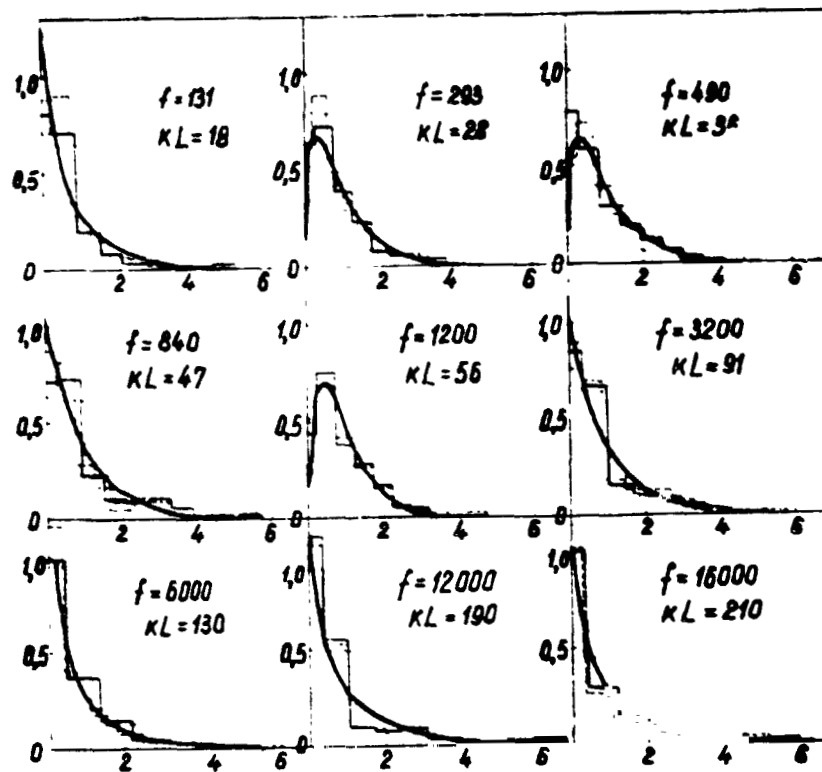
Fig. 3.

are estimates of the parameters **p** and α, where $\bar{x}$ and S^2 are estimates of the mathematical expectation and the dispersion.

The smooth curves (Figs. 2 and 3) correspond to the distribu- <u>/60</u> tion $G(x/\hat{\beta},\hat{\alpha})$, where $\hat{\beta}$ and $\hat{\alpha}$ are calculated by the method indicated above for n = 350. The empirical distribution is approximated well by the corresponding gamma distribution, for both uniform and for damped shells, at all exciting frequencies.

For an estimate of the effect of the structure shape on the nature of the distribution, similar measurements were carried out on uniform and damped shells of the combined type (Fig. 1a) <u>/61</u> (n = 280, 1 = 12.4 ᴄᴍ). The smooth curves on the histograms (Figs. 4 and 5) correspond to the distribution $G(x/\hat{\beta}, \hat{\alpha})$. In this case, the approximation of the histogram to the gamma distribution permits a better approximation to be produced.

In this manner, independently of the type of shell and internal losses, the empirical distribution has a stable shape and satisfactorily approximates the gamma distribution over the entire frequency range investigated. This permits the distribution $G(x/p, \alpha)$ to be used for estimation of the characteristics of the vibration fields of shells. We note that the wave dimensions of the shell kL = 16-210 (k is the wave number of the flexural
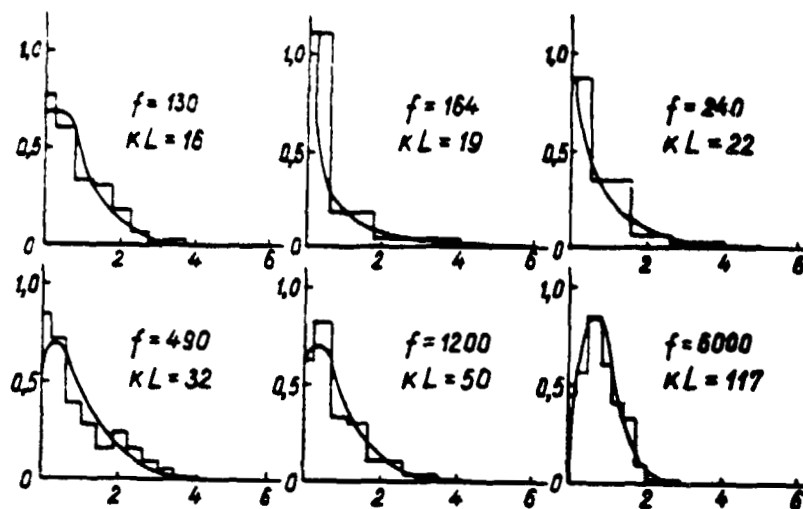
Fig. 4.
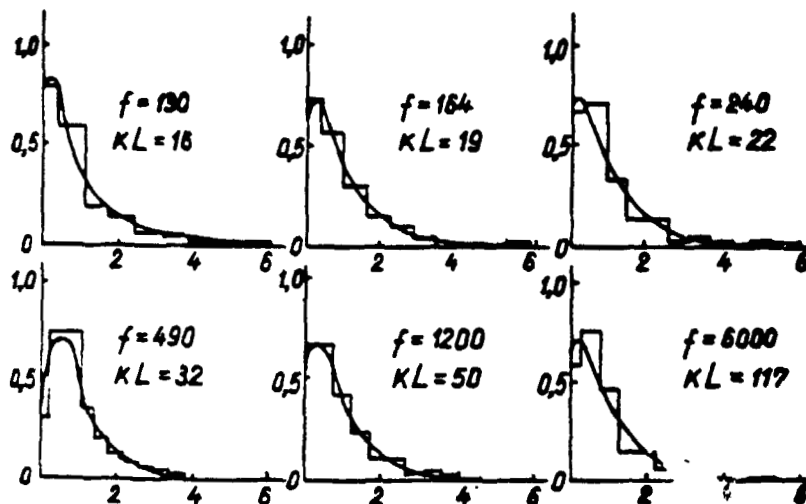
Fig. 5.

vibrations and $L = \sqrt{S}$, S = the shell surface area) correspond to the frequency range investigated.

The results obtained can be used for calculation of confidence estimates of the mean vibration amplitude structure. If the sample vibration amplitude values x_i are independent random values, distributed according to the pattern $G(x/p,\alpha)$, in accordance with the properties of the gamma distribution, $\bar{x}$ is distributed according to the pattern $G(x/p_1, \alpha_1)$ where $p_1 = np$ and $\alpha_1 = n\alpha$. By

64

substituting their estimates for the parameters p and α, we find
an approximate distribution pattern of the mean $G(x/\hat{p}_1, \hat{\alpha}_1)$.
Correspondingly, we find the limits of the confidence interval x_1
and x_2, for a given confidence coefficient ε, from the relation-
ships

$$\frac{\varepsilon}{2} = \int_0^{x_1} G(x/\hat{p}_1, \hat{\alpha}_1)\,dx = I(\hat{u}_1, \hat{p}_1);$$

$$1 - \frac{\varepsilon}{2} = \int_0^{x_1} G(x/\hat{p}_1, \hat{\alpha}_1)\,dx = I(\hat{u}_2, \hat{p}_1). \tag{1}$$

where $I(u, p) = \dfrac{1}{\Gamma(p)} \int_0^u x^{p-1}e^{-x}dx$ is the incomplete gamma function

[3], $\hat{u}_1 = \hat{\alpha}_1 x_1$ and $\hat{u}_2 = \hat{\alpha}_1 x_2$.

It is known that, under the conditional terms superimposed on
the distribution function by the random value ξ, the distribution
of the sample mean of this value is asymptotically normal [4]. If
ξ_i is distributed according to the pattern $G(x/p,\alpha)$, it can be
shown that the difference between the distribution functions F(x)
of the normalized sum

$$\xi = \frac{\alpha}{np} \sum_{i=1}^{n} \xi_i - 1\sqrt{np}$$

and the normal distribution pattern $\Phi(x)$ has an order of tendency /62
toward zero, equal to $(np)^{-(1/2)}$, with increase in n [3]. Conse-
quently, at large n the normal pattern $N(\bar{x}, (s/\sqrt{n}))$ can be used
for plotting the confidence intervals for the mean $\bar{x}$.

The relationship of the relative width of the confidence
interval $(x_2 - x_1)/\bar{x}$ to the confidence level $1 - \varepsilon$ is shown
in Fig. 6 as an example, for a uniform rectangular shell (f = 840 Hz).
The relationships obtained from relation (1) are shown by solid
lines, for sample values $\hat{\alpha}$ = 0.62 and $\hat{p}$ = 0.62 and various values
of n. The dashed curves correspond to the normal distribution,
with parameters $\bar{x}$ = 1.0 and S = 1.27, obtained experimentally under
the same conditions. It is clear that, for n < 40, with equal
confidence levels, the interval calculated from the gamma
distribution is smaller than the corresponding values obtained
for normal distribution. This discrepancy is decreased with
increase in n. For n > 40, the curves practically coincide. There-
fore, at np > 30, the confidence interval for the mean vibration
amplitude can be determined on the basis of normal distribution, /63
with an adequate approximation for practical purposes. However,
t np < 30, the gamma distribution, corresponding to the experi-
mental data obtained, should be used.
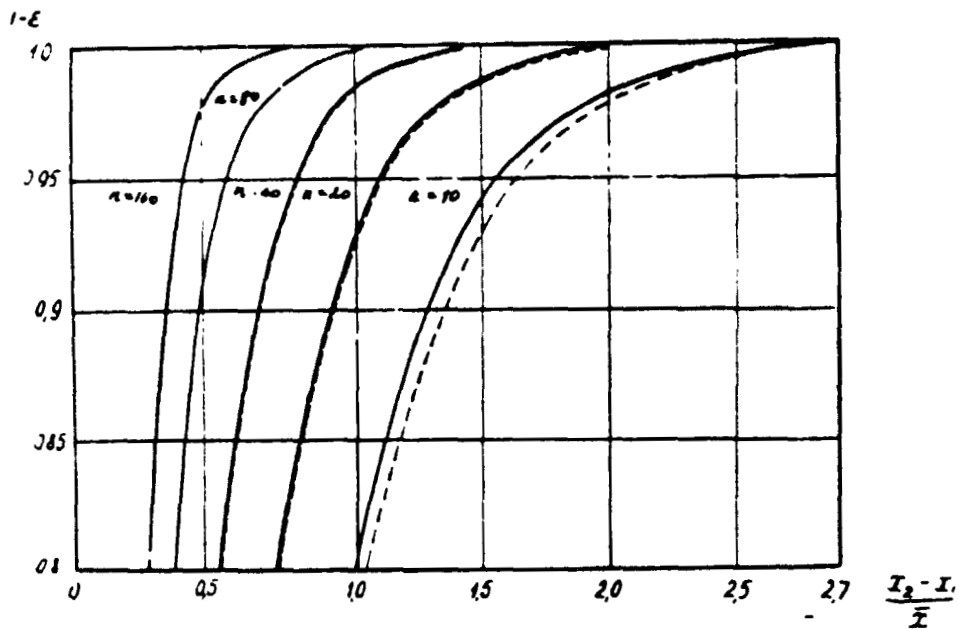
Fig. 6.

It can be assumed that such an amplitude distribution will
be observed for structures and shells which are different from
those investigated. However, further research is necessary for
estimation of the limits of applicability of the distribution
pattern found.

REFERENCES

1. Lyubashevskiy, G.S.,B.D. Tartakovskiy, and V.E. Frishberg, "Multichannel Method of Investigation of Distributed Vibratory Structures," in the collection Vibratsii i shumy (Fizicheskiye issledovaniya)[Vibration and Noise (Physical Studies)], USSR Academy of Sciences, Nauka Press, Moscow, 1969.

2. Rao, S. Lineynyye statisticheskiye metody i ikh primeneniya [Linear Statistical Methods and Their Use], Nauka Press, Moscow, 1968.

3. Pagurova, V.I., Tablitsy nepolnoy gamma-funktsii [Incomplete Gamma Function Tables],USSR All-Union Central Academy of Sciences Computation Center, Moscow, 1963.

4. Gnedenko, B.V. and A.N. Kolmogorov, Predel'nyye raspredeleniya dlya summ nezavisimykh sluchaynykh velichin [Limiting Distributions for Sums of Independent Random Values], State Publishing House for Technical and Theoretical Literature, 1949.

EXPERIMENTAL ESTIMATION OF THE STATISTICAL PARAMETERS
OF VIBRATIONS OF A SHELL
(USING A DIGITAL COMPUTER) II.

B.A. Kanayev, G.S. Lyubashevskiy, and B.D. Tartakovskiy
(Moscow)

In a number of cases, there is interest in obtaining statistical characteristics, not only of vibration amplitude modules [1], but of vibration phases. The statistical characteristics of complex vibration amplitudes of the same shells were examined, excited (as in work [1]) by harmonic force sources in the sound frequency range. The vibrations were measured with a multichannel unit, permitting the component values of a complex vibration amplitude, designated hereafter a_1 and b_1 respectively, for the i-th measurement point, to be obtained at each measured point. The amplitude and phase modules, respectively equal

$$A_i = |\sqrt{a_i^2 + b_i^2}| \quad \text{and} \quad \phi_1 = \arctan \frac{b_1}{a_1}$$

The most complete picture of a vibration field, with this type of multiple-point spatial measurements, permits presentation of the results in three-dimensional space, along the axes of which the amplitude module A_1, phase module ϕ_1 and coordinates of the measurement point relative to the exciting point r_1, respectively, are to be plotted. However, such a presentation of the results /64 is difficult to accomplish graphically. Therefore, the plotting of unidimensional distributions, the totality of which permits conclusions to be drawn as to the nature of the field, is advisable.

Unidimensional distributions of the vibration amplitude modules for various shells and exciting frequencies were examined in work [1]. Vibration phase distribution histograms of rectangular shells, for various exciting frequencies, with a sample volume n = = 350, are shown for a uniform shell in Fig. 1 and for a damped shell in Fig. 2. With increase in exciting frequency, the phase distribution, having two maxima at low frequencies, separated from one another by π, gradually tends towards a uniform distribution. For damped shells, the maxima in the low frequency range are less marked than for a uniform shell. The maximums separated by π correspond to standing waves. A decrease in the values of the /65 maxima is evidence of either an increase in diffuseness of the vibration field or of an increase in the fraction of direct waves in the total field. There can be a uniform phase distribution in both a diffuse field and in traveling waves. For determination of this, for example, the nature of change in the amplitude module as a function of distance to the source can be analyzed (Figs. 3
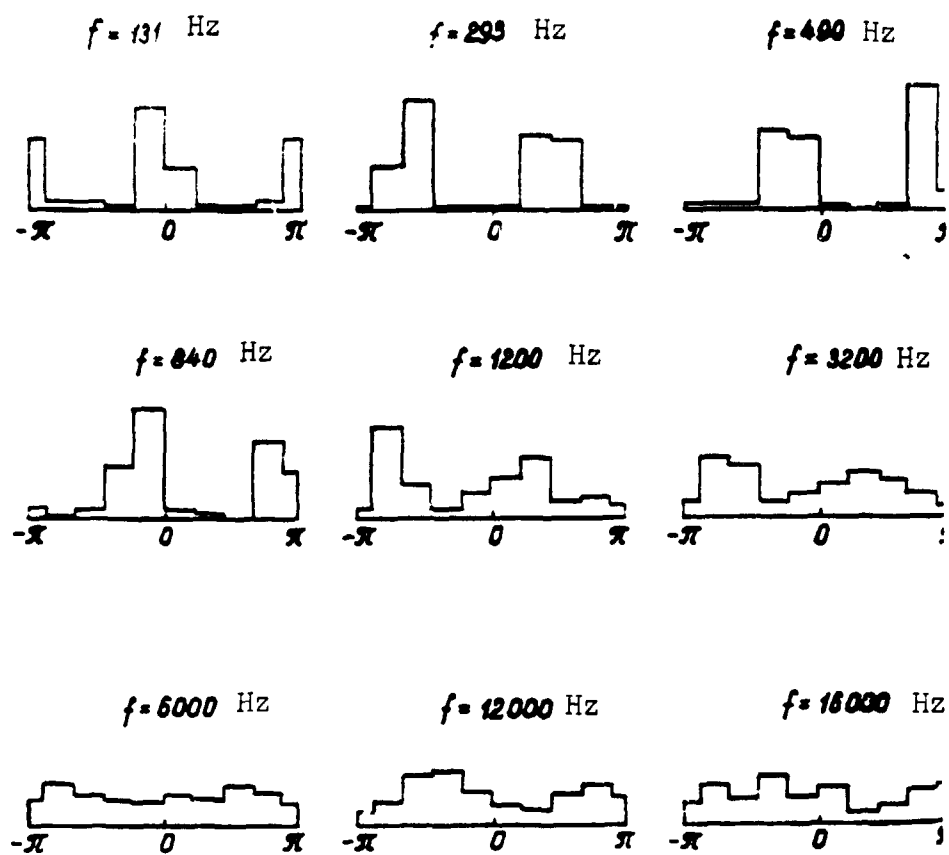
Fig. 1.
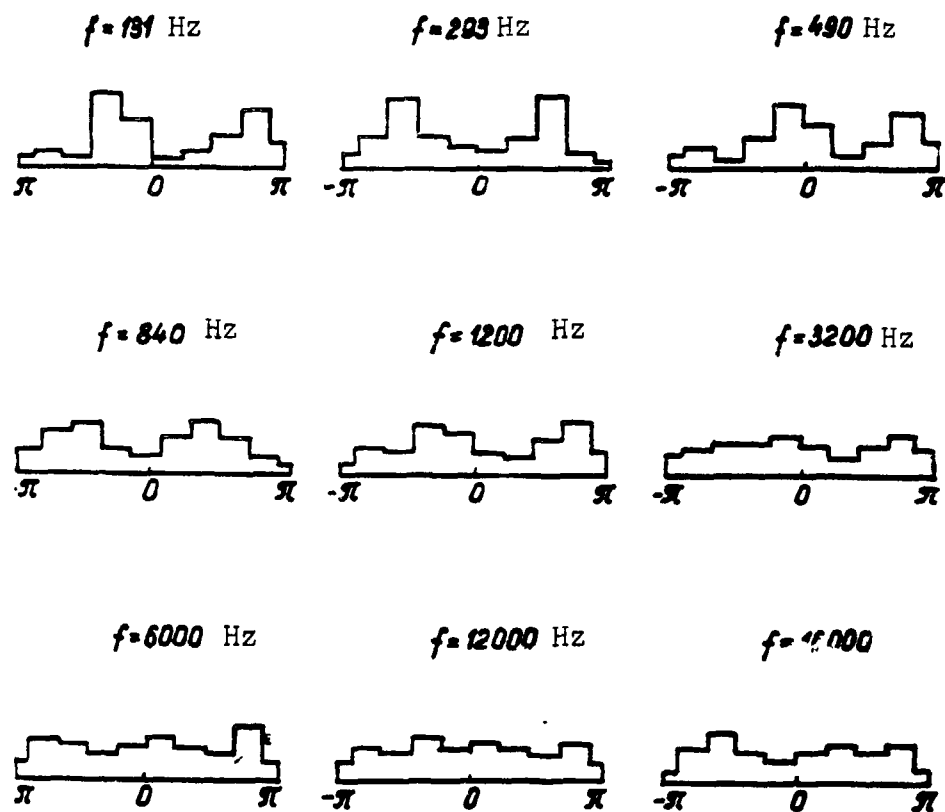
Fig. 2.

and 4). The mean amplitude A over a certain interval (r, r + Δr) vs. distance to the source r is designated in the figures by dashed curves. The solid curve corresponds to the calculated amplitude of a cylindrical wave

$$A = \frac{A_0 \, l^{-\gamma s}}{\sqrt{r}} \, .$$

where γ is an experimentally determined spatial attenuation coef- /66 ficient. The measured amplitude module, on the average, does not depend on distance, for a uniform shell, while the amplitude module is decreased with distance as well, for a damped shell, as in a traveling cylindrical wave with losses. Consequently, for a uni- /67 form shell, the uniformity of phase distribution and independence of the vibration energy from the distance to the source together are evidence of diffuseness of the field; for a damped shell, uniform phase distribution and decrease in energy as a function of distance are evidence of the presence of traveling waves.
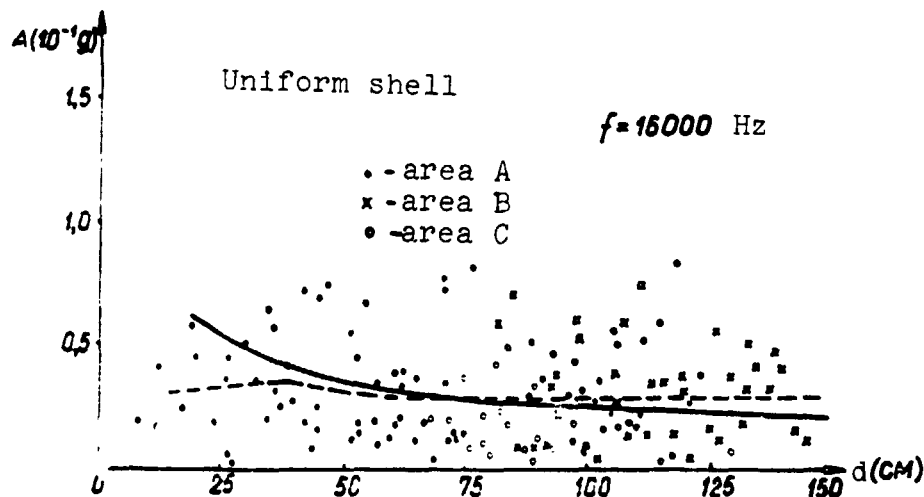
Fig. 3.

It is known that the complex amplitude components a and b are independent in a diffuse field and are distributed according to the normal law N(0,σ). In this case, the amplitude module is distributed according to the Rayleigh law [2]:

$$p(x) = \frac{x}{\sigma^2} \, e^{-\frac{x^2}{2\sigma^2}} \, .$$

70
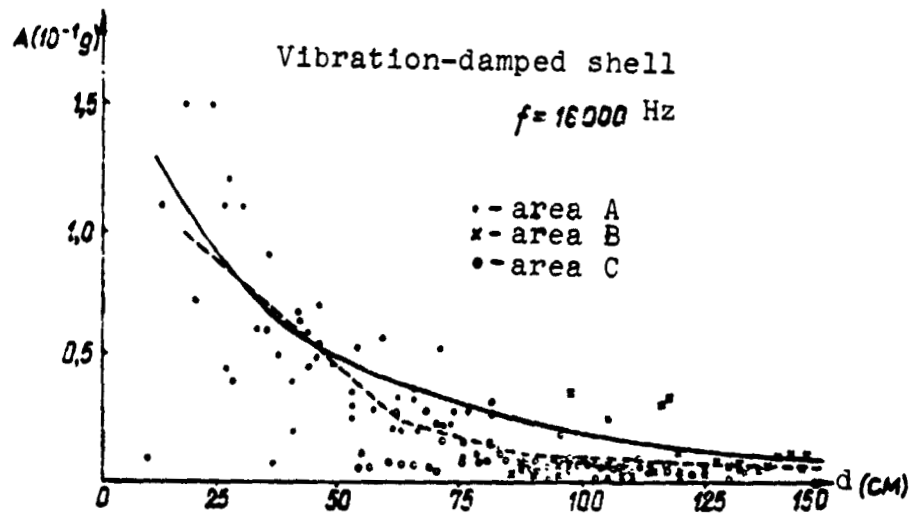
Fig. 4.

and the phase module is distributed uniformly. Therefore, the
diffuseness of the field can be judged, not only from the module
and phase distribution, but by the characteristics a and b.
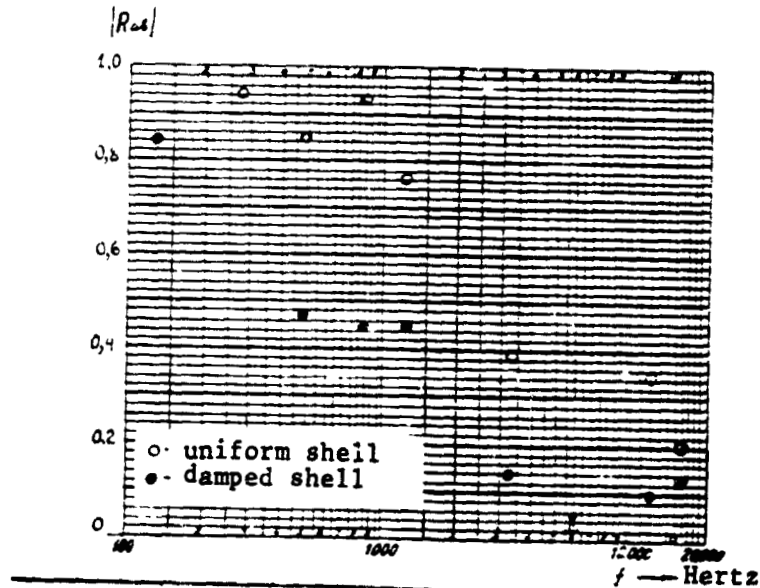
Fig. 5.

The degree of the statistical relation between the values a and b can be estimated from the magnitude of the correlation coefficient module

$$R_{ab} = \frac{m_{ab}}{S_a \cdot S_b} .$$

where m_{ab} is the empirical covariance and S_a^2 and S_b^2 are the empirical dispersions of the values a and b, respectively. The values of the correlation coefficient module are presented in Fig. 5, for rectangular (uniform and damped) shells. A standing wave predominates at low frequencies; therefore, $|R_{ab}| \simeq 1$. With increase in frequency, the correlation coefficient module decreases, approaching zero, which is evidence of the predominance of a diffuse vibration field.
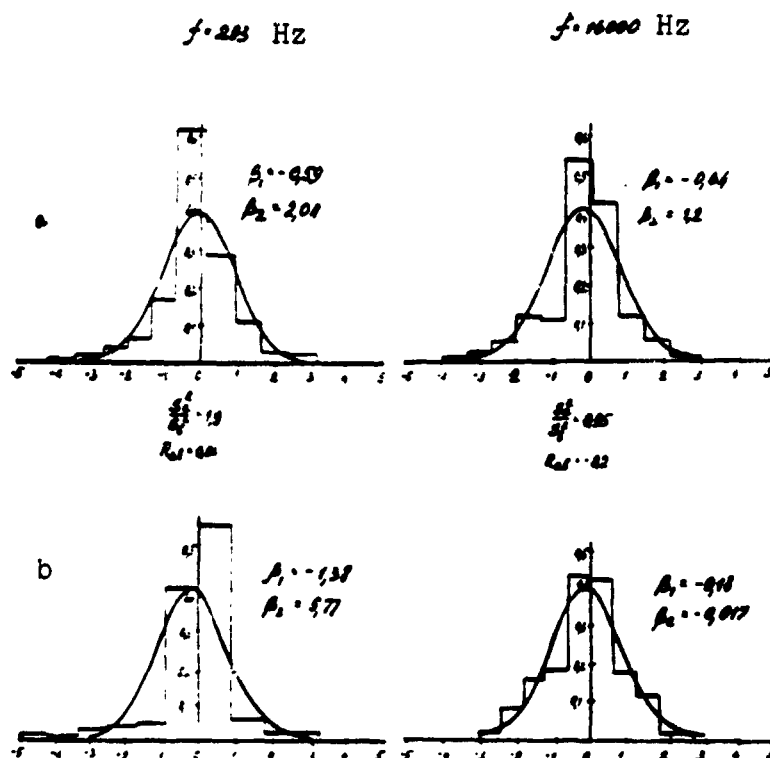
Fig. 6.

The distribution of the values of a_1 and b_1, normalized to a single dispersion, for a uniform shell, at n = 350 and exciting frequencies of 293 and 16,000 Hz, are presented in Fig. 6, as an example of component a and b distribution. The smooth curves

72

correspond to the normal distribution $N(0,1)$; the coefficients of asymmetry β_1 and excess β_2 and the ratio of the sample dispersion values S_a^2/S_b^2 also are indicated. In accordance with what has been said above, the distribution of the values of a and b at a frequency of 16,000 Hz are close to the normal distribution, with zero mean and equal dispersions, which, together with small values of $|R_{ab}|$, are evidence of the nearness of the field to diffuseness. /69 At a frequency of 293 Hz, the histograms are significantly different from the normal distribution; moreover, the value of $|R_{ab}|$ is close to unity. In this case, the field has a standing wave character.

The statistical approach to investigation of vibration fields of complex mechanical structures, using the distribution of phases and complex amplitude components and their interdependence, has been described for the first time, as far as is known. This statistical approach permits not only the probability-statistical estimation of the average vibration characteristics to be obtained, but an estimation of the nature of the vibration field structure.

REFERENCES

1. Kanayev, B.A., G.S. Lyubashevskiy, and B.D. Tartakovskiy, "Experimental Estimation of the Statistical Parameters of Vibrations of a Shell (Using a Digital Computer) I," (in this collection).

2. Levin, B.R., Teoreticheskiye osnovy statisticheskoy radiotekhniki [Theoretical Bases of Statistical Radio Engineering], Book 1, Sov. Radio Press, Moscow, 1969.

A MATHEMATICAL MODELING METHOD FOR DETERMINATION   OF
LOCAL VIBROACOUSTIC CHARACTERISTICS OF STRUCTURES

B.D. Tartakovskiy and A.B. Dubner
(Moscow)

One of the present problems in vibroacoustic diagnostics and techniques of noise control is determination of the layout of the distribution of acoustical (vibration) energy over a structure from the source to the observation point. Mathematical modeling of the vibration and acoustical signal propagation processes in complex structures requires a knowledge of local vibroacoustic characteristics. Such characteristics can be the magnitudes characterizing the passage of vibrational energy through the boundaries of structural elements, the mutual conversion of vibration and sound waves, absorption of vibrational energy in individual elements, etc. A method of determination of the vibroacoustic characteristics from the results of measurement of the distribution of vibrational energy in a structure is proposed, based on the energy model of a structure proposed by Westphal [1]. In con- /70 formance with work [1], we write equations describing the distribution of vibrational energy in a hypothetical diffuse energy state in structural elements:

$$- \mathit{n}_i \; \sum \; d_{ij} - \mathit{S}_i \; - \sum \; \mathit{n}_j d_{ji} - \mathit{W}_i = 0 . \tag{1}$$

where W_i is the vibrational energy density in the i-th structural element, W_j is the power of the vibrational energy source, d_{ij} is a value proportional to the coefficient of transfer of vibrational energy from the i-th section of the structure to the j-th section, n_i is a value proportional to the loss coefficient of the i-th section [2].

If exact values of the vibrational energy density were known, the vibroacoustic characteristics could be determined directly from Eq. (1) (in the case when the number of unknown values coincides with the number of structural elements). However, since the measured vibrational energy density distribution, in principle, has errors, it is necessary that the number of elements over which it is determined exceed the number of quantities sought. In this case, for determination of the vibroacoustic characteristics, the least squares method can be used [3]. In this case, it comes down to finding the values of the unknown parameters of the corresponding minimum value of the sum of the squares:

$$S = \sum_{i=1} \left[- n_i \left(\sum_{i=1} d_{ij} - S_i \right) - \sum_{j=1} n_j d_{ji} + W_i \right]^2 = \min . \tag{2}$$

where summing is carried out over all the elements of the structure. Taking the partial derivatives from expression (2) with the parameters sought and equating them to zero, we obtain a system of linear algebraic equations relative to the desired vibroacoustic quantities.

In structures with a high space attenuation value and strong sound and vibration isolation between individual elements, the vibration energy density value can differ by several times. In this case, the least squares method may not give the expected result, if the magnitude of expression (2) is determined with only a few terms.

Another approach is possible to solution of the reciprocal problem of the acoustic calculation, in which the unknown parameters occur in a set in such a manner that direct calculation by Eqs. (1) gives values which are closest to the fixed values of the sound (vibration) energy density. The value of the relative /71 root mean deviation can be considered as a criterion which characterizes the deg of deviation of the calculated energy density values of individual sections of the structure from the assigned distribution:

$$S = \frac{1}{N} \sum_{i=1}^{N} \left(\frac{w_i - w_i^*}{w_i} \right)^2. \tag{3}$$

where W_i is a value assigned to the i-th element of the structure and W_i^* is the calculated value for this element.

Further, the values of parameters corresponding to the minimum value of expression (4) must be found, which can be done by a search for the extreme in multidimensional space.

Even in the simplest cases, the proposed method requires a great number of calculations and, in practice, can be accomplished only with the aid of a digital computer. The program compiled for this purpose was compiled according to the block principle. Its core is composed of a block of search for the values of parameters corresponding to the minimum value of the relative root mean deviation. The Hook-Jivs algorithm [4] was put into practice in this program for the search for the extreme in narrow ravines on the response surface. The algorithm operates in the following manner. Initially, we calculate energy density values at assigned initial values of the parameters, and we calculate the value of the relative root mean deviation. Then, on each of the parameters in turn, we carry out test steps δx_i in directions leading to a decrease in this deviation. Assuming that the search direction found remains unchanged, we simultaneously change all the parameters by the value $\{\Delta x_i\}$. We find the components of the increment Δx_i after the k-th step:

$$\Delta x_{i_*} = 0,$$

$$\Delta x_{i_{k-1}} \begin{cases} \Delta x_{i_k} + \delta x_{i_*} \\ \Delta x_{i_k}. \end{cases}$$

if the test step in the direction δx leads to decrease in the error, if the test step does not lead to decrease in the error.

If, after the next step in the direction $\{\Delta X_1\}$, the value of the relative root mean error increases, we set $\{\Delta \bar{X}_1\} = 0$ and repeat the search process with the length of the test step $\{\delta x_1\}$ reduced to half, in this case. We continue the process until the length of the test step becomes less than the given value

$$\frac{\delta x_i}{x_i} < \varepsilon.$$

After determination of the /72 local vibroacoustic characteristics of the structure, using formula (1), the energy distribution over the structure can be determined and the contribution of the vibrational energy, passing through the structure by various paths, to the total energy of a given element can be estimated.
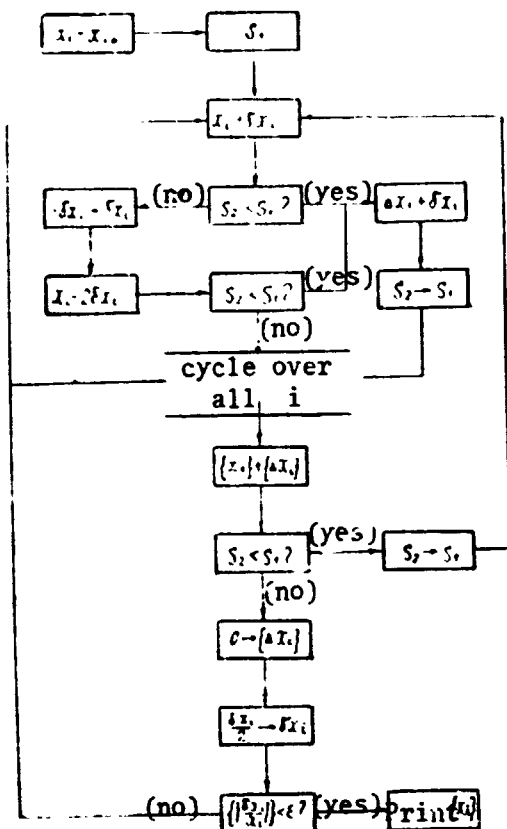
Fig. 1. Block diagrm of algorithm for search for the extreme.

REFERENCES

1. Westphal, W. _Akustiche Beihefte_ 1(1) (1957).

2. Nikiforov, A.S. and S.V. Budrin, _Rasprostraneniye i pogloshche-niye zvukovoy vibratsii na sudakh_ [Propagation and Absorption of Sound Vibrations on Ships], Sudostroyeniye Press, 1968.

3. Guter, R.S. and B.V. Ovchinskiy, _Elementy chislennogo analiza i matematicheskoy obrabotki rezul'tatov opyta_ [Elements of Numerical Analysis and Mathematical Processing of Test Results], Nauka Press, Moscow, 1970.

4. Child, D.G., _Metody poiska ekstremuma_ [Methods of Search for the Extreme], Nauka Press, Moscow, 1967.

OPTIMIZATION OF PARAMETERS OF THREE-LAYER VIBRATION-ABSORBING STRUCTURES USING A DIGITAL COMPUTER

T.M. Avilova
(Moscow)

Three-layer vibration-absorbing structures, consisting of metal plates with a viscous-elastic vibration-absorbing interlayer are more and more widely used for the damping of flexural vibrations. In connection with this, automation of the process of selection of the optimum parameters of such structures became necessary.

The loss coefficient of the three-layer structure depends on a large number of parameters: thickness of the layers, the complex modulus of elasticity, the complex shear modulus and density of the vibration-absorbing material, the modulus of elasticity and density of the metal layers and frequencies [1]. A number of works [2-5] have been devoted to investigation of the effect of these parameters on the frequency characteristics of the loss coefficient of the structure. Judging by the results obtained, some of these parameters can be left out of consideration, as a consequence of the smallness of their effect on the change in the loss coefficient of the structure. As a consequence of the fact that the density of the vibration-absorbing material usually changes within narrow limits, the frequency characteristic of the loss coefficient is displaced little on the frequency scale because of change in density.

Since the difference in the Poisson coefficient of vibration-absorbing interlayers, amounting to 0.3-0.5, shows up insignificantly on the frequency characteristic of the loss coefficient, one of the complex modules of the vibration absorbing layer, for example, Young's modulus, can be considered as a variable, considering the density and modulus of elasticity of the metal layers to be constant.

In this manner, only the thickness of the component layers, the complex modulus of elasticity and frequency remain variable.

As preliminary research has shown, the dependence of the frequency characteristics of the loss coefficient on the variables enumerated is not of an experimental nature; the task of optimization of the structure should result, not in finding the maximum loss coefficient from the variables enumerated, nor should it have an extreme character; the task of optimization of the structure should result, not in finding the maximum loss coefficient as a function of the four variables mentioned above, but in determina- /74 tion of the set of values of these variables, satisfying the given conditions (loss coefficient of the structure $\eta \geq 0.1$

in the frequency range $f_1 < f < f_2$).

A calculation program was compiled for the BESM-6 digital computer (Fig. 1).
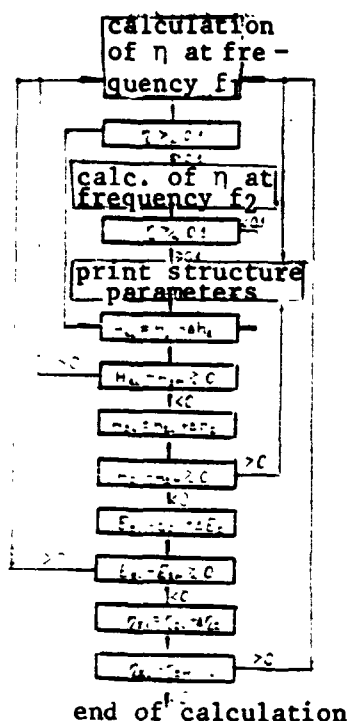
Fig. 1. Block diagram of program for calculation of optimum parameters of symmetrical three-layer vibration-absorbing structures.
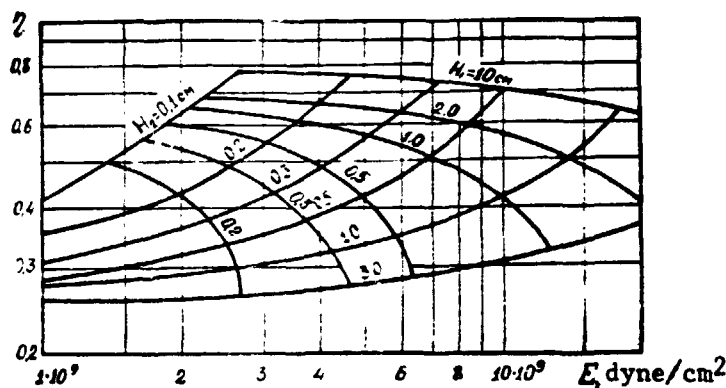
Fig. 2. Nomogram for structure with outer layers of steel.

For calculation according to the program, limiting values were assigned to the parameters H_1, H_2, E_2 and η_2; during the calculations, the value of the loss coefficients at frequencies f_1 and f_2 were determined in succession at all values of the variables H_1, H_2, E_2 and η_2, in the given range of values with selected change spacing. In the event the condition $\eta = 0$, 1 was satisfied, at $f = f_1$ and $f = f_2$, the parameters of the structures were printed out. A nomogram is presented (Fig. 2), which is plotted from the results obtained for a structure with outer layers of steel. The loss coefficients and modulus of elasticity η_2 and E_2 of the material of the intermediate layer were laid out on log-log coordinate axes. The lines of equal thickness of the outer and inner layers were plotted on the nomogram. The thicknesses of the layers of the structure, with a given intermediate layer viscous-elastic material, can be determined from the nomograms.

If thicknesses H_1 and H_2 /75 are given, the intersection point of the corresponding curves determines the minimum value of the loss coefficient of the material of the inner layer η_2 and the value of the modulus of elasticity E_2 corresponding to it. Using a material with a larger loss coefficient as the damping layer, the value of Young's modulus of the intermediate layer material can be varied, leaving the loss coefficient of the structure η unchanged.

79

The program compiled permits similar calculations to be carried out for a structure with outer layers of any metal.

The author takes the opportunity to express thanks to B.D. Tartakovskiy for discussion and valuable advice.

REFERENCES

1. Kerwin, E.M., D. Ross, and E.E. Ungar, Structural Damping, published by the American Society of Mechanical Engineers, 1959.

2. Avilova, G.M., N.I. Naumkina, and B.D. Tartakovskiy, "Optimum Parameters of a Two-Layer Vibration-Absorbing Coating," in the book   Bor'ba s shumami i vibratsiyami [Control of Noise and Vibrations], Moscow, 1966.

3. Kashina, V.I. and V.V. Tyutekin, "Experimental Study of a Reinforced Vibration-Damping Structure," Akusticheskiy zhurnal 13(3) (1967).

4. Braunisch, H., "Vibration-Damping by Three-Layered Sandwich System," Acustica 22(3) 136-144 (1969/70).

5. Avilova, G.M. and B.D. Tartakovskiy, O raschete parametrov trekhsloynykh vibropoglashchayushchikh konstruktsiy [Calculation of Parameters of Three-Layered Vibration-Absorbing Structures].

AUTOMATION OF MEASUREMENT OF SPATIAL DAMPING PARAMETERS /76

A.N. Akol'zin, A.I. Vyalyshev, B.D. Tartakovskiy, and T.N. Shmeleva
(Moscow)

In determination of the spatial parameters characterizing the loss of vibrational energy in various structures, use of a traveling wave unit leads to the necessity of processing quite a large amount of data.

A traveling wave unit was built, which permits introduction of measurement data, for automation of determination of the necessary parameters and for simplification of the statistical treatment of the results obtained. A processing program makes it possible to obtain mean values of the loss coefficients, lengths of flexural waves and wave propagation velocities for a given set of discrete frequencies.

The drop in level of vibrational acceleration in a unit distance D_1 dB/m was selected as a spatial damping parameter which an be determined. For a flexural wave in a uniform system, the loss coefficient η is connected with D_1 by the relation

$$\eta = \frac{M}{10} D_l \cdot \lambda.$$

(1)

where M = ln 10 and λ = the length of the flexural waves in the system.

In connection with this, the study was carried out in two stages: determination of the length of the flexural wave in the system and determination of the vibration level drop in a unit distance.

The length of the flexural wave is determined by the phase method. For a recording instrument of limited ϕ_{max} = 360°, the record of the phase of traveling waves is shown in Fig. 1.

Discrete phase values over equal distance intervals Δl are entered in the digital computer in the form of a block of numbers $\phi_1, \phi_2, \ldots, \phi_n$. To decrease the effect of random interference, a test of the maximum values of ϕ is introduced into the program and a limit is imposed on the minimum values of ϕ ($\phi_{min} > \pi$). In processing the data, the number n of intervals Δl between neighboring maxima is determined, which corresponds to the wavelength $\lambda = n\Delta l$ and an averaging over the entire distance measured L is carried out. The maximum error is determined by this method of calculation of λ:
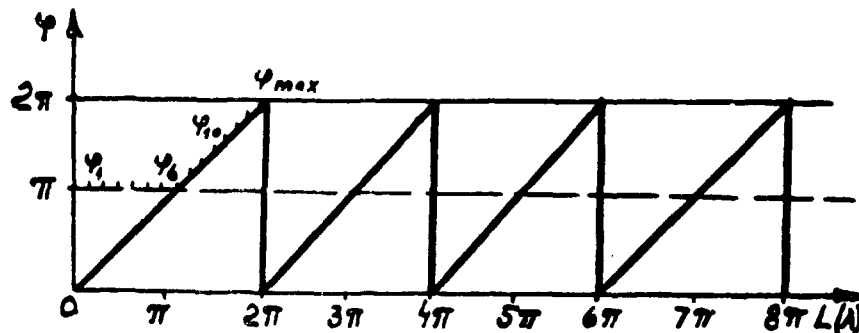
Fig. 1.

$$\Delta \eta_{ij} = \frac{\Delta l}{l} \cdot 100\% .$$

For determination of the mean drop in vibration level per unit /77
of distance D_1, the object of measurement is divided into equal
intervals ΔL along its length and m measurements are carried out
at each point over equal time intervals Δt. A second block of
numbers is entered into the digital computer: ξ_{11}, ξ_{12}, ..., ξ_{1m},
ξ_{21}, ξ_{22}, ..., ξ_{2m}, etc. As a result of the processing, the
mean change in level per interval ΔL is determined.

For given frequencies, the values of λ and D_1 obtained are
used in calculation of η by formula (1) and, for determination
of the propagation rate of the flexural waves, by the formula

$$c = f \cdot \lambda$$

The results of the measurements are reduced t) print.

f, Hz	λ, cм	η
10	156	0.19
15	126	0.17
20	108	0.16
31	96	0.15
63	62	0.13
125	45	0.12

The results of measurements of a steel rod, with a vibration-
absorbing covering applied, are presented in the table as an example.

THE USE OF A DIGITAL COMPUTER FOR INVESTIGATION OF /78
THE DYNAMIC CHARACTERISTICS OF A MAN WHILE PRESSING VERTICALLY
DOWNWARD WITH THE STRAIGHT ARM ON THE HANDLE OF A VIBRATOR (INSTRUMENT)

A.I. Zazhivikhina, G.S. Rosin, Aand Ye.I. Ryzhov
(Chelyabinsk)

The dynamic characteristics of a man were investigated by the resonance method, by means of recordings of the amplitude-frequency characteristics of a "vibrator-straight arm-human body" system on a standard automatic recorder (Fi₊ 1). The experiments were carried out with a specially constructed vibrator (Fig. 2), the moving system of which was fastened to a bronze suspension with small losses. Vibrations of the handle, fastened to the moving system, were recorded with an accelerometer. The mass of the moving system m, rigidity of the suspension k and friction coefficient r of the vibrator (calibration) were determined by exact formulas:

$$k = \frac{m_p \, \omega_p^2}{1 - (\omega_{p1} / \omega_{p2})^2} \cdot$$

$$(1)$$

$$m = \frac{m_p}{1 - (\omega_{p1} / \omega_{p2})^2} + \frac{r^2}{2K} \cdot$$

$$(2)$$

$$r = \frac{\frac{1}{2} K \omega_{p1} \left(\frac{1}{\omega_1^2} - \frac{1}{\omega_2^2} \right)}{\left[1 - \frac{\omega_{p1}^2}{4\omega_1^2} + \frac{\omega_{p1}^2 r^2}{4K^2} + \right] \left[1 - \frac{\omega_{p1}}{4\omega_2^2} + \frac{\omega_{p1}^2 r^2}{4K^2} \right]} \cdot$$

$$(3)$$

where ω_{p1} is the cyclic resonance frequency of vibration of the /79 unloaded vibrator, ω_{p2} is the resonance frequency of the unloaded vibrator without handle, m_p is the mass of the handle, $\omega_1 (< \omega_{p1})$ and $\omega_2 (> \omega_{p1})$ are the frequencies at which the resonance amplitude of the acceleration is reduced by half. The value of k, introduced in expression (3), was calculated by formula (1). Equation (3) was solved by the method of successive approximations, with an accuracy of 1%. In the first approximation, it was assumed that $\omega_{p1}^2 r^2 / 4K^2 = 0$. Then, the mass m was found by formula (2).

During the measurements, the operator pressed vertically downward on the vibrator handle with a straight arm. The dynamic rigidity K and the frictional coefficient R of the man were determined by the exact formulas:

$$K = \bar{K} - K,$$

$$(4)$$

$$R = \bar{r} - r,$$

$$(5)$$

$$\bar{K} = \bar{\omega}_p^2 (m - \bar{r}^2 / 2\bar{K}).$$

$$(6)$$

83
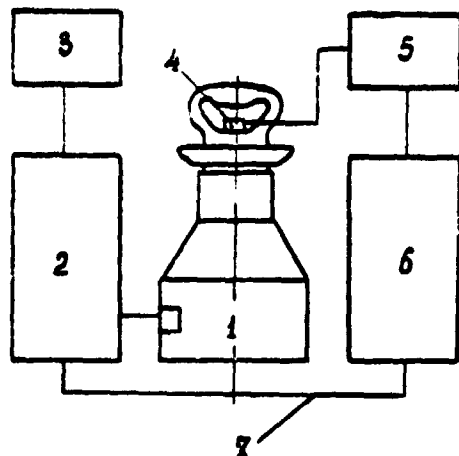
Fig. 1. Measuring unit block diagram: 1. vibrator; 2. generator 1022; 3. frequency meter F-532; 4. accelerometer 4332; 5. microphone amplifier 2603; 6. standard automatic recorder 2305; 7. flexible shaft.
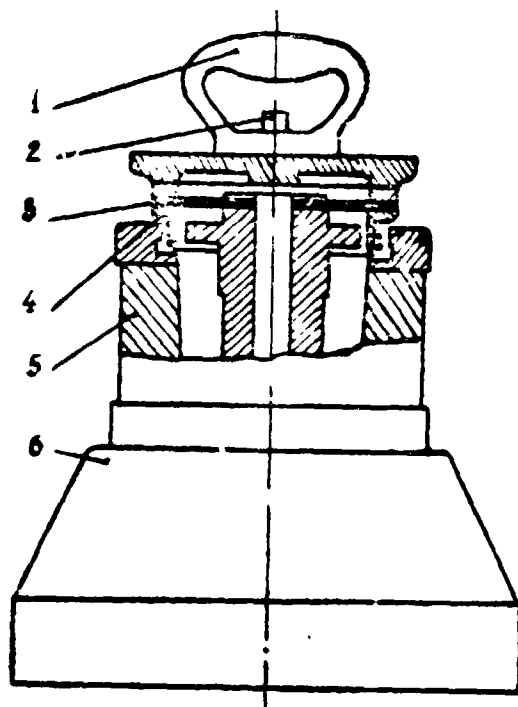
Fig. 2. Vibrator: 1. handle; 2. accelerometer 4332; 3. diaphragm; 4. moving system; 5. magnetic circuit; 6. base.

84

$$r = \frac{\frac{1}{2}\,\bar{K}\bar{\omega}_p\left(\frac{1}{\bar{\omega}_1^2} - \frac{1}{\bar{\omega}_2^2}\right)}{\left[\,1 - \frac{\bar{\omega}_p^2}{4\bar{\omega}_1^2} + \frac{\bar{\omega}_p^2 r^2}{4\bar{K}^2} + \right]\,\sqrt{1 - \frac{\bar{\omega}_p^2}{4\bar{\omega}_2^2} + \frac{\bar{\omega}_p^2 r^2}{4\bar{K}^2}}}\,(7)$$

Here, ω_p is the cyclic resonance frequency of the vibrator oscillations, loaded by the a.m of the man, $\bar{\omega}_1$ ($<\bar{\omega}_p$) and $\bar{\omega}_2$ ($>\bar{\omega}_p$) are the frequencies at which the resonance amplitude of acceleration of the loaded vibrator is decreased by half.

Seventeen men and 18 women were tested during the investigation of the dynamic characteristics. Five tests were carried out with each of them: 1. weak pressure on the handle (up to 10 kg) and weak grasp of the handle by the hand; 2. weak pressure and strong grasp; 3. strong pressure (over 20 kg) and weak grasp; 4. strong pressure and strong grasp; 5. the most convenient pressure and grasp for prolonged work with the instrument.

The results of all 1750 tests were calculated by formulas (4)-(7), by the method of successive approximations, according to the following algorithm.

The values of k and r were calculated by the iteration method, by formulas (6) and (7). The intial values were $\bar{k}_0 = 1$ and

$\bar{r}_0 = 0$. The iteration process was terminated upon reaching the conditions

$$100(r_a - \dot{r}_{a-1})/r_a \leqslant 1. \tag{8}$$

The values $\bar{K} = \bar{K}_n$ and $\bar{r} = \bar{r}_n$ were substituted in formulas (4) and (5), and then printed out in tabular form. A block diagram of the algorithm is shown in Fig. 3.
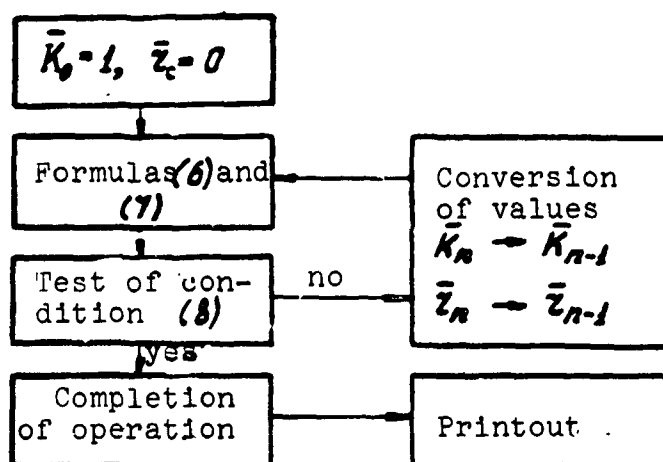
Fig. 3. Block diagram of calculation algorithm.

The average results for each group of test subjects and each <u>/81</u> group of tests are presented in the table.

Groups Tested		1	2	3	4	5
Men	$K \cdot 10^{-3}$, N/m	320	309	681	517	961
	R N-sec/m	280	280	449	365	904
Women	$K \cdot 10^{-3}$, N/m	188	236	464	425	223
	R, N-sec/m	247	235	462	321	244

Analysis of formulas (1)-(7) showed that the use of approximate expressions for calculation [1] leads to large errors in processing the results.

REFERENCES

1. Borisov, L.P., Yu.M. Vasil'yev, et al., "The Mechanical
    Impedance of the Straight Arm of a Man," in the collection
    Nauchnyye raboty instrumentov okhrany truda VTsSPS [Scien-
    tific Operations of Labor Protection Instruments, All-Union
    Central Trade Union Council], No. 5 (43), Profizdat Press,
    Moscow, 1966.

DIAGNOSTICS OF SOURCES OF DISTURBANCES AND DISTRIBUTION OF VIBRATIONS OVER THE WIDTH OF A TAPE IN TAPE-FEED MECHANISMS

A.-B.B. Kenstavichyus
(Kaunas)

Disturbances created by certain assemblies and components of tape-feed mechanisms (TFM) and acting on a moving magnetic tape are studied. The method, based on elements of digital logic, is established by stress-strain diagrams of the longitudinal deformations and vibrations across the width of a magnetic tape (Fig. 1).

The method of the experimental and theoretical research is presented.

Experimental studies were carried out for determination of the functional relationships of the longitudinal deformations in a section of magnetic tape to the magnitude of roller play, tension vibrations, rate of movement and elasticity of magnetic tapes. A block-diagram of the measurements is shown in Fig. 2.

Fig. 1. Distribution of deformations across the width of a magnetic tape: 1. magnetic tape; 2. roller; 3. roller play measurement sensor; F_{11} and F_{21} tape deformation in sections 1 and 2, respectively; ε_{11} and ε_{21} tape lengthening at measurement points on tracks 1, 2, 3; v_0 mean tape speed.

The play of guide and /82 inertia rollers, stress vibrations, rate of movement of the tape and deformation at each point of a cross section of magnetic tape are random in the assembly being studied; therefore, probability methods and stationary random function theory are applicable for further study of the dynamics of the system. Appropriate digital computer algorithms and programs were proposed for statistical analysis of the data obtained.

Estimates of the mathematical expectation, dispersion, inter-correlation function, energy spectral density and distribution /83 patterns of the random process values were calculated. The amplitude-phase-frequency characteristics and transfer functions of the variable longitudinal deformation processes of the magnetic tape, the magnetic tape tension vibrations and play of the rotating guide and inertial rollers were determined during various modes
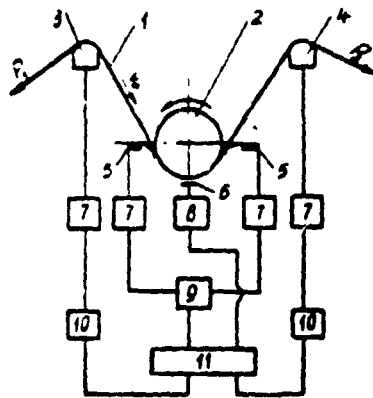
Fig. 2. Schematic block-diagram of measurements for one track: 1. magnetic tape; 2. roller-disturbance source; 3. multi-channel, two-slot magnetic head -- deformation measurement sensor; 4. multi-channel magnetic head; 5. magnetic tape tension vibration measurement sensors; 6. roller play measurement sensor; 7. amplifiers; 8. play gauge; 9. summation device; 10. deformation gauges; 11. multi-channel recording device; v_0. mean tape movement rate; P_1, P_2 tape tension forces.

ANALYSIS OF VIBRATION CHARACTERISTICS OF THIN PLATES COVERED WITH A THIN VISCOUS LAYER

A.K. Damashyavichyus, I.Sh. Rakhmatulin, V.K. Naynis,
and Yu.K. Konenkov
(Kaunas)

ﾍ certain technical problems, it is interesting to examine the problem of vibrations of a thin elastic plate, covered with a thin viscous layer of thickness H. The mathematical formulation of the problem is the following. We look for a solution of the equation of motion of a layer

$$\Delta \varphi + K_l^2 \varphi = 0,$$

$$- \operatorname{rot} \operatorname{rot} \bar{\psi} + K_t^2 \bar{\psi} = 0,$$

where

$$K_l^2 = \omega^2 / c_0^2 \left(1 - i\omega \left[\xi + \frac{4}{3} \eta \right] \Big/ \rho_0 c_0^2 \right); \qquad K_t^2 = i\rho_0 \omega \eta_t;$$

ρ_0, c_0, ξ, and η are parameters of the medium: density, speed of sound and viscosity coefficients, respectively; ω is the cyclic frequency of the oscillations. The boundary conditions reflect contact of the viscous layer with the thin plate (or rod):

$$\left. \begin{array}{l} D \dfrac{\partial^4 U_y}{\partial x^4} + \rho h \dfrac{\partial^2 U_y}{\partial t^2} = \dfrac{\partial}{\partial t} \left[q(x_1 t) + \sigma_{yy}(x_1 t) \right] \\ U_x = 0 \end{array} \right| \qquad \text{with } y = 0$$

$$\sigma_{yy} = \rho_0 \frac{\partial \varphi}{\partial t} - 2\eta_t \frac{\partial^2 \varphi}{\partial x^2} - 2\eta_t \frac{\partial^2 \psi}{\partial x \partial y} = 0$$

$$\sigma_{xy} = \eta_t \left(2 \frac{\partial^2 \varphi}{\partial x \partial y} - \frac{\partial^2 \psi}{\partial x^2} + \frac{\partial^2 \psi}{\partial y^2} \right) = 0 \qquad \text{with } y = 0$$

In this case, we restrict ourselves to the two-dimensional case. In this case, the velocity components u_x and u_y are carried with potentials:

$$u_x = \frac{\partial \varphi}{\partial x} + \frac{\partial \psi}{\partial y}$$

$$u_y = \frac{\partial \varphi}{\partial y} - \frac{\partial \psi}{\partial y}.$$

Solution of the problem, considering the smallness of the viscosity /84 coefficients, can be written in the form

$$\dot{u}_{\star} = -\int_{-\infty}^{-\lambda} \int_{-\infty}^{-\lambda} \frac{2\omega^2 e^{-i\omega t + ikx} q^{\star}(k, \omega) \, dk \, d\omega}{2(Dk^4 - \rho_s h \omega^2) - ik^2 H^2 \sqrt{2\tau_i \rho_0 \omega^3}}$$

With random vibrations of the plate, under the influence of a uniform, stationary random field q(x, t), we obtain the following expression for the spectral density of intensity of acceleration $S_{\ddot{u}_y}(\omega)$

$$S_{\ddot{u}_y}(\omega) = \int_{x}^{-x} \frac{\omega^4 S_q(k, \omega) \, dk}{Dk^4 - \rho_s h \omega^2 - ik^2 h^2 \sqrt{\dfrac{\tau_i \rho_0 \omega^3}{2}}^2}$$

It can be further assumed that, in the frequency range being examined, the spectral density of the action does not depend on k, i.e., $S_q = S_q(\omega)$. It follows from this that

$$S_{\ddot{u}_y}(\omega) = B(\omega) S_q(\omega),$$

where

$$B = \frac{1}{4} \sqrt{2\pi} \; \frac{D^{\frac{1}{4}}}{H^2 (\tau_i \rho_0)^{\frac{1}{2}} (\rho h + \rho_0 H)^{\frac{5}{4}}} .$$

For practical purposes, the case when a viscous layer is restricted to one side of the plate, with a thin membrane on the other, also is of interest. In this case, other conditions

$$\rho h \left(\frac{\partial^2 U_y}{\partial t^2} - c^2 \frac{\partial^2 u_y}{\partial x^2} \right) = \frac{\partial \sigma_{,y}}{\partial t} . \qquad\qquad U_x = 0 \text{ with } y = h$$

should be taken instead of the boundary conditions on the free surface

$$\sigma_{yy} = 0, \quad \sigma_{xy} = 0$$

90

DIAGNOSTICS OF THE TECHNICAL CONDITION OF ANTIFRICTION BEARINGS/85

A.-E.Yu. Vitkute, V.A. Pechkis, K.M. Ragul'skis, and
A.Yu. Yurkauskas
(Kaunas)

Antifriction bearings are part of various assemblies and mechanisms, and, in many cases, the condition of the bearings characterizes the entire mechanism.

Antifriction bearings and bearing assemblies can be diagnosed according to various characteristics and indications. One of the most reliable methods of diagnosis is the condition of the bearings and their assemblies by the characteristics of moments of resistance to rotation.

Under industrial conditions, it is important to know how to establish an approximate diagnosis of possible bearing deficiencies by the nature of the curves of the moment of resistance to rotation. For this, it is necessary to find out the effect of individual deficiencies of geometric shape, surface frequency, contamination, etc., on the components of the moment of resistance to rotation.

The characteristics obtained can be estimated by certain selected parameters or by a series of them. We present the following possible characteristic parameters (Fig. 1):
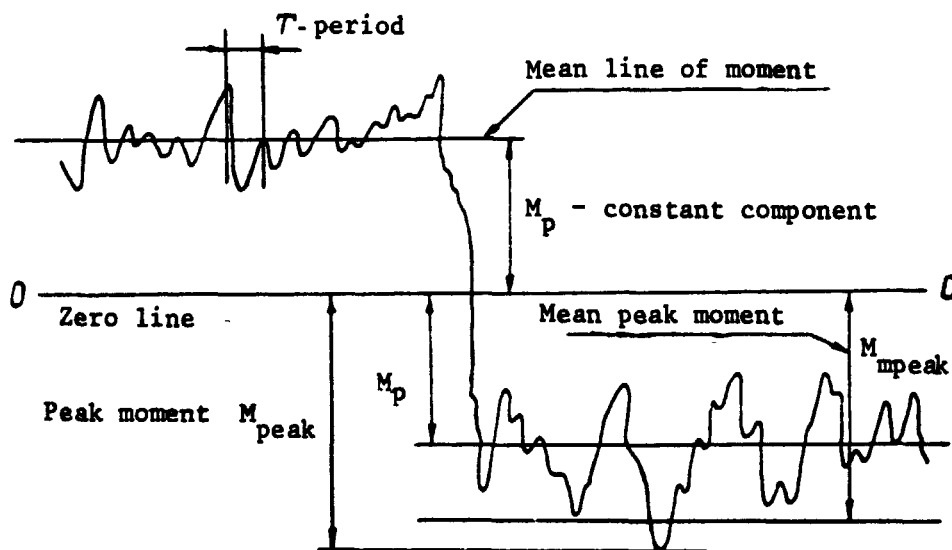
Fig. 1. Example of visualization of the moment of resistance to rotation.

1. The mean moment in the established mode -- constant component of the moment of resistance to rotation (M_D).

2. Peak moment (M_{peak}) in established mode of operation -- this is the maximum instantaneous value of the moment of resistance to rotation encountered during the test cycle.

3. Mean peak moment in established mode of operation -- this is the mean value of the instantaneous peak values of the moment encountered during the test cycle. The exact method of determination of this characteristic is the calculation of the values of each instantaneous peak on the recorded curve and finding their mean value.

4. The frequency characteristic of the moment is determined basically by spectral analysis; however, it can be visually determined approximately from the recorded curve.

Having characteristic curves for the greatest possible number of cases, methods for effective inspection can be provided.

The primary visual inspection can be carried out from the characteristics of the moment of resistance to rotation curve.

If other factors are not considered, it can be assumed that the characteristic moment of resistance to rotation curve is a function of the bearing geometry.

The condition of the separator, cleanliness of the rolling contacts, the presence of contamination, the amount and type of lubricant, as well as the operational conditions of the anti-friction bearings (loads, rotation rate, temperature of the surrounding medium and other things), have a great effect on the bearing characteristics.

Representative curves are plotted in Fig. 2, which characterize the effect of geometrical deviations, defects in the races and deformation of the rings on the variable component of the moment of resistance to rotation.

The characteristics of the moment of resistance to rotation take on a particularly characteristic appearance in the presence of play, ovalness or deformation of the bearing races. In these cases, we obtain a sharply expressed periodicity in multiples of the rotations. The moment of resistance to rotation provides a superior observational analysis of the cleanness of the surfaces of the raceways, balls and separators, as well as of accidentally encountered defects.

1)

1 revolution

2)

1 revolution

3)

1 revolution
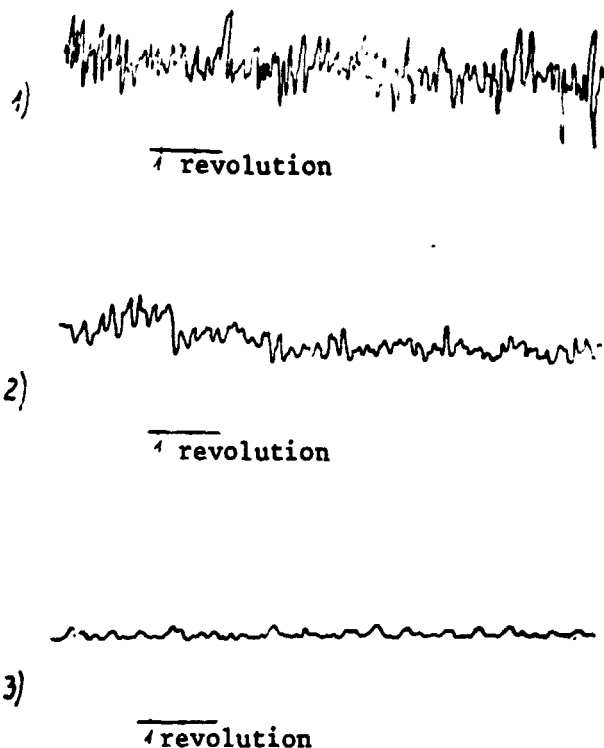
Fig. 2.   Characteristics of the
variable components of the moment
of resistance to rotation of a
type 26 bearing: 1. with deformed
outer bearing races; 2. with de-
formed inner bearing races;
3. with scratches in the race of
the outer ring.

Jamming of the separator
frequently is difficult to
distinguish from deviations
in the rolling contact geometry.
However, in the majority of
cases, jamming of the separator
can be identified by the random
nature of the overshoots, while
geometrical deviations are
almost sinusoidal curves.   /87
The effect of the separator
on the moment of resistance
to rotation is presented in
Fig. 3.

One of the basic causes
for the generation of stresses
in the separator, which cause
its destruction, is misalign-
ment of the inner bearing race
relative to the outer one.
The stresses can be reduced to
a minimum by ensuring the
necessary radial gap between
the balls and the race grooves.
As tests show [1], for each
value of the misalignment, the
maximum amplitude of the stress,
in the 0-3000 rpm range, does
not depend on the rotation
rate of a   ball   bear-
ing.   Curves are presented in
Fig. 4, which show the nature
of the stresses on the separator and increase in the amplitudes of
their vibrations, with increase in angular misalignment.

A characteristic trait of a dirty bearing is the presence of /89
fine overshoots. To establish contamination, it is sufficient to
carefully clean the bearings and then carry out the examination
again.

A lubricant usually causes an increase in the constant com-
ponents of the moment and reduction in its variable portion (Fig.
5).

In 1966, the SKF Company developed an impact-impulse method
of determination of damage to bearings by electrical measurements
of the high frequency vibrations which always exist in a damaged
bearing [2].
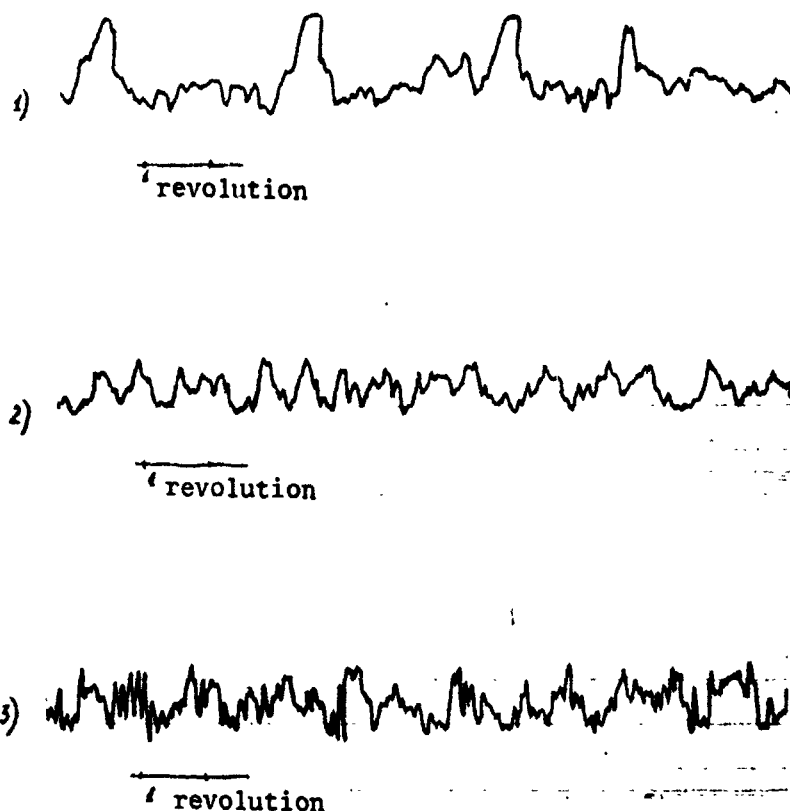
Fig. 3. Examples of characteristics of the moment of
resistance to rotation in the presence of separator
defects (type 26 bearing): 1. separator bent in;
2. separator deformed; 3. slight separator jamming.
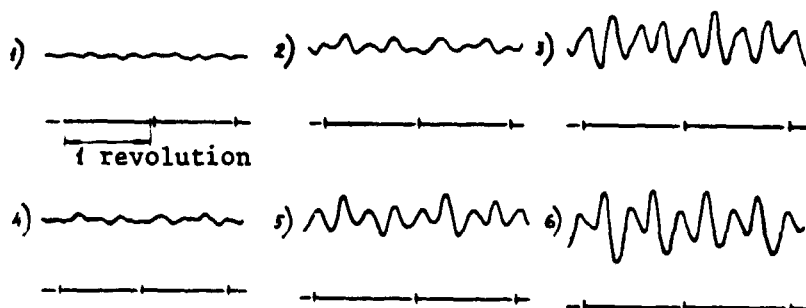
Fig. 4. Nature of stresses in the separator vs. angular
misalignment of bearing rings: 1. 0.26°; 2. 0.39°;
3. 0.46°; 4. 0.51°; 5. 0.56°; 6. 0.61°.
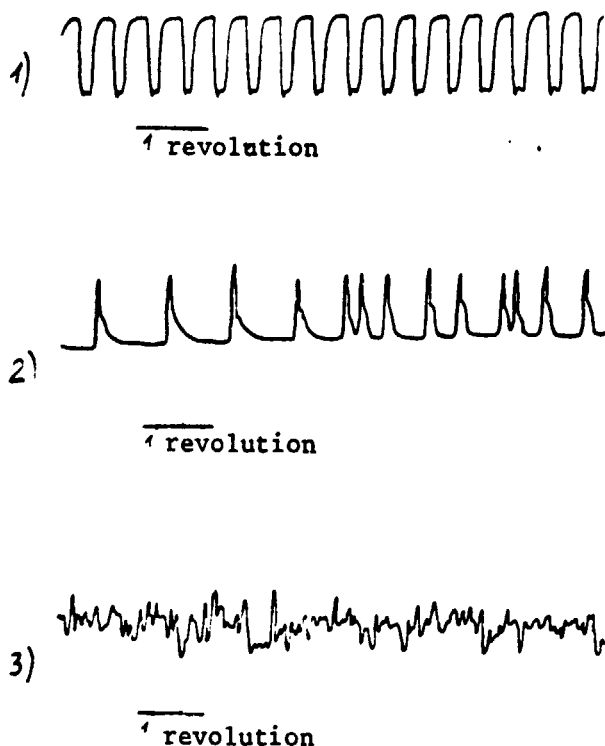
Fig. 5. Characteristics of variable component of the moment during various operational deviations (type 201 bearing): 1. with dirty bearing; 2. with clean, dry bearing; 3. with bearing lubricated with IS-45 grease.

In examination of all of the characteristics presented, account must be taken of the circumstance that, in each case, not a single factor, but several operate, and only one of them is predominant.

A visual diagnosis always has only a preliminary nature, and it requires great specialization by the inspector. Therefore, other methods of analysis of an experimental inspection of bearings is necessary for an objective diagnosis.

The purpose of interpretation of the visualized variable moment of resistance to rotation during examination is to obtain a judgment on the condition of the bearing. In the case of a complicated interpretation, a choice must be made between possible qualitative bearing conditions (qualitative interpretation) and certain unknown parameters on which this condition depends must be estimated. In this case, the presence of as small a random component as is desirable (in comparison with other determinative components) excludes the "null" criterion, since the difference between the values proposed by models of the experimental data and measured values turns out to be a random value, different from zero. Any effort to construct any kind of criterion leads to the necessity for taking the probability distribution characteristics of the difference obtained into account.

The interpretation can be presented in the two stages of synthesis of a certain "response" function $\lambda(\vec{\rho})$ in space of the bearing condition and determination of those values of the parameters $\vec{\rho} = \vec{\hat{\rho}}$, at which $\lambda(\vec{\rho})$ has a minimum (maximum). In the least squares case

$$\lambda(\vec{\hat{\rho}}) = \sum_k \sum_l [U_{kl} - f_{kl}(\vec{\rho})]^2.$$

where $f_{ki}(\vec{\rho})$ is a theoretical function characterizing possible conditions and U_{ki} is the experimental data.

Here, the entire series of observations is divided into individual groups, which are numbered by the subscript k (k = 0, ±1, ..., ±K), so that any pair of observations taken from different groups can be considered statistically independent. At the same time, observations included in any k-th group are correlatively connected together. The subscript designates the observation number within the k group, for example, the group of visualizations of the variable moment of resistance of a bearing with a deformed separator (race), clogged up with sandy dust, etc.

The task consists of determination of the optimum procedure for selecting among possible conditions, according to a given visualization of the observations. In order to guarantee the potential possibility of obtaining the maximum effective result of the "response" function, it is desirable to select probability conditions $P_n(\vec{u})$ for possible states n = 0, 1, 2, ..., N. They can be determined after obtaining experimental values of U_{ki}.

We obtain the probability density $P(\vec{U})$ of appearance of given vectors U_k(k = 0, ±1, ..., ±K), as a result of experiment, according to the Beyes formula:

$$P_u(n) = \frac{1}{P(U)} \cdot P(n) \cdot p_n(\vec{U}).$$

Here, P(n) is the a priori probability of each of the possible states and $P_n(\vec{u})$ is the conditional probability distribution density of the experimental data, in the absence of one of the possible states of the bearing being examined. These densities are determined according to the assigned model of the experimental material, by use of known probability theory relationships, and we consider them as functions of the bearing condition for a given set of experimental values, i.e., we have likelihood functions. In the case of a purely qualitative interpretation, the likelihood function is a discrete set of numbers (likelihood coefficients), characterizing the individual conditions.

In practical use of the theory set forth, we determine N values of λ_ν (ν = 1, 2, ..., N) of the logarithms of the ratios of the a posteriori probabilities

$$\lambda_\nu = \ln \frac{P_u(\nu)}{P_u(0)} = \ln \frac{P(\nu) L_\nu}{P(0) L_0},$$

$$L_n = p_n(U)$$

(1)

96

and we select that state of the object for which the value λ_ν is <ins>/92</ins> at a maximum and is positive. If all values of λ_ν ($\nu = 1, 2, \ldots,$ N) are negative, we select the condition at which n = 0.

We note that determination of the condition of the bearing being examined is made, not only on the basis of information obtained during processing of the assigned visualizations of the variable moment of resistance, but with consideration of previously existing a priori conceptions of these conditions, which are complicated as a result of processing the data of preceding tests. In this case, a nonrandom term, taking the a priori probability distributions into account, is added to expression (1) for determination of λ_ν:

$$\ln \frac{P_\nu(\nu)}{P_\nu(0)} . \tag{2}$$

All results concerning the specifications of the solution and evaluations of the effectiveness of the qualitative interpretation remain in force.

The maximum probability method leads to asymptotic, unskewed, effective and normal estimates [4]. Their effectiveness is determined by the covariance matrix B:

$$B = B_{ss'} \,{}_{ss'=1}^{N}, \qquad b_{ss'} = \sum_i \sum_k U_{ski} U_{s'ki},$$

where s is the number of states.

The diagonal elements of the matrix are the values of the dispersion of the corresponding estimates, and the nondiagonal ones are the correlation coefficients of the connections between the estimates. They must be taken into account in those cases when, for one and the same experimental material, we estimate somewhat different bearing conditions. The necessity for taking account of the connections between the estimates (and conditions) comes down to a requirement for unified variation of the parameters in searching for the maximum of the likelihood function. In selection of the observation system parameters, it must be considered that it depends essentially on the expected qualitative conditions of the bearings, on the properties of the random components and on the number and expected values of the parameter vectors, since the observations selected must ensure the production of the necessary information on the bearing conditions sought.

The following group of bearings was chosen: with scratches on the outer race 1, with deformed separators and lubricated 2,

97

lubricated with IS-45 lubricant 3, lubricated and dirty 4, dry 5, with deformed races and lubricated 6, dry, with deformed separator <u>/93</u> 7, with play 8, clogged with sandy dust 9 and with deformed outer races 10.

The mean number of overshoots beyond a specified level A_i (i = 1, 2, ..., N) during 20 revolutions is used as the parameters, according to which determination of the qualitative interpretation of the condition is carried out. The results of such an investigation for class 201 C bearings are presented in the table.

Bearing Group	Parameters												
	A_1	A_2	A_3	A_4	A_5	A_6	A_7	A_8	A_9	A_{10}	A_{11}	A_{12}	A_{13}
1	39	33.5	15.5	5	2								
2	55	54	56.5	50	42	29	20.5	9.5	4	2	0	0	0
3	70	50	29.5	19	16.5	10	8	4	2	0	0	0	0
4	36	39.5	33.5	25	18.5	14	10	8.4	6.5	4	3	2	2
5	61	45	45.5	30.5	24	13	7	5.5	1.5	1	0	0	0
6	35	35	35	35	34	33	23	15	10	4	1.5	0	0
7	23	19.5	1	0	0	0	0	0	0	0	0	0	0
8	51	51	51	51	51	51	51	51	51	51	51	38	11.5
9	145	145	138.5	71	65.5	88	64.5	34.5	7	2.5	0	0	0
10	27	29.5	24	23.5	19.5	7.5	5.5	3.5	2	2	1	0	0

We note that the criteria of comparison of the means and dispersion of the numbers of overshoots, as in a dispersion analysis, can be used for making a decision as to the bearing condition.

REFERENCES

1. Crawford, T.S., "The Experimental Determination of Ball Bearing Cage Stress," _Wear_ _16_(1) (1970).

2. Botö, P.A., "Detection of Bearing Damage by Shock Pulse Mea. ure-ments," _Eng. Dig._ _32_(9), Great Britain (1971).

3. Barnard, T.P. and R.S. Guyett, "Determination and Correlation of Fundamental Instrument Bearing Parameters," _Journal of the American Society of Lubrication Engineers_ (2) (1960).

4. Pugachev, V.S., _Teoriya sluchaynykh funktsiy_ [Theory of Random Functions], Fizmatgiz Press, Moscow, 1960.

DIAGNOSTICS OF THE VIBRATIONS OF COMPLEX ROTOR SYSTEMS   /94

I.Yu. Yugraytis, K.M. Ragul'skis, Rem.A. Ionushas, and
I.P. Karuzhene
(Kaunas)

It is advisable to establish an analytical connection between
the vibration parameters and the parameters of the unbalanced con-
dition of the system for an evaluation of the vibrations of a
rotor system.

Let us assume that a system, with n rotors, arranged in parallel
and rotating with different angular velocities, has six degrees of
freedom. Let us examine the movement of the system under the action
of unbalanced masses of the i-th rotor. Let us consider that the
unbalanced state of the i"-th rotor is characterized by three para-
meters (see Fig. 1, where C is the center of mass of the system,
and ξ, η and σ are the coordinates of the system center of mass:
by the unbalanced masses in two planes of corrections m_{1i} and m_{2i}
and angle α between them.
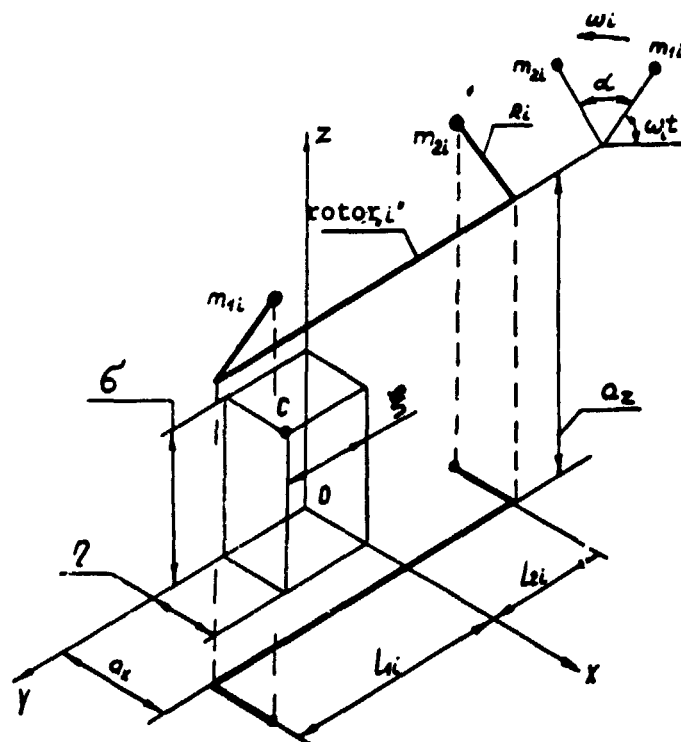
Fig. 1.

In the general case, a system of six nonlinear differential equations cannot be solved analytically. Therefore, locating the elastic elements of the system suspension in an appropriate manner, assuming that the origin of the coordinates of the axes coincides with the center of mass of the system, and omitting the terms of the second order of smallness as well, we obtain a system of differential equations in a simpler form:

$$\ddot{X}_{0i} - p_\lambda^2 \Sigma z \cdot \Psi'_{yi} + p_\tau^2 \cdot X_{0i} = [d_{1i} \cos \omega_i t + d_{2i} \cos (\omega_i t + \varkappa_i)] \omega_i^2 \qquad (1)$$

$$\ddot{Y}_{0i} + p_\tau^2 \Sigma z \cdot \Psi'_{xi} + p_\tau^2 \cdot Y_{0i} = 0 \qquad (2)$$

$$\ddot{Z}_{0i} + p_z^2 \cdot Z_{0i} = [d_{1i} \cdot \sin \omega_i t - d_{2i} \sin (\omega_i t + \varkappa_i)] \omega_i^2 \qquad (3)$$

$$\ddot{\Psi}_{xi} + \left[\left(\frac{p_\lambda}{\rho_\lambda} \right)^2 \cdot \Sigma z^2 + \left(\frac{p_z}{\rho_x} \right)^2 \cdot \Sigma y^2 \right] \cdot \Psi'_{xi} + \left(\frac{p_\tau}{\rho_\lambda} \right)^2 \Sigma z \cdot Y_{0i} =$$

$$= [-d_{1i} l_{1i} \cdot \sin \omega_i t + d_{2i} \cdot l_{2i} \cdot \sin (\omega_i t + \varkappa_i)] \omega_i^2 \qquad (4)$$

$$\ddot{\Psi}_{yi} + \left[\left(\frac{p_\tau}{\rho_y} \right)^2 \cdot \Sigma z^2 + \left(\frac{p_z}{\rho_y} \right)^2 \Sigma x^2 \right] \cdot \Psi'_{yi} - \left(\frac{p_x}{\rho_y} \right)^2 \Sigma z \cdot X_{0i} = 0 \qquad (5)$$

$$\ddot{\Psi}_{zi} + \left[\left(\frac{p_\tau}{\rho_z} \right)^2 \Sigma x^2 + \left(\frac{p_x}{\rho_z} \right)^2 \Sigma y^2 \right] \Psi_{zi} =$$

$$= [-d_{2i} l_{2i} \cos (\omega_i t + \varkappa_i) + d_{1i} l_{1i} \cos \omega_i t] \omega_i^2 \qquad (6)$$

Equations (3) and (6) are not connected with the remaining equations. It follows from this that solution of the problem given can be restricted to solution of only these two equations, and that the phase shift between the coordinates Z and Ψ_{zi} can be used.

The amplitude of the vibrations of the system under the action of the unbalanced condition of the i-th rotor will be

$$\lambda_{zi}^2 = \nu_z (d_{1i}^2 + d_{2i}^2 + 2d_{1i} \cdot d_{2i} \cos \varkappa_i) \qquad (7)$$

$$\lambda_{\Psi_i}^2 = \nu_\Psi \cdot (d_{1i}^2 l_{1i}^2 + d_{2i}^2 \cdot l_{2i}^2 - 2d_{1i} d_{2i} l_{1i} \cdot l_{2i} \cos \varkappa_i) \qquad (8)$$

where:
λ_{zi} and $\lambda_{\Psi i}$ are the system vibration amplitudes in the direction of the z axis and around the oz axis; ν_z, ν_Ψ are the dynamic coefficients of the system; d_{1i} and d_{2i} are the specific disbalances in the correction planes;

$$d_{1i} = \frac{m_{1i}}{M_0} \cdot R_i; \qquad d_{2i} = \frac{m_{2i}}{M_0} \cdot R_i;$$

M_0 is the system mass; and R_i is the radius of the unbalanced mass from the axis of rotation of the i-th rotor.

The phase shift between Z_1 and Ψ_{z1} is determined by this relation:

$$\tan\Delta = \frac{d_{zi}^2 \cdot l_{zi} - d_{1i}^2 l_{1i} - d_{1i} d_{zi} \, v_q \cdot v_z \, \cos \varkappa_i \, (l_{1i} - l_{zi})}{l_{0i} \cdot d_{1i} \cdot d_{zi} \, \sin \varkappa_i} \qquad (9)$$

Subsequently, we assume that

$$l_{1i} = l_{zi} = \frac{l_{0i}}{2} \; .$$

Then, solving the transcendental equations (7, 8, 9), we obtain the parameters of the unbalanced condition of the i-th rotor:

or

$$d_{1i} = l_{0i}^{-1} \cdot \Bigg] \overline{\left(\frac{l_{0i}}{2v_z}\right)^2 \cdot \lambda_{zi}^2 + \left(\frac{1}{v_q}\right)^2 \cdot \lambda_{\Psi i}^2 - \frac{l_{0i}}{v_z \cdot v_q} \cdot \lambda_{zi} \cdot \lambda_{\Psi i} \cdot \sin \Delta_i}$$

$$d_{1i} = l_{0i}^{-1} \cdot D_{1i}.$$

$$d_{zi} = l_{0i}^{-1} \Bigg] \overline{\left(\frac{l_{0i}}{2v_z}\right)^2 \cdot \lambda_{zi}^2 + \left(\frac{1}{v_q}\right)^2 \cdot \lambda_{\Psi i}^2 + \frac{l_{0i}}{v_z \cdot v_q} \cdot \lambda_{zi} \cdot \lambda_{\Psi i} \cdot \sin \Delta_i}.$$

or $\qquad d_{zi} = l_{0i}^{-1} \cdot D_{zi}.$

$$\sin \varkappa_i = \frac{\dfrac{l_{0i}}{v_z \cdot v_q} \cdot \lambda_{zi} \cdot \lambda_{\Psi i} \cos \Delta_i}{D_{1i} \cdot D_{zi}} \; ,$$

$$\cos \varkappa_i = \frac{\left(\dfrac{l_{0i}}{2v_z}\right)^2 \cdot \lambda_{zi}^2 - \left(\dfrac{1}{v_q}\right)^2 \cdot \lambda_{\Psi i}^2}{D_{1i} \cdot D_{zi}} \; .$$

In this manner, under specified conditions, the parameters of the imbalance of a complex rotor system, having n parallel rotors and having six degrees of freedom, can be determined from the parameters of the vibrations of two appropriate degrees of freedom. This considerably simplifies diagnostics of the vibrations of complex rotor systems.

DIAGNOSTICS OF LOAD VIBRATIONS AT THE INLET OF A MECHANISM

V.P. Dontsu, Z.T. Dontsu, K.M. Ragul'skis, and N.M. Savka
(Kaunas, Kishinyev)

One of the problems of investigation of the dynamics of a mechanism is a study of the forces of resistance to rotation during the operating cycle. Knowledge of the forces of resistance to rotation permits selection of the most economical mode of operation of the mechanism, and provision of stable and prolonged /97 operation of the unit at a given level in automatic control systems.

The torque on the drive shaft was studied, during steady movement of a precision tape-feed mechanism (TFM), used in precise magnetic recording devices. The visualizations obtained were considered as dynamic characteristics of a mechanism, subject to random actions, the complete investigation of which can only be carried out by statistical methods.
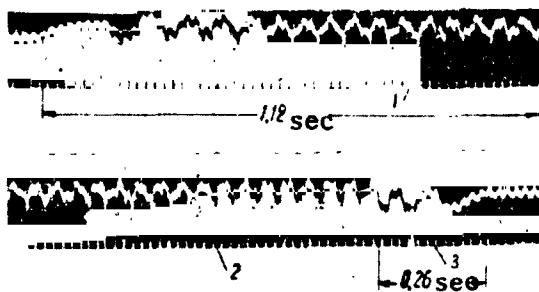
An oscillogram of the torque on a TFM drive shaft, with an endless spool of magnetic tape, is presented in Fig. 1. The stages of the operating cycle are visible on the oscillogram. There is no evident periodicity here, and the general appearance of the vibrations during steady movement remains unchanged during the observation period; therefore, it is referred to the stationary random processes class.

Fig. 1. Torque oscillogram.
1. Starting; 2. steady movement;
3. running down.
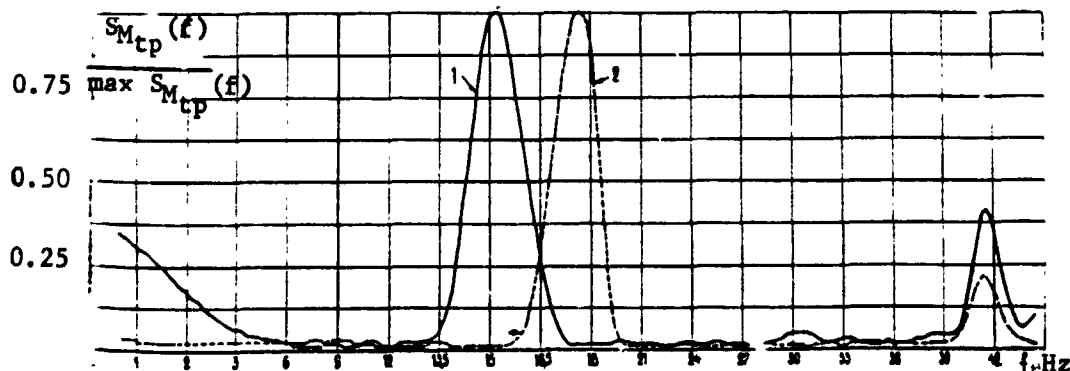
Fig. 2. Spectral densities M_{tp}, with various values of the inertial mass on the drive shaft: 1. with pulley; 2. without pulley.

The spectral densities are shown in Fig. 2. Curve 1 corresponds to the torque of the system with an inertial disk and curve 2, without disk. It is evident that the torque reaches the <u>/98</u> greatest amplitude for a system with inertial disk at frequencies of about 15.5 and 41 Hz and, for a system without inertial disk, at frequencies of 17.5 and 41.5 Hz. The peak values of the amplitude are reached at frequencies of 15.5 and 17.5 Hz. These frequencies are close to the drive shaft rotation rate (n = 20 rev/sec) and, as investigation has shown, are located close to the natural frequency of the system f_n = 16.5 Hz, which leads to resonance.

The principal source of disturbing forces is the drive shaft, since the rotation rates of all remaining elements are far different from the resonance peak frequency. The most probable cause of the disturbance is radial play of the drive shaft. Another peak is located in the 41-42 Hz frequency range. The reason for formation of this peak probably is the result of the effect of the first resonance peak and vibrating parts of the TFM.

The effect of an inertial disk on the system dynamics is clear from the graph (it shows up more in the low frequency spectrum). The low frequency resonance peaks are displaced with respect to one another and, as should be expected, the system without inertial disk (curve 2) reaches a peak value at a higher frequency than the system with an inertial disk (curve 1). However, this shift is insignificant, since its effect on the amplitude of the resonance peaks is negligible. It follows from this that change in the spectrum of location of resonance peaks by increase in mass of the inertial disk is ineffective.

INVESTIGATION OF VIBRATIONS OF WORKING ELEMENTS
OF A TWO-COORDINATE SCANNER

K.L. Kumpikas
(Kaunas)

Vibrations of the working elements of a two-coordinate, optical-mechanical scanner (OMS) were studied experimentally.

The working elements of the OMS are a scanning disk and a data storage board, kinematically connected to it (Fig. 1). An increase in the kinematic and dynamic precision of movement of the working elements makes it possible to create an OMS with a high information recording density per unit area of data storage.

The purpose of this work is the experimental determination of /99 the nature and magnitude of vibrations of OMS working elements, statistical processing of the experimental data, determination of the basic sources of excitation of the vibrations and the provision of recommendations for reduction in the vibration level of the device.

The measurement scheme is presented in Fig. 1.
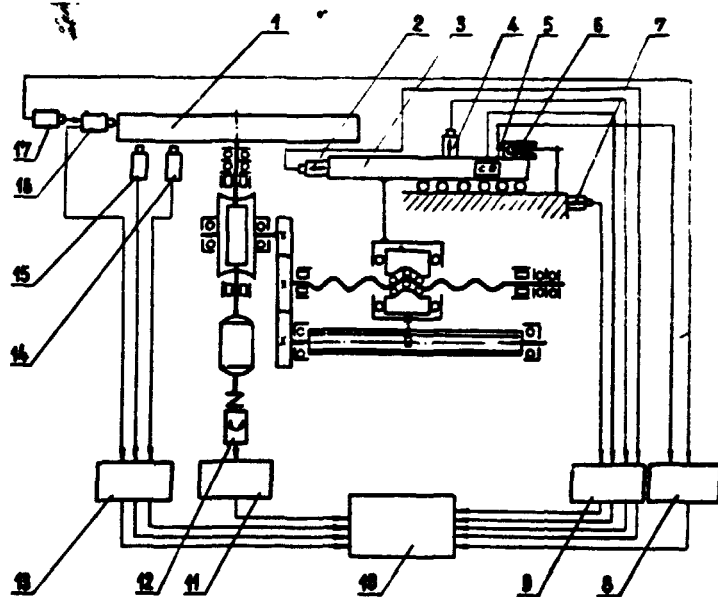
Fig. 1. Scheme for measurement of vibrations of OMS working elements: 1. scanning disk; 2,4,5,7. KD-21 acceleration sensors; 3. data storage board; 6. W10Z inductive displacement sensor; 7. KWS/T-5 vibration measurement apparatus; 9. SDM-132 vibration meter; 10. H105 loop oscillograph; 11. 51E01 vibration measurement apparatus; 12. type 9051D0074 torsion vibration sensor; 13. BE-5-2 vibration measurement apparatus; 14, 15, 16. capacitance displacement sensors of BE-5-2 vibration measurement apparatus; 17. W1T inductive displacement sensor.

Radial and axial vibrations of the disk were measured by no-contact capacitance sensors, with appropriate amplifying apparatus.

The behavior of the data storage board was investigated simultaneously with the disk vibrations. The torsion vibrations of the scanning disk shaft also were investigated.

All measurements were carried out simultaneously, and they <u>/100</u> were recorded by the loop oscillograph.

The oscillograms obtained are considered as visualizations of stationary, random, ergodic processes. To obtain the statistical characteristics of these processes by digital computer, the visualizations were replaced by a finite number of random process ordinates, corresponding to discrete, uniformly spaced moments of time. The curves were sampled and then statistically processed by digital computer. As a result of the processing, correlation functions and spectral densities of the vibrations of OMS working elements were obtained. The transfer functions between the vibrations of the scanning disk and the board also were determined.

Analysis of the results of the statistical processing of the experimental data permitted the sources of excitation of the vibrations of OMS working elements to be revealed, the effect of torsion vibrations of the disk on the data storage board to be determined, the possibility of use of the OMS created for recording and counting data to be evaluated, recommendations to be given on the reduction in vibration level, and recommendations to be given for design of new OMS, providing an information recording density of up to $4 \cdot 10^6$ million bits of information per cm^2 of data storage.

106

A METHOD OF DIAGNOSTICS OF THE DYNAMIC STABILITY
OF THE CARRIER IN A MAGNETIC RECORDING-PLAYBACK CIRCUIT

G.A. Petrulis and I. Gasyunas
(Kaunas)

The dynamic stability of the carrier in the magnetic recording-playback circuit of a multi-cassette tape-feed mechanism (TFM), a simplified diagram of which is shown in Fig. 1, was investigated. It was shown that, under specified conditions, transverse carrier vibrations can be excited, as a result of direct excitation, due to eccentricity of the drive elements or due to parametric excitation, as a consequence of periodic fluctuation in carrier tension. The transverse vibrations cause periodic, longitudinal displacements of the moving end of the carrier, located in the region of the magnetic head slot, which leads to stray frequency modulation of the output signal.

Assuming that the carrier, a flexible, uniform magnetic tape, is subjected to the action of periodically changing tension during longitudinal movement with velocity v_0, we write the equation for the transverse vibrations of the magnetic tape, taking account of the damping coefficient, in the form /101

$$\frac{\partial^2 y}{\partial t^2} + 2v_0 \frac{\partial^2 y}{\partial x\,\partial t} + 2\gamma \frac{\partial y}{\partial t} - \frac{P(t)}{m} \frac{\partial^2 y}{\partial x^2} = 0. \quad (1)$$
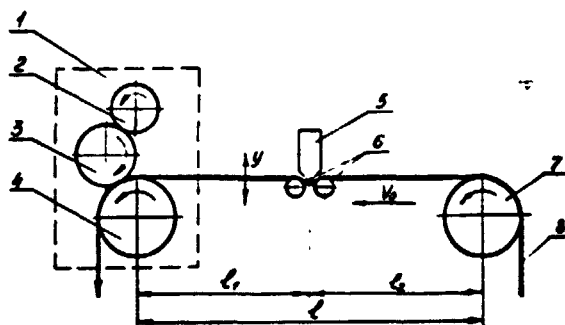
Fig. 1. Simplified diagram of multi-cassette TFM recording-playback circuit: 1. left pneumatic assembly (turned on); 2. drive shaft; 3. intermediate roller; 4. left cassette roller; 5. magnetic head; 6. magnetic tape tightening roller; 7. right cassette roller; 8. magnetic tape; l_1, l_2 vibrating portions of magnetic tape; l length of circuit; y direction of transverse vibrations of magnetic tape; v_0 rate of movement of tape.

where $p(t) = p_0 + p_t \cos\theta t$ is the tape tension exciting fluctuation; v_0 is the speed of movement of the magnetic tape; γ is the damping coefficient; and m is the mass of the vibrating section of magnetic tape.

Taking the limiting conditions into account (y = = 0 at x = 0 and x = l_1), after transformations, we write Eq. (1) in the form

107

of a modified Mathieu-Hill equation:

$$\ddot{f}+\Omega^{2}\left[1-\left(\frac{v_{0}\frac{k\pi}{l_{1}}-\gamma}{\Omega}\right)^{2}-2\mu\cos\Theta t\right]f=0 \qquad (2)$$

where $\Omega=\frac{k\pi}{l_{1}}\sqrt{\frac{P_{0}}{m}}$ is the natural vibration frequency of the carrier;

$\mu=\frac{P_{(t)}}{P_{0}}$ is the exciting coefficient; and

l_{1} is the length of the magnetic tape segment.
K = 1, 2, 3, ...

With specified ratios of the coefficients Ω, μ and Θ, Eq. (2) has an unbounded, increasing solution, with periods T and 2T, defining the dynamic instability region.

The second, fourth, sixth and eighth regions of dynamic in-
stability of the carrier, obtained experimentally, during move-
ment of the carrier at a speed of 4.76 cm/sec and in the static
state, are represented in Fig. 2. Broadening of the dynamic
instability regions is observed during movement of the carrier.
It is noted that the parametric transverse vibrations of the
magnetic tape section arise at frequencies of the exciting changes
in tape tension, at even numbers of times lower than the natural
vibration frequency, i.e., the boundaries of the dynamic instability
regions are located close to frequencies determined by the formula

$$\Theta_{*} = \frac{2\Omega}{K},$$

where K = 2, 4, 6, ... is the instability region order number.

The intensity of the transverse vibrations, taking place with
the frequencies of the external forces, increases considerably, in
proportion to approach to the frequency $\Theta = \Omega$, and the
frequency range is wider than that calculated theoretically.

Thus, diagnostics of the carrier behavior in the recording-
playback circuit, by plotting regions of dynamic instability,
according to a given carrier tension fluctuation spectrum, permits
the generation of transverse vibrations to be eliminated effectively
by a choice of the length of the free sections of tape.

108
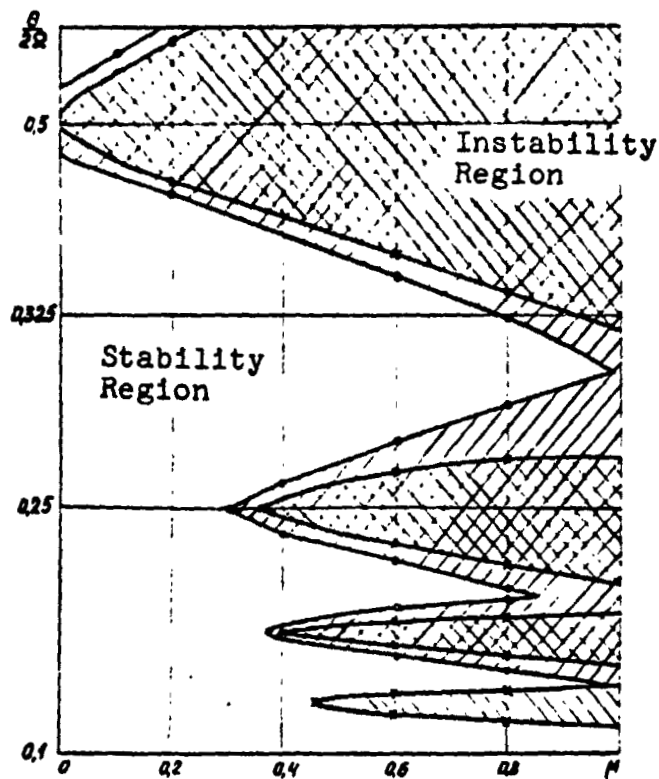
Fig. 2. Graph of a dynamic stability of magnetic tape in the recording-playback circuit at $\gamma = 0.018$ N-sec/m, $l_1 = 0.18$ m, p = 1 N: -o-o- region boundaries during magnetic tape movement at a speed $v_0 = 4.76$ cm/sec; -x-x- region boundaries in the static state of the magnetic tape.

COMPUTER DIAGNOSTICS OF SHOCK PROCESSES

A.-A.P. Laurutis, B.V. Rudgal'vis
(Kaunas)

The vigorous development of modern technology and automation of scientific research and production processes requires more and more reliable operation of elements of control, regulation, automation and computer technology systems, in particular, precision apparatus when acted on by external mechanical overloads (shocks, vibrations, linear accelerations). For successful control of these phenomena, as well as for increase in vibration and shock strength of apparatus, a deep understanding of the dynamics of the overloads mentioned is necessary. The most dangerous of all possible shock processes in this regard are impulses, which, as a rule, have complex forms, wide-band spectra and negligible duration. Such processes do not yield to mathematical description; consequently, /104 their physical action on various microelements of precision radio measurement apparatus cannot be determined by this means. The spectral characteristics of complex impulse processes can be determined by visualization of the analysis of their scanned oscillograms, obtained by means of a high-speed recorder.
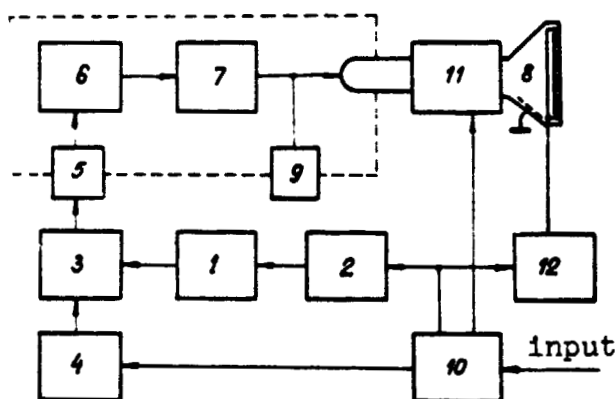
Fig. 1. Block diagram of ER-2 cathode ray electrostatic recorder.

The ER-2 wide-spectrum data, cathode ray electrostatic recorder, a block diagram and outward appearance of which are shown in Figs. 1 and 2, was specially developed for this. Special attention was given to precision in recording and the quality of the visual image in development of the recorder, since they fundamentally determine the precision of an experiment.

High quality of the visual image is guaranteed by a specially developed dynamic bias lighting system. High frequency generator 1 is connected with a device for fixing the duration of recording 2 and modulator 3, which, in turn, is connected with differentiating amplifier 4 and, through high-frequency, high-voltage dividing transformer 5, detector 6 and video amplifier 7, is connected to the cathode assembly of the cathode ray tube of electrostatic recorder 8, which is under high voltage from source 9. Recorded signal amplifier 10, connected with deflection system 11 and differentiating amplifier 4, also is connected to the device for fixing the recording duration 2

110

and time mark unit 12. In this manner, the signal being studied acts directly on the deflection of the recording tube beam and the beam current increases to the necessary value, at the moment and for the duration of recording, and it is recorded as a function of the speed with which the recorded process takes place. Uniform thickness of the lines of the visual image is guaranteed by this, over a wide speed range of rapidly-changing data. Simultaneous recording of the zero line and time mark (or sampling spacing) facilitates the elimination of amplitude and time distortions, which appear, due to vibration of the mechanical scanner assembly. This is especially important in study of the dynamics of precision systems.
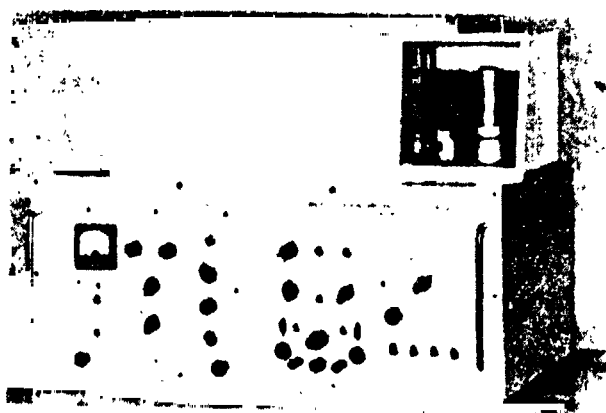
Fig. 2. External appearance of ER-2 electrostatic recorder.

The technical characteristics of the instrument are: maximum recording speed 2000 m/sec; data carrier feed speed up to 100 m/sec; recorded signal frequency range 0-50 kHz; maximum image sweep 100 mm; nonuniformity in line thickness, not more than 5% during measurement of the speed of flow of a process 100 times; recorded signal duration 0.0004-20 sec; time for production of visual image 60 sec.

The visualization of the pulse of an impact stand, obtained by means of this recorder, was processed by a Silhouette type automatic sampler and entered into the Minsk computer, for analysis according to the method presented.

In this case, the most important parameters are the complex spectral density of the shock pulse, energy spectrum, effective pulse duration and effective spectrum width, respectively:

$$S(\omega) = \int_{\tau}^{r} q(t) e^{-j\omega t} \, dt;$$

$$W = \int_{0}^{\tau} [S(\omega)]^2 \, d\omega;$$

$$\tau = \int_{t_0 + \frac{\tau}{2}}^{t_0 + \frac{\tau}{2}} q^2(t) \, dt = \varepsilon \int_{x_0}^{n} q^2(t) \, dt;$$

$$\Delta f = \int_0^{2\pi\Delta f} [S(\omega)]^2 \, d\omega = \varepsilon \int_\varepsilon^{\tau} [S(\omega)]^2 \, d\omega.$$

ε is the fraction of the total pulse energy arriving during an interval of time.

An analysis was made of the spectral density and energy spectrum as functions of the impact force, design of the stand and energy absorbed by the lining, rigidity of the base, etc. In this case, the solution was carried out according to these mechanical equations:

$$a_k = \frac{2}{N_s} \sum_1^{N_r} f(i \, \Delta t_r) \cos k \, \omega_r i.$$

$$b_k = \frac{2}{N_r} \sum_1^{N_s} f(i \, \Delta t_r) \sin k \, \omega_r i.$$

$$S(k) = \sqrt{a_k^2 + b_k^2}.$$

$$\varphi(k) = \arctan \frac{b(k)}{a(k)}.$$

$$\omega_r = 2\pi \, \Delta t_r.$$

Δt_r is the sampling interval in sec and k = 50 ... 30,000 is the frequency of the spectrum components.

A fragment of a shock pulse and examples of the shock stand spectral density are shown in Fig. 3a and b.

It was determined during the investigation that shock stand /108 pulses are random. Therefore, the method presented is incomplete. The information obtained was statistically processed.

112
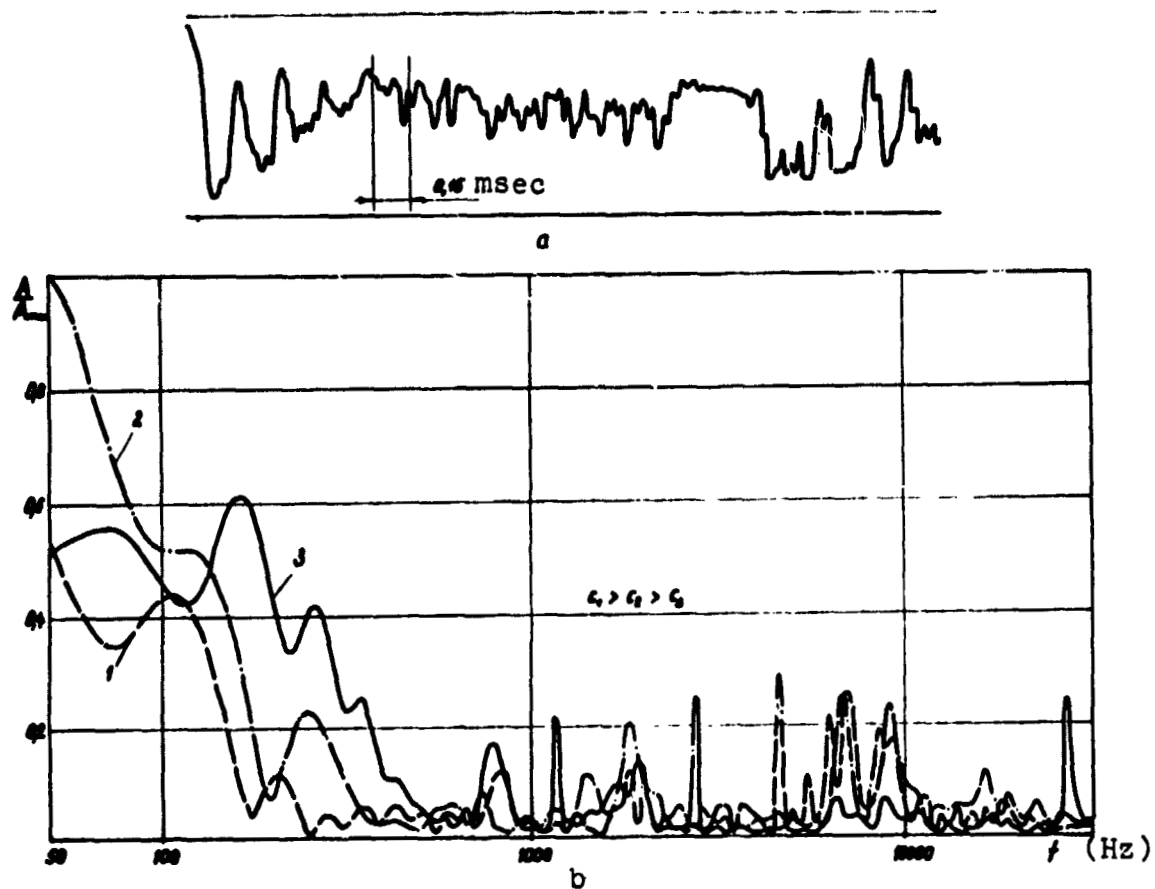
Fig. 3. a: Fragment of shock stand pulse visualization.
b: Spectral density of shock stand pulse, at various
rigidities of the energy-absorbing lining.

REFERENCES

1. Laurutis, A.-A. P., K.M. Ragul'skis, and B.V. Rudgal'vis, "Device for Control of Electrostatic Recording of a Recording Cathode Ray Tube," Resheniye o vydache avtorskogo svidet-el'stva po zayavke [Decision on Distribution of Authors Certificate on Claim]No. 1603309/26-9).

2. Rudgal'vis, B.V. and B.Ye. Gol'man, "Investigation of Shock Stand Pulses Used During Tests of a Relay," Voprosy radio-elektroniki. ser. Tekhnika provodnoy svyazi, Ministry of the Radiotechnical Industry, USSR, No. 4, 1970.

3. Khar'kevich, A.A., Spektry i analiz [Spectra and Analysis], State Publishing House of Technical and Theoretical Litera-ture, Moscow, 1962.

INVESTIGATION OF NOISE IN GEAR TRANSMISSIONS
BY THE METHOD OF MATHEMATICAL SMOOTHING OF EXPERIMENTS

B.T. Sheftel', G.K. Lipskiy, P.P. Ananov, and I.K. Chernenko
(Saratov)

Much attention is being given at the present time in instrument making to the development of low-noise high-speed rotation drives, using low-power (up to 40 watt) cylindrical reducers, with low module (0.1 + 0.5 mm) steel and metallopolymer gear wheels.

The basic factors forming the acoustical spectrum of a reducer are the rotation speed and load. The problem was posed of establishing the optimum ratios of these factors, which guarantee a given sound level for steel and metallopolymer gear pairs.

The cybernetic approach was used during the investigation, giving a new algebraic data language, which permitted a mathematical model of the process to be produced, in study of complex systems by the method of mathematical smoothing of experiments. The reducer noise investigation was carried out in an anechoic chamber, with Bruel and Kjaer Co. acoustical apparatus. Rotatable central-component smoothing (RCCS) was adopted for carrying out the experiments. A two-factor RCCS plan was presented, in the form of a matrix, in which randomized rows correspond to various tests and columns to values of the factors. In compiling the matrices, the levels of the factors were coded in accordance /109 with the table . Execution of this plan permitted a regression equation to be obtained:

$$\hat{y} = b_0 + b_1 x_1 + b_2 x_2 + b_{12} x_1 x_2 + b_{11} x_1^2 + b_{22} x_2^2$$

Matrix

X_0	X_1	X_2	$X_1 X_2$	X_1^2	X_2^2	V
+1	−1	−1	+1	+1	+1	2b
+1	+1	−1	−1	+1	+1	66
+1	−1	+1	−1	+1	+1	31
+1	+1	+1	+1	+1	+1	65
+1	−$\sqrt{2}$	0	0	2	0	36
+1	+$\sqrt{2}$	0	0	2	0	4b
+1	0	−$\sqrt{2}$	0	0	2	53
+1	0	+$\sqrt{2}$	0	0	2	57
+1	0	0	0	0	0	48
+1	0	0	0	0	0	59
+1	0	0	0	0	0	50
+1	0	0	0	0	0	52

Table

code	n rpm	mg-cm
−$\sqrt{2}$	700	15
−1	1500	215
0	3500	545
−1	5500	875
+$\sqrt{2}$	6300	1675

where Y is the experimental noise level value, X_1 is the rotation rate, rpm, and X_2 is the load.

After statistical analysis and determination of the significance of the regression coefficients, a test of the adequacy of the model selected was carried out.

As a result of canonical analysis of the regression equation, the following formulas were obtained.

Steel gear wheels:

-- first gear frequency

$$x_2^2 = -2.36 \left(x_1 - \frac{42.8 - \hat{y}}{13.7} \right).$$

-- second gear frequency

$$\frac{x_1^2}{a^2} + \frac{x_2^2}{b^2} = 1, \qquad a^2 = \frac{\hat{y} - 33.5}{5.35}, \qquad b^2 = \frac{\hat{y} - 33.5}{6.42}.$$

Metallopolymer gear wheels:

-- first gear frequency

$$x = \frac{\hat{y} - 34.3}{8.4}$$

-- second gear frequency

$$x_1^2 = -0.634 \left(x_2 - \frac{\hat{y} - 34.0}{3.17} \right).$$
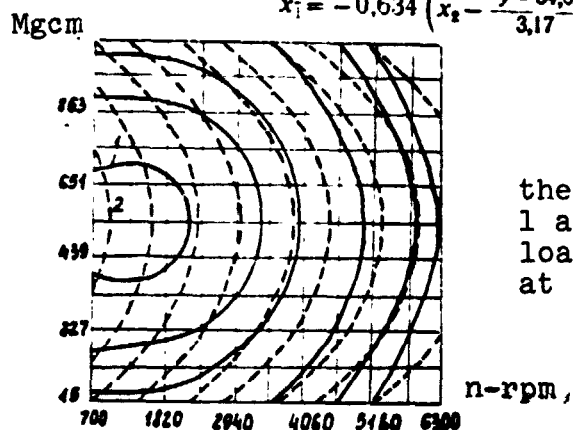
Fig. 1.

The formulas obtained and their geometric interpretation (Figs. 1 and 2) permit the optimum speed and load of a reducer to be determined, at a previously assigned sound level.

116

Mgcm
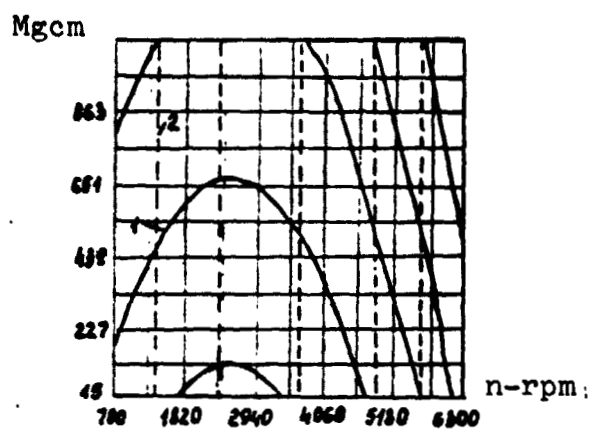
Fig. 2.

METHOD OF ESTIMATION OF ACOUSTICAL ENERGY
RADIATED BY INDIVIDUAL SURFACES OF AN INTERNAL COMBUSTION ENGINE

D.I. Yuknyus, V.N. Lukanin, and V.V. Efros
(Kaunas)

An estimate of the noise of an internal combustion engine usually is carried out on the basis of results obtained during measurement of the noise level at certain points around the engine. Such a method is applicable for an estimation of the noise characteristics of the engine overall, but it has low effectiveness or is completely inapplicable for obtaining information on the radiating power of individual surfaces or parts of the engine. Therefore, a new method was developed, which permits an estimation of the acoustical power radiated by a local surface of the engine.

The use of an acoustical waveguide horn, by means of which the acoustical energy is removed from the surface being studied and measured, lies at the base of the method. The pattern of change in transverse cross section of the horn is exponential.

The structural parameters of the horn were calculated so that it transmitted all audio frequencies above 37 Hz.

The dimensions and configuration of the horn inlet were determined by the shape of the surface being investigated. The dimensions of the output aperture of the horn were constant (they amounted to 2.5 × 3 m).

An experimental unit was built, which permitted the radiated acoustical power of any surface of an engine to be estimated.

Acoustical calibration of the horn circuit showed that distortion of the acoustical energy transmitted by it was insignificant, and did not exceed 1.5 dB over the entire frequency range investigated (50-16,000 Hz).

DETERMINATION OF CHANGES IN PROPERTIES
OF RANDOM PROCESSES WITH AN ACCURACY ASSIGNED IN ADVANCE

L.A. Tel'ksnis
(Vil'nyus)

The operation of machines and mechanisms is accompanied by vibroacoustic processes. These random processes can be used for determination of changes in the modes of operation of machines and mechanisms. In the solution of a number of practical problems, the change in properties must be determined, to an accuracy of a /112 certain interval of time assigned in advance. Let us examine the following problem in connection with this.

Let the random processes

$$X(t) = \begin{cases} x^{(1)}(t) & (u_0 < t \leqslant u_1) \\ x^{(2)}(t) & u_1 < t \leqslant u_2 \end{cases} \qquad (1)$$

be described by a mathematical expectation

$$m(t) = \begin{cases} m^1(t) & (u_0 < t \leqslant u_1) \\ m^2(t) & (u_1 < t \leqslant u_2) \end{cases} \qquad (2)$$

and correlation functions

$$k(\tau, \tau) = \begin{cases} k_1(\tau, \tau) & (u_0 < \tau, \tau \leqslant u_1) \\ k_2(\tau, \tau) & (u_1 < \tau, \tau \leqslant u_2), \end{cases} \qquad (3)$$

where $X^{(1)}(t)$ and $X^{(2)}(t)$ are normal and independent. The value of the variable u_1, at which a random process changes statistical properties, is unknown or random. An a priori distribution density $a(u_1)$ value of the variable u_1 is given. If the a priori distribution density is unknown, we assume that u_1 has a uniform a priori distribution density in the interval $u_0 < u_1 \leq u_2$.

There is one realization $x(t)$ $(u_0 < t \leq u_2)$ of the random process $X(t)$ $(u_0 < t \leq u_2)$. It is required that the values u_1^* of the argument u_1 at which the properties of the random process change be determined. In this case, the problem must be solved,

119

so that the mean risk achieves an error, with the loss function

$$l(u_1, \tilde{u}_1) = \begin{cases} 1, & u_1 - \tilde{u}_1 > \alpha \\ 0, & u_1 - \tilde{u}_1 \leqslant \alpha \end{cases} \qquad (4)$$

at a minimum. This can be achieved under condition that the requirement of a minimum arbitrary mean risk is satisfied, i.e.,

$$R(\tilde{n}_1) = M\{l(n_1, \tilde{n}_1) \mid \bar{x}\} = \sum_{n_1 = n_0 + 1}^{n_2} \omega(n_1 \mid \bar{x}) l(n_1, \tilde{n}_1) = min. \qquad (5)$$

where $\bar{x} = \{x(t_i)\}$ $(t_1 = hi; \ i = n_0 + 1, \ldots, n_2)$ is the realization of the random sequence

$$\bar{x} = \begin{cases} \bar{x}^{(1)} = \{x^{(1)}(t)\} \ (t_i = h_i; \ i = n_0 + 1, \ldots, n_1) \\ \bar{x}^{(2)} = \{x^{(2)}(t)\} \ (t_i = h_i; \ i = n_1 + 1, \ldots, n_2). \end{cases} \qquad (6)$$

of the mathematical expectation   /113

$$m = \begin{cases} m^{(1)} = \{m^{(1)}(t_i)\} \ (t_i = h_i; \ i = n_0 + 1, \ldots, n_1) \\ m^{(2)} = \{m^{(2)}(t_i)\} \ (t_i = h_i; \ i = n_1 + 1, \ldots, n_2) \end{cases} \qquad (7)$$

and correlation matrices described

$$K(n_1) = \begin{cases} [k_1(\tau_i, \tau_j)] \ (\tau_i = hi; \ \tau_j = hj; \ i, j = n_0 + 1, \ldots, n_1) \\ [k_2(\tau_i, \tau_j)] \ (\tau_i = hi; \ \tau_j = hj; \ i, j = n_1 + 1, \ldots, n_2). \end{cases} \qquad (8)$$

$k_r(\theta_i, \tau_j)$ $(r = 1, 2)$ are the values of the correlation function (3) at values of the variables $\vartheta = \theta_i$ and $\tau = \tau_j$; h is the quantization interval of the variable t of the random function $x(t)$; (in (4) and subsequent formulas, it is assumed, without loss in generality, that $h = 1$); n_r = Entier $(u_r h^{-1})$ $(r = 0, 1, 2)$; $\tilde{n}_1$ is the estimation of the parameter n_1 (nonoptimum); $\omega(n_1 | \bar{x})$ is the a posteriori probab'lity density of the parameter n_1; $l(n_1, \tilde{n}_1)$ are the values of the loss function, when $u_1 = hn_1$, $\tilde{u}_1 = h\tilde{n}_1$, $\alpha = ha$ and $h = 1$.

120

Since $u_{11}^* = hn_{11}^*$, and h, as a rule, is known, it is sufficient to find n_{11}^* for determination of u_{11}^*. Unfortunately, it is practically impossible to use expression (5) directly for evaluation of n_{11}^*. Calculation of the function $R(\tilde{n}_1)$ is an extremely cumbersome and laborious task, which is too difficult even for computers.

To obtain an estimate of n_{11}^*, it is necessary in practice to use the following expression:

$$(9)$$

$$n_{11}^* \simeq \underset{n_0-a-1 \leqslant \tilde{n} \leqslant n_2-a}{\arg\max} \sum_{n_1=\tilde{n}_1-a}^{\tilde{n}_1-a} \exp \beta_1(n_1 \ \bar{x}),$$

where

$$\beta_1(n_1 \ \bar{x}) = \begin{cases} -\frac{1}{2}\beta(n_1 \ \bar{x}) - \beta_{max}, & \text{if} \ -\frac{1}{2}\beta(n_1 \ x) - \beta_{max} \geqslant -c_1 \\ -\infty, & \text{if} \ -\frac{1}{2}\beta(n_1 \ \bar{x}) - \beta_{max} < c_1. \end{cases}$$

$$(10)$$

$$\beta_{max} = \underset{n_0-1 \leqslant n_1 \leqslant n_2}{\max} \left[-\frac{1}{2}\beta(n_2 \ \bar{x}) \right].$$

$$(11)$$

In this case, the function $\beta(n_1/\bar{x})$ can be calculated by the method set forth in works [1, 2].

An evaluation of a_{11}^* (which determines the change in properties of the random process, with an accuracy of the time interval, with a length of 2a, assigned in advance) can be calculated by formulas (9), (10) and (11) by computers.

An example of solution of the problem being examined by a digital computer is presented.

1. Tel'ksnis, L.A. and V. Chernyauskas, "Determination of Change
    in Properties of Random Signals," Statisticheskiye problemy
    upravleniya [Statistical Problems of Control], No. 1,
    Vil'nyus,1971.

2. Tel'ksnis, L.A., "Optimum Determination of Change in Proper-
    ties and Identification of Sources of Random Signals,"
    Vibrotekhnika (4/13) (1972).

122

THE ROLE OF STATISTICAL MEASUREMENTS
IN EXPERIMENTAL RESEARCH

V.V. Ol'shevskiy
(Moscow)

Experimental research, as a cognitive process, comes down to the production of quantitative data on previously unknown characteristics of an object (or phenomenon) studied. As a result of experimental research, we attempt to establish a quantitative model of the object, in order to use it subsequently for prognosis of previously unknown properties of the object, for solution of reciprocal problems, etc. The majority of experimental investigations in acoustics come down to the study of the probability characteristics of random processes (or fields). This means that, as a result of experiment, there is a statistical evaluation $\Theta(\hat{l})$ of the probability characteristic $\hat{\Theta}(\vec{l}/m)$, corresponding to one of the models $m \in M$, where M is the set of probability models of the random process $x(t)$. A structural diagram of quantitative experimental investigations is shown in the figure.

Formalization of a priori information	Hypotheses on the properties of the item being studied
Hypothetical items	**Item being studied**
Probability models of the random process $x(t=m) \; ;_i(t):$	**Sampling process** $\hat{x}(t)$
Probability characteristics $\Theta(l(m)=\mu_m \{\pi_i(\lambda)\}$	**Statistical measurement system**
Investigator	**Statistical estimates** $\hat{\Theta}(\vec{l})$
Results of investigation	**Experiment control system**

Let us examine certain aspects of organization of experimental investigations, based on the results of works [1-4].

It should be kept in mind that the scheme presented in the figure is of one, fixed, hierarchical level of experimental research. The question of where the formalized a priori information and hypothesis are taken from is not examined here.

By hypothetical items of investigation, we understand an idealized model of actual items. The item models are developed, using existing formalized a priori information and those hypotheses of their properties which the investigator thinks it possible to assume. Separation of the initial data into formalized a priori information and assumed hypotheses, in the problem being investigated, in our opinion, has a fundamental importance, since the basis of formalized a priori information is existing experience, obtained earlier during investigations of the properties of items, while hypotheses are formulated by the investigator at the /115 heuristic level. In this sense, formalized a priori information and hypotheses differ sharply in their confidence levels. The total of the hypothetical items must be sufficiently complete to encompass all possible modifications of the real item and conditions, under which the latter are found, which are of interest.

It is known that the random process $x(t)$ is determined by a set of random functions of time $x_k(t)$, k = 1, 2, ..., N and by the probability distributions, characterizing the properties of this set. Each function $x_k(t)$ is called the realization of the random process $x(t)$. A convenient (and, possibly, the only) form for considering existing a priori information and assumed hypotheses is the probability model of a random process, by which any presentation of instantaneous values of a process, which permits calculation or postulation of those of its probability characteristics which exist in the solved problem, are understood. /116 In this case, the random process $x(t)$ is presented in the following manner:

$$x(t) = m\left[\{\xi_i(t)\}\right].$$

(1)

where $m \in M$ is an operator characterizing the type of model selected (subsequently, we shall say that m is the model of the process); $\xi_i(t)$, i = 1, 2, ..., P are random processes, the probability characteristics of which are considered known.

Let $\theta(\vec{1}/m)$ be the probability characteristic of the process $x(t)$, corresponding to its m-th model; $\vec{1}$ are independent variables, on which the characteristic depends; and $\pi_1(\vec{\lambda})$ are the probability characteristics of the random processes; $\xi_1(t)$, $\vec{\lambda}$ are the corresponding independent variables. Mathematical model (1) must permit the probability characteristics $\theta(\vec{1}/m)$ to be calculated on the basis of known (assigned) characteristics $\pi_1(\vec{\lambda})$, i.e.,

124

$$\Theta(\vec{l}\,/m) = \mu_m[\{\pi_i(\vec{\lambda})\}].$$

where μ_m is the connection operator between characteristics $\pi_i(\vec{\lambda})$ and $\Theta(\vec{l}/m)$, corresponding to assumed model m of the random process. At the first (preparatory) stage of experimental investigations, the investigator must have available the probability characteristics $\Theta(\vec{l}/m)$ of the random processes, corresponding to their different models $m \in M$. The second stage is a study of the properties of the item studied (real), i.e., the conduct of experiments. Here, we produce a sampling process $\hat{x}(t)$, by which the set of the time functions $\hat{x}_r(t)$, r = 1, 2, ..., n, is understood, each of which corresponds to one experiment carried out. The functions $\hat{x}_r(t)$ should be called the sampling realizations. In distinction from the realizations $\hat{x}_k(t)$ of a random process, always of the corresponding probability models of the process and, consequently, possessing known probability properties, the sampling realization $\hat{x}_r(t)$ reflects the properties of the real item, and their properties are a priori unknown. On the other hand, after carrying out an experiment, the sampling realizations $\hat{x}_r(t)$, after their recording (storage), turn out to be known by their values. Since the purpose of the research is determination of the probability model of the process being investigated, nevertheless, known sampling realizations are necessary to obtain statistical estimates of the probability characteristics of interest to us. The sampling process $\hat{x}(t)$ further enters the statistical measurement system, at the output of which a statistical estimate $\hat{\Theta}(\vec{l}) = S_{\vec{L}}[\hat{x}(t),\vec{l}]$ of the probability characteristic $\Theta(\vec{l}/m)$ is formulated, in which $S_{\vec{L}} \in S$ is the estimate formation operator, selected with account taken of the form of the characteristic $\Theta(\vec{l}/m)$; $\vec{L}$ are the corresponding parameters of the statistical measurement system. The estimate $\hat{\Theta}(\vec{l})$, together with the characteristic $\hat{\Theta}(\vec{l}/m)$, becomes available to the investigator, who is drawing conclusions concerning the results obtained.

The investigator, on the basis of statistical measurements, can control the course of the investigation. The experiment control system serves this purpose. By means of it, the conditions in which the item being investigated are found can be purposefully influenced, and parameters of the statistical measurement system can be selected, as well. The task of such a relationship to the experiment is, first, the selection and provision of conditions, under which the results of investigation of the item will have presence. In other words, the question is of smoothing the imposing set of experimental investigations.

REFERENCES

1. Kotyuk, A.F. and V.V. Ol'shevskiy, "Problems of Metrology of Random Processes and Fields," First All-Union symposium, <u>Metody predstavleniya i apparaturnyye analiz sluchaynykh protsessov i poley (sbornik dokladov)</u> [Methods of Presentation and Instrumental Analysis of Random Processes and Fields (Collection of Reports)], 1, Novosibirsk, 1968.

2. Ol'shevskiy, V.V., "Mathematical Models and Statistical Description of Hydroacoustic Signals," <u>Trudy Pervoy Vsesoyuznoy shkoly-seminara po statisticheskoy gidroakustike</u> [Proceedings of First All-Union School-Seminar on Statistical Hydroacoustics], Nauka Press, Novosibirsk, 1970.

3. Ol'shevskiy, V.V., "Problems of Development of Mathematical Models of Random Processes and Fields," <u>Trudy Tret'yego Vsesoyuznogo simpoziuma 'Metody predstavleniya i apparaturnyye analiz sluchaynykh protsessov i poley'</u> [Proceedings of Third All-Union Symposium, 'Methods of Presentation and Instrumental Analysis of Random Processes and Fields'], Section P, Leningrad, 1970.

4. Ol'shevskiy, V.V., "Probability Models, Experimental Research and Statistical Measurement," Fourth All-Union Symposium, <u>Metody predstavleniya i apparaturnyye analiz sluchaynykh protsessov i poley</u> [Methods of Presentation and Instrumental Analysis of Random Processes and Fields], Section P, All-Union Scientific Research Institute of Electrical Measuring Instruments, Leningrad, 1971.

126

INTERPRETATION OF THE RESULTS OF STATISTICAL MEASUREMENTS /118

V.V. Ol'shevskiy
(Moscow)

In accordance with the examination carried out in work [1], an experimenter has two characteristics of a random process at his disposal, namely, the calculated probability characteristic $\Theta(\vec{l}/m)$ and the measured statistical estimate $\hat{\Theta}(\vec{l})$. Let

$$\rho_\Theta(m,\vec{L}) = \rho[\Theta(\vec{l},m), \hat{\Theta}(\vec{l})] \tag{1}$$

be a quality functional of the experimental investigation characteristic $\hat{\Theta}(1/m)$. This functional defines the difference in two functions $\Theta(\vec{l}/m)$ and $\hat{\Theta}(1)$, in the sense of operator ρ, the form of which is determined by the purpose of the experimental research and peculiarities of the problem to be solved. Of certain general properties of the quality functional $\rho_\Theta(m, \vec{L})$, we note the following: first, $\rho_\Theta(m, \vec{L}) > 0$; second, at $\Theta(\vec{l}/m) = \Theta(\vec{l})$, we have $\rho_\Theta(m, \vec{L}) = 0$; and, third, with increase in the difference between the functions $\Theta(\vec{l}/m)$ and $\hat{\Theta}(1)$, the value $\rho_\Theta(m/, \vec{L})$ increases monotonically. The following two forms of definition of the quality functional can be presented as an example:

$$\rho_\Theta(m,\vec{L}) = \langle \Theta(\vec{l}/m) - \hat{\Theta}(\vec{l}) \rangle . \tag{2}$$

as well as

$$\rho_\Theta(m,\vec{L}) = \langle [\Theta(\vec{l}/m) - \hat{\Theta}(\vec{l})]^2 \rangle . \tag{3}$$

Let us assume that the statistical measurement procedure is organized in such a manner that, for a selected model m, the parameters $\vec{L}$ of the measurement system are optimized, so that

$$\operatorname*{opt}_{\vec{L}} \hat{\Theta}(\vec{l}) = \operatorname*{opt}_{\vec{L}} S_{\vec{L}}[\dot{x}(t), \vec{l}/m]. \tag{4}$$

Realization of condition (4) corresponds to the specified minimum of functional (1), i.e., the solution of the system of equations

$$\nabla_{\vec{L}}\, \rho_\Theta(m,\vec{L}) = 0. \tag{5}$$

127

From this (under corresponding conditions of determination of the type of extremum), the value $opt\overset{o}{\Theta}(\vec{\mathit{l}})$ is found, at which func-tional (1) assumes the appearance

$$\hat{\rho}_\theta(m) = \rho\,[\dot{\Theta}(\vec{\mathit{l}},m), \quad \underset{\vec{\mathit{l}}}{\mathrm{opt}}\,\dot{\Theta}(\mathit{l})]. \tag{6}$$

It is evident that functional $\rho_\Theta(m)$ will have different values for different models m, as a consequence of the fact that hypotheses of the item being investigated equal its actual proper-ties to a nonuniform degree. We will understand model m_0 to be the basic model, corresponding to the smallest value of functional (6)

$$\hat{\rho}_\theta(m_0) = \inf_{m\in M}\hat{\rho}_\theta(m). \tag{7}$$

It can be expected that, the closer the values $\rho_\Theta(m)$ and $\rho_\Theta(m_0)$, the more accurately model m has been selected.

Let us turn attention to the nature of the formation of the set M of models m $\in$ M. Let us examine two arbitrary models m_1 and m_j. Their difference can be explained by both the amounts of a priori information taken into account and by those hypotheses which were assumed during their determination. In many cases, which are of interest in practice, it can be considered that, in development of various models, the amount of a priori information used is the same, and models (m_1 and m_j) are distinguished only by the nature of what has been assumed (h hypothesis and h_j).

Let us examine the value $\Delta\rho_\Theta(m)$ of functional $\rho_\Theta(m)$, which would correspond to the case of complete coincidence of the assumed models m and models of the real item (this, of course, is a hypothetical situation, but it deserves consideration from the methodical point of view). The value of $\Delta\rho_\Theta(m)$, taking what has been said into account, should be treated as errors in statis-tical measurement (methodical and instrumental). These errors can be calculated, if the probability characteristic $\Theta(\vec{\mathit{l}}'/m)$, cor-responding to the m-th model, is assumed as the true characteristic, i.e., the equality of $\Theta(\vec{\mathit{l}}/m) = \hat{\Theta}(\vec{\mathit{l}})$ is postulated. It is natural to expect that the smallest value of $\Delta\rho_\Theta(m)$, for an assumed set M, will occur for the basic model m_0, i.e.,

$$\inf_{m\in M}\Delta\rho_\Theta(m) = \Delta\rho_\theta(m_0). \tag{8}$$

128

Let ε be a positive number, the value of which is determined by proceeding from the specifics of the problem solved and characteristics of the research. Further, let the value

$$\Delta \rho_\theta (m, \varepsilon) = (1 + \varepsilon) \Delta \rho_\theta (m_\theta) \tag{9}$$

correspond to the magnitude of the error in statistical measure- /120 ments, increased by $(1 + \varepsilon)$ times. If, in carrying out experimental research, the condition

$$\Delta \rho_\theta (m_0, \varepsilon) > \rho_\theta (m_0). \tag{10}$$

is realized, the research task can be considered completed; if it turns out that

$$\Delta \rho_\theta (m_0, \varepsilon) < \rho_\theta (m_0). \tag{11}$$

the basic model cannot be considered sufficiently equal to the model of the real item. In this case, the set M of initial models must be replaced by another one M_1, so that $M \cap M_1 = \Phi$, further research should lead to a search among the models $m_1 \in M_1$ of the basic one m_0. This procedure should be repeated, introducing successive sets M_R, so that $M_{R-1} \cap M_R = \Phi$, $R = 1, 2, \ldots$, until conditions of type (10)

$$\rho_\theta (m_{R0}) > \Delta \rho_\theta (m_{R0}, \varepsilon_S) \tag{12}$$

do not occur, for the corresponding basic model m_{R0}.

The transition from set M to set M_R, $R = 1, 2, \ldots$, can either not be accompanied by the conduct of new experimental research or can require additional experiments. In the first case, the question is of the necessity for deducing additional hypotheses, which permit the set M_R to be determined and the already existing volume of experimental data to be used for subsequent statistical measurements. In the second case, experimental research is continued and its organization is carried out on the basis of taking account of the specific (new) properties of set M_R.

In this manner, interpretation of the results of experimental research comes down to a search for a basic probability model among all possible models.

REFERENCES

1. Ol'shevskiy, V.V., "The Role of Statistical Measurements in Experimental Research," (this collection).

130

LP-SEARCH AND ITS USE IN ANALYSIS OF THE ACCURACY /121
OF CONTROL SYSTEMS WITH ACOUSTICAL MODELS

V.I. Sergeyev, I.M. Sobol', R.B. Statnikov, and I.N. Statnikov
(Moscow)

One of the approximate methods of estimation of the accuracy of nonlinear statistical systems, containing significant nonlinearities with discontinuous characteristics, is the method of statistical linearization of I.Ye. Kazakov [1]: the actual relationship between the input and output signals of a noninertial nonlinear component is replaced by an approximate relationship, which is linear with respect to the centered input signal, which is equivalent in the statistical sense. The method is restricted in use for a number of reasons, among which can be such as the necessity for assuming the hypothesis of normal distribution of the input signal, and an obligatory analytical connection between the statistical characteristics of the input and output signals [2].

The universal method for solution of statistical problems of nonlinear systems is the Monte Carlo method. It permits the statistical characteristics of the output signals of any nonlinear systems to be found. The presence of an analytical connection between the statistical characteristics of the input and output signals is not obligatory for the method. Its essence is that the values sought in the problem are equated to the parameters of a certain random process. On the basis of the Chebyshev inequality, approximate values of the quantities sought are assumed to be equal to the estimates of the parameters of this process, obtained as a result of statistical treatment of experimental data.

A large number of tests is required to obtain a probability estimate of some event with a sufficiently high degree of accuracy. The errors of the method, at a given confidence level, decrease in inverse proportion to $\sqrt{N}$, where N is the number of tests.

A determinative analog of the Monte Carlo method, the LP-search [3, 4], is proposed for finding the values sought in nonlinear statistical systems. The LP-search is based on the use of nonrandom LP_τ-series of test points $Q_1, \ldots, Q_i \ldots$ [5]. This series has such properties that, for any region U in an n-dimensional cube, there takes place

$$\lim_{N \to \infty} \frac{S_N(U)}{N} = V(U). \tag{1}$$

where V(U) is the volume of this region and $S_N(U)$ is the number of /122 test points Q_i, with numbers $1 \le i \le N$, belonging to U.

131

The LP_τ-series belongs to the class of uniformly distributed series (uds). Convergence of the search with the test points of any uds results from (1), including LP_τ-series.[1] The advantage of the LP-search over the random method follows from estimates of the value of the difference $|S_N(U) - NV(U)|$. If, for random points, the difference $|S_N(U) - NV(U)|$ increases as $\sqrt{N}$, for points $Q_1, \ldots, Q_N$, at all N, the estimate calculated in [4, 5] holds true:

$$S_N(U) - NV(U) \leqslant c(n) \ln^n N \tag{2}$$

Statement of the Problem

To determine such a characteristic of the accuracy of a nonlinear statistical system as the probability of maintenance of the value of the output signal of the system in a given confidence interval. A variant of the block-diagram of the model for solution of the problem is proposed (Fig. 1). Here, 1 is the number sensor $Q_1, \ldots, Q_i, \ldots, Q_N$; 2 is the device for formation of input signals $\overline{X}(t) = \{x_1(t), \ldots, x_n(t)\}$; 3 is the system model; 4 is the counter of the number m of realizations of an output signal $\overline{Y}(t) = \{Y_1(t), \ldots, Y_n(t)\}$ in a given confidence interval; 5 is the counter of the total number N of realizations of an output signal $Y(t)$; and 6 is an m/N divider.

Fig. 1.

random input realizations, a table of nonrandom numbers is used [5].
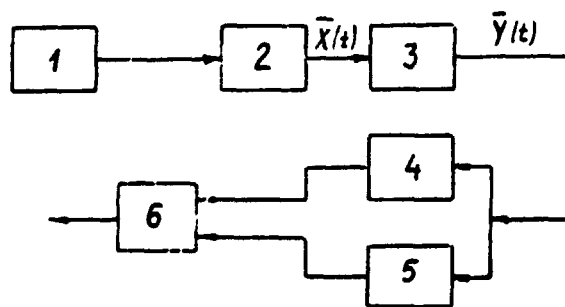
Conclusions

1. To attain the required accuracy in solution of the problem of control of a statistical system in the LP-search, a considerably smaller number of tests is required than in the Monte Carlo method.

2. The LP-search allows /123 the possibility of multiple repetitions of tests under identical conditions and observability of the output variables of the system, since, for processing of

---

[1]In use of the LP_τ-series, there is no difficulty in obtaining numbers, having normal, exponential or any other distribution.

REFERENCES

1. Kazakov, I.Ye. and B.G. Dostupov, <u>Statisticheskaya dinamika neleneynykh avtomaticheskikh sistem</u> [Statistical Dynamics of Nonlinear Automatic Systems], Fizmatgiz Press, Moscow, 1962.

2. Rosin, M.F., <u>Statisticheskaya dinamika i teoriya effektivnosti sistem upravleniya</u> [Statistical Dynamics and Theory of Effectiveness of Control Systems], Mashinostroyeniye Press, Moscow, 1970.

3. Artobolevskiy, I.I., M.D. Genkin, V.K. Grinkevich, I.M. Sobol', and R.B. Statnikov, "Optimization in Theory of Machines by LP-Search," <u>DANSSSR</u> <u>200</u>(6) (1971).

4. Grinkevich, V.K., I.M. Sobol', and R.B. Statnikov, "Determination of Optimum Dynamic Models in Parameter Space," <u>Izv. AN SSSR</u> (4) (1971).

5. Sobol', I.M., <u>Mnogomernyye kvadraturnyye formuly i funktsii Khaara</u> [Multidimensional Area Formulas and Haar Functions], Nauka Press, Moscow, 1969.

ALGORITHM FOR IDENTIFICATION OF A SINGLE CLASS

V.A. Kaminskas
(Vil'nyus)

1. Statement of the Problem

The class of nonlinear dynamic systems being discussed is described by the integral Hammerstein operator:

$$y(t) = \int_0^x w(\lambda) f[x(t-\lambda)] d\lambda. \tag{1}$$

Here, x(t) and y(t) are the input and output signals of the system. The nonlinear amplification coefficient f(x) and weighting function w(λ) are broken down by linear-independent functions:

$$f(x) = \sum_{i=0}^n a_i \varphi_i(x), \qquad \varphi_i(x) = H_i \left(\frac{x}{\sqrt{2\sigma_x}} \right). \tag{2}$$

$$w(\lambda) = \sum_{j=0}^m b_j \psi_j(\lambda), \qquad \psi_j(\lambda) = \sqrt{2x} \, e^{-x\tau} \cdot L_j(2x\lambda). \tag{3}$$

where $H_i(y)$ and $L_j(\lambda)$ are Hermite and Laguerre polynomials.

In accordance with (2) and (3), operator (1) is presented in /124 the form:

$$y(t) = a^T G(t, x) b. \tag{4}$$

where $a^T = (a_0, a_1, \ldots, a_n)$, $b^T = (b_0, b_1, \ldots, b_m)$ are unknown vector parameters; $G(t; \alpha) = \|h_{ij}(t; \alpha)\|$ is the dimensionality matrix $(n + 1) \times (m + 1)$, elements of which

$$h_{ij}(t; x) = \int_0^t \psi_j(\lambda; x) \times \varphi_i [x(t-\lambda)] d\lambda.$$

In connection with the use of computers, in place of operator (4), its discrete analog is studied:

$$y_k = a^T G_k(x) b. \tag{5}$$

134

where $y_k = y(k\Delta t)$, $G_k(a) = G(k\Delta t; \alpha)$ and Δt is the digitization interval.

The task of identification consists of determination of the estimates $\hat{a}$, $\hat{b}$, $\hat{\alpha}$ of the parameters a, b and α of operator (5), by observations under conditions of normal operations or experiment: $x^T = (x_0, x_1, \ldots, x_s)$ and $z^T = (z_0, z_1, \ldots, z_s)$, where $z_k = y_k + N_k$, and N_k are independent errors in observation of the values y_k of the output signal of the system. It is assumed that the mathematical expectation of error is zero and of the dispersion, finite.

2. Algorithm for Calculation of Parameter Estimates

In order for the parameter estimates to be minimized, a root mean quality criterion is required:

$$Q(a, b, x) = \sum_{k=1}^{s} \left(z_k - a^T G_k(x) b \right)^2. \tag{6}$$

The mathematical search for the minimum in the function (6) is carried out in the following manner. The function

$$I(x) = \min_{a \ b} Q(a, b, x). \tag{7}$$

is interpolated and estimates $\hat{a}$, $\hat{b}$ and $\hat{\alpha}$ are determined by solution of the extreme problem

$$\min_{x} I(x) = \min_{x} \min_{a \ b} Q(a, b, x). \tag{8}$$

The technical process of calculation of the estimates looks this way. An initial approximation $\hat{\alpha}_\xi$ is selected, and the extreme problem (7) is solved. For the search for the extreme of criterion (6), at a fixed $\hat{\alpha}_\xi$, the principle of lowering by components, with the Gauss method, is used, leading to an iterated algorithm of the type:

$$\left. \begin{array}{l} \hat{a}_l^z = \left(A_l^T(\hat{x}_\xi) A_l(\hat{x}_\xi) \right)^{-1} A_l^T(\hat{x}_\xi) z \\[2mm] \hat{b}_l^z = \left(B_l^T(\hat{x}_\xi) B_l(\hat{x}_\xi) \right)^{-1} B_l^T(\hat{x}_\xi) z \end{array} \right\} \quad l = 1, 2, \ldots, \tag{9}$$

135

where $\quad A_i(\dot{x}_z) = b_i^{-T} G_k^T(\dot{x})_z$, $B_i(\dot{x}_z) = a_i^{-T} G_k(\dot{x}_z)$, $k = 1, s.$

Further, by known methods [1] of the search for the extreme of the function of one variable $I(\alpha)$, for example, by the Fibonacci method, a new value $\hat{\alpha}_{+1}$ is determined. After this, we immediately turn to algorithm (9), etc., while the process converges.

3. Reduction of the Estimates of $\hat{f}(x)$ and $\hat{w}(\lambda)$

As investigation has shown, the algorithm described above permits calculation only of the estimates $\hat{c}$, corresponding to the products of the parameters of the type $a \cdot b^T = c$. For reduction of the estimates $\hat{w}(\lambda)$ of the weight function $w(\lambda)$ and estimates $\hat{f}(x)$ of the nonlinearity $f(x)$, a method was developed, using the equality

$$\int_0^x w(\lambda)\,d\lambda = K. \tag{10}$$

where K is the amplification coefficient of the linear portion of the model. The estimates $\hat{a}$ and $\hat{b}$ are reduced by estimates of $\hat{c}$, of the corresponding equations:

$$\left. \begin{aligned} \frac{\hat{b}_j}{\hat{b}_v} &= \frac{\displaystyle\sum_{i=0}^{n} \hat{c}_{ij}}{\displaystyle\sum_{i=0}^{n} \hat{c}_{iv}} \\ \sum_{j=v}^{m} \hat{b}_j \int_0^{\alpha} \hat{\psi}_j(\lambda; \hat{x})\,d\lambda &= K \end{aligned} \right\} \quad j = 0, 1, \dots \partial-1, \partial+1, \dots m \tag{11}$$

$$\hat{a}_i = \frac{\displaystyle\sum_{j=0}^{m} \hat{c}_{ij}}{\displaystyle\sum_{j=0}^{m} \hat{b}_j}, \qquad i = 0, 1, \dots, n \tag{12}$$

In those cases when k is unknown, it should be assumed as unity. Then, the estimates $\hat{w}(\lambda)$ and $\hat{f}(x)$ are reduced only with an accuracy of the factors 1/ and k, respectively.

136

4.   Generalization in the Case of a Multidimensional System

The results obtained above are easily generalized in the class of multidimensional systems of the type:

$$y(t) = \sum_{\mu=1}^{q} \int_{0}^{z} w^{\mu}(\lambda) f^{\mu}[x^{\mu}(t-\lambda)] d\lambda.$$

(13)

If it is designated that

$$\left. \begin{array}{l} A_i(x_z) = b_{zi}^{iT} G_k^{zT}(x_z) , \quad B_i(x_z) = a_{zi}^{iT} G_k^{z}(x_z^{i}) \\ a^T = (a^{z}), \quad b^T = (b_i^{z}) \quad x^T = (x^{\mu}), \quad k = 1, s, \quad \mu = 1, q \end{array} \right\}.$$

(14)

the formal mathematical record of the algorithm of identification of the system (13) coincides with the algorithm for a unidimensional system.

5.   Physical Interpretation of the Class of Systems Examined

Structurally, this class of systems is a series combination of the noninertial nonlinearity $f(x)$ with the linear dynamic element, the weight function of which is $w(\lambda)$. Applying a Laplace transform to operator (1), in accordance with (3), we obtain:

$$y(p) = \sum_{j} b_j \frac{(p-z)^j}{(p-z)^{j-1}} \cdot f(p).$$

(15)

where $y(p)$ and $f(p)$ are the Laplace transforms of the functions $y(t)$ and $f[x(t)]$, respectively. From the latter equality, the dynamic characteristics of the system (transmission function, differential equations, etc.) of interest to us can be obtained.

The program putting the algorithm described above into practice was developed in ALGOL-60 algorithmic language.

137

REFERENCES

1. Wild, D.G., Metody poiska ekstremuma [Methods of Search for the Extreme], Moscow, 1967.

138

IDENTIFICATION OF AN OBJECT
BY INPUT AND OUTPUT SPECTRAL CHARACTERISTICS

S.F. Red'ko, V.F. Ushkalov
(Dnepropetrovsk)

The problem is discussed of identification of a linear object of known structure, the movement of which is described by a system of differential equations of the type

$$\dot{y} = Ay + Bu \tag{1}$$

where y is an n-dimensional output vector, u is an m-dimensional vector of staticnary, random disturbances (inputs), A and B are matrices of unknown parameters of the dimension, $n \times n$ and $n \times m$, respectively. The spectral and reciprocal spectral densities of the inputs and outputs are used as the initial information on the object.

The relations connecting the unknown parameters of the object with the input and output spectral densities can be presented in the form

$$i\omega S_{yu} = A S_{yu} + B S_{uu}, \tag{1a}$$

where S_{uu} and S_{yu} are the vectors of the spectral and reciprocal spectral densities of the inputs and outputs. Construction of a model of the object

$$i\omega \hat{S}_{yu} = C \hat{S}_{yu} + D S_{uu}, \tag{2}$$

which is the best in the sense of the minimum root mean error, is conveniently carried out [1] in the following manner. We present the estimate of $\hat{S}_{yu}$ in the form

$$\hat{S}_{yu} = S_{yn}^{(0)} + \Gamma_p, \tag{3}$$

where $S_{yn}^{(0)}$ is determined from the equation

$$i\omega S_{yu}^{(0)} = C_0 S_{yu}^{(0)} + D_0 S_{uu}, \tag{4}$$

139

p is the vector of increment of the parameters of the matrices C and D, and Γ is the sensitivity function of the evaluation $\hat{S}_{yu}$, by elements of the vector

$$p \left(\text{i.e.} \ \Gamma = [(\hat{S}_{yu})_{p_1}, \ (\hat{S}_{yu})_{p_2}, \dots, (\hat{S}_{yu})_{p_n}] \right).$$

C_0 and D_0 are the initial values of the matrices C and D.

Estimation of the vector $\hat{p}$, the best in the sense of the minimum root mean error [1, 2], equals

$$\hat{p} = \left[\int_{\omega_{\text{init}}}^{\omega_{\text{end}}} \Gamma^T W \Gamma \, d\omega \right]^{-1} \left[\int_{\omega_{\text{init}}}^{\omega_{\text{end}}} \Gamma^T W (S_{yu} - \hat{S}_{yu}) \, d\omega \right]. \tag{5}$$

where W is the weight matrix.

Elements of the vector Γ are determined as the solution of the system of equations of sensitivity

$$i\omega (\hat{S}_{yu})_{p_j} = C_0 (\hat{S}_{yu})_{p_j} + \frac{\partial F}{\partial p_j} S_{yu} + \frac{\partial G}{\partial p_j} S_{uu}. \qquad j = 1, 2, \dots \tag{6}$$

where F and G are the matrices of the increments of matrices C and D, respectively:

$$C = C_0 + F, \quad D = D_0 + G \tag{7}$$

The procedure for estimation of the unknown parameters was reduced to numerical solution of Eqs (4)-(7). The use of the input and output spectral characteristics as the initial information leads to substitution of differential equations (1) by algebraic ones (1a). The initial approximation $S_{yu}^{(0)}$ and the elements /128 of vector Γ are determined by way of solution of the system of algebraic equations (4) and (6):

$$S_{yu}^{(0)} = [i\omega E - C_0]^{-1} D_0 S_{uu}.$$

$$(\hat{S}_{yu})_{p_j} = [i\omega E - C_0]^{-1} \left[\frac{\partial F}{\partial p_j} S_{yu} + \frac{\partial G}{\partial p_j} S_{uu} \right]. \qquad j = 1, 2, \dots$$

140

Substitution of the differential equations by algebraic ones leads to decrease in the quantity of calculations and amount of data which must be stored in the computer memory.

The algorithms were put into practice in the Minsk-22 computer. Examples of identification of dynamic objects are presented.

REFERENCES

1. Deneri, "Identification Algorithm, Insensitive to Errors in Initial Estimates of Parameters," Raketnaya tekhnika i kosmonavtika 9(3) (1971).

2. Ruban, A.I., "Observation and Identification Algorithm for Nonlinear Dynamic Objects," Izv. AN SSSR, Tekhnicheskaya kibernetika (3) (1971).

SYNTHESIS OF AN OBSERVATION OPERATION
AND THE PROPERTY OF COMPLETE OBSERVABILITY OF NONLINEAR OBJECTS

Ye.A. Gal'perin
(Moscow)

The statement and solution of the problem of observation of a linear object from incomplete information is well-known. The problem of observation of a nonlinear system is similar and consists of the following. The known dynamic properties of the object are expressed by the equation

$$\frac{dx}{dt} = f(x,t) \quad x \in \{R^n\}. \quad t \geqslant t_0 \tag{1}$$

The initial data $x(t_0)$ are unknown; however, the quantities comprising the l-vector of information are measured on trajectories (1)

$$y(t) = h(x,t) \quad y \in \{R^l\} \quad l < n \tag{2}$$

Equations (2) cannot be solved for x. It is required that the motion be restored, i.e., that x(t) be found, using (1) and (2) in a certain interval $[\alpha, \beta]$ of the previous history of the process.

Since an inverse resolving operation cannot be synthesized, as is done for linear systems, an operation-procedure is synthesized, including solution of a certain experimental problem. The /129 generally accepted meaning of the ALGOL procedure is included in the understanding of the procedure.

The observation operation is set by synthesis of an observable signal Y, generating the N-vector-function Φ, defining the observation procedure. Computing by the known integration operator

$$x(t) = g(x_0, t_0, t) \quad t \geqslant t_0 \tag{3}$$

and assuming normal properties of continuity or differentiability in (1), (2) and (3), we can synthesize the following observation operations.

1. Integral observation operations.

142

Signal	Generating function

$$Y_0(t) = y(t); \qquad \Phi_0(z, t) = h(z, t)$$

$$Y_1(t) = \int_t^{t_s} y(\tau) d\tau; \qquad \Phi_1(z, t) = \int_t^{t_s} h[g(z, t, \tau)] \, d\tau \qquad (4)$$

$$t_s = t + \Theta z_s, \quad \Theta > 0, \quad 0 < z_s \leqslant 1 \ (s = 1, \ldots, p); \quad z \varepsilon \{R^n\}$$

2. Differential observation operations.

Signal	Generating functions

$$Y_0(t) = y(t);$$
$$\Phi_0(z, t) = h(zt)$$

$$Y_1(t) = \frac{dy}{dt}; \qquad \Phi_1(z, t) = \frac{d\Phi_0(x, t)}{dt}\bigg|_{x=z} = \frac{\partial h(z, t)}{\partial t} +$$

$$+ \sum_{i=1}^{n} \frac{\partial h}{\partial z_i} \cdot f_i(z, t) \qquad (5)$$

$$Y_s(t) = \frac{d^s y}{dt^s}; \qquad \Phi_s(z, t) = \frac{d\Phi_{s-1}(x, t)}{dt}\bigg|_{x=z} \qquad (s = 2, \ldots, p)$$

3. Combined observation operations.

These operations include repeated integration or mixed integral-differential syntheses.

Let us examine the system $N = 1 \cdot (p + 1)$ of equations with n unknowns

$$\Phi(z, t) = Y(t) \qquad (6)$$

System (6) always has a solution: obviously, the actually realized condition x(t) in (1) is such. However, it is not simple to find this condition, in view of the following: 1. The inverse operator $\Phi^{-1}(z, t)$ does not exist everywhere and, in any case, is not expressed in explicit form; 2. the function $\Phi(z, t)$ does not exist in explicit form in integral observation operations, but only in the form of procedures which can be put into practice in a computer; 3. the set of solutions (6) can be finite, countable /13 or continual. These circumstances lead to the necessity for a synthesis and solution of the extreme problem in place of Eq. (6).

Let us designate any vector appropriate to the standard by $||x||$, let us select the closed set $Z(t)$, presumably containing the conditions sought $x(t)$, and let us formulate the mathematical programming problem

$$\begin{cases} F(z, t) - \Phi(z, t) - Y(t)|| \to \min_z \\ z \in Z(t) \subset \{R^n\} \end{cases} \tag{7}$$

The procedure of observation of movement $x(\tau)$, $\tau \geq t$ consists of the following stages. formation of an observable signal and the generating function, solution of problem (7) and search among the "null" $\{F(z, t = 0\}$ solutions of the actual condition $x(t)$, and integration of (1), at $x_0 = x(t)$.

In this form, with a one-time solution of the extreme problem, the procedure is a prediction system. If the integration limits are presented in (4), $\theta < 0$ is assumed, the left differentiation is implied in (5) and a continuous solution of the series of extreme problems is carried out, a servo system is produced, which is suitable for use in a control device. The presence of a controlling action in (1) does not introduce significant complications.

The system (1)-(2) is fully observable at moment t in region $Z(t)$, if the observation operation can be synthesized so that the set of "null" solutions of problem (7) is finite or empty.

Theorem

The generating function $\Phi(z, t)$ ensures complete observability of system (1)-(2), in a closed vicinity of points z_0 at moment t, if the rank of its Jacoby matrix $E\Phi/\partial z$ at point z_0 equals the order of the system.

Fulfilment of the conditions of the theorem in the region $Z(t)$ guarantees that the calculation procedure of the observation can be put into practice. In linear systems, this condition is necessary and sufficient, and, in stationary ones, is reduced to the known R.Ye. Kalman condition: rank $(H', A'H', \ldots, A'^{(n-1)}H') = n$.

144

ANALYSIS OF SPECTRA OF ACOUSTICAL SIGNALS
AT THE OUTLET OF A NONLINEAR SYSTEM UNDER THE ACTION OF THE
SUM OF THE HARMONIC SOURCES

Yu.D. Sverkunov
(Moscow)

A system for analysis of components of the noise and vibration spectra of an internal combustion engine was described in work [1], and the problem was stated of determination of the transfer function of a noise or vibration propagation channel, by means of measurement of the amplitudes and phase of discrete components of the spectra. Such an analysis can be greatly simplified, if specific relations between components of the spectra at the outlet of a nonlinear system are established. This report is devoted to establishment of such relations.

Let there be an input action

$$u_{in} = u_0 + \sum_{i=1}^{n} u_i \cos(\omega_i t + \varphi_i)$$

A characteristic of a noninertial, nonlinear element $u_{out} = f(U_{in})$ is the exponential polynomial

$$f(U_{in}) = k_0 + k_1(u_{in} - u_0) + \ldots k_s(u_{in} - u_0)^s + \ldots + $$
$$+ k_{sm}(u_{in} - u_0)^{Sm}$$

(1)

We assume that frequencies ω_i are not multiples. The signal at the nonlinear system outlet consists of a set of combinations of frequencies (CF). It is convenient to assign a set of coefficients $[b_1, \ldots, b_n]$, taking the values of any whole numbers, as well as zero, to any CF, for example, $b_1\omega_1 + b_2\omega_2 + \ldots + b_n\omega_2$, during the action of a sum n of harmonic signals at the inlet. For the CF amplitudes $[b_1, \ldots, b_n]$, which we designate $U_{[b_2, \ldots, b_n]}$, at the outlet of a nonlinear system, the formula was obtained in work [2], with the given expression (1),

$$U_{[b_1, \ldots, b_n]} = \sum_{s=0}^{\left[\frac{Sm-q}{2}\right]} \frac{k_{q+2s}}{2^{q+2s-1}} (q+2s)! \times$$

(2)

$$\times \sum_{i=1}^{C_{s+n-1}^{n-1}} \frac{u_1^{2a_{1i}^{(n)}-b_1} \dots u_n^{2a_{ni}^{(n)}-b_n}}{a_{1i}^{(n)}! \dots a_{ni}^{(n)}! (a_{1i}^{(n)}+b_1)! \dots (a_{ni}^{(n)}+b_n)!}$$

where $a_{1_i}, \dots, a_{n_i}$ is the i-th partitioning of the quantity s in /132
n whole, nonnegative terms;

$$q = \sum b_i$$ is called the order of the given CF;

[d] is the integral part of d; C_m^n is the number of combinations of
m with n.

Let us examine formula (2) for only one term of the external

sum, which is the CF amplitude $U_{[b_1,\dots,b_n]}^{(q+2s)}$ at the outlet of a

parabola of degree q + 2s.

Extracting the quantity s in n nonnegative terms from the
set of partitionings of the subsets with $a_p = 0, 1, 2, \dots, s$, a
lower order formula of the representation $U_{[b_1,\dots,b_n]}^{(q+2s)}$ over the
CF amplitude can be obtained:

$$U_{[b_1,\dots,b_n]}^{(q+2s)} = \sum_{j=0}^{s} \frac{U_p^{(b_p)-2j}}{j!(j-b_p)!} U_{[b_1',\dots,b_{n-1}']|b_p|-2j}^{(q_{n-1}+2s-2j)} \qquad (3)$$

where $U_{[b_1,\dots,b_n]/|b_p|+2j}^{(q+2s-2j)}$ is the CF amplitude $[b_1', \dots, b_{n-1}'] =$

$= [b_1, \dots, b_{p-1}, b_{p+1}, \dots, b_n]$ at the outlet of a parabola of

degree $q_{n-1} + 2s - 2j$, with the proportionality coefficient

$$K_{q+2s}, \quad q_{n-1} = \sum_{i=1}^{n-1} b_i'; \qquad p \in \{1, 2, \dots, n\}.$$

All CF of order q can be broken into subsets of adjustable CF
(ACF), which are produced by means of every kind of adjustment of

the set of n numbers, m of which are different, $b_1, \dots, b_n \left(b_i \geqslant 0, \sum_{i=1}^{n} b_i = q \right)$.

146

The number of such ACF equals $n!/(n-m)!$. Expression (3) permits the relation between the ACF amplitudes to be made apparent. We will assume below that $u_1 \geq u_2 \geq \ldots \geq b_1 \geq b_2 \geq \ldots \geq b_n$. Then, for $n = 2$, it can be shown that $U_{[b_1,b_2]}^{(q+2s)} \geq U_{[b_2,b_1]}^{(q+2s)}$ for any s.

For $n = 3$, there are six ACF in all. The correlation among their amplitudes is determined by means of (3) and can be shown schematically with the aid of Fig. 1. In Fig. 1, the ACF amplitudes are provisionally designated by numbers obtained from their subscripts, which are ordered in sequence by columns from top to bottom in each column. The sign $\geq$ is conditionally replaced by an arrow here, directed from the greater amplitude to the lesser one, and the sign $\leftrightarrow$ designates an indefiniteness correlation. For example, $132 \rightarrow 231$ means that $U_{[b_1,b_3,b_2]}^{(q+2s)} \geq U_{[b_2,b_3,b_1]}^{(q+2s)}$, and

$132 \leftrightarrow 231$, that $U_{[b_1,b_3,b_2]}^{(q+2s)} \lesseqgtr U_{[b_2,b_3,b_1]}^{(q+2s)}$. The latter is easily <u>/133</u> established, assuming initially that $u_1 = u_2 > u_3$, and then that $u_1 > u_2 = u_3$, at $b_1 > b_2 > b_3$.

Let us examine the correlation for arbitrary n. By analogy with polynomials of several variables, we will call the ordered set ACF a lexicographic series (LG series), i.e., we will consider that the CF $[b_1',\ldots,b_n']$ is located higher in the LG series than its ACF $[b_1'', b_n'']$, if $b_1' \geq b_1''$, in which, if $b_1' = b_2'$, $b_2' \geq b_2'$ at $b_2' = b_2''$, $b_3' \geq b_3''$, etc., so that, in the final analysis, $b_k' > b_k'$, where $k \leq n - 1$.

Theorem

If CF $[b_1', \ldots, b_n']$ is higher in the LG series than CF $[b_1'', \ldots, b_n'']$, there always are such correlations of the initial amplitudes, not going beyond permissible limits, at which $U_{[b_1',\ldots,b_n']}^{(q+2s)} > U_{[b_1'',\ldots,b_n'']}^{(q+2s)''}$.

Proof

In the ACF being examined, let b_k' and b_k'' be the first different coefficients, i.e., $b_k' > b_k''$. Then, assuming that $u_k > u_{k+1} = u_{k_2} = \ldots = u_n$, all coefficients b_i' and b_i'' can change places, for $k + 1 \leq i \leq n$, so that they all coincide in pairs in both ACF,

except one pair. After this, using break-down formula (3) n-K-2 times, we reduce the comparison of the initial ACF amplitudes to a comparison of $U_{[b'_k, b''_k]}^{(q+2s)}$ and $U_{[b''_k, b'_k]}^{(q+2s)}$. It follows from their inequality that $U_{[b''_1, \ldots, b'_n]} < U_{[b''_1, \ldots, b''_n]}$, which was required to be proven.

Breaking down the LG series, in the form of a sequence of n columns, by (n - 1) amplitudes in each column, we obtain a table, which can be called a lexicographic matrix (LG matrix). By means of the latter, a set of correlations between the ACF amplitudes is established. In each column of the LG matrix, the correlations between amplitudes are the same as in a LG matrix with a smaller dimension per unit, which we will consider known. The sign → always stands between neighboring elements of an LG matrix in a single row, as in Diagrams 1 and 2, so that they will always differ by only two coefficients.

It is easy to establish the correlations between any ACF amplitudes in neighboring columns, if they are not obviously of the same LG matrix. For this, it is sufficient to assume $b'_1 = b''_1$, after which the comparison of amplitudes of neighboring columns is reduced to a comparison of the amplitudes located in a single column.

A matrix for n = 4 is presented in Fig. 2 as an example. In this manner, a lexicographic matrix graphically shows the correlations between the amplitudes of the overwhelming majority of ACF.
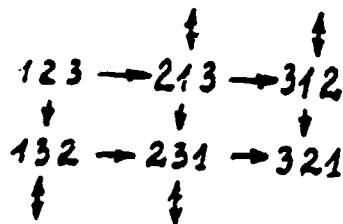
Fig. 1.

The established correlations, /134 all coefficients of the same parity of which have the same sign, hold true for nonlinear systems, described by polynomials or exponential series. since the inequalities obtained are intensified in this case. Thus, the correlations obtained prove to be true for a quite extensive class of functions.

$$
\begin{array}{ccc}
\uparrow & \uparrow & \uparrow \\
1234 \rightarrow 2134 \rightarrow 3124 \rightarrow 4123 \\
\uparrow & \uparrow & \uparrow & \uparrow \\
1243 \rightarrow 2143 \rightarrow 3142 \rightarrow 4132 \\
\uparrow & \uparrow & \uparrow & \uparrow \\
1324 \rightarrow 2314 \rightarrow 3214 \rightarrow 4213 \\
\uparrow & \uparrow & \uparrow & \downarrow \\
1342 \rightarrow 2341 \rightarrow 3241 \rightarrow 4231 \\
\uparrow & \updownarrow & \uparrow & \uparrow \\
1423 \rightarrow 2413 \rightarrow 3412 \rightarrow 4312 \\
\downarrow & \downarrow & \downarrow & \downarrow \\
1432 \rightarrow 2431 \rightarrow 3421 \rightarrow 4321 \\
\uparrow & \uparrow & \uparrow
\end{array}
$$
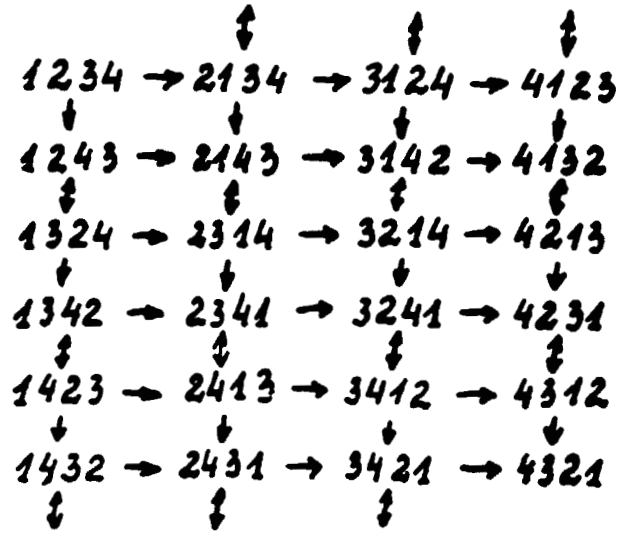
Fig. 2.

REFERENCES

1. Urban, P., "Noise Analysis by Synchronous Filtration," Acustica 20(5) (1968).

2. Sverkunov, Yu.D., "Analysis of Spectra at the Outlet of a Non-linear System," Radiotekhnika 7 (1972).

THE USE OF STATISTICAL CHARACTERISTICS OF REDUCER VIBRATIONS AS DIAGNOSTIC SYMPTOMS

F.Ya. Balitskiy, M.D. Genkin, M.A. Ivanova, and A.G. Sokolova

(Moscow)

The vibrations of a gear drive are a random process, carrying information on various parameters, i.e., on the condition of the transmission [1, 2].

It is well-known [3] that complete information on a random process can be obtained from an n-dimensional amplitude probability distribution pattern. Nevertheless, the most widespread characteristic of a random process up to this time is the spectral density, owing to its accessibility. In fact, in some cases, the spectral characteristic is a good diagnostic symptom, for example, when various spectral components are unambiguously connected to specific kinematic pairs. Otherwise, it is useful to have data on the connections between various frequency components of the spectrum [4]. Such a possibility was revealed during study of two-dimensional distribution patterns and their accompanying torque characteristics.

The results of a statistical analysis of the vibrations of the experimental RS-1 reducer stand, with a spiral-gear transmission, operating on a closed circuit, are presented. The analysis was carried out on the Minsk-2 and Minsk-32 digital computers, with two-channel analog-digital converter, built in the Institute of the Science of Mechanics. Two-dimensional distribution patterns, conditional dispersions and dispersion ratios were calculated. The octave-band-filtered first harmonics of the tooth frequency f_z of the vibrations at two different measurement points were considered as the components of the vibration process to be analyzed. The regression lines, corresponding to different values of the loading torque, are represented in Fig. 1. Since it was not the gear drive parameters which were determined by diagnostic methods, but the characteristics most sensitive to change in state of the object of the investigation, the loading torque, which is the simplest and most accessible for measurement, was chosen as the condition parameter.

The slope of the regression lines changes from 0 to $\pi/4$ with increase in load (Fig. 1), i.e., the angle of inclination of the regression line can serve as a characteristic of the condition. The regression lines become essentially nonlinear at large loads, and the $\bar{x}(y)$ and $\bar{y}(x)$ curves run together in the middle sections, which is evidence of the appearance of a strong connection between the processes. The square of the dispersion ratio $\eta_{Y/X}^2$ can serve as a quantitative estimate of such a characteristic as closeness of a connection (see Table 1).

150
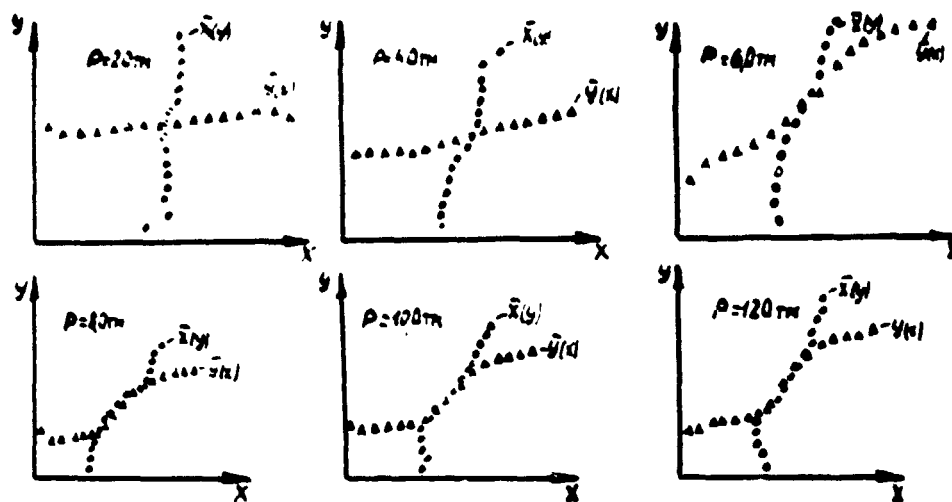
Fig. 1.

TABLE 1.

Load, P (kg-m)	2	4	6	8	10	12
$\eta^2\, Y\, X$	0.033	0.064	0.211	0.43	0.464	0.423

The filtered first x(t) and second y(t) harmonics of the tooth frequency also were considered as components of the vibration process to be analyzed. The nature of the regression lines $\bar{y}(x)$ changes with change in load (Fig. 2). The dispersion ratio, the values of which are presented in Table 2, also can serve as a quantitative estimate of the closeness of the connection between the first and second harmonics of the tooth frequency. Convex regression lines are arbitrarily indicated by the symbol (+), and the concave ones, by the symbol (-), in the bottom row of the table.

The conditional dispersions were calculated for the same vibration components and values of the loading torque. The schedastic lines DY/X, illustrating the relationship of the trend /138 of these curves to the value of the condition parameter, are represented in Fig. 3. The more characteristics are used for identification, the greater the probability of a correct identification of the dynamic condition of a complex object.
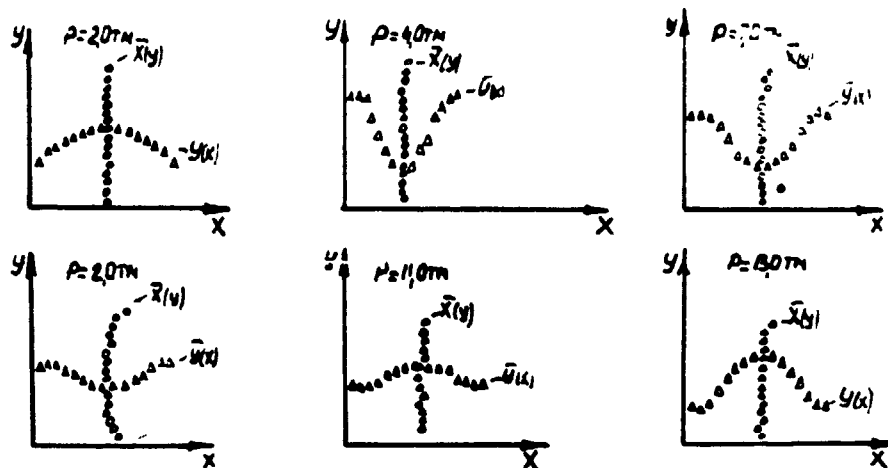
Fig. 2.

TABLE 2.

Load, P (kg-m)	2	4	7	9	11	13
r_i^2 $Y_i X$	0.03	0.53	0.52	0.35	0.08	0.65
Sign	+	–	–	–	+	–
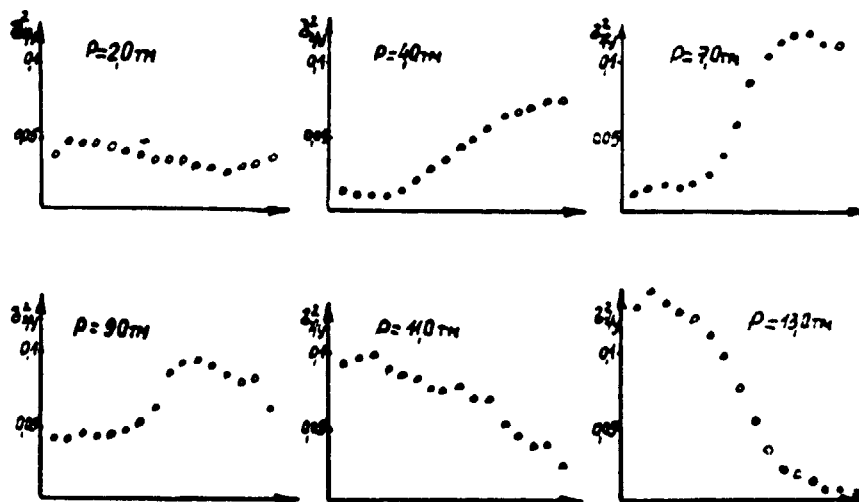
Fig. 3.

The statistical characteristics described above are a set of informative diagnostic characteristics for other condition parameters of a gear drive, and they facilitate making a mathematical model of gear meshing more precise, as well.

REFERENCES

1. Balitskiy, F.Ya. and A.G. Sokolova, "Diagnostics of the Condition of a Planetary Reducing Gear for Certain Parameters, Materialy Vsesoyuznogo simpoziuma 'Novyye metody issledovaniya shumov i vibratsiy i kiberneticheskaya diagnostika mashin i mekhanizmov'[Materials of All-Union Symposium, 'New Methods of Investigation of Noises and Vibrations and Cybernetic Diagnostics of Machines and Mechanisms'], Kaunas, 1970.

2. Petrusevich, A.I., M.D. Genkin, and V.K. Grinkevich, Diagnosticheskiye nagruzki v zubchatykh peredachakh s pryamozubnymi kolesami [Diagnostic Loads in Gear Drives with Spur Gear Wheels], USSR Academy of Sciences Press, 1956.

3. Levin, B.R., Teoriya sluchaynykh protsessov i eye primeneniye v radiotekhnike [Theory of Random Processes and Its Use in Radio Engineering], Sovetskoye Radio Press, Moscow, 1957.

4. Gershman, S.G. and V.D. Svet, "The Use of the Methods of General Correlation Theory for Analysis of Acoustical Noises," Tezisy dckladov VII Vsesoyuznoy akusticheskoy konferentsii [Summaries of Reports, VIIth All-Union Acoustical Conference], Leningrad, 1971.

THE USE OF BISPECTRA FOR PURPOSES OF ACOUSTICAL DIAGNOSTICS

F.Ya. Balitskiy, M.D. Genkin, M.A. Ivanova, and A.G. Sokolova
(Moscow)

In a diagnostic examination, it always is useful to extract from the entire volume of information included in a visualization of a vibroacoustical process that part which reacts most sharply to change in the condition parameters of the diagnostic object. Most often, the frequency range of the examination is limited.

In a number of cases, a priori determination of the informative sections of the spectrum presents great difficulties; therefore, additional information is necessary. Thus, for example, in mathematical modeling of such objects of diagnostics as a gear drive, the accuracy of the linear approximation or degree of nonlinearity of this vibrational system must be estimated. To estimate the degree of nonlinearity of the system, for example, by the dispersion ratio [1] over a wide frequency range is inadvisable, because of the great magnitude of error. At the same time, for an esti- /139 mate of the degree of nonlinearity in a narrow frequency band, frequency subranges must be chosen, in which it is expedient to make such an estimate. It is proposed to use a bispectral analysis of 2,3 vibroacoustical processes for this.

If a random process can be considered as the linear superposition of statistically independent components, the power spectrum (two-dimensional characteristic) is adequate for its complete characterization:

$$F(\omega) = \frac{1}{2\pi} \int B(\tau) e^{-i\omega\tau} d\tau = X(\omega) X^*(\omega). \tag{1}$$

where $B(\tau) = \overline{x(\tau)x(t + \tau)}$ is a unidimensional correlation function, and

$$X(\omega) = \frac{1}{2\pi} \int_{-\infty}^{\infty} x(t) e^{i\omega t} dt.$$

In nonlinear systems, the spectrum becomes nontrivial, dif- /140 ferent combination frequencies appear and the interrelation of different portions of the spectral range can be detected by the bispectrum, a three-dimensional frequency characteristic:

154

$$S(\omega_1, \omega_2) = \left(\frac{1}{2\pi}\right)^2 \int\limits_x^x \int B(\tau_1, \tau_2) e^{-i(\omega_1 \tau_1 + \omega_2 \tau_2)} d\tau_1 d\tau_2 = \quad (2)$$

$$= X(\omega_1) X(\omega_2) X^*(\omega_1 + \omega_2)$$

Here, $B(\tau_1, \tau_2) = x(t) x(t + \tau_1) x(t + \tau_2)$ is a two-dimensional correlation function.

The results of a bispectral analysis of vibrations produced by a III 8 experimental reducer stand, with a spur gear single-stage transmission, in the mode n = 700 rpm, at various values of the loading torque (p_1 = 100 kg-m, p_2 = 250 kg-m), are shown in Figs. 1 and 2. The frequency <u>/141</u> count numbers are laid out along the coordinate axes, at 156 Hz intervals and the tooth frequency harmonics f_z are designated; the level lines are represented on the sheet. The pole projections on the coordinate axes indicate the interacting frequencies of the vibration spectrum, and the bispectrum amplitude in the pole characterizes the magnitude of the connection between frequencies.

Fig. 1.

A mode, for which the system studied can be considered as linear (the bispectral function maximum is observed only at the exciting frequencies), is indicated in Fig. 1. The appearance of a series of combination frequencies, which are the result of non-linear interaction of the tooth frequency harmonics and the exciting frequencies of the ball bearing support, are evident in Fig. 2.

2 4 6 8 10 12 14 16 18 20 22 24 26 28 30

f_2
$2f_2$
$3f_2$
$4f_2$

2 4 6 8 10 12 14 16 18 20 22 24 26 28 30

f_2 $2f_2$ $3f_2$ $4f_2$

Fig. 2.

In this manner, in this mode of operation of the reducer stand (p = 250 kg-m), the vibrations of the system have a clearly nonlinear nature, and the two-dimensional simplex (Fig. 2) permits specific frequency bands to be selected for quantitative estimates of the degree of nonlinearity by other well-known methods [1].

REFERENCES

1. Balitskiy, F.Ya. et al., "Use of the Dispersion Ratio in Estimating the Nonlinear Properties of an Object of Diagnosis," (article included in this collection).

156

USE OF THE DISPERSION RATIO IN ESTIMATING
THE NONLINEAR PROPERTIES OF AN OBJECT OF DIAGNOSIS

F.Ya. Balitskiy, M.D. Genkin, M.A. Ivanova, A.A. Kobrinskiy,
and A.G. Sokolova
(Moscow)

One of the most significant moments in the process of diagnosing the condition of an object by its vibroacoustical characteristics is the construction of a mathematical model of the object and estimation of those parameters of this model (i.e., corresponding to the coefficients of the equations), direct measurement of which is impossible, for one reason or another. In those cases, when the mathematical model is described by a system of linear differential equations, the method of determination of such coefficients has been developed in sufficient detail [1]. However, the question as to whether or not a linear mathematical model describes the characteristics of the object being examined sufficiently well is fundamental in a number of cases. The basic factors determining the nonlinear properties of an object are /142 the relationships of certain of its parameters or acting forces to its condition, i.e., the vector of the phase coordinates of the object.

There is significant interest in estimating the nonlinear properties of such complex objects of diagnosis as gear drives. A relation of the rigidity of the meshing to wheel position, the generation of shock pulses upon entry of the teeth into the mesh [2] and significantly nonlinear vibroshock modes of motion, connected with systematic wear of the profiles of the meshing teeth [3, 4] can be observed in them. Direct measurement of the forces of interaction of the teeth arising during operation is impossible for gear meshing, as a consequence of which, data of the diagnostic analysis is restricted to only the vibrations of the gears stimulated by these forces, which can be considered as a vibroacoustical signal at the system outlet.

Known methods of estimation of the nonlinear properties of an object have been developed for automatic control systems, based on measurements of the so-called dispersion ratio [5]

$$\eta_{yx}^2 = \frac{D[M(y\,|\,x)]}{D[y]}$$

between signals x at the inlet and y at the outlet of the object. The dispersion ratio defines the degree of functional connection

between random values of x and y (at $\eta = 1$, we have an exact functional relationship $y = f(x)$), in distiction from the correlation coefficient R_{xp}, which describes the extent of the linear connection of these values. The dispersion ratio lies in the range

$$R_{yx} \leqslant \tau_{\iota yx} \leqslant 1.$$

the relatiorship between the values of x and y is linear at $\eta_{xp} = |R_{yx}|$. Considering these properties of the dispersion ratio, we determine the degree of nonlinearity of the object of control by the connection of the signals at the inlet and outlet in the following manner [6]:

$$\nu_{yx}^{j} = 1 - \frac{R_{yx}^{j}}{\tau_{iyx}^{2}}.$$

(2)

Similarly, the degree of nonlinearity of the diagnostic object can be determined by two output signals, if the two corresponding outlets are separated by a term, the linearity of which is hypothetical. In the linear case, Eq. (2) becomes zero and, with significant nonlinearity of the object, ν_{yx} differs sharply from zero.

An expe.imental investigation for estimating the nonlinearity $\underline{/143}$ of a diagnostic object was carried out on a single-stage, spur gear reducer. The linearity of the properties of spur gearing (including the linearity of its mode of operation) was tested. Torsional vibrations of the driven wheel and transverse (to the meshing plane) vibrations of the drive wheel on its support were taken as the two outputs of the object to be analyzed. The results of the investigation showed that the degree of nonlinearity of a reducing gear is essentially connected with its operating mode, so that different mathematical models of it can correspond to different values of the system parameters.

REFERENCES

1. Genkin, M.D. V.I. Sergeyev, and L.V. Sukhorukov, "Calcula-
    tion-Experimental Investigation of the Dynamics of Reducing
    Gears, Using Computers," in the collection Vibroakustiches-
    kaya aktivnost' mekhanizmov s zubchatymi peredachami [Vibro-
    acoustical Activity of Mechanisms with Gear Drives,], Nauka
    Press, Moscow 1971.

2. Petrusevich, A.I., M.D. Genkin, and V.A. Grinkevich, Dinamiches-
    kiye nagruzki v zubchatykh peredachakh s pryamozubnymi
    kolesami [Dynamic Loading of Gears with Spur Gear Wheels],
    USSR Academy of Sciences Press, 1956.

3. Kovalev, N.A., "Vibrations of Gears with Scoured Teeth," in
    the collection Teoriya peredach v mashinakh [Theory of Trans-
    missions in Machines], Mashinostroyeniye Press, Moscow, 1966.

4. Bansevichyus, R.Yu. and V.L. Ragul'skene, "Vibroshock Phenomena
    in Lightly Loaded Gear Drives." Nauchnyye trudy vuzov Lit.
    SSR Vibrotekhnika $\underline{2}$(2), $\underline{1}$(23), $\underline{1}$(4) (1968-1969).

5. Raybman, N.S. and V.M. Chadeyev, Adaptivnyye modeli v sistemakh
    upravleniya [Adaptive Models in Control Systems], Sovetskoye
    Radio Press, Moscow, 1966.

6. Raybman, N.S., Identifikatsiya ob"yektov upravleniya [Identi-
    fications of Objects of Control], Central Electromechanical
    Institute Publications, 1967.

A USE OF REGRESSION ANALYSIS IN ACOUSTICAL DIAGNOSTICS
OF GEAR DRIVES

F.Ya. Balitskiy, M.D. Genkin, M.A. Ivanova, A.A. Kobrinskiy,
and A.G. Sokolova
(Moscow)

The most complicated time in diagnostics of gear drives is
the comparison of a mathematical model of the gearing and the
forces acting on it. Although a whole series of works [1, 2, 3]
have been devoted to explanation of the nature of the excitation,
there still is much confusion here. For example, in the vibration
spectra of gearing, the amplitude of the second harmonic /145
(and sometimes the harmonics of higher orders) very often con-
siderably exceeds the amplitude of the first harmonics, which is
determined basically by the form of the exciting pulses. Thus,
a study of such components of the vibration spectrum as the
filtered first $x_1(t)$ and second $x_2(t)$ harmonics of the tooth
frequency f_z permits information to be obtained on the physical
characteristics of the vibration excitation process and an approach
to be made to comparison of models of the gearing. It was proposed
in (4) to use the methods of general correlation theory for solution
of such problems.

Regression analysis of two random processes x_1 and x_2 (in the
band $\Delta f = 0.06\ f_z$) has shown a strong dependence of the second
harmonic on the first and independence of the first from the second
(Fig. 1). The nature of change in the regression line $\bar{x}_2(x_1)$, with
change in loading moment P, gives rise to the idea of a variable
phase shift between the first and second harmonics.
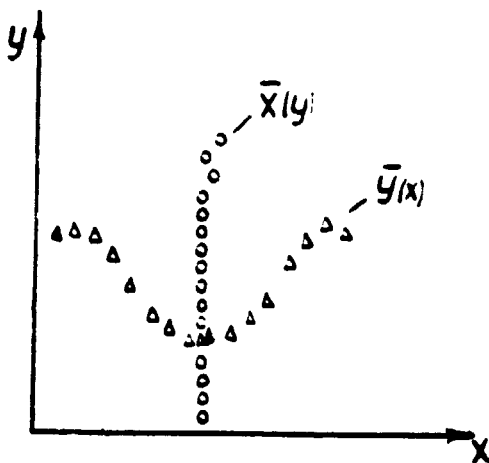
If, for simplicity, discussion
is restricted to the sinusoidal
functions $x_1 = \cos\ \omega t$ and $x_2 =
= \cos\ (2\omega t + \phi)$, $\bar{x}_2(x_1) = (2x^2 -
- 1)\cos\phi$. The family of regression
lines for different values of the
phase shift angle ϕ (relative to the
period of the second tooth frequency)
is represented in Fig. 2. From a
comparison of Figs. 1 and 2, we
obtain a relationship (with specific
assumptions) of the phase shift angle
between the two harmonics of the
vibration process (see Fig. 3).

The data obtained are used for
comparison of models of vibration
excitation in the reducing gear.

Fig. 1.

160
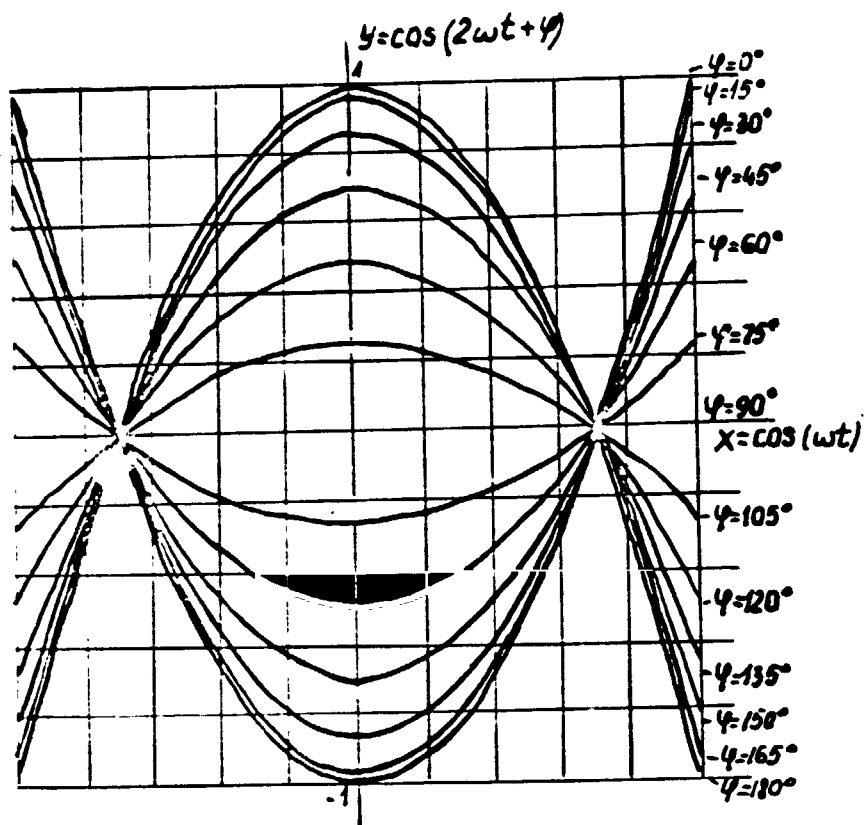
Fig. 2.
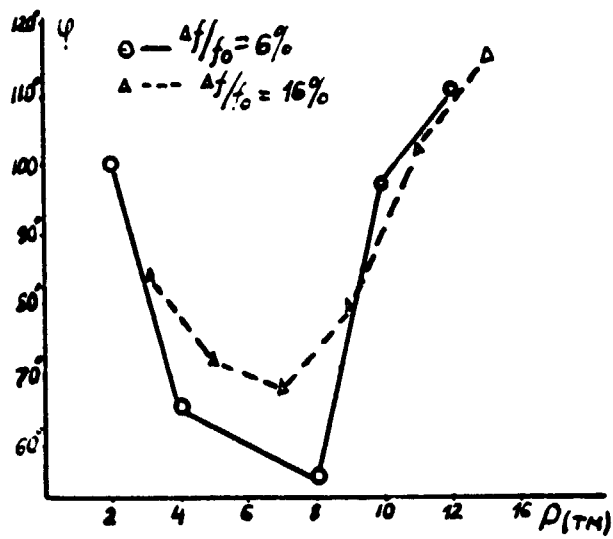
Fig. 3.

1. Petrusevich, A.I., M.D. Genkin, and V.A. Grinkevich, <u>Dinamiches-kiye nagruzki v zubchatykh peredachakh s pryamozubnymi kolesami</u> [Dynamic Loading of Gears with Spur Gear Wheels], USSR Academy of Sciences Press, 1956.

2. Kovalev, A.I., "Fundamental Results of Study of the Dynamics of High Frequency, High Speed Gear Drives," <u>Sb. dokladov nauchno-tekhnicheskoy konferentsii MEI</u> [Collection of Reports of Scientific-Technical Conference of the Moscow Power Engineering Institute], 1967.

3. Abramov, B.M., <u>Kolebaniya pryamozubnykh zubchatykh koles</u> [Vibrations of Spur Gear Wheels], Khar'kov State University Press, Khar'kov, 1958.

4. Gershman, S.G. and V.D. Svet,"The Use of the Methods of General Correlation Theory for Analysis of Acoustical Noises," <u>Tezisy dokladov VII Vsesoyuznoy akusticheskoy konferentsii</u> [Summaries of Reports, VIIth All-Union Acoustical Conference], Leningrad, 1971.

DIGITAL MODELING OF VIBROACOUSTICAL PROCESSES GENERATED BY GEARING

F.Ya. Balitskiy, M.D. Genkin, A.A. Kobrinskiy, and A.G. Sokolova
(Moscow)

Vibroacoustical processes generated by transmission gears are caused by the simultaneous effect of a number of factors, which are different in their mechanical natures, on gearing [1, 2]. For acoustical diagnostics of mechanisms with gear drives, a detailed study of the effect of each of these factors on the vibroacoustic processes is necessary. It is convenient to carry out the investigation by the mathematical modeling method, which leads to the necessity for construction of a mathematical model of a transmission gear, taking account of the statistical nature of the excitation [3, 4].

Problems of analog modeling of vibroacoustical processes, assuming the determinative nature of the excitation, were developed in [5, 6].

We limit ourselves to analysis of the high frequency components of the vibroacoustical process generated by spur gearing. In this case, the basic factors in vibration excitation are profile errors in the gearing, variable rigidity of the gearing, and errors in the basic spacing and deformation of the teeth, as well, leading to collisions as the teeth mesh. The action of these factors is steady, it is repeated with the frequency of meshing of the teeth and, in addition, is different for each pair of meshing teeth. The periodic vibrations of spur gear wheels, with periodic excitation, as a consequence of the effect of each of these factors, has been studied in a number of works [6-10]. We present equations, describing the torsional and transverse vibrations of pairs of gear wheels when meshing, with account taken of the flexibility of their supports (Fig. 1): /147

$$\left.\begin{aligned}
I_1 \ddot{\varphi}_1 + r_1 h_3 \ddot{x} + r_1 [c_3(t)x - F(t)] &= 0 \\
m_1 \ddot{y}_1 + h_1 \ddot{y}_1 + h_2 \ddot{x} + c_1 y_1 + c_3(t)x - F(t) &= 0 \\
I_2 \ddot{\varphi}_2 + r_2 h_3 \ddot{x} + r_2 [c_3(t)x - F(t)] &= 0 \\
m_2 \ddot{y}_2 + h_2 \ddot{y}_2 - h_3 \ddot{x} + c_2 y_2 - c_3(t)x + F(t) &= 0
\end{aligned}\right\} \tag{1}$$

Here, $x = \varphi_1 r_1 + \varphi_2 r_2 + y_1 - y_2 - \Delta(t)$ is the magnitude of deformation of the gearing; $c_3(t)$ is the variable rigidity of the gearing; $\Delta(t)$ is the gearing profile error function; and $F(t)$ is a function describing the impact interactions of the teeth.

163
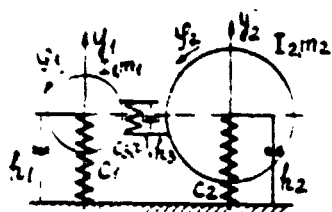
Fig. 1.

To plot the excitation function, we divide the time axis into intervals of moments t_i, corresponding to the engaging and disengaging of successive teeth,

$$t_{2i} = T(i + \varepsilon - 1), \qquad t_{2i+1} = t_{2i} + T(1 - \varepsilon), \qquad (2)$$

where $T = 2\pi/f_z$ is the gear meshing period and E is the period of contact. The function $c_3(t)$ assumes constant values c' and c" in the one-pair and two-pair meshing intervals. F(t) is a delta function, synchronized with moments t_{2i} of tooth engagement, equal to:

$$F(t) = \sum_{i=1}^{z} F_0 \delta(t - t_{2i}).$$

The magnitude of the shock pulse upon engagement of a tooth can be determined by formulas [7]. This magnitude depends on the gear wheel spacing error and deformation of the teeth. The function $\Delta(t)$, describing the profile errors of the gearing is in harmony with the frequency determined by the number of teeth in the indexing wheel used in manufacture of the gears.

Plotting of the amplitude-frequency characteristics of system (1) and their comparison with similar characteristics, obtained experimentally for a pair of sour gear wheels, permits the inertial-rigidity parameters of the system to be precisely specified, according to the frequencies of the fundamental spectral components, and the dissipative parameters and amplitudes of the exciting forces, by the intensity of these components [5].

In fact, functions $c_3(t)$, F(t) and $\Delta(t)$ in system (1) are random, as a result of which, vibrations of the continuous components appear in the spectrum. A significant feature of these random functions is the fact that they are determined by the /148 sequence of time intervals, corresponding to the meshing of different teeth. Thus, these functions can be modeled by digital computer, with a succession of realizations of random values generated by a random numbers generator. Subsequent statistical processing of the random vibrational processes produced by the computer [3, 4] permits the statistical relationships of the excitation processes to be determined and technical measures to reduce the noise level of gear transmissions to be proposed.

164

REFERENCES

1. Artobolevskiy, I.I., M.D. Genkin, and V.I. Sergeyev, "Acousti-
   cal Dynamics of Machines," Vestnik AN SSSR (11) (1968).

2. Genkin, M.D., O vibroakusticheskoy aktivnosti mekhanizmov s
   zubchatymi peredachami [Vibroacoustical Activity of Mechanisms
   with Gear Drives], Nauka Press, Moscow, 1971.

3. Balitskiy, F.Ya., M.D. Genkin, M.A. Ivanova, and A.G. Sokolova,
   "Problems of Modeling Acoustical Processes in Machines," in
   the collection Dinamika i akustika mashin [Dynamics and Acous-
   tics of Machines], Nauka Press, Moscow, 1972.

4. Balitskiy, F.Ya., M.D. Genkin, M.A. Ivanova, and A.G. Sokolova,
   "Statistical Analysis of Vibroacoustical Processes in Gear
   Drives Applicable to Problems in Diagnostics," ibid.

5. Genkin, M.D., V.I. Sergeyev, and L.V. Sukhorukov, "Calculation-
   Experimental Investigation of the Dynamics of Reducing Gears
   Using Computers," in the collection Vibroakusticheskaya
   aktivnost' mekhanizmov s zubchatymi peredachami [Vibro-
   acoustical Activity of Mechanisms with Gear Drives], Nauka
   Press, Moscow, 1971.

6. Bosch, M., "Dynamic Behavior of Gear Drives, with Particular
   Consideration of Cog Fit," Ind.-Anz. (102) (1965); (14) (1966).

7. Petrusevich, A.I., M.D. Genkin and V.A. Grinkevich, Dinamich-
   eskiye nagruzki v zubchatykh peredachakh s pryamozubnymi
   kolesami [Dynamic Loading of Gears with Spur Gear Wheels],
   USSR Academy of Sciences Press, 1956.

8. Grinkevich, V.K., "Forced Vibrations of Gear Wheels of a Single
   Stage Reducer," in the collection Vibroakusticheskaya aktiv-
   nost' mekhanizmov s zubchatymi peredachami [Vibroacoustical
   Activity of Mechanisms with Gear Drives], Nauka Press,
   Moscow, 1971.

9. Kovalev, A.I., "Fundamental Results of Investigation of the
   Dynamics of High-Speed Gear Drives," Sb. dokladov nauchno-
   tekhnicheskoy konferentsii MEI [Collection of Reports,
   Scientific and Technical Conference, Moscow Power Engin-
   eering Institute], 1967.

10. Abramov, B.M., Kolebaniya pryamozubnykh zubchatykh koles
    [Vibrations of Spur Gear Wheels], Khar'kov State University
    Press, Khar'kov, 1958.

ALGORITHM FOR PROCESSING VIBROACOUSTICAL SIGNALS, FOR THE PURPOSE OF EARLY DETECTION OF CHANGE IN CONDITION OF A MACHINE

V.I. Povarkov
(Moscow)

As experience has shown, a change in the condition of a machine, the appearance of a fault or wear of a part, leads to a change in the vibroacoustical signals of the machine. Therefore, diagnostics of the condition of a machine consists of comparison of reference vibroacoustical signal curves of the machine with the current (investigated) characteristics.

However, since vibroacoustical signals of a machine are random processes and the analysis time for these processes is restricted, only an estimate of the characteristics of the signals, which, in turn, have random values, can be obtained. Therefore, with small defects in the early stages of development, leading to slight changes in the vibroacoustical signals and their characteristics, the question can arise as to whether one change or another, for example, in the spectral or correlation characteristics, is connected with the random nature of the signals or with the appearance of a defect, i.e., comparison of these characteristics must be approached from the probability point of view.

Let X_{ij} be a certain estimate of the i-th statistical characteristic (for example, spectral or correlation) at point j. The distribution function of the random values X_{ij} tends towards the normal, with increase in integration time or number of independent samples. Therefore, it can be assumed that random values $X_{ij}^{(1)}$ (reference condition) and $X_{ij}^{(2)}$ (the condition investigated) are distributed according to the normal law and that the magnitudes of their dispersions are identical and equal to σ_z^2.

Then the magnitude $y_{ij} = X_{ij}^{(2)} - X_{ij}^{(1)}$ also will be distributed normally and have a mean $E[y_{ij}] = 0$, if the mean $X_{ij}^{(1)}$ and $X_{ij}^{(2)}$ are identical (i.e., the condition of the machine has not changed), or $E[y_{ij}] = a \neq 0$, if the mean $X_{ij}^{(1)}$ and $X_{ij}^{(2)}$ are different (i.e., the condition of the mechanism has changed), and the dispersion is $2\sigma_z^2$. That is, the hypothesis H_0 that $E[y_{ij}] = 0$ must be tested against complex alternatives K, that $E[y_{ij}] = a \neq 0$, where the value of a is unknown. If the dispersion of values of y_{ij} is known precisely, the Neyman-Pearson criterion can be used as the most powerful in testing the hypotheses of the magnitude of the mean value. In conformance with [2], the hypothesis is rejected at a selected level of significance, if

166

$$y_{ij} \geqslant \frac{\sigma_z}{2\sqrt{n}} X_{a}. \tag{1}$$

Here n is the number of samples or number of degrees of freedom of <u>/150</u> the random values of y_{ij} and X_{α} is a level selected from the equality

$$P_{H_s}(y_{ij} > X_a) = \alpha. \tag{2}$$

where P_{H_0} $(y_{ij} \geq X_{\alpha})$ is the probability that y_{ij} has a value $\geq X_{\alpha}$ when hypothesis H_0 is correct.

However, as a rule, the dispersion of values $X_{1j}^{(1)}$ and $X_{1j}^{(2)}$ is not known precisely; perhaps only certain sample dispersions of these values $S_X^2(1)$ and $S_X^2(2)$ were measured. Therefore, to test the hypothesis of the distribution of the means, it is necessary to rest on the criterion constructed according to the Student method [3]. If $\overline{X_{1j}^{(1)}}$ and $\overline{X_{1j}^{(2)}}$ are certain sample mean measured characteristics, the following statistic is formed

$$t_{ij} = \frac{\overline{X_{ij}^{(2)}} - \overline{X_{ij}^{(1)}}}{\sqrt{S_{x^{(2)}}^2 + S_{x^{(1)}}^2}} \sqrt{n-1}. \tag{3}$$

having a Student distribution, with a number of degrees of freedom K = 2(n - 1), where n is the number of samples of the measured values. Hypothesis H_0 is rejected if t_{1j} exceeds a certain level $t_{k,\alpha}$ in absolute value:

$$t_{1j} > t_{k,\alpha} \tag{4}$$

depending on the selected level of significance of α and the number of degrees of freedom k.

Therefore, the algorithm for comparison of statistical characteristics can be reduced to measurement of sample means $\overline{X_{1j}^{(2)}}$ and $\overline{X_{1j}^{(1)}}$ and sample dispersions S_{1j}^2 and S_{1j}^2, to formation of statistic t_{1j} according to formula (3) and comparison with the selected threshold and solution adopted.

Such a comparison must be carried out over several most informative points j.

The spectral characteristics of vibrations of an aircraft engine were processed, during an imposed defect, simulating partial breaking away of the blades. In this case, the integration time was ∿1 sec, the number of samples n = 10 and the level of signifi-- cance α = 0.2.

The use of statistic t gave a clear spread of the spectrogram in this case, which was not noticeable during a simple visual examination.

REFERENCES   /151

1. Gershman, S.G., V.I. Povarkov, and N.G. Dubrovskiy, "Spectral-
      Correlation Analysis of Vibrations of an Aircraft Engine
      During Tests Under Test Stand Condicions," Doklad na Bsesoyuz-
      nom simpoziume [Report to All-Union Symposium], Kaunas, 1970.

2. Levin, B.R., Teoreticheskiye osnovy statisticheskoy radio-
      tekhniki [Theoretical Foundations of Statistical Radio
      Engineering], Vol. 2, Sovetskoye radio Press, Moscow, 1968.

3. Dunin-Barkovskiy, I.V. and N.V. Smirnov, Teoriya veroyatnosti
      i matematicheskaya statistika v tekhnike [Probability Theory
      and Mathematical Statistics in Technology], Technical-Theo-
      retical Literature Press, Moscow, 1955.

METHOD OF STUDY OF THE POSSIBILITY OF PREDICTING THE QUALITY OF TREATMENT IN POLISHING BY VIBROACOUSTICAL PROCESSES

V.V. Trubnikov and B.Ye. Bolotov
(Kuybyshev)

One of the major parameters of quality of polishing is deviation from roundness of the profile of the treated surface (waviness, graininess). Analysis of these deviations permits examination of the profile as the accomplishment of a random process. In connection with this, a model of profile formation was assumed, which is depicted in Fig. 1, where $S_F(\omega)$ is the spectrum of the disturbing forces; $S_a(\omega)$ is the relative spectra of vibrations of the polisher and the part; $S_x(\omega)$ is the spectrum of deviation from circularity of the profile of the treated surface; w_1 is the APFC of a closed dynamic system of the polishing mill; and w_2 is the APFC of the process of shaping the profile of the treated surface.
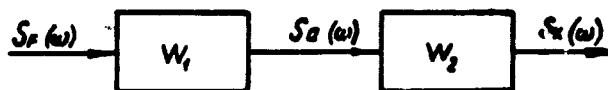
Fig. 1

For experimental investigation of the process of formation of deviations of the profile of the treated surface from circularity, an experimental unit, based on a polishing mill was built, which permitted study of the following characteristics of the dynamic /152 system of the mill and of the vibroacoustical processes: overall level and spectral composition of vibration accelerations and vibration displacements of individual elements of the dynamic system of the mill; precision of rotation of the polishing circle spindle in the static and dynamic modes of operation (at no load, in the process of setting the polishing circle and in polishing); the nature of the process and spectral composition of the relative vibrations of the polishing circle and the part being processed; the statistical and dynamic rigidity of individual elements of the elastic system of the mill (in particular, of the polishing mill spindle assembly); and APFC of the elastic system of the stand.

Considering that the spindle assemblies are the fundamental source of disturbance of high-accuracy polishing mills, a method of investigation of the effect of individual parameters of them (the magnitude of the preliminary clearance gap on the supports, the magnitude of the clearance gap during fitting of the bearing wheels, vibroacoustical characteristics of the bearings, magnitude of imbalance, etc.) on the vibroacoustical characteristics of the system was developed; besides this, provision was made for measurement of the spectrum of the disturbing forces, due to the operation of the spindle assembly.

The experimental data were processed by a digital computer for further use in modeling the process of formation of deviations of the profile of the treated surface. Interpretation of the experimental and calculated data permits the problem of predicting the quality of the treatment to be solved and, subsequently, the problem of optimization of the system to be approached.

170

THE USE OF CORRELATION RECEIVING SYSTEMS
FOR DETECTION OF NOISE SOURCES AT SHORT DISTANCES

V.V. Tarabarin
(Moscow)

The correlation method of determination of the direction to a noise source is widely used in hydroacoustics, for noise direction finding purposes [1], and in radio astronomy, for determination of the location of sources of radio wave radiation [2]. However, the use of this method has been studied little for those cases, in which the correlation receiving system is used for detection of noise sources, masked by isotropic noise field inter- /153 ference, at distances comparable with the distance between receivers [3, 4, 5]. This problem is part of the general problem of localization of noise sources, on the background of interference, and it can be solved by use of sharply directional receiving systems.

It is known that a system, composed of two microphones, located at a fixed distance   apart, and a correlator is directional [1]. The correlation coefficient between the microphone signals as functions of orientation of the microphones can be considered as the directionality coefficient of such a system.

Making appropriate assumptions [5], we find an expression, in conformance with work [2], for the correlation function of the signal of a source at a finite distance, characterized by mean power S in a selected frequency band Δf, with a uniform spectrum, which is determined by the following relationships:

$$R = S \cdot \frac{\sin\left[\frac{2\pi\Delta f d}{c}\left(K^2 - \frac{1}{4} - K\sin\Theta\right)^{\frac{1}{2}} - \left(K^2 - \frac{1}{4} - K\sin\Theta\right)^{\frac{1}{2}}\right]}{\frac{2\pi\Delta f d}{c}\left(K^2 - \frac{1}{4} - K\sin\Theta\right)^{\frac{1}{2}} - \left(K^2 + \frac{1}{4} - K\sin\Theta\right)^{\frac{1}{2}}} \times$$

$$\times \cos\left[\frac{2\pi f_0 d}{c}\left(k^2 + \frac{1}{4} + K\sin\Theta\right)^{\frac{1}{2}} - \left(K^2 + \frac{1}{4} - K\sin\Theta\right)^{\frac{1}{2}}\right]. \tag{1}$$

where Θ is the angle between the axis of the base and the direction to the signal source; f_c is the mean frequency; c is the rate of propagation of sound, and k = r/d.

Assuming K in (1) to be infinitely large, it can be shown that Eq. (1) has the well-known expression in this case,

$$R_x = S \cdot \frac{\sin\left(\frac{2\pi\Delta f d}{c} \cdot \sin\theta\right)}{\frac{2\pi\Delta f d}{c}} \cdot \cos\left(\frac{2\pi f_0 \cdot d}{c} \cdot \sin\Theta\right). \tag{2}$$

which defines the directionality of the correlation system in detection of a signal of a source at an infinite distance.

Consequently, finiteness of the distance to the source does not introduce errors in determination of the direction of the sound source. This conclusion holds true for cases when the direction to the source of the noise is at the maximum of the correlation function obtained by the method of mechanical rotation of the base of the receiving sy.tem. If the method of synthetic rotation of an immovable base (delay lines) is used, the error in the assumed direction to the noise source, the value of which depends on θ and r, must be taken into account.

To test the p⸱⸱ ⸱bility of determination of the location of <u>/154</u> noise source 1, masked by an interference field, by a receiver correlation system, containing two nondirectional microphones, experimental studies were carried out on the directionality of a device containing two nondirectional microphones 2, the signals from which enter the input of analog correlator 4 through microphone amplifiers 3 (Fig. 1). The standardized correlation functions at the correlator output were measured, as a function of orientation ⸱ᵒ the receiving system base to noise source 1, at k ≤ 1.
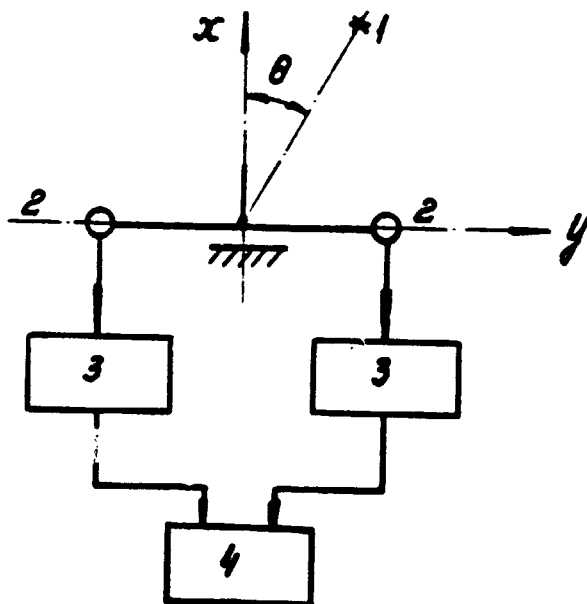
Fig. 1.

In determination of the direction to a point source of wide-band noise, having a flat spectrum in the 2000-5000 Hz frequency band, in accordance with (1), an increase in d improves the directionality of the system; however, in this case, the value of the mean output signal of the correlator is decreased (Fig. 2a). Change in the relative distance from the base of the receiving system to noise source 1 K = = r/d = 0.25-1) has no significant effect on the accuracy of determination of the source location (Fig. 2b). Measurement of the directionality of the system in finding

172

the direction to a source, radiating a frequency-modulated signal at a mean frequency f_0 = 100 Hz, frequency modulation f_1 = 4 Hz, and at various values of the deviation frequency Δf = 100, 150 and 200 Hz, showed (Fig. 2c) that the directionality of the system /155 is considerably impaired with decrease in the width of the uniform spectrum of the signal source.
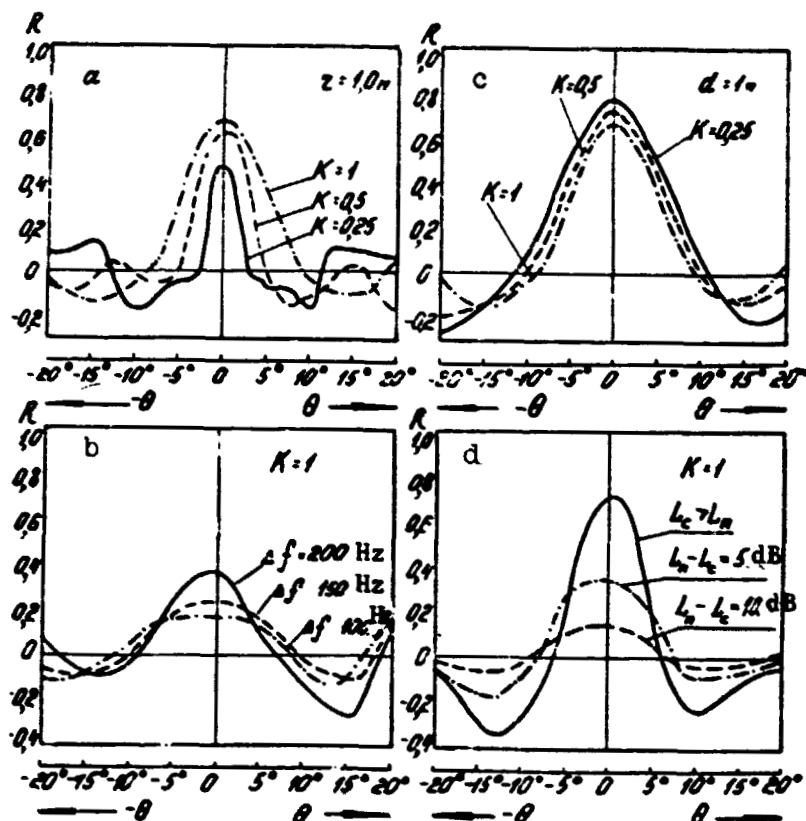
Fig. 2.

Investigation of the effect of the input signal-to-noise ratio on the directionality of the system (Fig. 2d) permits the conclusion to be drawn that satisfactory results can be obtained in detection of a wide-band noise source, if the level of the interference noise field exceeds the signal level by not more than 5-6 dB. The capacity of the receiver correlation system to distinguish sources which are located close together was determined by measurement of the direction to the sources of air jets, radiating a wide-band, high-frequency noise. The minimum distance at which well expressed maximums of the correlation functions were obtained was about 50 mm, which is in agreement with the results presented in [4]. Consequently, a receiver correlation system containing two non-directional microphines can be used in measurements for localiza- /156 tion of noise sources at short distances (K = 1); however, the

following limitations on its use must be taken into account:

1. The system is directional only in the plane of the base;

2. The directional power of the system is impaired with decrease in the bandwidth of the noise source spectrum;

3. The system does not permit unambiguous determination of the direction to noise sources, located on both sides of the base line;

4. The system has a comparatively low output signal-to-noise ratio.

174

REFERENCES

1. Prostakov, A.L., *Gidroakustika i korabl'* [Hydroacoustics and Ships], Sudostroyeniye Press, Leningrad, 1967.

2. Novikov, A.K., *Korrelyatsionnyye izmereniya v korabel'noy akustike* [Correlation Measurements in Marine Acoustics], Sudostroyeniye Press, Leningrad, 1971.

3. Pisarevskiy, N.N., "Correlation Methods in the Investigation of Noises," in the book *Bor'ba s shumom* [Noise Control], ed. Yudina,Ye.Ya., Stroyizdat Press, Moscow, 1964.

4. Gilbrech, D.A., *JASA* 30(9) (1958).

5. Jacobson, M.J., *JASA* 31(4) (1959).

NEW PRINCIPLES OF CONSTRUCTION OF ELECTROMECHANICAL VIBRATION INDUCERS

K.-A.P. Ashmonas, R.Yu. Bansevichyus, A.I. Vaznelis,
and K.M. Ragul'skis
(Kaunas)

More and more rigid requirements for long life, reliable operation, uniform noise and synchronous operation of individual vibration inducers are being placed at the present time on vibration machines for industrial purposes. One of the basic causes for electromechanical vibration inducers getting out of order is premature loss of operating capacity of support bearings. Great centrifugal forces of the disbalances act on the bearings, and they quickly wear out. For solution of these problems, electromechanical vibration inducers of high reliability and a low noise level were created and studied.

The vibration inducer (Fig. 1) consists of housing 1 and disbalance rotor 2, with adjustable disbalances 3 set on. On the periphery of the housing, adjacent to the disbalance rotor, a /157 space is built in, into which compressed air or oil under pressure is supplied through an orifice in the rotor. Air pressure on the inner surface of the housing creates a disturbing force. Upon rotation of the disbalance rotor, the centrifugal force arising is equalized with the force acting on the rotor, caused by the air pressure, and only a   torque acts on the rotor. The disturbing force is given by the pressure of the compressed air, and complete unloading of the bearings is accomplished by the adjustable disbalances 3.
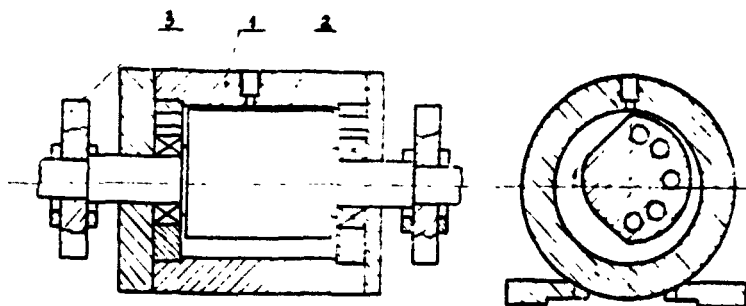
Fig. 1. Vibration inducer.

The vibration inducer (Fig. 2) consists of housing 1, dynamically balanced rotor 2 and adjustable external disbalances 3. The rotor is made with a cylindrical outer surface of varying radius,
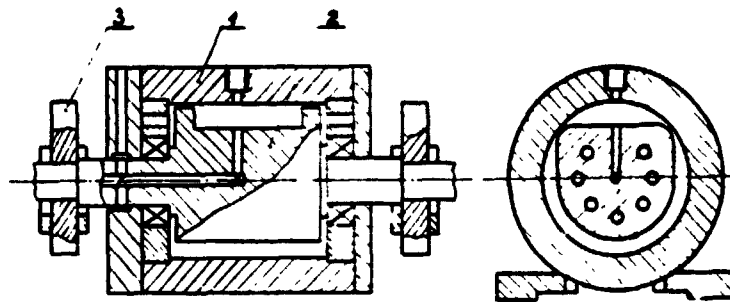
Fig. 2. Vibration inducer.

forming a gap, in the shape of a circular wedge, with the inner
surface of the housing. During rotation of the rotor, a moving
zone of increased air pressure arises in the circular wedge gap. /158
A disturbing force is created by the air pressure, which acts on
the inner surface of the housing. The active force of the com-
pressed air on the rotor is balanced with the centrifugal force,
at approcriate settings of the adjustable external disbalances,
and only a torque acts on the rotor.

The air pressure at individual points on the inner part of
the housing, the disturbing force on the housing and the force
acting on the supports were measured during the investigations.
Much attention was given to determination of the optimum profile
of the cylindrical outer surface of the dynamically balanced rotor.

Some new methods of synchronization of vibration inducers
were introduced in the work. The ensurance of synchronization of
the operation of several vibration inducers, operating in one
vibration unit, is an urgent problem at the present time. To
ensure synchronous operation of all vibration inducers, forced
synchronization, by use of rigid connections, which are bulky,
short-lived and which create a high noise level, are very often
used. To eliminate all these deficiencies, a new method of syn-
chronization of vibration inducers was created. This method uses
the fact that the synchronizing links are made in the form of
permanent magnets or electromagnets.

A diagram of a device for synchronization of vibration
inducers, operating at any distance apart and at any position in
space, is presented in Fig. 3. The device consists of several
vibration inducers, driven by asynchronous electric motors. Dis-
balances 2 are installed on the shafts of vibration inducers 1.
Electromagnets 3 and 4 are securely installed at a specified   /159
distance from the disbalances. Their windings are connected in
series and, in this case, electromagnet 4 has supplementary
winding 5, which is connected to an alternating current source.

177
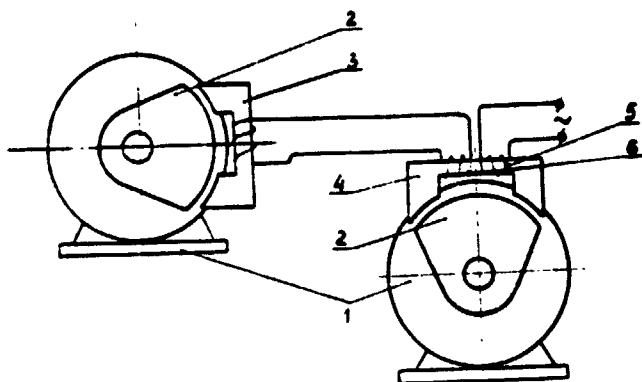
Fig. 3. Device for vibration
inducer synchronization.

A variable voltage of a fre-
quency which depends on the
angular position of disbalance
2, is induced in winding 6 of
electromagnet 4. In the case
of the least losses (when the
disbalance is in the extreme
right position, as shown in
Fig. 3), the voltage on winding
6 is at a maximum, i.e., a
maximum current, created by
the supplementary magnetic
circuit flows in the circuit
of electromagnet 3. In the
case when disbalance 2 is
distant from electromagnet 4,
the current in the winding of electromagnet 3 has a very small
value.

The supply frequency of winding 5 must be different from the
frequency of rotation of the electric motors, which always is easy
to accomplish, since, in the case of asynchronous electric motors,
they always are different, due to slip.

Upon starting up, the vibration inducers rotate with non-
uniform angular velocities, because of slip, which is character-
istic of asynchronous electric motors. Synchronization of their
rotation is provided by means of the electromagnets, which also
assist in approaching the resonance zone in the still unsynchronized
mode of operations.

The possibility of producing stable synchronous operation of
two vibration inducers, rigidly fastened to a solid body with and
without a flexible suspension, was investigated. It was found
that stable synchronous operation of the vibration inducers is
possible over a quite wide range of change in the parameters.

178

STRUCTURAL ANALYSIS OF VIBROACOUSTICAL PROCESSES

A.P. Gromov, L.L. Myasnikov, Ye.N. Myasnikova, and B.A. Finagin
(Leningrad)

The method of automatic identification of acoustical signals, by means of the segmentation [1], can be generalized and used for investigation of noises and vibrations in machines and mechanisms, for cybernetic diagnostics.

The structural analysis consists of presentation of a noise or vibroacoustical signal as a sequence of segments, determined by time quantization (if the segment is maintained longer, it is /160 recorded again), in which each segment is characterized by specific spectral characteristics. The structural spectrum is plotted as a histogram of the segments, i.e., as a relation of the probability density of appearance of a segment to the segment type. It is assumed that the conditions of ergodic processes are maintained.

A measuring apparatus was used in the work, which contained an acoustical vibration analyzer, which is a Stseptron (Fig. 1). The Stseptron, as is well known, is a set of optical fiber mechanical filters; the output ends of the light guides form a matrix, which gives an image of the signal(Stseptronogram). A signal is supplied to the input from the sound recording of a vibration, made previously in a machine part; excitation of the Stseptron is accomplished through an electrodynamic converter or piezoelectric bimorph.
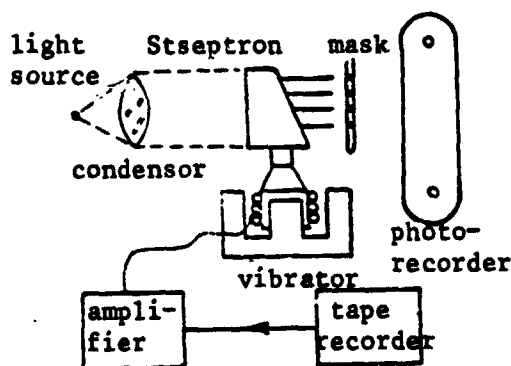
Fig. 1.

Observation of the images given by this Stseptron leads to determinatior of the segment type of each quantizaticn interval. Usually, the conclusion concerning the segment has the approximate nature of a "guess," i.e., an approximate attribution of the figure to one class or another. A short dictionary of reference images of the segments (numbering 10) was compiled. Tests carried out on considerable material (containing over 15,000 segments) by a team of independently working operators showed that structural spectra, plotted on the basis of statistics of the "guessed" segments, permits the signal to be classified and identified with a reliability of not less than 90%.

The possibility of automation of the segmentation process was
established. For this purpose, stseptronograms of segments were
counted by means of a photoelectronic mosaic, constructed of photo-
diodes and coded in accordance with the combinations of fields char-
acterizing the segments. The coded electrical signals serve for a
digital computer input. The program for compiling the structural
spectra consists of counting the frequency of each segment, plot-
ting histograms, comparing them with reference histograms and
establishment of a diagnostic conclusion.

There is interest in "semiautomatic" structural analysis of
vibrations for operations control. A stseptron has been developed
which can be directly stimulated by a vibrating body (Fig. 2). This
stseptron fulfills the role of a vibroscope; it is equipped with a
cassette with different masks, which facilitate visual definition
of the segments. For plotting histograms, the operator uses a
mechanical counter, pressing the keys corresponding to the dif-
ferent segments.
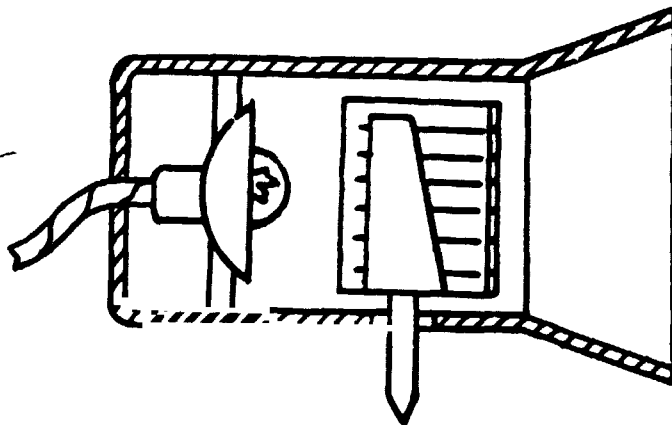
In many cases, it is
sufficient to determine the
two most frequent segments
for noise classification,
with determination of which
of them is most probable.
Segments with low proba-
bilities can be disregarded.
This permits an approximate
judgment on the structural
spectrum, after a certain
amount of training, on the
basis of visual impressions
of change in the stseptrono-
grams.

Fig. 2.

REFERENCES

1. Myasnikov, L.L. and Ye.N. Myasnikova, Avtomaticheskoye raspoz-
   navaniye zvukovykh obrazov [Automatic Sound Image Identifica-
   tion], Energiya Press, 1970.

180

SELECTION OF INFORMATIVE PARAMETERS OF VIBROACOUSTIC PROCESSES

L.N. Koshek
(Novosibirsk)

The problem of selection of parameters of processes to be measured arises during investigation of vibroacoustical processes for the purpose of diagnostics or identification of systems, since existing identification and diagnostics strategies were developed only for finite-dimensional spaces.

The problem of selection of informative parameters of vibroacoustic processes and construction of apparatus for their determination are discussed in the report. It is assumed that the processes being investigated are structurally uniform and either purely random or contain not very many determinative components.

Exhaustive data on the process $x(t)$ is contained in infinite-dimensional characteristics of the distribution type $w_n(x_1, x_2, \ldots, t)$, $n \to \infty$; however, already at $n > 2$, serious difficulties arise in obtaining and processing such characteristics. Based on experience in analysis of random processes in the theories of communications, automation, radio technology and other sciences, it can be assumed that the most useful data on the process $x(t)$ is contained in unidimensional characteristics: density $w(x)$ and standardized correlation functions $R(\tau)$.

Within the framework of these assumptions, the problem can be formulated in the following manner: to synthesize N functionals $B_j[x]$, carrying the most valuable data on the process $x(t)$.

The requirement that the parameters sought be orthogonal flows from the additive property of information dimension I, and the problem can be reduced to selection of orthogonal series, which are suitable for obtaining the "best" estimates of $w^*(x)$ and $R^*(\tau)$. In estimating the quality of the approximation with the loss functionals $c_1[w_1, w^*]$ and $c_2[R_1, R^*]$, the synthesis problem is reduced to minimization of the mean losses:

$$V_{01} = \inf_{w^*(x)} \int_{(w)} c_1[w_1 w^*] \Psi_1[w] \, dw.$$

$$(1)$$

$$V_{02} = \inf_{R^*(\tau)} \int_{(R)} c_2[R, R^*] \Psi_2[R] \, dR,$$

$$(2)$$

181

where $\psi_1[w]$ and $\psi_2[R]$ are the continual densities of distribution of the characteristics $w(x)$ and $R(\tau)$ (probability functionals).

It is clear that solution of problems (1, 2) will differ for /163 each specific class of processes $[X(t)]$ and, moreover, will depend on the types of functionals c_1 and c_2.

In particular, the solution obtained for a broad class of vibroacoustical processes, having $R(\tau)$, is reminiscent of the exponent, and the distributions $w(X)$ are not too much different from the normal one. The problem was solved by the numerical method. ψ_1 and ψ_2 were given by tables, compiled on the basis of experimentally obtained $w(X)$ and $R(\tau)$. The approximation was estimated by the functionals

$$c_1[w_1,w^*] = \left[\frac{1}{\sigma} \int\limits_{-\infty}^{x} \left(w(X) - w^*(X) \right)^2 e^{-\frac{x^2}{2\sigma^2}} \, dx \right]^{\frac{1}{2}}, \tag{3}$$

$$c_2[R, R^*] = \left[\frac{1}{T_k} \int\limits_{0}^{x} \left(R(\tau) - R^*(\tau) \right)^2 e^{-\frac{\tau}{T_k}} \, d\tau \right]^{\frac{1}{2}}, \tag{4}$$

where σ^2 is the dispersion of the process being investigated and T_k is the correlation index [1]. The Hermite $H_H(X)$ and Laguerre $L_n(\tau)$ polynomials turned out to be the best orthogonal series in the sense of (3, 4), for $n = 2, 4, 6, 8, 10$, and the most informative parameters of this class of processes are the coefficients of the series produced:

$$b_n = \frac{1}{\sqrt{n!}} \int\limits_{-\infty}^{\infty} w(x) H_n \left(\frac{x}{\sigma} \right) dx, \tag{5}$$

$$a_n = \frac{1}{T_k} \int\limits_{0}^{\infty} e^{-\frac{\tau}{T_k}} R(\tau) L_n \left(\frac{\tau}{T_k} \right) d\tau. \tag{6}$$

For determination of the necessary number of parameters $N = N_B + N_a$ and accuracy of their measurement, information value functions (2) must be synthesized. For $w(x)$ and $R(\tau)$, they take the following form:

$$V_1(I) = V_{01} - \inf_{\Sigma(w_k)} \int\limits_{(w)} \left[\inf_{w^* \in (w_k)} \times \right.$$
$$\left. \times \int\limits_{(w_k)} c_1[w, w^*] \Psi_1[w] \, dw \right] \Psi_1[w] \, dw \tag{7}$$

$$V_2(I) = V_{02} - \inf_{\Sigma(R_k)} \int_{(R)} \left[\inf_{R^* \alpha(R_k)} \times \right.$$
$$\left. \times \int_{(R_k)} c_2[R, R^*] \Psi_2^*[R] dR \right] \Psi_2^*[R] dR \qquad (8)$$

The results of calculations for the class of processes being examined, obtained for the case when the permissible value loss levels were assumed to be no more than 10%, were reduced to a table, in which the necessary amount of data on each parameter and the corresponding accuracy of measurement Δ are presented, together with a summary of the informative parameters enumerated. The informative parameters obtained (5, 6) can be used, not only for identification and diagnostics of objects, but, naturally, for obtaining estimates of $w^*(X)$ and $R^*(\tau)$.

/164

TABLE.

Parameter	b_0	b_1	b_2	T_k	a_0	a_1	a_2
I (bit)	9	6	5	5	5	4	3
Δ (%)	0.2	1.5	3	3	3	6	12

The instrument used for obtaining data on the parameters should contain N_b nonlinear units and integrators for determination of the coefficients b_n and N_a of the orthogonal filters and the multipliers and integrators for determination of coefficients a_n. An experimental model of an instrument using the idea of orthogonal filtration (3) was developed and built at the Novosibirsk Electrotechnical Institute, based on standard analog computer components. Experimental test of the model demonstrated satisfactory values of the accuracy of determination of all parameters, with the exception of coefficient a_2.

REFERENCES

1. Koshek, L.N., "Correlation Analysis of 'Slow' Processes," in the collection Tekhnicheskaya kibernetika [Technical Cybernetics], Novosibirsk, 1965.

2. Stratoncvich, R.L., "The Value of Information," Izv. AN SSSR, Tekhnicheskaya kibernetika (5) (1965).

3. Lampard, D.G., "A New Method of Determining Correlation Function of Stationary Time Series," Proc. IIE (1) (1955)

DIGITAL METHODS OF EXTRACTING SPECTRAL CHARACTERISTICS IN A TRANSIENT SIGNAL

V.K. Maslov, G.A. Rozenberg
(Moscow)

An effective algorithm for digital spectral analysis of wide-band steady signals was proposed in work [2], on the basis of BPF (band-pass filters), permitting the excessive amount of initial description to be significantly reduced, as a result of the fact that a discrete Fourier transform is carried out on a fragmentary-logarithmic frequency grid, with continual storage, independent of the width of the spectrum and duration of the processes being examined. In this case, the dispersion of the spectral estimates is approximately uniform over the entire frequency range. In this report, the use of method [2] is discussed, for analysis of transient, random signals, of the type

$$x(t) = A(t) \cdot N(t) \tag{1}$$

where $N(t)$ is a steady random signal and $A(t)$ is a slowly changing (by comparison with the lower frequency spectrum of the signal) determinate time function.

In acoustical measurements, moving transportation means (aircraft, automobiles and the like), with a stationary microphone, $A(t)$ has the meaning $1/r(t)$, where $r(t)$ is the current distance between the radiator and the receiver.

It is known [1] that the spectrum of the product of two functions equals the package of the spectra of these functions, i.e., the spectrum of the diagnostic signal $N(t)$ is distorted, the more significantly, the larger the spectrum of function $A(t)$ differs from the δ function. The proposed method of "steadying" is based on the approximate calculation of certain statistical characteristics of the signal $x(t)$ over an interval of time, during which $A(t)$ can be assumed constant. If the mathematical expectation of the process $N(t)$ equals zero, it proves to be simplest of all to measure the "moving" dispersion, using the sliding mean operator [3]:

$$\sigma^2_{xT}(t_i) = \int_{t_i-\frac{T}{2}}^{t_i+\frac{T}{2}} x^2(t)\,dt = \int_{t_i-\frac{T}{2}}^{t_i-\frac{T}{2}} A^2(t)\,N^2(t)\,dt \approx$$

$$\approx A^2(t_i) \int_{t_i-\frac{T}{2}}^{t_i+\frac{T}{2}} N^2(t)\,dt \approx A^2(t_i)\,\sigma^2_{NT} \tag{2}$$

On the assumption that N(t) is steady, in the broad sense of the signal, σ_{NT}^2 is independent of t_1 and the relation

$$A(t_i) = \text{const} \cdot \sigma_{xT}(t_i) \tag{3}$$

follows from (2). The requirement for interval T is contradictory: a decrease in T decreases the displacement error for $A(t_1)$, but leads to an increase in the dispersion of the estimate σ_{NT} [4]. The selection of interval T can be carried out roughly, according to the criterion of the number of degrees of freedom K, which is necessary for obtaining a certain fixed dispersion of the estimates σ_{NT} [1]

$$T \geqslant \frac{1}{2B} \, K[D(\sigma)] \tag{4}$$

where B is the frequency bandwidth of the initial process. Thus, for example, to obtain an estimate with a dispersion of ±1 dB, at a confidence level of 80%, it is required that K = 63; if B = 20 kHz,

$$T = \frac{63}{4 \cdot 10^4} \approx 16 \cdot 10^{-4} \, \text{sec}$$

In the majority of practical cases, during such an interval of time, it can be considered that A(t) is unchanged.

The procedure for analysis of a transient signal (1), with known $A(t_1)$, is reduced to analysis of the sequence of segments of the signal

$$\dot{x}_i(t) = \frac{x(t)}{A(t_i)} \approx N_i(t) \tag{5}$$

with

$$t_i - \frac{T}{2} < t < t_i + \frac{T}{2}$$

For an estimate of the degree of correspondence between the spectrum of the steadied signal (5) and the spectrum of the initial steady signal N(t), a spectral analysis, with resolving powers of 1/24, 1/12, 1/6 and 1/3 octaves and a modulating function of the type

186

$$A(t) = \frac{A_0}{\sqrt{1+z^2\left(t-\frac{T}{2}\right)^2}}$$ (7)

where T is the total length of the realization analyzed, A_0 = const and α is a parameter, is carried out on a BESM-4 digital computer, by means of an inverse algorithm [2]. The signal N(t) was presented as the sum of a steady random signal with a given auto-correlation function and five discrete components. For each of three values of the parameter α (0, 0.1, 0.5), statistically independent realizations of the signal x(t) were analyzed over ten smoothings, in accordance with expression (5). The results of the /167 processing of the spectral estimates sampled showed that their dispersion, for the process N(t), corresponds to the theoretical values [8] and is independent of A(t). The mean values of the estimates of the spectra, at values of parameter α = 0.1 and α = = 0.5, were practically indistinguishable from the values obtained at α = 0 (steady signal). Only in the 1/24 and 1/12 octave bands, adjacent to bands into which the discrete components enter, is a certain positive displacement observed, on the order of 1-3 dB, due to "washing" of the discrete components, caused by modulation. As should be expected, this displacement increases with increase in α, i.e., with increase in the rate of change of the signal envelop.

VIBRATIONAL SENSITIVITY OF A MEASURING INSTRUMENT
AND METHODS OF INCREASING THE ACCURACY OF ITS DETERMINATIONS

Yu.S. Mironov
(Leningrad)

The properties and peculiarities of two groups of measuring systems reacting to vibrations are discussed.

The results of the action of a three-dimensional, cophasal, monoharmonic vibration on the linear system of a measuring instrument were analyzed. For a change in the instrument reading, the following relation was obtained: $u = \text{grad}\, u \cdot \bar{\psi}$, where $\bar{K} = \text{grad}\, u$, $\bar{\psi} = \{x,y,z\}$ are the vectors of the vibration sensitivity of the instrument and of the vibration action. Ways to decrease or increase u were examined in the cases when the vibrations are the acting or measured values, respectively. In measurement of the vibrations, on the basis of the direction of z, the action of the transverse components leads to a relative error $\delta_1 = (\bar{\psi}_{xy} \cdot \bar{K}_{xy})/u_z$. In order that $\delta_1 \sim 0$, it is necessary and sufficient that

a) $\bar{\psi}_{xy} \approx 0$, b) $\bar{K}_{xy} \approx 0$ and c) $\cos\varphi(\bar{\psi}_{xy} \wedge \bar{K}_{xy}) = 0$

In experimental determination of $\bar{K}$, monotonic oscillations should be given successively in the directions x, y and z, determining u_x, u_y and u_z by the known method. However, this leads to considerable error, in connection with inaccuracy of the experimental means. To increase the accuracy in determination of $\bar{K}$ for /168 linear systems, it is proposed to measure u and the components $\{x_1, y_1, z_1\}$ in succession, by rotation of this instrument in the X, Y and Z directions, and then by compiling a system of equations, which is written, in matrix form

$$\bar{A} \cdot \bar{K} = u, \text{ where } A = \begin{pmatrix} x_1 & y_1 & z_1 \\ x_2 & y_2 & z_2 \\ x_3 & y_3 & z_3 \end{pmatrix}, \quad u = \begin{pmatrix} u_1 \\ u_2 \\ u_3 \end{pmatrix}, \quad \bar{K} = \begin{pmatrix} \partial u/\partial x \\ \partial u/\partial y \\ \partial u/\partial z \end{pmatrix}.$$

Since $\bar{A}$ and u are found by experiment, at $\bar{A} \neq 0$, $\bar{K} = u \cdot \bar{A}^{-1}$ is determined.

Let us examine the error δ_2 in determination of the vibration sensitivity, during tests of the instrument, for which the vibration is affecting the value, by a unidirectional vibration action, in the case of the presence of nonlinear distortions. Together with the basic signal $w_1 \cos 2\pi\nu_1 t$, let $w_2 \cos 2\pi\nu_2 t$ act, in which $w_1 \leq 2w_2$ and $\nu_2 \neq n\nu_1$, where n is a whole number and

$\nu_1 \geq 10$ Hz. The following is obtained in this case

$$\delta_2 = \Theta_{21} \frac{w_2}{w_1} - \frac{1}{2} \frac{w_2^2}{w_1^2} \left(1 + \Theta_{21} \frac{w_2}{w_1}\right),$$

where Θ_{21} is the ratio of the sensitivities of the instrument at ν_2 and ν_1. At $w_2 = 0$ and in the nontrivial case, with

$$\frac{w_2}{w_1} = \sqrt{2 + \left(\frac{\Theta_{12}}{2}\right)^2} - \frac{\Theta_{12}}{2}$$

the error $\delta_2 = 0$. Thus, for example, this takes place at

$$\Theta_{12} = 4 \quad \text{and} \quad \frac{w_2}{w_1} = 0.45.$$

A method for decrease in the error δ_2 also was proposed.

The connection between vibration sensitivity and vibration resistance was analyzed, for instruments not measuring vibrations; known and proposed new criteria for estimates of vibration resistance were analyzed. The form for expression of the results of tests of vibration resistance was given. Experimental data were presented on decreasing the errors in nonlinear systems during vibrations.

MEASUREMENT OF THE VIBRATION OF STRUCTURES
WITH A THREE-COMPONENT VIBRATION SENSOR

V.V. Yes'kov, V.S. Konevalov, and A.S. Nikiforov
(Leningrad)

A method is described for measurement of transverse displacements of a plate, caused by transverse waves, and longitudinal displacements, caused by the total effect of longitudinal and transverse waves, by means of a three-component vibration sensor.

Limitations arising during measurements of the relationship of displacements of a plate, caused by transverse and longitudinal-transverse waves are:

1. Connection of the vibration sensor to the plate studied leads to change in the transverse displacement of points on the surface of the plate, due to the finite impedance of the vibration sensor [2];

2. The vibration sensor has a finite magnitude of selectivity, with respect to vibrations, accomplished in the direction of the axes of different channels of the vibration sensor;

3. Longitudinal displacements of the plate surface, caused by transverse waves, create a restriction on the relative sensitivity of the vibration sensor to longitudinal-transverse waves. This restriction equals

$$\frac{\xi_{x,y}}{\xi_z} = \frac{hK_{tr}}{2} \tag{1}$$

where $h = h_{pl} + 2H$, $\xi_{x,y}$ and ξ_z are the displacements of the plate surface in the longitudinal and transverse directions, respectively; h_{pl} is the plate thickness; H is the ele ation of the vibration sensor axis above the plate surface and K_{tr} is the wave number of the transverse waves in the plate;

4. The transverse displacement of the plate surface during propagation of longitudinal waves, due to the Poisson ratio, also creates a restriction on the sensitivity of the vibration sensor to transverse waves. It equals

$$\frac{\xi_z}{\xi_{x,y}} = v, \tag{2}$$

where v is the Poisson coefficient.

190

The region of values of the ratio of the amplitudes of the longitudinal (ξ_x and ξ_y) and transverse (ξ_z) displacements of the surface of a plate 20 mm thick, characterizing the ratio of the amplitudes of these displacements, caused by longitudinal-transverse and by transverse waves, is shown in Fig. 1. The measured ratios ξ_x/ξ_z and ξ_y/ξ_z cannot be sufficiently reliably applied to the waves referred to above beyond the limits of these restrictions.

The results of measurements of the ratios ξ_x/ξ_z and ξ_y/ξ_z, by means of a three-component vibration sensor, of a structure 20 mm thick, fastened parallel to the stiffening ribs, at a distance of 50 cm from one another, also are presented as an example in Fig. 1. Excitation was accomplished with a wideband noise source. It is evident that the amplitudes ξ_x and ξ_y are close to one another and approach ξ_z with increase in frequency. It also is evident that, in this case, the results of the measurements fit into the limitations discussed above.

Fig. 1. Ratio of the amplitudes of longitudinal (ξ_x and ξ_y) displacements of a plate surface to transverse (ξ_z): 1. ξ_y/ξ_z; 2. ξ_x/ξ_z; 3. restriction dependent on selectivity of the vibration sensor; 4. restriction according to formula (2); 5. restriction according to formula (1).

The ratio of the amplitudes of the transverse and longitudinal vibrations of models, which were plates of various thicknesses, fastened with stiffening ribs, were investigated by means of the three-component vibration sensor. Similar measurements also were carried out on plates without stiffening ribs.

The dimensions of the models and plates were on the order of 70×100 cm^2, with thicknesses of 6 to 12 mm.

The results of the measurements show, in particular, that the amplitudes of the longitudinal vibrations increase considerably and approach the values of the amplitudes of the transverse

vibrations, with the plates fastened by stiffening ribs. The ratio of the amplitudes of the longitudinal and transverse vibrations in plates with stiffening ribs increases with increase in frequency. This ratio also increases with increase in thickness of plates fastened by stiffening ribs.

The results of the measurements of longitudinal and transverse vibrations of plates in certain real engineering structures coincide qualitatively with the results of investigations carried out on models.

REFERENCES

1. Keller, F., _Acustica_ 10, · 349 (1960).

2. Klyukin, I.I., _Akusticheskiy zhurnal_ 5(1), 38 (1959).

METHOD OF ACCOUNTING FOR INSTRUMENTAL DISTORTIONS DURING OBSERVATION OF SIGNALS

K.A. Kazlauskas and Ts.Ts. Paulauskas
(Vil'nyus)

A method is proposed in the work for accounting for instrumental distortions in linear systems with known dynamic characteristics.

A signal x(t), passing through the system, is distorted and causes signal y(t) at the outlet. For a linear system, the connection between signals y(t) and x(t) is described by the packet integral:

$$y(t) = \int_{-\infty}^{\infty} k(t-\tau) x(\tau) d\tau,$$ (1)

where k(t) is the pulse transfer function of the system.

Applying a Fourier transform to Eq. (1), we obtain

$$S_y(w) = K(w) S_x(\omega),$$ (2)

where $S_y(\omega)$ and $S_x(\omega)$ are Fourier images for signals y(t), x(t) and /172 the function k(t), respectively.

From Eq. (2), we have

$$S_x(\omega) = \frac{S_y(\omega)}{K(\omega)}.$$ (3)

The pulse transfer function of an ideal system is the δ function.

We reduce expression (3) to the form

$$S_x(\omega) = S_y(\omega) + \left[\frac{1}{K(\omega)} - 1 \right] S_y(\omega),$$ (4)

where the factor(1/K(ω)) - 1 characterizes the instrumental distortion. In proportion to approach to the ideal system, (1/K(ω)) - 1

tends toward zero. In practice, as $\omega \to \infty$, $K(\omega) \to 0$; consequently, $1/K(\omega)$ increases without limit and it is impossible to calculate $S_x(\omega)$ precisely by formula (4).

A calculation by formula (4) can be carried out approximately. Using the expansion

$$\frac{z}{1-z} = z + z^2 + \ldots + z^n + \ldots,$$

where $|z| < 1$, we reduce Eq. (4) to the form

$$S_{x_n}(\omega) = S_y(\omega) \{1 + [1 - k(\omega)] + [1 - k(\omega)]^2 + \ldots + [1 - K(\omega)]^n\}. \tag{5}$$

where $|1 - K(\omega)| < 1$.

Applying a reverse Fourier transform to Eq. (5), we obtain

$$x_n(t) = y(t) + y(t) * [\delta(t) - k(t)] + y(t) * [\delta(t) - k(t)]^{2*} + \ldots$$
$$\ldots + y(t) * [\delta(t) - k(t)]^{n*} = y(t) * d_n(t), \tag{6}$$

where $d_n(t) = \delta(t) + [\delta(t) - k(t)] + [\delta(t) - k(t)]^{2*} + \ldots + [\delta(t) - k(t)]^{n*}$, $\delta(t)$ is the Dirac delta function and $n*$ is the n-fold taking of the packing operation.

According to formula (5) in the frequency region or according to formula (6) in the time region, approximate values of the signal $x(t)$ are calculated, taking account of the instrumental distortions.

Recommendations are presented as to how to proceed in cases when the condition $|1 - K(\omega)| < 1$ is not satisfied. Cases are discussed, in which the signal $y(t)$ is observed in a mixture with additive noise.

An experimental verification by digital computer showed the workability of the method, permitting the data characteristics of the results of measurements or observations to be improved.

194

METHOD OF INVESTIGATION OF VIBROACOUSTIC CHARACTERISTICS OF CENTRIFUGAL PUMPS

B.V. Pokrovskiy, V.Ya. Rubinov, and A.M. Yurgin
(Moscow)

A method has been used in acoustical diagnostics of pumps, which consists of taking sonograms of the pump, by means of an audio spectrograph. In distinction from usual analyzers, the spectrograph makes it possible to obtain a three-dimensional image of the signal being analyzed, in which its frequency-amplitude characteristics developed over time, with a resolving power of 0.004 sec, are depicted. As an example, a sonogram of an electrically driven pump, in the 40-4000 Hz frequency range, is presented in the figure. The amplitude ratios are determined on the sonogram by the contrast of individual contours, with an accuracy of 6 dB.

f, Hz
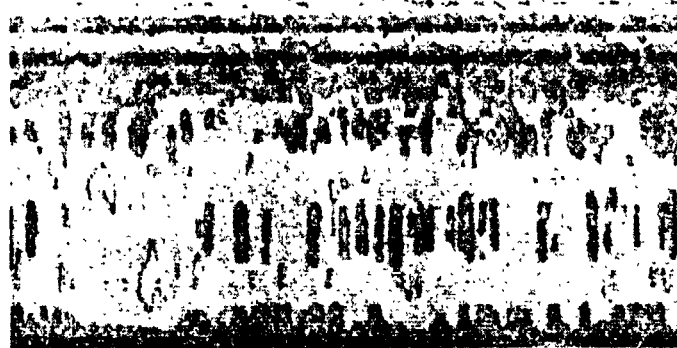
Fig. 1.

A comparison of the spectrograms and sonograms of a series of experimental pumps, with previously known characteristics of the vibrational processes, permitted it to be determined that the completely defined "images" on the sonogram correspond to individual sources of hydrodynamic vibrations of the pump (from irregularities in the flow, vortical and cavitation). The possibilities of the spectrograph, supplemented by the use of multispeed magnetic recordings by tape recorder, were used in investigation of periodic, transient processes during flow around the grating of a centrifugal pump, leading to the generation of discrete vibrations at the /174

breaking frequency and its harmonics.

The results of experimental investigations of vibroacoustical characteristics of centrifugal pumps, by means of the spectrogr, are evidence of the promise of this method for revealing the fundamental sources of vibrations, which can be identified by means of specific "images" on the sonogram, and their study.

METHOD OF APPROXIMATE DETERMINATION OF THE
CHARACTERISTICS OF NONLINEAR VIBRATIONAL SYSTEMS

R.P. Atstupenene and V.-R.V. Atstupenas
(Kaunas)

Methods of determination of the characteristics of elements of nonlinear vibrational systems, from the result of analysis of forced vibrations [1,2], are approximate in themselves, since they are based on the use of experimental data. The constant components of the linearized characteristics and linearization coefficients are determined experimentally by finding the values of these quantities at different vibration amplitudes and frequencies and subsequent approximation of their analytical expressions. Therefore, it is important to have simple and convenient, although approximate, formulas for determination of the characteristics of vibrational systems from experimentally known functions.

If it is assumed that solution of the equation of motion of a nonlinear system

$$m\ddot{x} + F_1(\dot{x}) + F_2(x) = E \sin \omega t \tag{1}$$

can be written with sufficient accuracy in the form

$$x = x_0 + a \sin(\omega t + \varphi), \tag{2}$$

using the method of statistical linearization, we obtain [2] the following formulas for the constant damping components and elastic forces and the corresponding linearization coefficients:

$$F_0(Z) = -\frac{2}{\pi} \int_0^Z \frac{P(z)}{\sqrt{Z^2 - z^2}}\, dz, \tag{3}$$

$$q^{(1)}(Z) = \left\{ \frac{2}{Z^2 \pi} \int_{-Z}^{Z} \frac{F^2(z)\, dz}{\sqrt{Z^2 - z^2}} - F_0^2(Z) \right\}^{\frac{1}{2}}, \tag{4}$$

$$q^{(2)}(Z) = \frac{4}{Z^2 \pi} \int_0^Z \frac{Q(z)\, z\, dz}{\sqrt{Z^2 - z^2}}. \tag{5}$$

Here, z = x, Z = a for the elastic characteristic and Z = $\dot{x}$, Z = aω for the damping characteristics, P(z) and Q(z) are the even and odd

components of the characteristic $F(z)$, $q^{(1)}$ is the linearization coefficient, obtained by use of the first approximation criterion, conditions of equality of the mathematical expectations and dispersions of the true and approximating functions, $q^{(2)}$ is the coefficient of linearization, obtained by use of the second approximation criterion, the conditions of the minimum mathematical expectation of the square of the difference between the true and approximating functions.

For determination of the system characteristics from known $F_0(Z)$ and $q(Z)$, integral Eqs. (3)-(5) should be solved. In view of the fact that $P(z)$ has a slight effect on the magnitude of q (in conformance with expression (5), this effect is completely absent), as well as for obtaining a simpler expression of $F^{(1)}(z)$, we assume $F(z) = Q(z)$ and $F_0(Z) = 0$ in Eq.(4). Precise solution of these equations gives

$$F^{(1)}(z) = \text{sign}\, z \left\{ \frac{1}{2}\, \frac{d}{dz} \int_0^z \frac{Z^2 q^2(Z)\, dZ}{\sqrt{z^2 - Z^2}} \right\}^{\frac{1}{2}} - \frac{d}{dz} \int_0^z \frac{F_0(Z)\, Z\, dZ}{\sqrt{z^2 - Z^2}} \,. \tag{6}$$

$$F^{(2)}(z) = \text{sign}\, z \int_0^z \frac{d}{d(Z^2)}\, [Z^2 q(Z)]\, \frac{Z\, dZ}{\sqrt{z^2 - Z^2}} - \frac{d}{dz} \int_0^z \frac{F_0(Z)\, Z\, dZ}{\sqrt{z^2 - Z^2}} \,. \tag{7}$$

For an approximate solution of integral Eqs. (3)-(5), we use the mechanical quadrature formulae of V.A. Steklov [3]:

$$\frac{1}{\pi} \int_{-1}^{1} \frac{f(y)\, dy}{\sqrt{1 - y^2}} = \frac{1}{6} \left[f(1) + f(-1) + 2f\left(\frac{1}{2}\right) + 2f\left(-\frac{1}{2}\right) \right] + R_1, \tag{8}$$

where the residual term

/176

$$R_1 = -\frac{f^{(6)}(\zeta)}{2^6 \cdot 6!} \qquad \text{at} \quad -1 < \zeta < 1 \tag{9}$$

and the more precise formula

$$\frac{1}{\pi} \int_{-1}^{1} \frac{f(y)\, dy}{\sqrt{1 - y^2}} = \frac{1}{12} \left[f(1) + f(-1) + 2f\left(\frac{1}{2}\right) + 2f\left(\frac{1}{2}\right) + \right.$$

$$\left. + 2f\left(\frac{\sqrt{3}}{2}\right) + 2f\left(-\frac{\sqrt{3}}{2}\right) \right] + R_2. \tag{10}$$

198

where the residual term

$$R_2 = - \frac{f^{(12)}(\zeta)}{2^{11} \cdot 12!} \qquad \text{at} \quad -1 < \zeta < 1. \tag{11}$$

After appropriate transformation of the right sides of Eqs (3)-(5) and application of formula (8), without the residual term, to them, we obtain

$$F_0(Z) = -\frac{1}{3}\left[P(Z) + 2P\left(\frac{Z}{2}\right)\right], \tag{12}$$

$$q^{(1)}(Z) = \left\{\frac{2}{3Z^2}\left[Q^2(Z) + 2Q^2\left(\frac{Z}{2}\right)\right]\right\}^{\frac{1}{2}}, \tag{13}$$

$$q^2(Z) = \frac{2}{3Z}\left[Q(Z) + Q\left(\frac{Z}{2}\right)\right]. \tag{14}$$

The presence of values of functions P and Q, at two values of the argument, in Eqs. (12)-(14) hampers solution of these equations for the even and odd components of the unknown function. It is clear from equalities (12)-(14) that, in the first approximation, $F_0(Z)$ depends on the argument as $P(z)$ and $Zq(Z)$ as $Q(z)$. If functions $F_0(Z)$ and $Zq(Z)$ are formed from the basic elementary functions, without the summing and calculation operations,

$$\frac{P\left(\frac{Z}{2}\right)}{P(Z)} \approx \frac{F_0\left(\frac{Z}{2}\right)}{F_0(Z)}; \qquad \frac{Q\left(\frac{Z}{2}\right)}{Q(Z)} \approx \frac{q\left(\frac{Z}{2}\right)}{2q(Z)};$$

$$\frac{Q^2\left(\frac{Z}{2}\right)}{Q^2(Z)} \approx \frac{q^2\left(\frac{Z}{2}\right)}{4q^2(Z)}. \tag{15}$$

Taking (15) into account, Eqs. (12)-(14) assume the form

$$F_0(Z) = -\frac{1}{3} P(Z)\left[1 + 2\frac{F_0\left(\frac{Z}{2}\right)}{F_0(Z)}\right]. \tag{16}$$

$$q^{(1)}(Z) = \left\{ \frac{2}{3Z^2} \; Q^2(Z) \left[1 + \frac{q^{(2)}\left(\frac{Z}{2}\right)}{2q^{(1)}\left(\frac{Z}{2}\right)} \right] \right\}^{\frac{1}{2}} .$$ (17)

$$q^{(2)}(Z) = \frac{2}{3Z} \; Q(Z) \left[1 + \frac{q^{(1)}\left(\frac{Z}{2}\right)}{2q^{(2)}\left(\frac{Z}{2}\right)} \right] .$$ (18)

and their solution for P and Q becomes elementary. After substituting z for Z, we have:

$$F^{(1)}(z) = \frac{\sqrt{3} \; zq(z) \; \text{sign} \, z}{\left\{ 2 + \frac{q^2\left(\frac{z}{2}\right)}{q^2(z)} \right\}^{\frac{1}{2}}} - \frac{3F_0(z)}{1 + 2 \frac{F_0\left(\frac{z}{2}\right)}{F_0(z)}} ,$$ (19)

$$F^{(2)}(z) = \frac{3z \, q(z) \, \text{sign} \, z}{2 + \frac{q\left(\frac{z}{2}\right)}{q(z)}} - \frac{3F_0(z)}{1 + 2 \frac{F_0\left(\frac{z}{2}\right)}{F_0(z)}} .$$ (20)

The first term in these formulas is taken with the sign of the argument, and the argument in the second term according to the absolute value, because P and Q are even and odd components of the characteristics sought, by definition.

If the analytical expressions of $F_0(Z)$ and q(Z) are formed from the sum of the functions of the class referred to, formulas (19) and (20) are used for each term separately, and the characteristics are determined termwise.

It is evident from expressions (8) and (9), taking (15) into account, that the approximate formulas (19) and (20) are the more accurate, the smaller the six derivatives of $F_0(Z)$ and $Z^2q(Z)$. If function $F_0(Z)$ is expressed by an even, and function $Z^2q(Z)$, by an even, polynomial in Z steps, not higher than five, formulas (19) and (20) give the same results as formulas (6) and (7).

If the accuracy must be increased, formula (10) can be used <u>/178</u> without the residual term. In this case, we obtain:

$$F_0(Z) = -\frac{1}{6} \left[P(Z) + 2P\left(\frac{Z}{2}\right) + 2P\left(-\frac{\sqrt{3}}{2} Z\right) \right] ,$$ (21)

200

$$q^{(1)}(Z) = \left\{ \frac{1}{3Z^2} \left[Q^2(Z) + 2Q^2\left(\frac{Z}{2}\right) + 2Q^2\left(\frac{\sqrt{3}}{2} - Z\right) \right] \right\}^{\frac{1}{2}}.$$ (22)

$$q^{(2)}(Z) = \frac{1}{3Z}\left[Q(Z) + Q\left(\frac{Z}{2}\right) + 3Q\left(\frac{\sqrt{3}}{2} - Z\right) \right].$$ (23)

Making such an assumption concerning the structure of functions $F_0(Z)$ and $Zq(Z)$ and carrying out similar actions, we obtain:

$$F^{(1)}(z) = \frac{\sqrt{3}\, zq(z)\, \mathrm{sign}\, z}{\left\{ 1 - \dfrac{q^2\left(\frac{z}{2}\right)}{2q^2(z)} + \dfrac{3}{2}\dfrac{q^2\left(\frac{\sqrt{3}}{2} - z\right)}{q^2(z)} \right\}^{\frac{1}{2}}}$$
$$- \frac{6F_0(z)}{1 + 2\dfrac{F_0\left(\frac{z}{2}\right)}{F_0(z)} + 2\dfrac{F_0\left(\frac{\sqrt{3}}{2} - z\right)}{F_0(z)}}.$$ (24)

$$F^{(2)}(z) = \frac{3zq(z)\, \mathrm{sign}\, z}{1 + \dfrac{q\left(\frac{z}{2}\right)}{2q(z)} + \dfrac{3}{2}\dfrac{q\left(\frac{\sqrt{3}}{2} - z\right)}{q(z)}}$$
$$- \frac{6F_0(z)}{1 + 2\dfrac{F_0\left(\frac{z}{2}\right)}{F_0(z)} + 2\dfrac{F_0\left(\frac{\sqrt{3}}{2} - z\right)}{F_0(z)}}.$$ (25)

These formulas are the more accurate, the smaller are 20 derivatives of $F_0(Z)$ and $Z^2q(Z)$, and, if the sum of these functions is expressed by a polynomial in Z steps, not over 11, the error in formulas (24) and (25) equals zero, in comparison with the formulas (16) and (17).

Example

Let the following be obtained as a result of processing the experimental data: $F_0(a) = -c_1 a^3 c_1 a^3$, and $q(a) = c_2 a^4$. Determine the elastic characteristics of the system.

Substituting the known values of $F_0(a)$ and $q(a)$ in the formulas obtained, we obtain:

$$F^{(1)}(x) = 2.3562\, c_1\ x^3 + 1.4254\, c_2 x^5,$$
$$F^{(2)}(x) = 2.3562\, c_1\ x^3 + 1.6000\, c_2 x^5,$$

according to formulas (6) and (7);

$$F^{(1)}(x) = 2.4000 \, c_1 \, x^3 + 1.2235 \, c_2 \, x^5,$$

$$F^{(2)}(x) = 2.4000 \, c_1 \, x^3 + 1.4545 \, c_2 \, x^5.$$

according to formulas (19) and (20);

$$F^{(1)}(x) = 2.3538 \, c_1 \, x^3 + 2.4254 \, c_2 \, x^5,$$

$$F^{(2)}(x) = 2.3538 \, c_1 \, x^3 + 1.6000 \, c_2 \, x^5.$$

from formulas (24) and (25).

The example presented demonstrates the simplicity and effectiveness of the proposed method.

REFERENCES

1. Kononenko, V.O. and N.P. Plakhtiyenko, "Determination of the Characteristics of Nonlinear Elements of Vibrational Systems from Analysis of the Motion," <u>Prikladnaya mekhanika</u> <u>5</u>(10) (1969).

2. Atstupenas, V.-R.V. and R.P. Atstupenene, "Determination of the Characteristics of Nonlinear Vibrational Systems with One Degree of Freedom, from the Results of Vibration Tests," <u>Nauchnyye trudy VUZ Litovskoy SSR, Vibrotekhnika</u> <u>3</u>(16) (1971).

3. Stekloff, W., "Quadratures, Note 1," <u>Izvestiya Rossiyskoy Akademii nauk</u>, Series VI (17) (1918).

THE RELATIONSHIP OF TRANSIENT VIBRATIONAL PROCESSES AT A POINT IN A PLATE TO THE NATURE OF SUDDEN KINEMATIC DISTURBANCES

Yu. K. Konenkov
(Moscow)

A solution is given in this work to the problem of a transient vibration process in a fastened plate, during a sudden displacement of the edge. Let us take the equation of motion of the plate in the form

$$D \; \frac{1}{r} \; \frac{\partial}{\partial r} \; r \; \frac{\partial}{\partial r} \; \frac{1}{r} \; \frac{\partial}{\partial r} \; r \; \frac{\partial}{\partial r} \; \omega + \rho h \; \frac{\partial^2}{\partial t^2} \; \omega = 0$$

with limiting and initial conditions

$$\omega(R, t) = f_1(t), \qquad \frac{\partial}{\partial r} \, \omega(R, t) = f_2(t),$$

$$\omega(R, 0) = 0, \qquad \frac{\partial}{\partial t} \, \omega(r, 0) = 0.$$

Usually, a problem of this type is solved with the aid of a Laplace transform. It is more convenient in this case to reduce the equation to a nonuniform one and to make the limiting conditions uniform, assuming

$$\omega(r, t) = \left(\frac{r^2 - R^2}{2R} \right) f_2(t) + f_1(t) + \psi(r, t)$$

For the function introduced $\psi(r,t)$, we obtain the following problem

$$D \; \frac{1}{r} \; \frac{\partial}{\partial r} \; r \; \frac{\partial}{\partial r} \; \frac{1}{r} \; \frac{\partial}{\partial r} \; r \; \frac{\partial}{\partial r} \; \psi + \rho h \; \frac{\partial^2 \psi}{\partial t^2} =$$
$$= - \rho h \left[\left(\frac{r^2 - R^2}{2R} \right) f_2''(t) + f_1''(t) \right]$$

with limiting conditions

$$\psi(R, t) = 0, \qquad \frac{\partial}{\partial r} \, \psi(R, t) = 0,$$

204

and initial conditions

$$\ddot{\psi}(r,0) = -\left(\frac{r^2-R^2}{2R}\right)f_2(0)-f_1(0),$$

$$\frac{\partial}{\partial t}\ddot{\psi}(r,0) = -\left(\frac{r^2-R_2}{2R}\right)f_2'(0)-f_1'(0)$$

Solution of this problem by the separation of variables method is presented in the form

$$\ddot{\psi}(r,t) = \sum_n \left\{I_0(i\,\varkappa_n)I_0\left(\varkappa_n\,\frac{r}{R}\right) - I_0(\varkappa_n)I_0\left(i\,\varkappa_n\,\frac{r}{R}\right)\right\} \times$$

$$\times \left[a_n\sin\omega_n t + b_n\cos\omega_n t + \int_0^t \frac{\sin\omega_n(t-\tau)}{\omega_n}\,\Phi_n(\tau)\,d\tau\right]$$

where $\omega_n^2 = D\varkappa_n^4/\rho h$, $\Phi_n(\tau)$ are coefficients of the generalized Fourier /181 series

$$\Phi_n(t) = -\frac{\int_0^R\left[I_0(i\,\varkappa_n)I_0\left(\varkappa_n\,\frac{r}{R}\right) - I_0(\varkappa_n)I_0\left(i\,\varkappa_n\,\frac{r}{R}\right)\right][(r-R)f_2''(t)+f_1''(t)]\,r\,dr}{\int_0^R\left[I_0(i\,\varkappa_n)I_0\left(\varkappa_n\,\frac{r}{R}\right) - I_0(\varkappa_n)I_0\left(i\,\varkappa_n\,\frac{r}{R}\right)\right]^2 r\,dr}$$

α_n is the solution of the frequency equation

$$I_0(i\,\varkappa_n)\dot{I}_0(\varkappa_n)-i\,I_0(\varkappa_n)\dot{I}_0(i\,\varkappa_n)=0$$

n	1	2	3	4	5	6	7
$\varkappa_n$	3.1961	6.3064	9.4395	12 577	15.716	18 850	21.992

The integration constants a_n and b_n are found from the initial conditions. Let us examine the interesting partial case, when $f_2(t) = 0$

and there is no action at t = 0, i.e., $f_1(0) = f_2(0) = 0$, in greater detail. To obtain the closed form of the solution, the Fourier-Bessel coefficients must be calculated explicitly. This is achieved by means of the Lommel functional relation, which is suitable for any cylindrical functions $Z_\lambda(\alpha x)$ and $Z_\mu(\beta x)$:

$$\int \left[(\alpha^2 - \beta^2)x - \frac{\lambda^2 - \omega^2}{2} \right] z_\lambda(\alpha x)\, z_\mu(\beta x)\, dx =$$

$$= x \{ \beta\, z_\lambda(\alpha x)\, \dot{z}_\mu(\beta x) - \omega\, z_\mu(\beta x)\, \dot{z}_\lambda(\alpha x) \}$$

In this manner, the solution of the problem finally takes the form

$$\dot{\psi}(r,t) = - \sum_{n=1}^{\infty} \times$$

$$\times \frac{2\,[I_0(i\varkappa_n)\,I_1(\varkappa_n) + I_0(\varkappa_n)\,i I_1(i\varkappa_n)] \left[I_0(i\varkappa_n)\,I_0\left(\varkappa_n\,\frac{r}{R}\right) - I_0(\varkappa_n)\,I_0\left(i\varkappa_n\,\frac{r}{R}\right) \right]}{\varkappa_n\,\{I_0^2(i\varkappa_n)\,[I_0^2(\varkappa_n) + I_1^2(\varkappa_n)] - I_0^2(\varkappa_n)\,[I_0^2(i\varkappa_n) + I_1^2(i\varkappa_n)]\}} \times$$

$$\times \int_0^t \frac{\sin \omega_n(t-\tau)}{\omega_n}\, f_1(\tau)\, d\tau$$

Finally, it is of interest to examine some partial cases of exci- /182 tation, in which the packing can be calculated and the explicit type of change in a deformation over time can be found. Some examples are presented in the table on the following page.

206

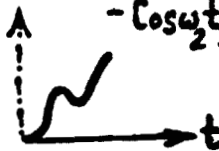| Type of function $f(t)$	Corresponding type of packing $\Phi_n(t) = \int_0^t \dfrac{\sin \omega_n (t-\tau)}{\omega_n} f'(\tau)\, d\tau$
$f(t) = Qt$	$\dfrac{Q \sin \omega_n t}{\omega_n}$
$f(t) = Q$	$+Q \cos \sqrt{\dfrac{D \alpha_n^4}{\rho h}}\, t$
$f(t) = Qt^2$	$\dfrac{\rho h (1 - \cos \omega_n t)}{D \alpha_n^4}$
$f(t) = Q(\cos \omega_1 t - \cos \omega_2 t)$	$\Phi_n(t) = \dfrac{Q}{\omega_n} \left\{ -\sin \omega_n t \left[\dfrac{\sin(\omega_n - \omega_1)t}{\omega_n - \omega_1} + \dfrac{\sin(\omega_n + \omega_1)t}{\omega_n + \omega_1} \right] \dfrac{\omega_1^2}{2} \right.$ $+\cos \omega_n t \left[\dfrac{1-\cos(\omega_n - \omega_1)t}{\omega_n - \omega_1} + \dfrac{1-\cos(\omega_n + \omega_1)t}{\omega_n + \omega_1} \right] \dfrac{\omega_1^2}{2}$ $+\sin \omega_n t \left[\dfrac{\sin(\omega_n - \omega_2)t}{\omega_n - \omega_2} + \dfrac{\sin(\omega_n + \omega_2)t}{\omega_n + \omega_2} \right] \dfrac{\omega_2^2}{2}$ $\left. -\cos \omega_n t \left[\dfrac{1-\cos(\omega_n - \omega_2)t}{\omega_n - \omega_2} + \dfrac{1-\cos(\omega_n + \omega_2)t}{\omega_n + \omega_2} \right] \dfrac{\omega_2^2}{2} \right\}$

INVESTIGATION OF THE NOISE CHARACTERISTICS
OF ROOM AIR CONDITIONERS

S.I. Tret'yakova
(Moscow)

In recent years, room air conditioners have become widely used in the national economy. However, control of them is restrained by the absence of standard documentation, regulating the noise characteristics of room air conditioners. Standards, established by the method of measurement of the noise characteristics of the machines and fans, have not spread to methods of control of noise characteristics of room air conditioners, for the following reasons:

-- The presence of discrete components in the noise spectrum;
-- The transient nature of the noise;
-- The features of the air conditioner unit in rooms, dependent on radiation in 1/8 and 1/4 space.

Methods of measurement of the noise characteristics of room air conditioners in anechoic and reverberation chambers, according to All-Union State Standard 11870-66 and the machines, are examined in the work. Methods of determination of the noise characteristics are the ASRAE recommendations on methods of measurement of ventilation unit noise. It was shown that the most acceptable method is the standard source method in a reverberation room, with time and space averaging. Quantitative estimates of the errors in measurement by comparable methods are presented.

SYNTHESIS OF VIBRATION DAMPERS

V.A. Kamayev and S.V. Nikitin
(Bryansk)

Widely used for vibration quenching are shock absorbers, with characteristics of the type

$$F(x, \dot{x}) = cx + f(x, \dot{x}),\qquad(1)$$

in the dampers of which there is Coulomb friction, leading to discontinuities of the first or second kind of characteristics $f(x, \dot{x})$ and shock absorber reaction (acceleration of vibration-isolatable object $\ddot{x}$). The perturbation function, acting on the isolated object, in turn, often has a discontinuity. In these cases, the synthesis /184 of dampers, especially with polygonal characteristics, on the basis of the usual quality criteria of the type

$$\Phi = \Phi(K_{\omega, \Delta t}, \ddot{x})\qquad(2)$$

($K_{\omega, \Delta t}$ is the weight coefficient, dependent on the frequency and time of operation at it) will not always be sufficiently successful, and sometimes leads to trivial outcomes. A synthesis, resting on criteria which take account of the third derivative of the displacement of the object, of the type

$$\Phi' = \Phi'(K'_{\omega, \Delta t}, \dddot{x}).\qquad(3)$$

provides great advantages. In this case, a filtering process is a supplementary differentiation, which permits low-frequency vibrations to be suppressed and high-frequency ones, transmitting great energy, to be extracted. Moreover, we note that there are data [1, 2], which permit standardization of the action of the vibrations on a human by type (3) criteria.

The use of type (3) criteria, in turn, causes definite difficulties in the use of analytical methods of synthesis (the first approximation is insufficient). In this case, a synthesis using an analog or digital computer is effective.

Producing $\dddot{x}$ by an analog computer, by means of differentiation of $\ddot{x}$ leads to large systematic errors. A method is proposed for determination of $\dddot{x}$ by means of measurement of the acceleration $\dot{x}$, with the aid of a mathematical accelerometer. The mathematical

accelerometer is an electronic model of the regular mechanical accelerometer hooked up to an analog computer. The natural frequency of the accelerometer $\omega_c \gg \omega_1$, where ω_1 is the highest of the frequencies of the object measured.

Using type (3) quality criteria, a synthesis of a series of dampers was carried out. In this case, their structural systems, determined by the possibility of being put into practice structurally, were given. The damper characteristics were optimized from among those shown in Fig. 1, in which the number of optimization factors (parameters) changed from one (Fig. 1a, 1b) to three (Fig. 1e).
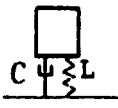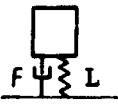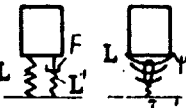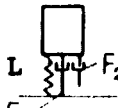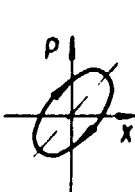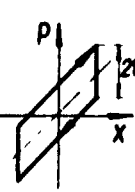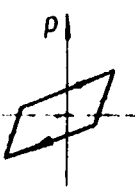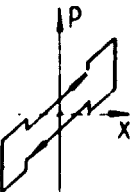
Damper structural diagram					
	$C \, \downarrow \, L$	$F \, \downarrow \, L$	$L \, \curlyvee \, \Psi$	$L \, L' \, F$	$L \, \Psi \, F_2 \, F_1$
	a)	b)	c)	d)	e)
Damper characteristics					
Optimization factors $L = const.$	$\dfrac{C}{\sqrt{LM}}$	$\dfrac{F}{L \cdot X}$	Ψ	1) $\dfrac{F}{L \cdot X}$; Ψ 2) $\dfrac{L}{L}$; $\dfrac{L}{L}$	1) $\dfrac{F \cdot L}{L \cdot X}$ 2) $\dfrac{F L}{F_2}$ 3) $\dfrac{C}{X}$

Fig. 1.

In the first stage, optimization was carried out by the scanning method. Subsequent improvement was achieved by the use of the Gauss-Zaydel method. Determinative functions, which are continuous and have a first order discontinuity, were used as the disturbances.

After synthesis of the damper characteristics, the optimum structure in a specified disturbance range was developed.

The investigations carried out showed the advisability of the method presented in investigation of dynamic systems, the vibrations of which have discontinuities of the first derivative, as well as in disturbances having a discontinuity of the first kind.

210

REFERENCES

1. Bronshteyn, Ya.I., "Methods of Testing Automobiles for Smooth- ness of Ride," in the collection _Podveska avtomobilya_ [Auto- mobile Suspensions], USSR Academy of Sciences Press, 1951.

2. Rotenberg, R.V., _Podveska avtomobilya i yego kolebaniya_ [The Automobile Suspension and Its Vibrations], Mashgiz Press, Moscow, 1960.

SYNTHESIS OF A SYSTEM WITH ACTIVE VIBRATION ISOLATION, CONSIDERING THE VIBROACOUSTICAL CHARACTERISTICS OF THE SOURCE AND OF THE ISOLATED OBJECT

M.D. Genkin, V.G. Yelezov, and V.V. Yablonskiy
(Moscow)

For the purpose of increasing the vibration isolation effect of a damper, it has been proposed [1] that electromechanical converter 4 (Fig. 1) be included in parallel with the former. In the operating mode, it decreases the combined rigidity of dampers 2.

The efficiency and resistance of an active vibration isolation (AVI) system are analyzed in work [2], for the case of unidirectional vibrations of a mass (a source) on a spring, with a damper (damping system), resting on a quite rigid base (the isolated object).
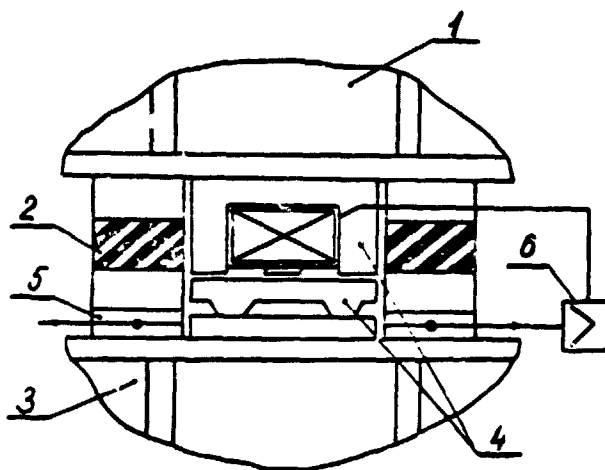
The purpose of this work /187 is to consider the effect of certain vibroacoustical characteristics of real objects on AVI resistance and synthesis of AVI, which are effective over a wide frequency band.

Fig. 1.

In the vibrational system (Fig. 1), $z^s(j\omega)$ and $z^l(j\omega)$ are the mechanical resistances of source 1 and load 3; $z^{sl} = z^s z^l / (z^s + z^l)$ and $z^r(j\omega) = (k/j\omega)(1 + j\lambda) = k/\omega + \gamma$ is the resistance of damping system 5 as one spring, with rigidity k and loss coefficient λ; $\omega_0 = \sqrt{k/m}$ is the natural frequency of the uncontrolled system; $f(j\omega)$ is the force transmitted by the dampers to the isolated object (input action to the control system) and f_a is the active compensating force; $K_f(j\omega) = f_a/f$ is the transfer coefficient of the control circuit (disturbance compensation principle).

The problem is to ensure effective quenching (damper "softening") in the $\omega > \omega_{min}$ frequency band, while maintaining the rated rigidity k at zero frequency ($K_f(0) = 0$) and with a lower limit on the effective rigidity (for example, $k_{eff} = k(1 + K_f) \geq$ $\geq 0.5k$) in certain low frequency regions $0 < \omega \leq \omega_k < \omega_0$. A single-section, high-frequency RC or LCR filter is inserted into the control circuit for this, in which the limiting frequency $\omega_{RC} = 1/RC$ and the natural frequency $\omega_{LCR} = 1/\sqrt{LC}$ lies in the interval ω_k-ω_{min}.
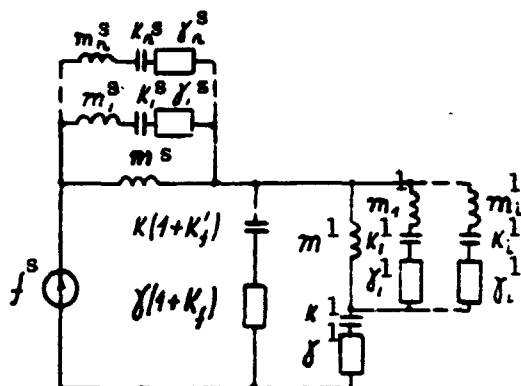
212

Fig. 2

LCR circuits are inserted in series [3] into the equivalent system (Fig. 2), with a multi-resonance load source. Under these conditions (especially, if $Z^s(j\omega)$ and $Z^l(j\omega)$ are experimentally measured characteristics), it is convenient to use the immitance resistance criteria, when the necessary and sufficient condition for resistance in the system being examined has the following form [4]: /188

with

$$Re\{ \quad \omega_i)[1 + K_f(j\omega_i)] - P \quad (j\omega_i) > 0$$
$$Im\{ \quad \omega_i)[1 - K_f(j\omega_i)] - I_\omega \quad (j\omega_i) = 0$$

(1)

Here, $Z^s(j\omega)[1 + K_f(j\omega)]$ is the controlling immitance, reflecting the electromagnetic reciprocal connection through the dynamic force to the damper-isolated object cross section.

In this case, the basic task of AVI synthesis is reduced to determination of those vibration frequency filter parameters (with dimensionless frequency $\Omega_{RC} = \omega_{RC}/\omega_0$ or $\Omega_{LCR} = \omega_{CR}/\omega_0$, as well as the loss coefficient $\lambda_{LRC} = R\sqrt{C/L}$) at which:

-- Resistance condition (1) is maintained over the entire frequency range $0 < \omega < \infty$;

-- The condition $|k_{eff}/k| \geq 0.5$ is maintained in the assigned range $0-\Omega_k = \omega_k/\omega_0$; and

-- The maximum possible vibration quenching is ensured at frequency $\Omega_{min} = \omega_{min}/\omega_0$.

The relationships of the values found for Ω_{LCR}^0 (curves 1 and 2) and Ω_{RC}^0 (curves 3 and 4) to frequency Ω_k, at $\lambda_{LRC} = 1$ and various values of the loss coefficient λ, are shown in Fig. 3. These filter parameters were determined from a joint analysis of the boundaries of the resistance region and the boundaries of the regions of parameters which satisfy the given restrictions.

Calculation and investigation by electrical models showed that, in the majority of practical cases, when the internal resonance frequencies are consider ly higher than the basic frequency ω_0 and moreover, $\Omega_k << 1$, $\Omega_{min} \sim (2-3)$, the system resistance is

213

Fig. 3

fully defined by the low-frequency parameters of the system. At $\Omega_k \sim 1$ and $\Omega_{min} \gg \gg 1$, the mass m^1 and internal resonance of the system must be taken into account. Resistance condition cab, with a high frequency RC filter at the i-th critical frequency ω_i, at an arbitrary value of Ω_{RC}, is determined by the following expression:

$$1 - K_{,0}\left[\frac{\lambda(\lambda - \sqrt{\lambda^2 + 1})^2 + (\lambda + \sqrt{\lambda^2 + 1})}{\lambda[1 + (\lambda + \sqrt{\lambda^2 + 1})^2]}\right] \geqslant -1 - \frac{k_i \lambda_i}{k\lambda}$$

where K_{f0} is the transfer coefficient of the control circuit in the operating frequency range, and k_i and λ_i are the equivalent rigidity and loss coefficients of the "source-load" system, with resistance $z^{s1}(j\omega)$ at the i-th resonance frequency.

The boundaries of the internal resistance region (conditional, <u>/189</u> but passive resistance $z^{s1}(j\omega)$ of the system with a RC filter) are defined by the expression:

$$-1 + (1 + \lambda)^{-2} \leqslant K_{,0} \leqslant -1 + (1 - \lambda)^{-2}.$$

214

REFERENCES

1. Genkin, M.D., A.V. Rimskiy-Korsakov, A.N. Tselebrovskiy, and V.V. Yablonskiy, "Damper with Automatic Control," Avt. svid. SSSR kl 47a [Author's Certificate, USSR, Class 47a], 20, No. 259568, claimed 6 September 1968, published 12 December 1969.

2. Genkin, M.D., V.G. Yelezov, and V.V. Yablonskiy, "Method of Active Quenching of Vibrations of Mechanisms," in the collection Dinamika i akustika mashin [Dynamics and Acoustics of Machines], Nauka Press, 1971, pp. 70-88.

3. Skuchik, Ye., Prostyye i slozhnyye kolebatel'nyye sistemy [Simple and Complex Vibrating Systems], Mir Press, Moscow, 1971.

4. Kulikovskiy, A.A., Ustoychivost' aktivnykh linearizovannykh tsepey s usilitel'nymi priborami novykh tipov [Stability of Active Linearized Circuits with New Types of Boosters], Gosenergoizdat Press, 1962.

ACTIVE DAMPING OF UNIDIMENSIONAL STRUCTURES /190

B.D. Tartakovskiy
(Moscow)

A unidimensional structure is examined, along which a wave $u = u_0\exp[i(\omega t - kx)]$ propagates (a rigid pipe, in which a wave propagates; an infinite string, along which a transverse wave propagates; a rod, along which longitudinal or torsional columns propagate, generally a unidimensional propagation of some one mode of vibrations which is nondegenerating with distance). We superimpose the location of the receiver system x_p on the axis origin $x = 0$. Designating the phase shift of the vibrations between the locations of the receiver x_p and sender (radiator) x_g by ψ, between the location of the sender and the monitoring point by θ and the degree of decrease in amplitude of the field at the monitoring point x_k by α, we find that, with the radiator located behind the receiver [1], the transformation coefficient of the compensating system

$$\varphi = \frac{1}{\exp(-i\psi) - \frac{1}{1-\alpha}\exp(i\psi)} \tag{1}$$

is independent of θ. In the case of total compensation ($\alpha = 0$)

$$\varphi = \frac{i}{2\sin\psi} \tag{2}$$

If $\psi < \pi$, the phase shift is $\pi/2$. Assuming $u_0 = 1$, the total field at the receiver point amounts to

$$u_\Sigma = 2i\sin\psi \cdot \exp(-i\psi). \tag{3}$$

The converter, multiplying the total vibration by the value $1/2\sin\psi$, makes its wave $\exp(-i\psi)$, with the opposite sign, which arrives at the monitoring point. At $\pi < \psi < 2\pi$, the phase shift must be $-(\pi/2)$, accordingly. Thus, the phase shift in a reciprocal connection electromechanical system (with distributed parameters), in the general case, does not equal $\pm\pi$ overall, as happens in electronic devices (consisting of discrete elements). The modulus of the quantity ϕ must change within the limits of $0.5-\infty$, periodically repeating through the value $\psi = 2\pi$. At distances of $\psi = (\pi/2)(2n + 1)$, i.e., in the antinodes, the value of ϕ is at a minimum, amounting to $\pm i/2$. If $\alpha \neq 0$, the gain factor must change within /191

216

smaller limits than at $\alpha = 0$, continuing to become minimum in the antinodes of the standing-traveling waves $u_0[1 - (1-\alpha)\exp(-2i\psi)]$, established ahead of the radiator. Upon bringing the receiver close to the radiator ($\psi \to 0$), the phase coefficient of the electromechanical converter tends towards $-\pi$. If it is assumed that the conversion coefficient ϕ is independent of frequency and equals the value of (2), with subscript 0, over the entire frequency range examined, the compensation coefficient modulus is determined by the relation

$$ x_{\omega \cdot x} = \frac{2_{\cdot 3} \cdot \psi_0 - \sin \psi}{\sqrt{1 + 4(\sin \psi_0 - \sin \psi) \sin \psi_0}} . \tag{4}$$

Total compensation ($\alpha = 0$) takes place at $\psi = \psi_0$. Oscillations, corresponding to the Nyquist criterion [$\mathrm{Re}(\overline{k\phi_0}) \geq 1$, $\mathrm{I_m}(\overline{k\phi_0}) = 0$], arises at the ratios

$$ \text{a)} \quad \psi_0 = \left[\frac{\pi}{6} ; \frac{5\pi}{6}\right] + 2\pi n; \qquad \psi = \frac{\pi}{2} + 2\pi n; \tag{5}$$

$$ \text{b)} \quad \psi_0 = \left[\frac{7\pi}{6} ; \frac{11\pi}{6}\right] + 2\pi n; \qquad \psi = \frac{3\pi}{2} + 2\pi n. $$

Thus, if the signal is white noise, the receiver, to avoid auto-excitation, should be set in a restricted wave band interval, for example, $\pi/6 < \phi_0 < 5\pi/6$. The bands $0 < \phi_0 < \pi/6$, $5\pi/6 < \psi_0 < 2\pi$, etc., are forbidden for signals with solid frequency spectra, since the values $\phi_0 = 1/2\sin\psi_0$, the modules of which exceed unity, correspond to them. Therefore, at frequencies satisfying the relation $\sin\psi \geq 2\sin\psi_0$, the amplitude oscillation condition will be satisfied and, consequently, at frequencies, at which the phase oscillation condition $\psi = \pi/2$ also is satisfied, and oscillations arise. With increase in frequency, the phase oscillation condition is disrupted, arising again under the condition $\psi = (\pi/2) + 2\pi n$. Approaching the compensating frequency, the oscillation frequency will occur in the range $0 < \psi_0 < \pi/2$ at $\psi_0 = \pi/6$, being double the compensating frequency ($\psi_{osc} = \pi/2$). Since the quantity $\psi_{osc} = \pi/2$, independently of ψ_0, with decrease in ψ_0, the ratio ψ_{osc}/ψ_0 increases and tends towards ∞ as $\sin\psi_0 \to 0$. In this manner, theoretically, signal compensation is possible with a solid frequency spectrum without oscillation, if the relation $\psi_0 = 0$ can be achieved. With periodically repeating different ratios of ψ and ψ_0, the quantity /192 α changes correspondingly within the limits $\alpha = 0-\infty$. In case the signal is harmonic or has a certain finite frequency spectrum (for example, with a frequency limiting rectangular filter), there is

interest in determination of the frequency characteristics $\alpha(\psi)$ at a certain given value ψ_0. For values of ψ_0 lying outside the oscillation region, within the limits of $\phi_0 = 0-\pi$, at frequencies corresponding to $\psi = (3\pi/2) + 2\pi n$, the coefficient α is maximum, with the minimum-maximum values ($\alpha = 1.33$) occurring at $\phi_0 = \pi/2$.

Inclusion of a filter in the reciprocal connection circuit changes the oscillation conditions. Accordingly, the oscillation amplitude and phase conditions can be written in the form

$$Re \; \frac{ie^{-i\psi}}{2\sin\psi_0} \; \Phi(\omega) \geqslant 1; \quad I_m \; \frac{ie^{-i\psi}}{2\sin\psi_0} = 0, \tag{6}$$

where $\Phi(\omega)$ is the frequency standardized characteristic of the filter. Assuming $\Phi(\omega) = \dfrac{1}{1+i\tilde{Q}\left(\frac{\omega}{\omega_0}\right)} \cdot \tilde{Q}$ and that $\tilde{Q}$ is the actual value, (6) can be presented in the form

$$\frac{\sin\psi - \cos\psi\,\tilde{Q}}{2\sin\psi_0\,(1+\tilde{Q}^2)} \leqslant 1 \; (a); \quad \cos\psi - \sin\psi\,\tilde{Q} = 0 \; (b). \tag{7}$$

It follows from (5a) that introduction of a filter changes both the frequency at which the oscillation amplitude conditions are fulfilled and the frequency at which the phase condition is fulfilled. In this case, for example, in the region of values $0 < \psi_0 < \pi/6$ and $\psi = 0-2\pi$, the phase conditions are fulfilled at frequencies which are closer to normal, and the amplitude conditions at frequencies which are further away. The term $1/(1+Q^2)$ plays the predominant role in increase of Q, as a consequence of which, frequencies at which oscillation is possible are sharply increased. In this case, the region of values of ψ_0 at which both oscillation conditions can be realized is constricted.

Let us examine, for example, constriction of the autoexcitation region adjacent to the value $\psi_0 = \pi$, which can be achieved by use of one of two widespread types of filters, having frequency characteristics of the type

$$a) \; \tilde{Q} = 2Q \; \frac{\omega - \omega_0}{\omega}, \quad b) \; \tilde{Q} = 2Q\left(\frac{\omega}{\omega_0} - \frac{\omega_0}{\omega}\right). \tag{8}$$

218

In accordance with (8), the oscillation conditions have the
appearance, with filter a

$$\sin \psi \geqslant 2 \sin \psi_0. \quad Q = \frac{\operatorname{ctg} \psi}{2\left(\frac{\psi_0}{\psi}-1\right)}. \tag{9a}$$

and with filter b

$$\sin \psi \geqslant 2 \sin \psi_0: \quad Q = \frac{\operatorname{ctg} \psi}{2\left(\frac{\psi}{\psi_0}-\frac{\psi}{\psi}\right)}. \tag{9b}$$

With increase in Q, the region of values of $\psi_0 = \pi \pm (\pi/6)$, at the
boundary of which autoexcitation takes place in the absence of a
filter (Q = 0), is constricted asymptotically, approaching the
value π as $Q \to \infty$. In this case, the value of ψ, at which auto-
excitation takes place, also is contracted toward the value π.
This indicates, for example, the possibility of expanding the
working frequency region downwards, by use of filter a, with Q-
factor Q = 4, to values corresponding to $\psi_0 = 0.9\pi$ and $\psi = 0.78\pi$,
while, without the filter, $\psi_0 = 0.833\pi$ and $\psi = 0.5\pi$. With removal
of frequency ω from the rated value, the autoexcitation suppression
effect increases with the same Q-factor. Filter b acts approximately
the same. At those values of Q, the autoexcitation region left
boundaries are somewhat different, corresponding to the lower fre-
quencies at which the forms of the frequency characteristics of both
filters differ strongly. The boundaries of the autoexcitation region,
defined by three values Q, ψ_0 and ψ, depend essentially on the rated
value ψ_0. The action of the filter in constricting the autoexcita-
tion region increases in proportion to increase in the wave interval
ψ_0. In all bands, except the "zero," an increase in Q contracts
the autoexcitation region towards the central value $\psi_0 = n\pi$. In
the "zero" region of ψ_0 (adjoining the vibration radiator), the
limiting curves asymptotically converge, ith certain finite, and,
moreover, small values of Q, on the order of 10^{-2}.

The autoexcitation regions are similar to the control system
stability regions, used in automation theory, in two parameters;
however, they have a more complex nature than the stability regions
of discrete systems, due to the multilobed frequency characteristics
of the signals.

If the system receiver is installed behind the sender, in the
traveling wave region, the conversion coefficient must amount to

$$\varphi_0 = - \frac{1-\alpha}{\alpha} \exp(i\psi_0).$$

The total signal at an arbitrary point, located at a wave interval Q from the system receiver, at frequency ω, equals

$$u_z = \frac{a_z \exp[-i(\psi - \Omega)]}{1 - \frac{1-\alpha}{\alpha} \exp[-i(\psi - \psi_0)]} \tag{10}$$

Accordingly, with a degree of attenuation of the field $\alpha \lessgtr 0.5$, the coefficient $|\phi| \gtrless 1.$[1] Oscillation arises under the conditions

$$Re\left\{ \frac{\alpha-1}{\alpha} \exp[-i(\psi - \psi_0)] \right\} > 1; \quad Im\left\{ \frac{\alpha-1}{\alpha} \exp[-i(\psi - \psi_0)] \right\} = 0,$$

from which it follows that, at $\alpha > 0.5$ oscillation does not arise at all. If $\alpha \leq 0.5$, oscillation arises at frequencies satisfying the condition $\psi - \psi_0 = \pi(2n - 1)$.

The vibration attenuation effect of the compensation system radiators can be considered as an active method of isolation of vibrations at point x_g. The magnitude of the "active sound isolation" is determined by the relationship:

$$3n = 20 \lg \frac{1}{\alpha}.$$

At $\alpha < 0.5$ and, consequently, ZI [sound insulation] > 6 dB, it is advisable to place the receiver of the system in a "high level space," i.e., in front of the sender. The "sound isolation" effect generated can be considered as creating a point reflecting surface at x_d. The "active reflecting surface" behaves like a soft boundary, having an impedance $z = z_0 \frac{\alpha}{2-\alpha}$, where z_0 is the wave resistance of the medium.

---

[1]We recall that, here, we have in mind the gain factor of the electro-mechanical circuit as a whole. As a consequence of binary electro-mechanical conversion and attenuation of the gain factor connected with this, the electrical part of the circuit always must be greater than unity (on the order of 100-1000).

The impedance and energy characteristics (at the monitoring point, located behind the radiator) have the following form: the compensation coefficient at the radiator point $\alpha_n = \alpha$; the load impedance at the radiator point

$$z_{load}(x_d) = -\frac{1-\alpha}{\alpha} \, z_{in}$$

where z_{in} is the wave resistance of an infinite waveguide; the /195 power of the compensating radiator is

$$p = -\frac{1}{2} \, Re\,[x(1-x)\, z_{in} \, w] = x(1-x)\,P_0.$$

where P_0 is the primary wave radiator power, in the absence of compensation. The maximum power which can be drawn by the compensating system radiator is $0.25\,P_0$, at $\alpha = \alpha_{max} = 0.5$.

REFERENCES

1. Tartakovskiy, B.D., "Multichannel Electromechanical Reciprocal Connection System of a General Type," _Nauchnyye trudy vuzov Lit. SSR, Vibrotekhnika_ 4(13), 267-280 (1970).

COMPENSATION OF VIBRATIONS OF A UNIDIMENSIONAL STRUCTURE AND A PLANE ACOUSTICAL FIELD

B.D. Tartakovskiy
(Moscow)

Endless structures are realized in practice, in the presence of loss and to an adequate extent, owing to which, reflections from the edges to the center part of the structure can be disregarded. In the absence of losses, reflections from the boundary frequently have to be taken into account. In this case, besides compensation for waves passing through the boundary, the reciprocal connection system can be used for compensation of the total field ahead of the boundary. In these cases, the system converters can be located in a different manner relative to the boundary and to one another. Each of the locations shown in Fig. 1 has inherent peculiarities, which must be taken into account in solving specific problems. For compensation of incident, reflected and summary waves, scheme 5a can be used, for example, scheme 1b for compensation for waves passing through the boundary, etc.
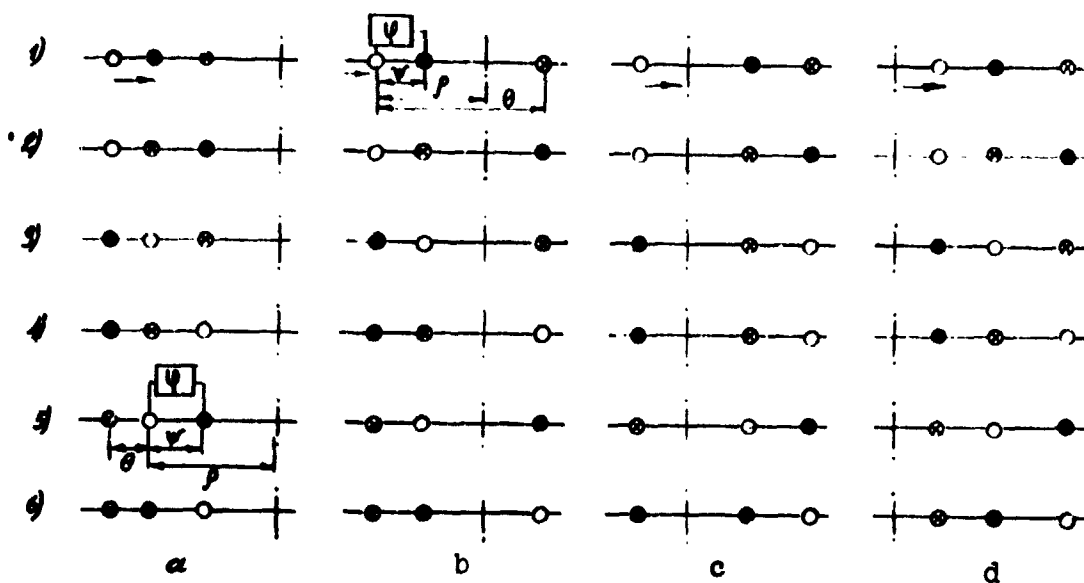

Fig. 1.

Compensation for the summary wave can be considered as active "space absorption" (a type of distributed wave absorption), and compensation for waves passing through can be treated as active vibration or sound isolation. Active local absorption of elastic vibrations or sound waves is adequate compensation for waves

reflected from the edge of a semi-infinite structure (field), for example, at the edges of the space. The action of active methods <u>/197</u> of "isolation" and "absorption" is propagated to any distance from the edge, and it is not restricted to a narrow region or series of regions, as is the case with compensation for the summary field (in a uniform structure in the presence of boundaries). With the compensating system located ahead of the boundaries, direct and reflected compensating waves and waves radiated by the system sender act on the system receiver. The waves radiated by the sender also can be considered as a sum of the direct waves and waves reflected from the boundary. We introduce the subscript Σ to designate the summary initial wave and that radiated by the system sender and the subscript i for waves subject to compensation (i = 1, incident wave; 2, reflected wave; 3, field ahead of the boundary; 4, wave passing through the boundary), and we designate

$$K_\Sigma = \frac{v_\Sigma(x_n)}{v_\Sigma(x_g)} ; \qquad \varkappa_\Sigma = \frac{v_\Sigma(x_k)}{v_\Sigma(x_g)} ;$$

$$\eta_\Sigma = \frac{u_\Sigma(x_k)}{u_\Sigma(x_n)} ; \qquad M_i = \frac{u_i(x_k)}{u_\Sigma(x_k)} ,$$

where us a wave subject to compensation, v is the compensating wave, $x_k(0)$ is the coordinate of the location of the monitoring receiver, $x_p(0)$ is the compensating system receiver and $x_g(\theta)$ is the sender (radiator) of the system. We obtain

$$\varphi_{\Sigma,i} = \frac{1}{K_\Sigma - \dfrac{\varkappa_\Sigma}{(1-\alpha)\eta_\Sigma M_i}} . \tag{1}$$

With location system 5a, accordingly

$$\varphi_{\Sigma,i} = \frac{M_i[1 + R\exp\{-i2(\rho-\psi)\}]}{M_i \exp(-i\psi)[1+\exp\{-i2(\rho-\psi)\}] - \dfrac{\exp(i\psi)}{1-\varkappa}[1+R\exp(-i2\rho)]} . \tag{2}$$

where ψ, Θ and ρ are the wave intervals indicated in Fig. 1. With compensation, only the incident waves

$$\phi_{\Sigma,1} = \frac{\exp{(i\varphi)}}{1 - \frac{1}{1-\alpha}\exp{(-i2\Theta)}[1 + R\exp{(-i2\rho)}]} \qquad (3)$$

only the reflected waves

$$\phi_{\Sigma,1} = \frac{-R(1-\alpha)\exp{(-2i\rho)} \cdot \exp{(i\varphi)}}{1 + R\alpha\exp{(-2i\rho)}}, \qquad (4)$$

the entire field ahead of the boundaries

/198

$$\phi_{\Sigma,1} = \frac{\exp{(i\varphi)}}{1 - \frac{\exp{(-2i\Theta)}[1 + R\exp{(-2i\rho)}]}{(1-\alpha)[1 + R\exp{(-2i(\rho+\Theta)}]}} . \qquad (5)$$

In the case of compensation for waves passing through the boundary (scheme 1b)

$$\phi_{\Sigma,1} = \frac{1}{\exp{(-i\varphi)} - \frac{\exp{(i\varphi)}}{1-\alpha} \cdot \frac{1 - R\exp{(-2i\rho)}}{1 - R\exp{(-2i(\rho-\varphi)}}} . \qquad (6)$$

At $R = 0$, the values of ϕ_{Σ} change to corresponding values of ϕ for a uniform waveguide. The system used for compensation for reflected waves is autoexcited under the conditions

$$Re\left[\exp\{-i[\varphi(\omega)-\varphi_0]\} \cdot \frac{R(1-\alpha)\exp{(-2i\rho)}}{1 + R\alpha\exp{(-2i\rho)}}\right] \geqslant 1,$$
$$Im\left[\exp\{-i[\varphi(\omega)-\varphi_0]\} \cdot \frac{R(1-\alpha)\exp{(-2i\rho)}}{1 - R\alpha\exp{(-2i\rho)}}\right] = 0. \qquad (7)$$

At $R < 1$, such a system is not excited at any frequencies. Physically, this is explained by the fact that, at $R < 1$, the modulus ϕ is less than unity, independent of α. It follows from the expressions obtained that, with compensation of reflected waves, the system cannot create a signal, equal in amplitude to the reflected one and opposite to it in phase, at all. The signal radiated by the sender must be such that mutual compensation for the primary and reflected waves, themselves and their reflections from the boundary, takes place. Moreover, besides the direct waves

224

and waves radiated by the sender, two reflected waves enter the receiver. If the sender is located at the very boundary ($\rho = \psi$), some simplification takes place

$$\varphi_{\Sigma,2} = \frac{-R(1-\alpha)\exp(-i\psi)}{1 + R\alpha\exp(-2i\psi)} .\qquad(8)$$

However, in this case, the wave radiated by the sender is not in antiphase to that reflected from the boundary. Only with simultaneous location of the system receiver and sender at the boundary ($\rho = \psi = 0$), is the phase of the wave radiated by the sender opposite to the phase of the reflected wave ($\phi_{\Sigma,2} = -\frac{R(1-\alpha)}{1 + R\alpha}$), and at $\alpha = 0$, equals its module ($\phi_{\Sigma,2} = -R$). The diversity of possible schemes for location of elements of the compensation system permits the optimum scheme to be selected, taking account of conditions super- /199 imposed by the conditions of the specific problem. The requirement for constriction of the autoexcitation frequency region has the greatest effect. Using (1), the action of other compensation schemes presented in Fig. (1) can be analyzed.

In distinction from plane wave compensation in a waveguide, attenuation of the acoustical pressure of the wave created by the compensating radiator takes place in compensation of a plane propagated wave, due to expansion of the wave front, and the possibility arises of compensation for the primary field in directions different from that of the plane wave propagation.

Let us examine two of the simplest models, a sphere, pulsating and oscillating (in the direction of propagation of the primary wave).

Let us assume that a sphere of radius a is located at point $r = 0$, the acoustical pressure receiver (microphone, hydrophone) at point (r_1, v_1) and that the coordinates of the monitoring point are (r_2, v_2).

In the first case, acoustical pressure p, at a distance r from the center of the sphere, is connected with the acoustical pressure on the surface of the sphere p_a by the ratio $p = p_a(a/r)\exp[-ik(r-a)]$. The value of p_a, providing the assigned compensation coefficient of the field α at the monitoring point, is determined by the equation

$$p_a = -(1-\alpha)p_0\left(\frac{r_2}{a}\right)\exp\{ik[r_2(1-\cos r_2)-a]\}.\qquad(9)$$

225

where p_0 is the amplitude of the acoustical pressure of the primary plane wave. The total acoustical pressure at any point in the compensation frequency amounts to

$$p_\Sigma = p_0 \left\{ \exp(-ikr\cos v) - (1-x)\frac{kr_2}{kr} \times \right.$$
$$\left. \times \exp\left\{ -ik[r - r_2(1 - \cos v_2)] \right\} \right\} \tag{10}$$

Assigning a position to the monitoring point (kr_2, v_2), the sound pressure attenuation can be determined as a function of the coordinates (r, v) and a profile of the equal attenuation regions $p_\Sigma/p =$ = const can be plotted in a plane passing through the radiator, perpendicular to the wave front. The coordinates Δx and Δy relative to the monitoring point, corresponding to the given attenuation p_Σ/p, are determined by equation

$$\frac{p_\Sigma}{p} = 1 - \frac{r_2}{\sqrt{(r_2 + \Delta x)^2 + (\Delta y)^2}} \exp\left(-ik\right] \overline{(r_2 + \Delta x)^2 + (\Delta y)^2 - r^2}\right). \tag{11}$$

With the monitoring point located on the radiator axis $(\theta_2 = 0)$, the change in sound pressure along the axis from the radiator $(\theta = 0)$ is $p_\Sigma/p = 1 - r_2/r$, and along the line passing through the monitoring point, perpendicular to the axis,

$$\frac{p_\Sigma}{p} = 1 - \cos \vartheta \cdot \exp[-ikr_2(1\cos \vartheta - 1)].$$

With the monitoring point located on the axis in front of the radiator $(\theta_2 = \pi)$, the acoustical pressure attenuation along the axis $(\theta = \pi)$ is

$$\frac{p_\Sigma}{p} = 1 - \frac{r_2}{r} \exp[-2ik(r - r_2)].$$

The acoustical pressure p, at distance r from the center of the sphere, oscillating in the X direction, is connected with the acoustical pressure on the surface of the sphere P_a by the relationship

226

$$p = p_a \frac{a^2}{r^2} \frac{1+ikr}{1+ika} \cdot \exp\left[-ik(r-a)\right]. \tag{11}$$

The magnitude of the acoustical pressure required for a given acoustical pressure compensation coefficient at the monitoring point, is found from the condition

$$p_a = -(1-x) p_0 \left(\frac{r_2}{a}\right)^2 \frac{1+ika}{1+ikr_2} \exp\left\{ik\left[r_2(1-\cos\vartheta_2)-a\right]\right\} \tag{1 }$$

The total acoustical pressure at any point in the compensation frequency amounts to

$$p_\Sigma = p_0 \left\{ \exp(-ikr\cos\vartheta) - (1-x)\left(\frac{kr_2}{1+ikr_2}\right) \times \right.$$
$$\left. \times \exp\left\{-ik\left[r-r_2(1-\cos\vartheta_2)\right]\right\}\right\}. \tag{13}$$

At $k_r \cdot k_{r_2} \ll 1$, a more rapid decrease in acoustical pressure of the oscillating radiator takes place, as a result of which the compensation region in the x direction is constricted. In connection with the directionality of the oscillating radiator, the acoustical pressure created by it at angle v, compensates the plane wave acoustical pressure at closer distances than along the horizontal axis, as a consequence of which the compensation region turns back towards the radiator.

227

1. Blackman, R.B. and I.W. Tukey, The Measurement of Power Spectra, Dover Publications, New York, 1958.

2. Maslov, V.K. and G.A. Rozenberg, "Algorithm for Digital Spectral Analysis of Wide Band Random Signals," in the collection Trudov III Vsesoyuznogo simpoziuma Metody predstavleniya i apparaturnyy analiz sluchaynykh protsessov i poley [Proceedings of IIIrd All-Union Symposium, Methods of Presentation and Instrumental Analysis of Random Processes and Fields], All-Union Scientific Research Institute of the Electrical Industry, Leningrad, 1970.

3. Kotyuk, A.F., V.V. Ol'shevskiy, and E.I. Tsvetkov, Metody i apparatura dlya analiza kharakteristiki sluchaynykh protsessov [Methods and Apparatus for Analysis of the Characteristics of Random Processes], Energiya Press, Moscow, 1967.

4. Vollerner, N.F., "Some Problems of Instrumental Analysis of Transient Random Processes," Trudy Akusticheskogo in-ta (1) (1966).

228

A NEW METHOD OF MEASUREMENT OF TENSION
ON A MOVING MAGNETIC TAPE

A.K. Kurtinaytis and Ye.S. Lauzhinskas
(Kaunas)

Let us examine the possibility of no-contact measurement of the tension on a moving magnetic tape, assuming that the magnetic tape is uniform. A scheme for calculation of the natural frequency of transverse vibrations of the magnetic tape is depicted in Fig. 1, where T is the tape tension, 2l is the magnetic tape chord length and ρ is the weight of a unit chord length of tape.
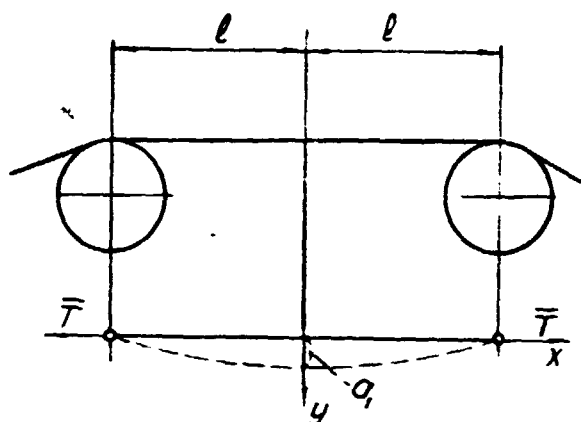
It is well-known that a /202 moving magnetic tape accomplishes spatial vibrations, including natural frequency transverse tape vibrations. If the section of magnetic tape vibrates in one of the normal shapes, the deviation can be presented by the equation

$$y = X \cos pt \qquad (1)$$

where X is a function of x, defining the shape of the vibrating magnetic tape section and p is the angular frequency of vibration. The increase in potential energy of deformation, as a consequence of the deflection, is obtained by multiplying T by the tape length. Then, the potential energy expression is

Fig. 1.

$$\Pi = T \int_0^l \left(\frac{\partial y}{\partial x}\right)^2 dx. \qquad (2)$$

We obtain the greatest potential energy when the vibrating magnetic tape occupies the extreme position. In this position, cos pt = 1 and

$$\Pi = T \int_0^l \left(\frac{dX}{dx}\right)^2 dx. \qquad (3)$$

229

The kinetic energy of the vibrating magnetic tape equals

$$T = \frac{\rho}{g} \int_0^l (\dot{y})^2 \, dx \qquad (4)$$

and it reaches a maximum under conditions, when the tape is in the middle position, i.e., when cos pt = 0; then,

$$T = \frac{p^2 \rho}{g} \int_0^l X^2 \, dx. \qquad (5)$$

In the assumed case of a uniform magnetic tape, the flexure curve during the vibrations is sinusoidal; therefore,

$$X = a_1 \cos \frac{\pi x}{2l} . \qquad (6)$$

Assuming that there is no energy dissipation, Eqs. (3) and (5) can be equated and, substituting in Eq. (6), we obtain

$$p^2 = \frac{\pi^2 g T}{4 l^2 \rho} \qquad (7)$$

and, accordingly,

$$f = \frac{p}{2\pi} = \frac{1}{4l} \sqrt{\frac{gT}{\rho}} \quad \text{Hz}. \qquad (8)$$

It is evident from formula (8) that the natural frequency of the magnetic tape section depends on the magnetic tape tension.

Measuring the natural frequency of the transverse vibrations of the magnetic tape section f and knowing the numerical values of ρ and l, it is easy to calculate the magnetic tape tension.

A schematic block diagram of a device for measurement of the tension on a magnetic tape by the no-contact method is depicted in Fig. 2, where 1 is the magnetic tape, 2 is an inductive sensor, 3 is an amplifier, 4 is an analyzing device, 5 is a frequency meter and 6 is a computing device.
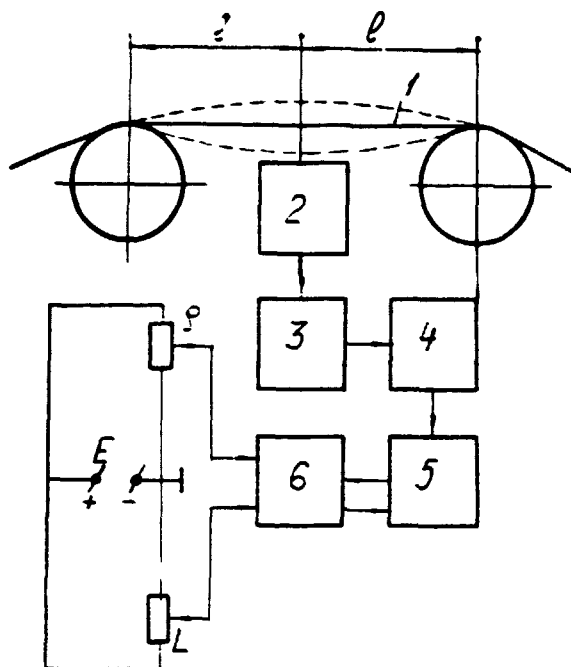
230

Fig. 2.

Magnetic tape 1 accomplishes spatial vibrations during movement, including vibrations caused by disturbance of the support and transverse vibrations at the natural frequency. The signal from inductive sensor 2 passes through amplifier 3 and enters spectrum analyzer 4, where the predominant frequencies of the natural vibrations of the magnetic tape section are clearly isolated. The numerical values of the frequency of these vibrations is determined by frequency meter 5. They enter the computing device, which is equipped with devices for entering the values of ρ and 1. In this manner, we obtain T at the computing device output.

/204

Not only constant, but variable, components of the magnetic tape tension can be measured with this device. The frequency range of measurement of the tension vibrations of the magnetic tape can be changed by changing the time interval between frequency meter readings.

The method set forth can be used widely in study of highly accurate tape feed mechanisms. However, to create a more nearly perfect and accurate device of this type, the consequences of irregularities in the magnetic tapes must be taken account of and corrections must be introduced into formula (8), and limiting conditions for the magnetic tape section (in our case, it was assumed that $y_{x=\pm 1} = 0$) also are necessary.

EXPOSURE OF DEFECTS IN GEAR DRIVES OF AN EXCAVATOR
BY THE VIBROACOUSTICAL METHOD

R.A. Makarov, Yu.A. Gasparyan
(Moscow)

Recordings of the vibrations of the gear drive housing of an excavator with its parts in faulty condition were analyzed. The spectrum is changed in the low-frequency portion by displacement of the shaft (coaxial misalignment, nonperpendicularity).

By introduction of an artificial defect (cutting a tooth of a gear pair), the spectrum is changed in the low and medium frequency regions. The greatest vibration pulse amplitude is observed at low frequencies, in all modes of operation of the gear drives. With a defect in the antifriction bearing (breaking of the separator and outer race), a change in the continuous vibration spectrum is observed. Various harmonics of the shaft rotation frequency are increased in amplitude. Overshoots in frequencies and multiple repetition rates of the balls in the outer race appear. The general level and spectral characteristics of the vibrations are changed by painting the gears and antifriction bearings. With peeling and scaling of the gear cogs, this effect is not observed. Introduction of defects by turns permitted the approximate frequency range to be determined for diagnosing gear drive parts.

It was established that the defects of the gear drive enumerated can be defined by 17 1/3 octave filters.

R.A. Dashevskiy
(Khar'kov)

The requirements as to vibration levels of electrical machines have considerably increased in recent years. Reduction of vibration is an important problem, encompassing questions of not only technology, but of working conditions and living conditions of men. In addition, the vibration level of an electrical machine determines its quality to a certain extent.

The basic sources of vibrations in electrical machines are disbalanced masses of the rotor, bearings and electromagnetic field air gap.

One of the ways for improvement in the vibration characteristics of electrical machines produced by mechanical sources can be the use of dampers in them, of materials with increased friction between parts, dissipating the energy of the vibrations generated in the machine, installed in the paths of their propagation. The effectiveness of the use of dampers depends to a considerable extent on the compatibility of their characteristics with the vibration parameters.

A method is proposed for calculation of the damping elements located between the bearings and mounts.

Equilibrium conditions for such a system have been worked out in the polar coordinate system:

$$(1-2\sigma)\left[\frac{1}{r}\frac{\partial}{\partial r}\left(r\frac{\partial U}{\partial r}\right)+\frac{1}{r^2}\frac{\partial^2 U}{\partial \varphi^2}-\frac{U}{r^2}-\frac{2}{r^2}\frac{\partial U}{\partial \varphi}\right]-$$

$$+\frac{\partial}{\partial r}\left[\frac{1}{r}\frac{\partial}{\partial r}(rU)+\frac{1}{r}\frac{\partial V}{\partial \varphi}\right]=0;$$

$$(1-2\sigma)\left[\frac{1}{r}\frac{\partial}{\partial r}\left(r\frac{\partial V}{\partial r}\right)+\frac{1}{r^2}\frac{\partial^2 V}{\partial \varphi^2}-\frac{V}{r^2}-\frac{2}{r^2}\frac{\partial U}{\partial \varphi}\right]-$$

$$+\frac{1}{r}\frac{\partial}{\partial r}\left[\frac{1}{r}\frac{\partial}{\partial r}(rU)+\frac{1}{r}\frac{\partial V}{\partial \varphi}\right]=0.$$

where U and V are dimensionless components of the displacement vector in the radial and peripheral directions, respectively; σ is the Poisson coefficient; and r and φ are the polar coordinates.

Solving the system and changing to the Descartes coordinate /206 system, an expression was obtained which permitted determination of the damping element parameters:

233

$$\frac{P}{l} = \frac{8\pi\lambda E(3-4\eta)(1-\eta)}{(1+\eta)(1-4\eta)\xi K}\left(r_0^2 - \frac{1}{r_0^2}\right).$$

where P is the load acting on the damping element; l is the width of the damping element; E is the modulus of elasticity of the element material; K is a test coefficient; r_0 is the ratio of the outer diameter of the element to the inner diameter, and

$$\xi = \frac{2(3-4\eta)^2}{1-4\eta}\left(r_0^2 - \frac{1}{r_0^4}\right)\ln r_0 - \frac{2}{1-4\eta}\left(r_0^2 + \frac{1}{r_0^4}\right) + \frac{4}{1-4\eta}.$$

One of the basic causes of magnetic vibrations in electrical machines is radial forces, variable over time, acting on the air gap:

$$P_r = \frac{2\delta_0}{\mu_0}\left[\frac{1}{K_\delta} - \sum \beta b_\mu \cos \mu Z_2(x - \omega t)\right]^2 \cdot F_{(x)}^2.$$

where μ_0 is the magnetic permeability of air; δ_0 is the magnitude of the air gap; k_δ is the air gap coefficient (Carter coefficient); β and b_μ are structural coefficients; μ is the order of the acoustical harmonic; Z_2 is the number of channels in the armature; ω is the angular velocity; and $F_{(x)}$ is the magnetomotive force.

For reduction of the time-variable components of the radial forces (and, as a consequence, the vibration level), it is proposed that the armature channels be bridged over with magnetodielectric wedges, made of a special ferromagnetic dielectric substance. The results of investigation show that, in this case, not only the vibroacoustical, but the energy characteristics of electrical machines are improved by installation of these wedges, and their efficiency is increased.

ELECTRICAL AND ACOUSTICAL RESONANCES OF VIBRATORS /207

M.V. Khvingiya, T.G. Tatishvili, and A.G. Zil'berg
(Tbilisi)

The cause of noise in electrical vibrators is the resonance properties of electromechanical systems, the vibrations of individual box and plate type parts.

Let us examine the interconnections between the basic components of the noise spectrum created by the machine and the characteristics of the forced vibrations of the system.

Nonlinear vibration stimulators are used in electrical vibrators. The nonlinear properties are inherent in both the electromagnetic and elastic elements. The spectrum of vibrations excited in a working part is characterized by harmonics of the type $\sin k\omega$, where ω is the frequency of the exciting force (usually, $\omega = 50$ Hz) and k is a fractional or whole number, corresponding to the sub- and ultraharmonics.

The differential equations for vibration of a single-cycle machine, with resonant elastic elements, has the form

$$\ddot{x}_1 + 2n_1\dot{x}_1 + \omega_{01}^2 x_1(1 + \varepsilon x_1^2) = 0.051\, \Phi^2/\mu_0\, sm;$$

$$\ddot{x}_2 + 2n_2\dot{x}_2 + \omega_{02}^2 x_2(1 + \varepsilon x_2^2) = 0; \qquad (1)$$

$$\dot{\Phi} = \frac{U_0}{w}\sin\omega t - (\delta - x_{1,2})\, r\Phi/\mu_0\, s\omega^2.$$

For a machine with cylindrical springs, $n_1 = i_2$, $\omega_{01} = \omega_{02}$ and $\varepsilon = 0$. In these equations, δ is the initial gap, S is the electromagnet surface area, w is the number of turns in the coil, r is the active coil resistance, m is the corrected mass, μ_0 is the magnetic constant, ε is a dimensionless coefficient, accounting for the nonlinear lengthening of the spring, $2n_{1,2} = c_{1,2}/\psi_{1,2}2\pi m\omega_{1,2}$ are the corrected coefficients of the inelastic resistances, $c_{1,2}$ is the rigidity of the system in the exciting (1) and no-load (2) modes, $\psi_{1,2}$ are the damping coefficients, $\omega_{01,2}$ are the natural angular frequencies, u_0 is the amplitude of the voltage supplied and Φ is the magnetic flux of the electromagnet.

The amplitude-frequency characteristics, corresponding to mass-production specimens of the 184-PT (with springs) and C-920 (with coils) machines are shown in Fig. 1.

The characteristics were obtained with a power amplifier and /211 a low-frequency generator, with deep frequency modulation of the
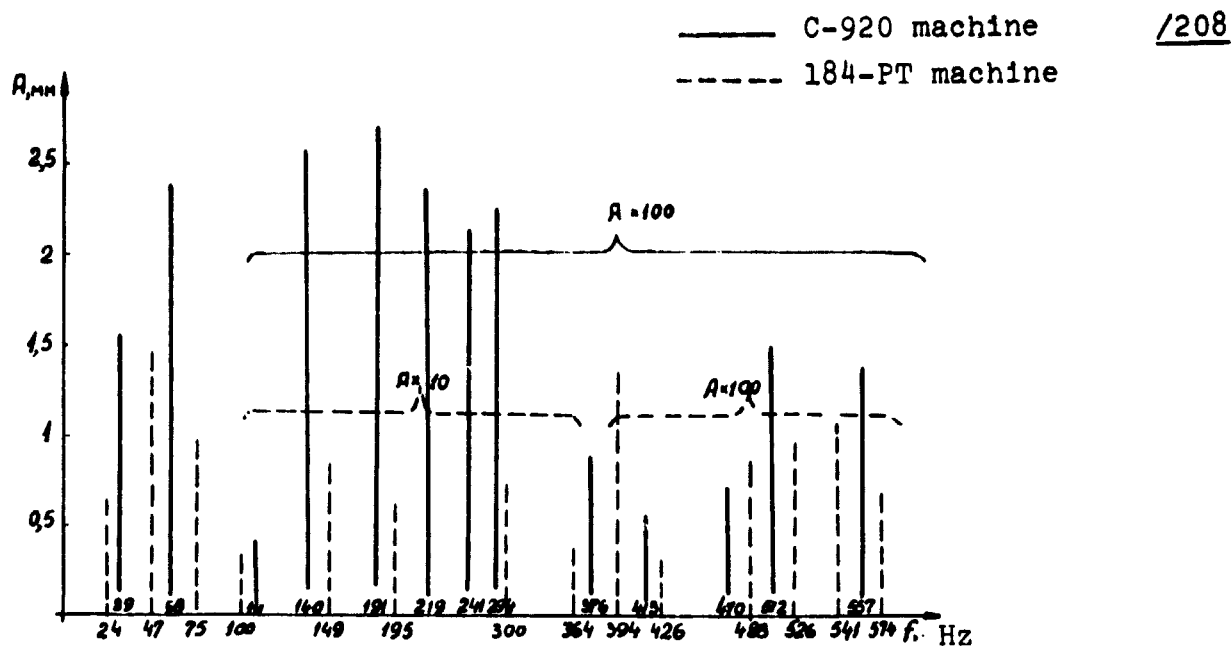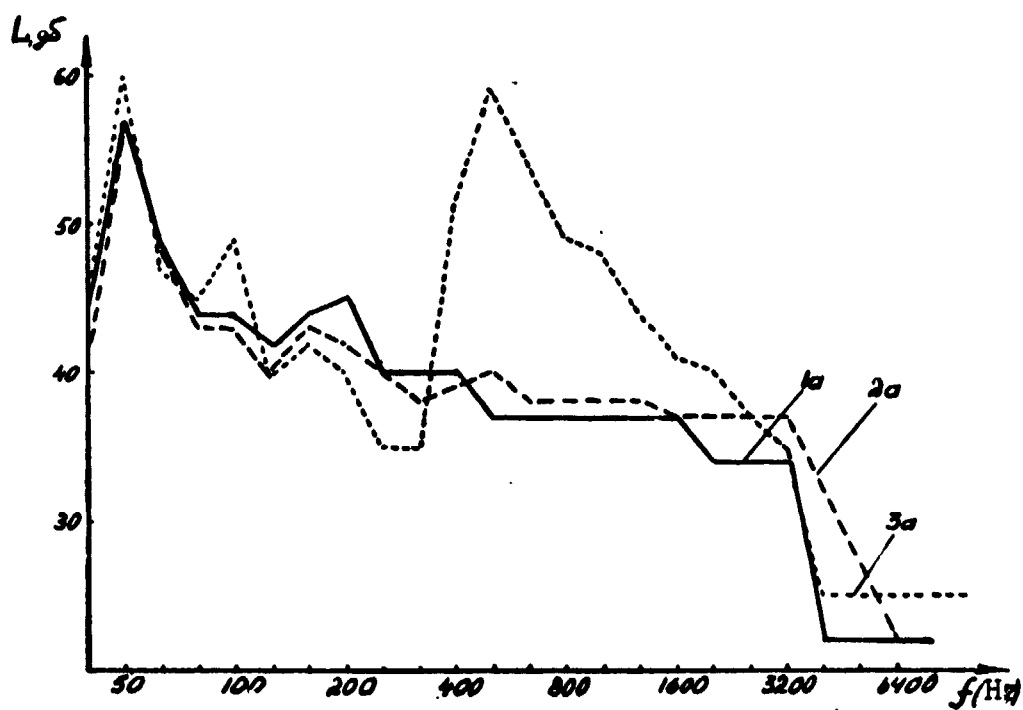
Fig. 1.

Fig. 2.

supply voltage.   Similar resonance characteristics for the system
of equations (1) also were reproduced by analog computer [1].

The noise characteristics of the machine were taken off with
a measuring circuit, consisting of a noise meter, noise spectrum
analyzer and electronic oscillograph with memory, according to
the generally accepted method [2, 3].   The measurement points were
located at a distance of 1 meter from the machine.   Considering the
total symmetry of the operating elements of the machine relative
to its longitudinal axis, measurements were restricted to five
measurement points (four points around the perimeter and the fifth
over the exciter).
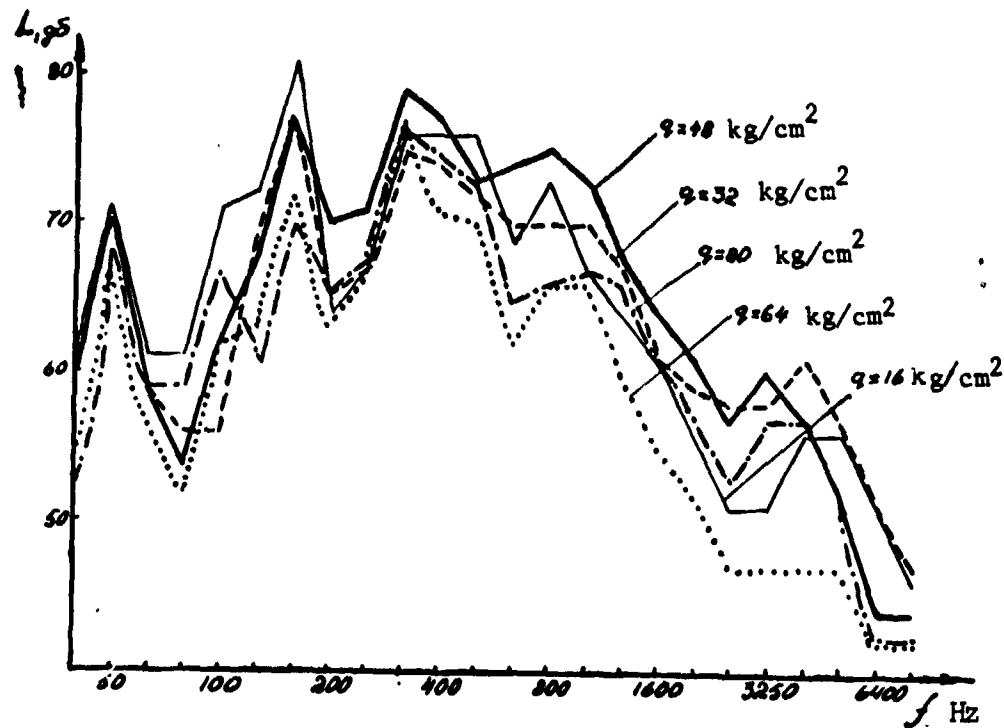
Fig. 3.

Curves of the acoustical pressure level spectra of the C-920
machine, at a supply voltage frequency of 50 Hz and magnetic biasing
currents, equal to 1a, 2a and 3a, corresponding to the measurement
point along the side of the machine in the plane of the elastic
elements, are depicted in Fig. 2.   Curves of the acoustical pressure
level spectra of the 184-PT machine are plotted in Fig. 3, with a
supply voltage frequency of 50 Hz and prestresses on the springs
at the fastening points, q = 16-80 kg/cm^2.   It is evident from the
curves than an optimum prestress between springs, ensuring a minimum

237

level of acoustical pressure is observed.

In this manner, correspondence between the acoustical spectra and nonlinear forced vibrations of the electromechanical system is observed in the electrical vibrator. The characteristics of the nonlinear system can be used for diagnosing a noise spectrum.

REFERENCES

1. Tatishvili, T.G., M.V. Khvingiya, and G.G. Tsulaya, "Investigation of Vibrations of an Electromagnetic Vibrator, Considering Structural Damping and Asymmetry of the Characteristics," Tezisy dokladov konferentsii po probleme konstruktsionnogo dempfirovaniya kolebaniy [Summaries of Reports of Conference on the Problem of Structural Damping of Vibrations], Riga, 1971.

2. Osipov, G.L., D.E. Lopashov et al., Izmereniye shuma mashin i oborudovaniya [Measurement of Noise of Machines and Equipment], Committee on Standards, Measures and Measuring Instruments of the Council of Ministers USSR Press, Moscow, 1968,

3. Bachyulis, R.I. and S.G. Butsevichyus, Nauchnyye trudy vuzov Lit. SSR, Vibrotekhnika 4(9), Vilnyus (1970).

PROBLEMS OF VIBROACOUSTICAL DIAGNOSTICS OF TEXTILE MACHINES

L.N. Ivanov, O.N. Pobol', G.T. Gevorkyan'
(Moscow)

Analysis of existing methods of monitoring the assembly and adjustment of such mechanisms as the shed forming and slay mechanisms of types STB, ATPR and other nonshuttle looms and the cam drives of conveyor-type machines has shown that the vibroacoustical method is the most suitable method for diagnostics.
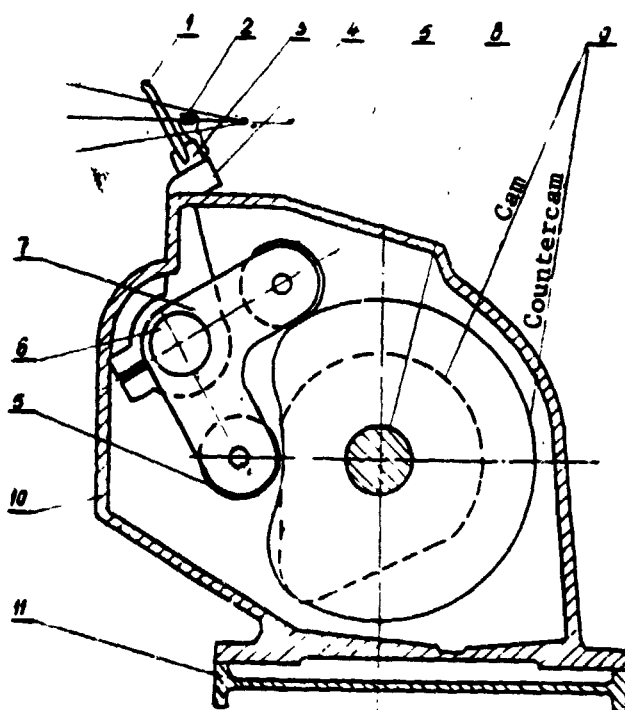

Fig. 1.

A diagram of the slay mechanism of a type STB loom is shown in Fig. 1. The assembly adjustment of this mechanism is carried out by a selection of rollers (Nos. 5) and, in this case, the necessity frequently arises for repeated dismantling and new selection of rollers.

The reciprocating action slay mechanism operates at a speed of up to 280 rpm, depending on the width of the loom. The exciter of the basic /213 acoustical signal is the impact of the rollers on the cams during change in direction of movement, with the frequency of rotation of the camshaft (Nos. 8).

Since the mechanism is enclosed in a closed housing of small size, installed on the loom with a vibration isolating drive, it can be considered a point radiator, and the power of the high-frequency noise is determined by the equation

$$w = k \left(\frac{S}{BM}\right)^2 h^{0.8} \cdot m^{1.2} \cdot \omega^{1.4},$$

where S is the area of the radiating surface, B is the rigidity of the housing, M is the specific mass, n is the gap, m is the specific impact mass, ω is the frequency and k is a constant.

The spectra of the acoustical pressure, obtained for two different gaps between the rollers and cams, are presented in Fig. 2.
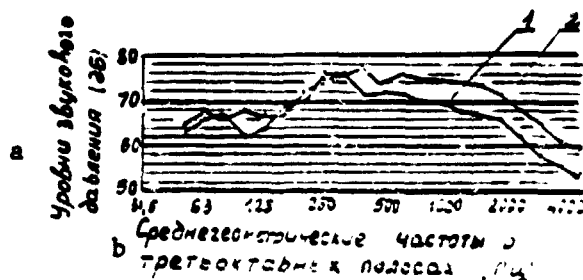

Fig. 2.

Key: a. Acoustical pressure
         level (dB)
     b. Mean geometric frequency
         in 1/3 octave bands (Hz)

The acoustical pressure in the high-frequency maximum radiation of the spectrum, at frequencies of 300-1500 Hz (which corresponds to an impact duration of 10^{-3}) changes by 4 dB. Consequently, carrying out the diagnosis by means of a sensor-microphone is impossible in this case.

An accelerometer can be used as the sensor. Its point of installation is selected so that there will be a dip in the frequency characteristic of the vibrating part, on which the sensor is installed, in the region of the maximum acoustical signal from the rollers. This allows there to be a drop in the vibrations for those values of the gap in the mechanism which amount to 10-20 dB.

DIAGNOSTIC DEVICE FOR MONITORING THE TECHNICAL CONDITION OF MECHANICAL ASSEMBLIES

V.I. Osovskiy, V.V. Shergin, and V.I. Shumilin
(Rostov-on-Don)

An automatic diagnostic device for monitoring the condition of tractor transmission gears is described.

The structural noise spectrum of the gearshift box and rear axle of the tractor were analyzed in a digital computer, by an algorithm based on the multiple correlation method.

The optimum assembly of operating frequencies, by use of which the errors in measurement were minimized, was selected from the entire frequency spectrum.

Selected frequencies are necessary for choosing the measurement range of the diagnostic device. It turned out that, to obtain a relative error of no more than 2%, it was sufficient to use two filters, vibrating only at the frequencies carrying the maximum data of the mechanical parameter being investigated.

The measurement system consists of frequency-selection filters, amplifiers and quadratic detectors, at the outlets of which constant voltages are created, which are proportional to the signal level at the frequencies selected.

The analysis and logic system consists of a series of sensitive threshold elements, with control relays and indicators, permitting identification of three classes of conditions of the gear. Delayed blocking generators, with diode-thyristor outlets, were used as threshold elements.

The diagnostic device was regulated and tested in one of the factories. The threshold voltage values $\beta_{ij} = \alpha_{ij}$ were calculated, by proceeding from the equality presented and then were set into the instrument:

$$\frac{1}{\sigma_I \sqrt{2\pi}} e^{-\frac{(m_I - \beta)}{2\sigma_I^2}} = \frac{1}{\sigma_{II}\sqrt{2\pi}} e^{-\frac{m_{II}}{2\sigma^2}}.$$

where σ_I and σ_{II} are the root mean deviations of the signal of the corresponding class from the mathematical expectation m_I and m_{II}.

The instrument was tested on 18 objects, and it showed an error of no more than 8%. The presence of exchangeable and rebuildable filters in the instrument permits the possibility in principle of monitoring any mechanical assemblies, thereby making it universal to a certain extent.

DIAGNOSTICS OF AUTOMOBILE ENGINE MECHANISMS BY VIBRATION PARAMETERS

B.I. Tarantsev, V.G. Makarov
(Riga)

The use of the vibroacoustical method of diagnostics of the technical condition of an engine is based on a series of premises: the generation of impacts in the linking mechanisms of carburetor engines; periodicity of repetition of impacts in linking mechanisms; the presence of specific frequency characteristics of both individual parts and of the entire engine, as a total system.

The selection of the method and development of means for diagnostics of the technical condition of an engine are based on these premises.

Based on an instrument for estimating the technical condition of engine mechanisms by the vibration parameters (HRI-1 [height-range indicator]), a method of frequency phase selectivity, developed at the Moscow Highway Institute, was proposed.

The engine, in specific modes of operation, firmly maintained under SDA-70 conditions by an automatic mode selector, was tested by the HRI-1 instrument. An estimate of the technical condition of the engine mechanisms is accomplished by the vibration acceleration amplitude of the vibration pulse being investigated, as well as according to the shape of the latter.

The results of diagnosis by an automobile inspection team were favorable and demonstrated the acceptability of the diagnostic method under operational conditions.

Experience in development and test of the HRI-1 instrument permitted general requirements for means for diagnostics of engine mechanisms by the vibration parameters to be formulated.

DIAGNOSTICS OF SOURCES OF ERRORS
IN GYROSCOPIC INSTRUMENTS

M.K. Lyutkevichyus, Z.Yu. Potsyus, and B.B. Rinkevichyus
(Kaunas)

Measurement of the accuracy of operation of gyroscopic instruments is particularly urgent, with regard to increased accuracy in control of inertial systems. A major problem is the study of gyroscopic drift and its causes. Disturbances causing drift in gyroscopes, such as friction in the frame suspension bearings, stress /216 on the angle sensor, dynamic disbalance of the rotor, the "turbine effect" of the air bearings, etc., are random and chaotic, and the drift caused by them in tests tends towards zero. Moreover, the rate of drift is insignificantly small in absolute value; however, errors introduced by them can affect the operation of inertial systems in a significant manner. Therefore, it is especially important to carry out measurements of gyroscope drifts over small intervals of time.

The test stand developed has 12 fixed positions of the rotating table on which the test gyroscopic instrument is installed. The chuck of the rotating table, suspended on air bearings, is turned by a torque generator at a speed, equal to and opposite in direction to the speed of rotation. The earth and, thus, the apparent drift, caused by the speed of rotation of the earth, are eliminated. The magnitude of the natural drift of the gyroscope is measured by an angular position sensor converter. A computing device ensures automatic processing of the digital data.

ANALYSIS OF THE RELATIONSHIP BETWEEN ERRORS
IN MANUFACTURE OF SLOT CONNECTIONS AND GEAR DRIVE NOISES

M.K. Bodronosov
(Moscow)

On the basis of experimental research, an analysis was carried out of the effect of certain errors in manufacture of straight-barrel slots on the noise characteristics of gear drives. In carrying out the experiments, the gear crowns of the test wheels were held immovable, and only the geometric dimensions of the slots and the mutual locations of the individual elements were varied. The investigation of the effect of each factor was carried out under otherwise equal conditions, on $34:56$ cog ratio gear pairs ($m = 2mm$), made of 40 C steel, with a gear crown accuracy of 7 X, machining fineness $\Delta 7$, at a speed $v = 7.1$ m/sec. The number of slots was 6.

The clearance in slot pairs in dimension D, equal to 0.015, 0.05, 0.08 and 0.110 mm, was obtained by change in the outer diameter of the spindle by means of polishing.

The results of the tests of the experimental wheels showed /217 that their noise level increases with increase in clearance.

Curve 1 (Fig. 1) corresponds to the noise level of gear pairs as a function of clearance in diameter D. Increase in noise of the gears with increase in clearance in diameter D can be explained by increase in shock pulses in the slot connection, and then by increase in the dynamic forces directly on the gears.
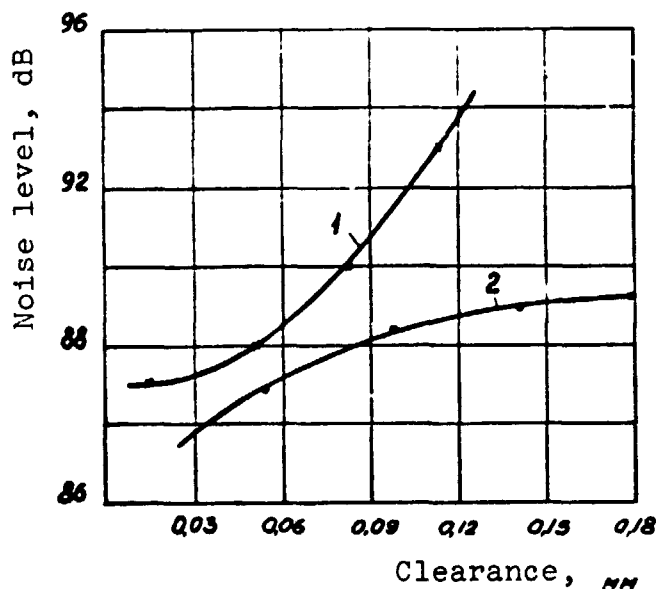
Fig. 1.

A comparative analysis of the noise frequency spectra (Fig. 2a) shows that the acoustical pressure increases with increase in clearance in dimension D, in both the harmonic of the reciprocal frequency Z_s (on the order of $f_s = 200$ Hz), and on the tooth frequency ($f_t = 1140$ Hz) and its higher harmonics ($2f_t$ and $4f_t$).

The different size clearances in the slot pairs were produced by change in the widths of the notches in the gear

hubs. The effect on the noise level of the size of the clearance in dimension b is not so significant as the effect of the clearance in dimension D (curve 2, Fig. 1). The noise level is increased overall by 2 dB, with increase in clearance to 0.09 mm and more. Here, the acoustical pressure increases more rapidly on the second and third harmonics of the tooth frequency f_t (Fig. 2b) with increase in clearance in dimension b. The increase in the high-frequency components of the noise is explained by increase in   /218 intensity of vibration of the wheel, as a result of impacts while meshing. An increase in components, on the slot frequency (f_s = = 150 Hz) and on the subharmonics of the tooth frequency (660 and 440 Hz) also is seen in Fig. 2b. This can be explained by an increase in the degree of separation of the teeth, due to deterioration in conditions of centering of the wheel on the slot shafts.

a
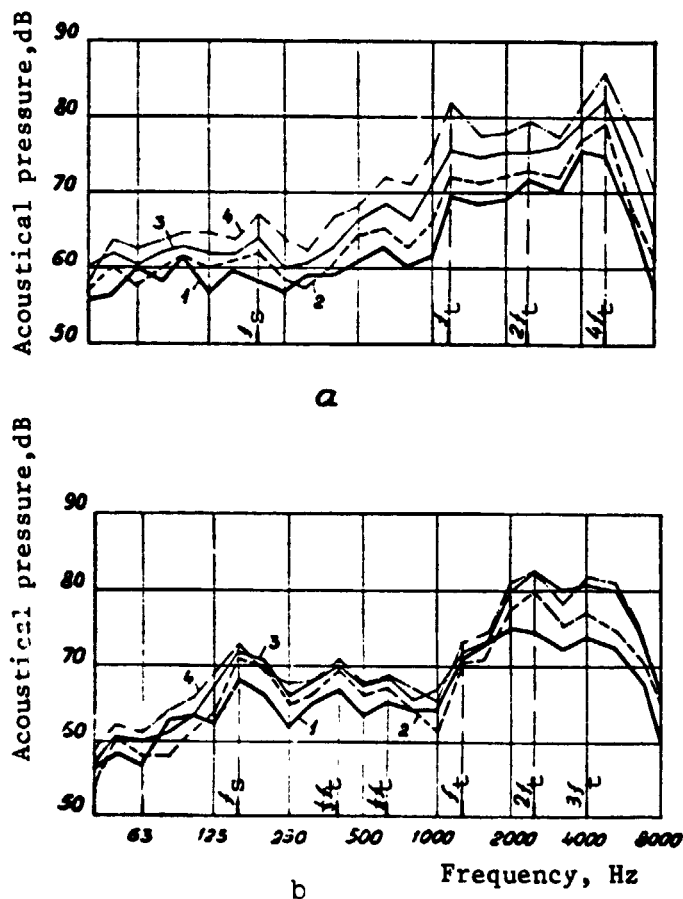
Errors in the mutual locations of slot elements also affect the vibroacoustical characteristics of the gear drive. In particular, increase in aparallelism of the lateral surfaces of the slots, by a value of 0.020-0.030 mm in a length of 100 mm (at a dimension D = 34 mm), leads to an increase in noise level by 1.5-2 dB.

Deviations in slot   /219 spacing show a less noticeable effect on the noise.

In gear drives, having considerable errors in the mutual location of slot elements, the contact point deteriorates and conditions for smooth operation are disrupted.

b

Frequency, Hz

Fig. 2.

THE PROBLEM OF CARRYING OUT A DIAGNOSIS
OF AN INTERNAL COMBUSTION ENGINE BY VIBROACOUSTICAL PARAMETERS

V.N. Lukanin and V.I. Sidorov
(Moscow)

Investigation of the physics of noise formation in an internal combustion engine, carried out in the Transport Engines Problems Laboratory, Moscow Highway Institute, revealed a series of patterns in this phenomenon. A dependence of the acoustical radiation on the engine operating process, its construction, and operational parameters, as well as on the degree of wear of its parts, has been established.

At the present time, test specimens of instruments and devices, which permit evaluation of the condition of individual mechanisms, systems, assemblies and connections in an engine by the nature of the vibrations or noise, already are operating in some automobile plants, diagnostic stations and motor transport establishments.

However, the complex relationship of the vibroacoustical parameters to many factors operating in a dynamic system, in operation of an internal combustion engine and, besides, worn ones, can be learned with maximum accuracy only with the aid of cybernetics.

The necessity for use of an automotive type piston engine in diagnosis is a distinction in setting up the problem of the use of cybernetic methods of accomplishing diagnosis of such a mass of parts as an automotive type piston engine is. This is dependent on the fact that the final purpose of a diagnosis, apart from evaluating the ability of the engine to operate, is predicting its life and the duration of economically advisable operation.

What has been set forth can be followed by the example of   /220
evaluation of the technical condition of the connecting rod bearings of a GAZ-51 engine, having different clearances between the shaft journals and bushings. It has been established experimentally that the amplitude of the natural vibrations at the moment of impact of these parts is increased by 2 dB for each 0.1 mm of increase in the clearance between them. This phenomenon is noted in a definite band of the frequency spectrum of the vibrations, excited in the engine at definite speeds, heat and load modes, at specific advances in the angle of ignition of the operating mixture in the cylinders. However, these relationships are not rectilinear. For example, a change in the ignition advance from 10 to 22° of the deflection angle of the crankshaft causes an increase in the amplitude of 0.6 dB per degree, and from 28 to 34°, only 0.17 dB per degree. The effect of the motor oil temperature shows up to a great extent in the bearings, with increase in the clearances in them. Thus, an increase in the amplitude of the vibrations by 2 dB takes place

in bearings with a clearance of 0.27 mm, with an oil temperature of from 30 to 44°C, and, in bearings with a clearance of 0.18 mm, from 30° to 55°C. Consequently, in evaluating the condition of an internal combustion engine there must be an inverse negative connection between the vibroacoustical parameters and the factors affecting them. This permits the error in extrapolation (prediction) of a specific technical condition of the engine to be reduced to a minimum, and its weakest assemblies or mechanisms to be revealed.

Predicting the reliability of an engine, in turn, must take place with consideration of the effect of the degree of wear of its assemblies and connections, as well as of the operating conditions, which will affect the rate of wear of parts in the future. In this case, an inverse connection with the factors causing such an effect is necessary.

A system for cybernetic diagnostics of an internal combustion engine by vibroacoustical parameters is shown in the diagram.

In particular, it is clear from this diagram that the problem of diagnostics is not only in detection of deviations of the engine from the normal dynamic condition, but in predicting its operating capability during the succeeding operating period.
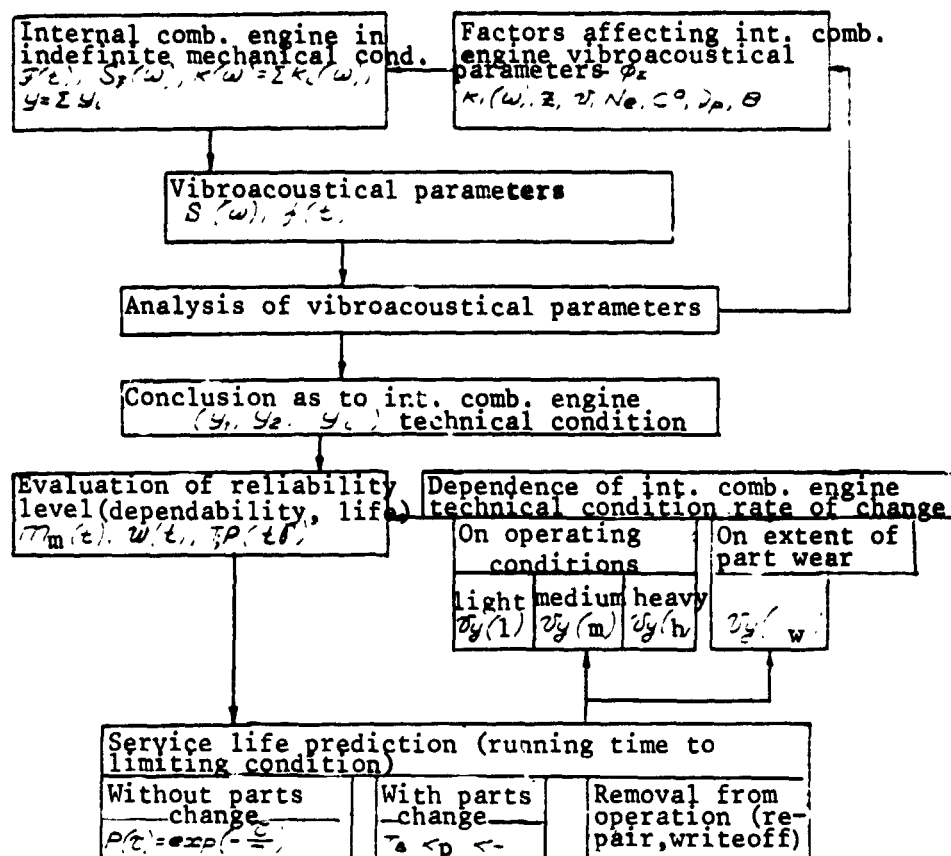
248

Fig. 1. Diagram of system of cybernetic diagnostics of an internal combustion engine by vibroacoustical parameters.

F(t) work completed; $S_J(w)$ force spectrum; k(w) frequency characteristic; y condition of assemblies; S(w) vibration spectrum; f(t) time characteristic of vibrations; $k_1(w)$ fluctuation in k(w); Z irregularity in cylinder operation; v speed conditions; N_e load conditions; °C temperature conditions; ν motor oil viscosity; Θ spark advance; Vy(w) rate of parts wear with different degrees of wear; Vy(l), Vy(m), Vy(h) rate of parts wear under various operating conditions; $m_m(t)$ mean number of breakdowns; (t) breakdown flow parameter; T running time to breakdown; P(t, γ) gamma-percent service life; $P(\tau) = \exp(-\tau/T)$ probability of breakdown-free operation; T_B mean time for restoration; K_p technical readiness coefficient; K_t technical use coefficient.

TRANSITIONAL MODES OF MOTION AND CAPTURE REGIONS OF VIBROSHOCK SYSTEMS

V.L. Ragul'skene
(Kaunas)

In view of the fact that, because of their intrinsic non-linearity, vibroshock systems have the property of multiplicity of periodic modes of motion, it is urgent that the capture regions be determined, i.e., the initial motion parameter regions, from which the system is drawn into diverse, periodic shock modes of motion. The transitional modes of motion must be determined for solution of this problem. There are three initial parameters for a nonautonomous vibroshock system with one degree of freedom: coordinates, velocity and time. It was shown earlier [1] that it is possible and expedient to investigate the transitional modes and capture regions of vibroshock systems in the phase plane of two variables (phases and shock velocity).

It also was proposed [1], for a more complete investigation of the transitional modes of motion, as well as for determination of the capture regions, to use calculations, not only in the direction of increase, but in the direction of decrease, in time (indices). Transitional modes (parameters of motion at two neighboring impact points) were investigated in the work by the mathematical modeling method on an analog computer, in the directions of increase and decrease in time, with stabilized exciting pulse amplitudes and widths. For nonlinear systems, we immediately obtain the boundary of the capture region from an unstable point modeled in the reverse direction. If the system does not have unstable points (as, for example, the single mass vibroshock system investigated in this work), modeling in the reverse direction, we can change the scale (for example, five times, in our case) and, thereby, follow the transitional process under the initial conditions over a wider range than by the direct solution.

Thus, if the motion of a system in the direction of increase is described by the following differential equation:

$$F\left(\frac{d^n x}{dt^n}, \frac{d^{n-1} x}{dt^{n-1}}, \ldots, \frac{dx}{dt}, x, t\right) = 0.$$

(1)

the motion in the direction of decrease in time is described by the following equation:

$$F\left[(-1)^n \frac{d^n x}{dt^n}, (-1)^{n-1} \frac{d^{n-1} x}{dt^{n-1}}, \ldots, -\frac{dx}{dt}, -t\right] = 0.$$

(2)

where x is a generalized coordinate, t is the time in the direc-
tion of increase and $\xi = -t$ is the time in the direction of decrease.

Let us proceed to examination of specific systems.

Let us examine a single mass vibroshock system, in the case when the interaction is accounted for by the theorem of pulses to the coefficient of restoration of the impact velocity. In this case, we assume that periodic pulses act on the mass on the stop side [2].

The equations of motion in the direction of increase in time have the form

$$m \frac{d^2 x}{dt^2} = F(t) \qquad \text{with } x < 0$$
$$\left(\frac{dx}{dt}\right)^- = -R\left(\frac{dx}{dt}\right)^- \qquad \text{with } x = 0 \tag{3}$$

and on the side of decrease,

$$m \frac{d^2 x}{dt^2} = -F(t) \qquad \text{with } x < 0$$
$$\left(\frac{dx}{dt}\right)^+ = -\frac{1}{R}\left(-\frac{dx}{dt}\right)^- \qquad \text{with } x = 0 \tag{4}$$

In Eqs. (3) and (4)

$$F(t) = F \sum_k \delta(t - kT)$$

and
$$\sigma = \int_{kT-0}^{kT+0} \delta(t - kT)\, dt, \tag{5}$$

where F = const, k = 0, 1, 2, ... is an expanded natural number, T is the period of the external force, σ is the external periodic force pulse, and the superscripts + and - in the first derivatives designate the velocity at the moments before and after impact, respectively, here and subsequently.

In solution of the problem in the direction of decrease in time, the impact velocity restoration coefficient (1/R) > 1 (by

the forward solution, R > 1). Moreover, we change the sign of the velocity (the velocity before impact is negative and after impact, positive). The pulses also are negative.

The velocity before impact in the forward solution corresponds to the velocity after impact in the reverse one.

We reckon phase ϕ_1 from impact to pulse. For n-fold modes (n is the number of pulses of the external force between two shocks), phase $\phi_1 + 2\pi(n - 1)$ is plotted in the figures, i.e., from a shock to the following pulse. We designate the phase in the opposite /224 direction $2\pi - \phi_1$, since the phase period between two pulses is 2π ($\phi_1 = 2\pi\frac{T_*}{T}$, where T_* is the time from impact to pulse). We reckon the phase between succeeding pulses and shocks; this corresponds to the phase between a shock and the first pulse in the forward solution.

At moment t = 0, the mass is in the catch (x_0 = 0). We set $\dot{x}_0$. The phase ϕ_0 is from the starting moment to the first pulse of the external force.
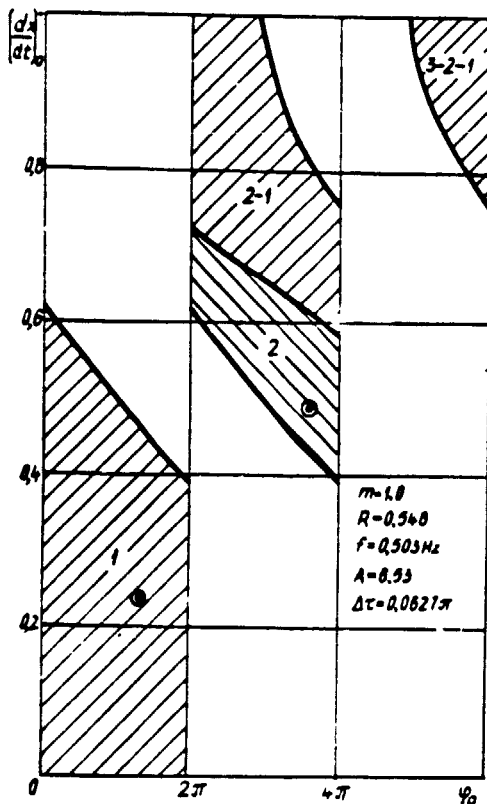
Capture regions in the direction of increase in time are shown in Figs. 1, 2 and 3, at various widths of the exciting pulse (pulse height is 6.53).

At large pulse widths, the zones are less diverse and wide, and with narrower pulses, they are all diverse and narrower. Thus, for example, at $\Delta\tau = 0.0627\pi$, the last zone filling the entire region investigated (1x = 100 v) is 3-2-1; at $\Delta\tau = 0.052\pi$, this zone will be /226 4-3-2-1; and, at $\Delta\tau = 0.034\pi$, 8-5-3-2. (The figures designate a multiplicity factor, the number of pulses between two neighboring impact points; for example, the designation 8-5-3-2 means that, after eight pulses between two neighboring impact points, five pulses follow, then three pulses /228 and a mode with two pulses between shocks is established.)

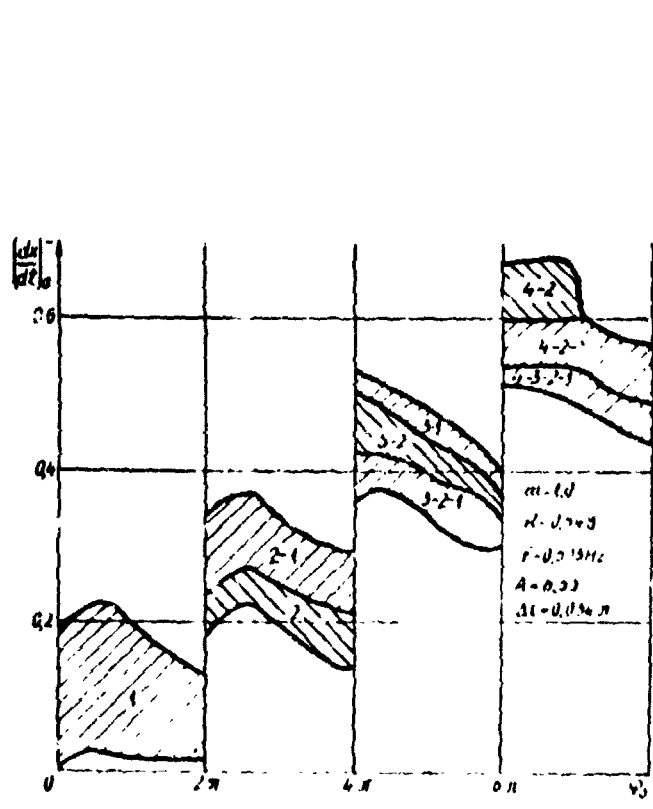Fig. 1. Capture regions.

252

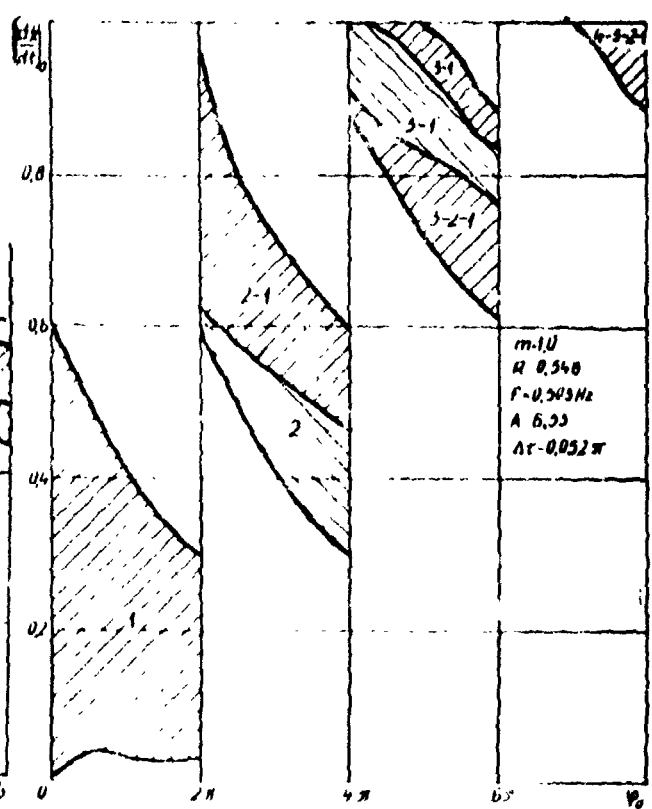Fig. 2.   Capture regions.

Fig. 3.   Capture regions.
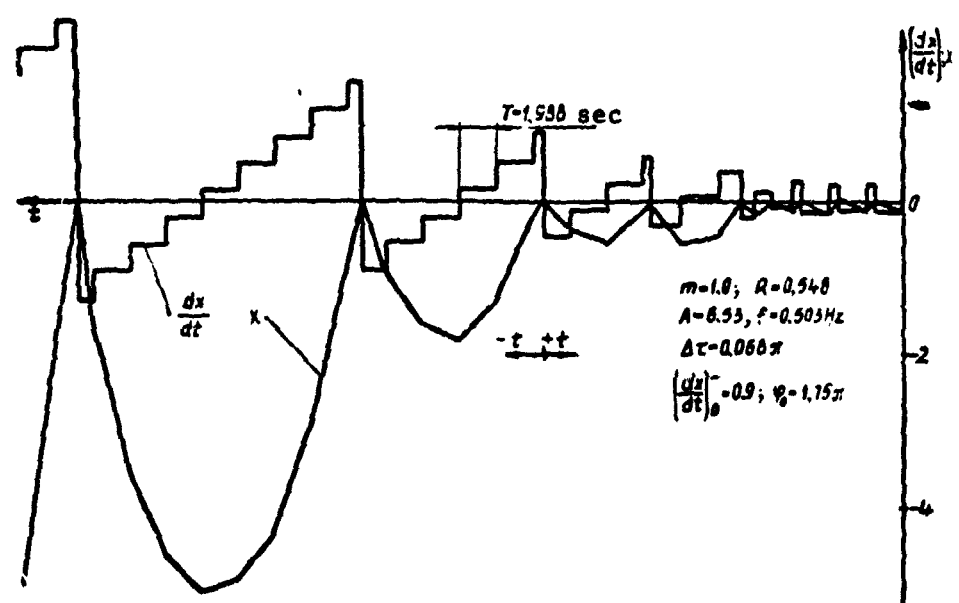
Fig. 4.   Trajectory of motion of mass with time, by solu-
tion of differential equations during increase and decrease
in time.

Fig. 5. Phase plane.
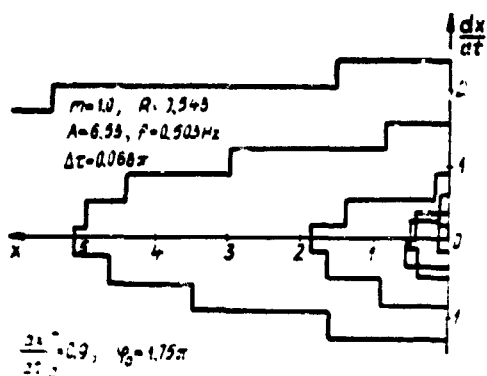
It has been determined that the zones are repeated precisely from bottom to top. That is, at a pulse width $\Delta\tau = 0.0034\pi$, the zones are located in the following order: 1, 2, 2-1, 3-2-1, 3-2, 3-1, 4-3-2-1, 4-2-1, 4-2, 5-3-1, 5-3-2, 5-3-2-1, 5-2-1, etc., up to 8-5-3-2. At $\Delta\tau = 0.052\pi$, we have 1, 2, 2-1, 3-2-1, 3-2, 3-1, 4-3-2-1, and at $\Delta\tau = 0.062\pi$, only 1, 2, 2-1 and 3-2-1.
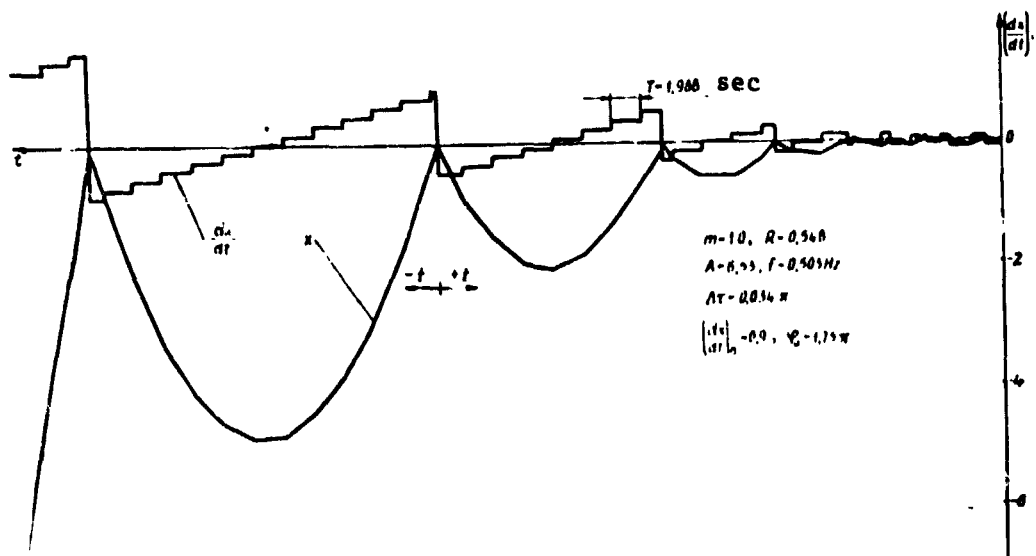
Fig. 6. Trajectory of motion of mass with time.
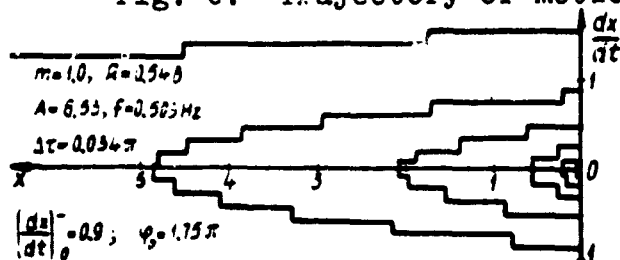
Fig. 7. Phase plane.

The trajectories of the motion of the masses with time and in the phase plane, by solution of the differential equations of motion with increase and decrease in time, are shown in Figs. 4, 5, 6 and 7.

254

REFERENCES

1. Ragul'skis, K.M., I.I. Vitkus, and V.L. Ragul'skene, <u>Samosin-khronizatsiya mekhanicheskikh sistem (I. Samosinkhronnyye i vibroudarnyye sistemy)</u> [Autosynchronization of Mechanical Systems (I. Autosynchronized and Vibroshock Systems)], Vil'nyus, 1965.

2. Ragul'skene, V.L., "Capture Regions in Vibroshock Systems (Method: Single-Mass Vibroshock System with Immovable Stops)," <u>Nauchnyye trudy vuzov Lit. SSR, Vibrotekhnika</u> 1(1) (1967).

CERTAIN CHARACTERISTICS AND CAPTURE REGIONS
OF NONLINEAR VIBRATING SYSTEMS

V.L. Ragul'skene
(Kaunas)

It has been shown that, not only free vibrations of a system, but vibrations which are multiples of them in frequency, are of importance in research. The corresponding periodic forced vibrations of the type n/m (n is the number of periods of disturbance /229 between periods of movement and m is the number of periods of movement in one period of disturbance), generated by a harmonic or close to harmonic disturbance, are propagated close to the corresponding curves of the free vibrations, i.e., close to the "skeleton" curves and their frequency multiples:

$$f(A) = mA \left(\omega \, \frac{m}{n} \right)^2 .$$

where m is the mass, A is the maximum deviation and ω is the frequency.

In our example (Fig. 1), subharmonic vibrations of the type n = 3 (m = 1) are propagated close to the curve

$$f(A) = mA \left(\frac{\omega}{3} \right)^2 .$$

It has also been proposed that investigation of transitional /231 modes of motion and capture regions be carried out by precise methods in phase space, with the least number of coordinates. Thus, for example, for nonautonomous second order equations (for example, the Duffing equations), in place of three variables (coordinates, velocity, phases), it is proposed to use two: velocity during transition of the coordinate through zero and phase

$$\left[\left(\frac{dx}{dt} \right)_{x=0} \text{ и } \varphi_i \right] .$$

Plotting the transitional modes in this coordinate system (Fig. 2) considerably simplifies the investigation, since it is plotted in a plane, in a coordinate system with two variables.

256

Transitional modes were investigated by the mathematical modeling method on an analog computer, in the directions of increase and decrease in time. Modeling in the reverse direction from the unstable point, we immediately obtain the capture region (Fig. 3).

Fig. 1. Amplitude-frequency characteristics: 1. free vibrations; 2. multiple frequencies of the free vibrations (n = 3); 3. forced harmonic vibrations; 4. subharmonic third order vibrations (n = 3).

Fig. 2. Transitional modes of motion and capture regions.

257

Fig. 3. Bifurcation curve of harmonic modes
of motion n = 1, determined by solution of
differential equations of motion in the direc-
tion of decrease in time from an unstable
singular point.

REFERENCES

1. Khoyasi, T., _Nelineynyye kolebaniya v fizicheskikh sistemakh_ [Nonlinear Vibrations in Physical Systems], Mir Press, Moscow, 1968.

2. Ragul'skene, V.L., "Capture Regions in Vibroshock Systems (Method: Single-Mass Vibroshock System with Immovable Stops)," _Nauchnyye trudy vuzov Lit. SSR, Vibrotekhnika_ 1(1) (1967).

ELECTRONIC DAMPING OF MECHANICAL VIBRATIONS

P. Vasil'yev and A. Navitskas
(Vil'nyus)

In measuring and recording the patterns of vibration of a process being investigated, for example, tensile stress vibrations of a magnetic carrier (tape or wire), the frequency of the process being investigated must be an order of magnitude lower than the natural frequency of the sensitive receiving element, for sufficient accuracy.

The elastic element must damp, for the frequency range of the vibrational patterns being investigated to be expanded, in particular, of the tensile stresses of a moving signal carrier. The natural frequency of the flexural vibrations of the sensitive /232 element is determined by the following expression:

$$f = \frac{\alpha^2}{2\pi l^2} \sqrt{\frac{E \cdot I}{m}} ,$$

where l is the length of the arm, E·I is the flexural rigidity, m is the mass of a linear unit of the arm, α is from equation

$$ch\alpha \cdot \cos\alpha + 1 = 0$$

and the roots of this equation are

$$\alpha_0 = 1.875,$$
$$\alpha_1 = 4.694,$$
$$\cdots\cdots\cdots$$
$$\alpha_i \approx \frac{2(i+1)-1}{2} \pi .$$

A method is proposed for damping mechanical vibrations of elastic sensitive elements with semiconductor strain gauges, based on electronic compensation of their natural (resonance) vibrations, a schematic diagram of which is depicted in Fig. 1.

The **arm**, which is sensitive to bending, consists of bimorph /233 glued or soldered piezoceramic plates 1 and 2, on the outer sides of which semiconductor strain gauges 3 and 4 are glued. The piezoceramic plates are included in a closed electrical circuit: plate 1, resistor 5, amplifier 6, phase shifter 7, plate 2.
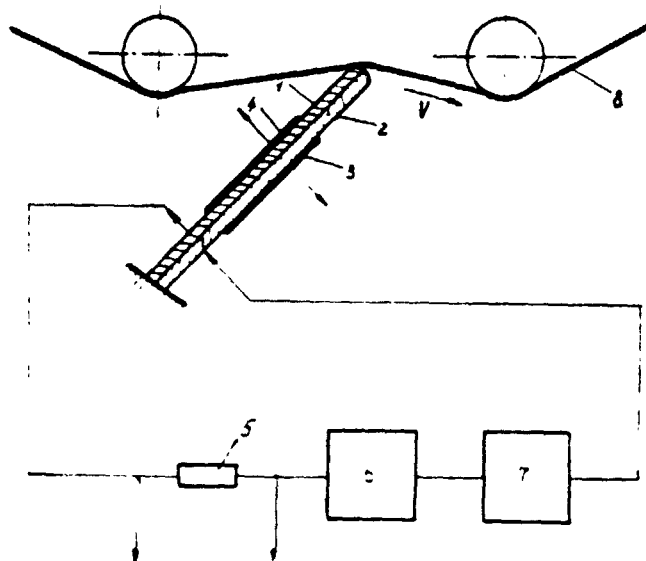
Fig. 1. Meter block diagram -- stress sensor construction: 1, 2 piezoceramic plates; 3, 4 strain gauges; 5 load resistance; 6 amplifier; 7 phase-shifting circuit.
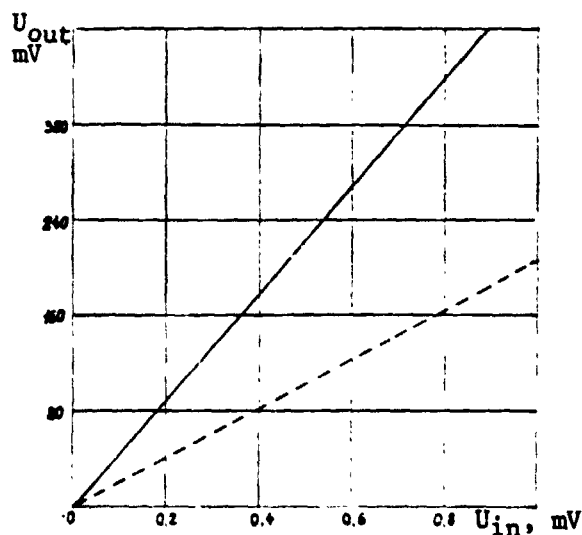

Fig. 2. Meter amplitude characteristic: solid line, glued plates; dashed line, soldered piezoplates.

During tension vibrations of the moving carrier, an emf is generated in plate 1, which includes the stress measurement vibration signal plus stray natural vibrations of the arms. The latter are extracted by resonance amplifier 6 and, passing through phase shifter 7, by means of creating flexural antiphase vibrations in plate 2, they damp the arm.

The nature of the variable component of the stress vibration signal can be determined with resistor 5. Strain gauges 3 and 4 register changes in the stress on the moving signal carrier, taking account of its initial level. The calibration does not differ from the normal calibration of the arm with the strain gauges.

The output voltage, excited in the piezoceramic plate, can be subtracted from the coefficient of longitudinal deformation of the piezo material:

$$h = g \cdot E$$

where g is the longitudinal deformation coefficient and E is the Young's modulus of the material. From /234 this,

$$U_{out} = h \cdot \varepsilon \cdot t$$

where ε is the relative deformation due to stretching and t is the plate thickness.

261

The amplitude and frequency characteristics of specific sensors (arm length l = 25 mm, width b = 7 mm, thickness d = 0.5 mm, TsTS-19 piezoceramic) are shown in Figs. 2 and 3. The characteristics of glued sensors are indicated by dashed lines and of soldered ones, by solid lines [sic].
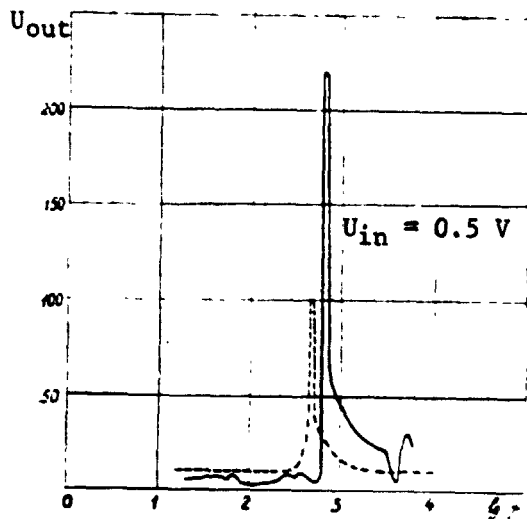
Fig. 3. Meter frequency characteristic: the solid line, glued piezoplates; dashed line, soldered piezoplates.

The spectral density of the patterns of change in stress, measured by the sensor without damping (solid line) and with electronic damping (dashed) is shown in Fig. 4.

The proposed method of /235 damping mechanical vibrations, by means of injection of electrons through a reverse connection, permits the range of the frequencies measured to be sharply expanded, in various systems of measurement of stress vibrations of moving signal carriers, and it also finds use for damping the natural vibrations of mechanical stress stabilizers of tape and wire record carriers.
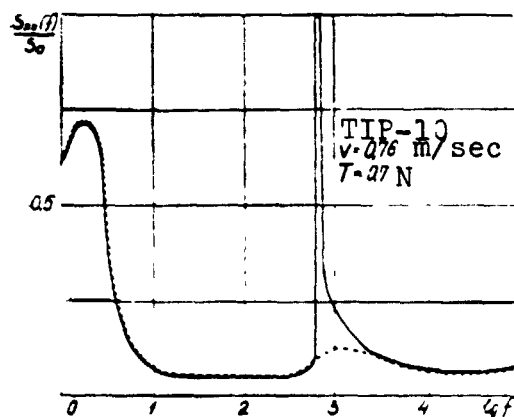
Fig. 4. Tape stress vibration oscillogram: solid line, with undamped arm; dashed line, using electronic damping.

262

REFERENCES

1. Navitskas, A.I., "Stress Measurement in a Moving Tape," _Nauch-nyye trudy vuzov Lit. SSR, Vibrotekhnika_ 2(2) (1967).

2. Kurtinaytis, A. and K. Ragul'skis, "Device for Measurement of Stress Vibrations in a Magnetic Tape," _Avt. svid. SSSR_ [Author's Certificate, USSR], No. 24035, published 21 March 1969.

3. Nubert, G.P., _Izmeritel'nyye preobrazovateli neelektricheskikh velichin_ [Nonelectrical Quantity Measurement Converters], Energiya Press, Moscow, 1970.

4. Khemmond, P., _Teoriya obratnoy svyazi i eye primeneniye_ [Inverse Connection Theory and Its Use], Fizmatgiz Press, 1961.

SYNTHESIS OF MECHANISMS WITH FLEXIBLE
CENTRIFUGAL-INERTIAL CONNECTIONS ACCORDING TO
FIXED DYNAMIC CHARACTERISTICS

K.M. Ragul'skis and I.K. Yaroslavskiy
(Kaunas)

A designer, creating a strong and light instrument, guaranteeing uniform movement of the performing elements, independent of what vibrations are accomplished by the remaining part of the unit, taking the nature of the measurement of external loads into account, operates with two parameters: the moments of inertia of the mass and rigidities of the transmission lines, of which, with relatively constant geometric dimensions of the drive assembly, the more easily measured parameter is the rigidity of the transmission line of the drive or, more likely, the most pliable part of it, the couplings.

There are a number of criteria for selection of dynamic characteristics of the couplings at the present time, which are indicators of a number of basic properties of the transmission: vibration isolation, vibration quenching, etc. The most promising are couplings with a nonlinear relation between the magnitude of the torque transmitted and the magnitude of deformation of the coupling, since couplings with nonlinear characteristics convert a linear torsional-vibrating system into a nonlinear one.

The problem of the optimum planning of dynamic systems has /236 been solved by a number of authors. A.N. Golubentsev [1] examined the question of the minimum dynamicity coefficient under conditions of a constant external load. S.A. Pankratov [2] obtained an equation of motion of a dynamic system under external loads, which change according to a monoharmonic pattern. P.F. Pankovich [3] examined a two-mass system (steam engine-turbine), connected by two types of couplings: flexible and hydraulic, and he developed a method for defining recommendations for decrease in the torsional vibrations of ship turbines. V.S. Gaponov and N.F. Kirkach [4, 5] proposed a general method for obtaining the relation of one of the system parameters to the remaining parameters, and they obtained a second kind of solution of a system of differential equations of a mechanical system with elastic coupling, by means of the Volterra equation. This solution does not contain the roots of a characteristic equation as constants, but parameters of the system, i.e., a change in any parameter directly affects the magnitude of the transition process function.

The creation of mechanisms, the structures of which provide given dynamic characteristics, was examined in work [6], for self-synchronizing speed transmissions, and in the work of B.L. Dikovskiy and A.T. Poletskiy [7]. In this work, the profile of the cam

of an ungraduated pulser of the system of M.F. Balzhi was determined, corresponding to the desired pattern of movement of the driven shaft of the pulser. The Minsk-1 digital computer was used for processing the data in work [7].

The construction of mechanisms, with flexible centrifugal-inertial (FCI) connections [8], by introduction of curvilinear profiles into them also can ensure the production of a given /237 dynamic characteristic.
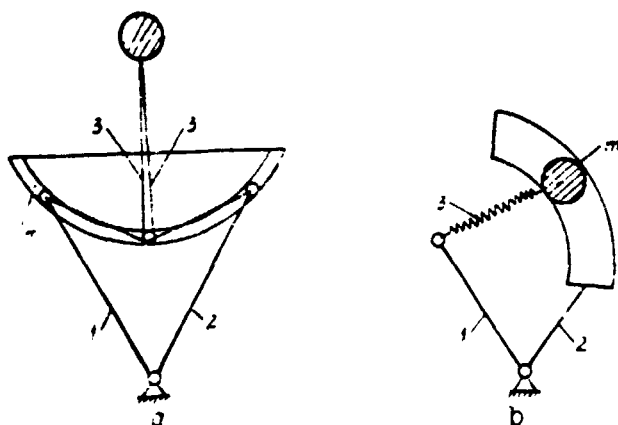

Fig. 1.

Examples of mechanisms with FCI, with symmetrical a and asymmetrical b curvilinear profiles, are presented in Fig. 1. In these mechanisms, movement from drive link 1 to the driven one 2 is transmitted oy flexible elements 3 and centrifugal masses m (4 are massless rigid links).

For these mechanisms, in the steady-state mode of movement, i.e. during rotation of shafts 1 and 2 with uniform angular velocities, the dynamic characteristic has the form

$$\frac{M}{mr^2 \omega^2} = F_1(x, m, \omega^2, c).$$

(1)

where M is the mean value of the torque transmitted by tne coupling; m is the corrected total mass of the centrifugal weights; r is the corrected external force arm; ω is the mean angular velocity of rotation of shafts 1 and 2; $\alpha = \phi_1 - \phi_2$ is the difference in phase between the deflection angles of the driving and driven links; and c is the total rigidity of the flexible elements.

We illustrate determination of the theoretical shape of the curvilinear profile of a system with FCI, providing the given dynamic characteristic, by the example of a symmetric system with FCI, the calculation scheme for which is shown in Fig. 2.

For this type of mechanism, with the aid of the Lagrange equation of the second kind, the following relationship was obtained in work [8]:
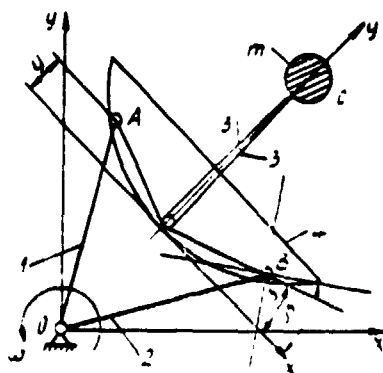
265

Fig. 2.

$$\mathcal{V}_C = -\omega^2 \frac{\partial}{\partial \dot{\partial}} W_1 - \frac{\partial}{\omega} \cdot \quad (2)$$

where   <u>/238</u>

$$M_C = \frac{M}{mr^2 \omega^2} , \quad (3)$$

$$W_1 = 0.5\,(I_1 + I_2) + \frac{mr^2}{2} , \quad (4)$$

$$\hat{r} = \frac{c}{m\omega^2}\,\Delta, \quad (5)$$

$$\Pi = c\Delta^2. \quad (6)$$

Here, I_1 and I_2 are the moments of inertia of links 1 and 2, respectively; Δ is the deformation of the flexible elements; and Π is the potential energy.

We introduce the designations

$$k\omega = \frac{c}{m\omega^2} , \quad d = \frac{l_0}{r} , \quad \frac{Y}{r} = U, \quad \frac{X}{r} = V, \quad \frac{dY}{dX} = \frac{dU}{dV} = \tan\beta, \quad (7)$$

where l_C is the initial elasticity length; r is the crank length OA = OB; and X and Y is a coordinate system moving together with the mechanism.

Taking expressions (2)-(7) into account, we obtain an equation of the connection characteristics from expression (1):

$$\frac{M}{mr^2\omega^2} = \frac{k\omega}{k\omega-1}\left(\cos\frac{\alpha}{2} + d - U - \sqrt{U^2 + \sin^2\alpha}\right)\times \quad (8)$$

$$\times\cos\alpha(\tan\frac{\alpha}{2} + \tan\beta + \cos\mu - \sin\mu\tan\frac{\alpha}{2})$$

from which we derive the differential equation of the theoretical profile

266

$$\frac{dU}{dV} = \frac{k_\omega - 1}{k_\omega} \frac{F_z}{\sqrt{1 - V^2}\,(\sqrt{U^2 - V^2 - d - U - \sqrt{U^2 + V^2}})} \times$$

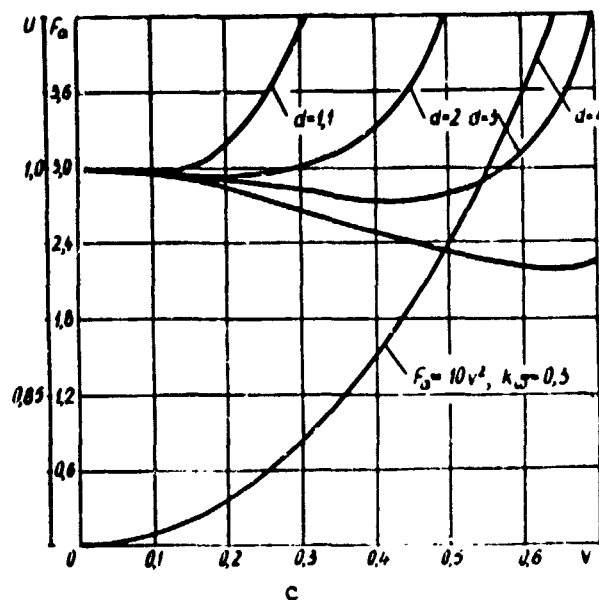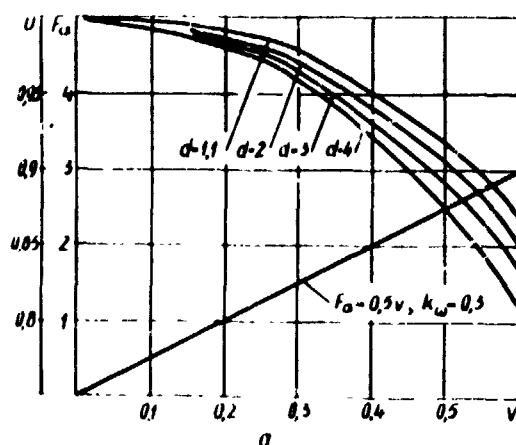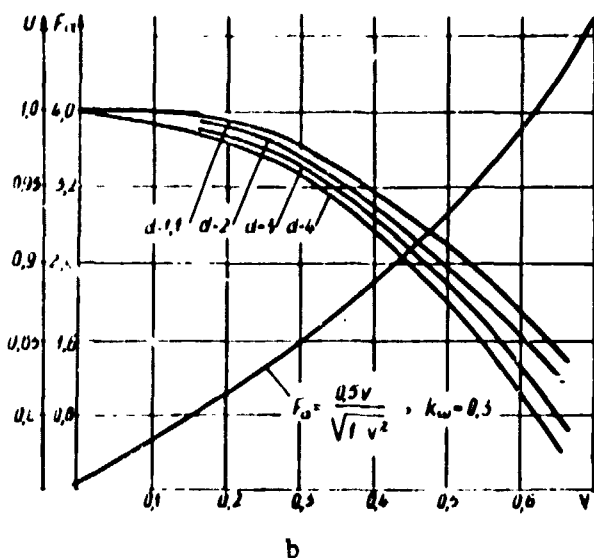$$\times \frac{\sqrt{U^2 - V^2}}{V + \sqrt{U^2 - V^2}} - \frac{V}{\sqrt{1 - V}} . \tag{9}$$

Fig. 3.

Solution of Eq. (9) by digital computer permits a number of theoretical curvilinear profiles to be plotted for given dynamic characteristics F_α. Examples of these profiles are shown in Fig. 3, in the form of curves. These examples illustrate the possibility of using FCI as mechanisms with given dynamic characteristics.

267

1. Golubentsev, A.N., Dinamika perekhodnykh protsessov v mashinakh so mnogimi massami [Dynamics of Transition Processes in Machines with Many Masses], Mashgiz Press, Moscow, 1959.

2. Pankratov, S.A., Dinamika mashin dlya otkrytykh gornykh i zemlyanykh rabot [Dynamics of Machines for Open-Pit Mining and Excavation Work], Mashinostroyenie Press, Moscow, 1967.

3. Pankovich, P.F., Trudy po vibratsii korablya [Works on the Vibration of Ships], Mashgiz Press, Moscow-Leningrad, 1960.

4. Kirkach, N.F. and V.S. Gapanov, "Synthesis of Characteristics of Flexible Couplings for Drives," in he collection Dinamika i prochnost' mashin [Dynamics and Strength of Machines], No, 2, 1970.

5. Kirkach, N.F. and V.S. Gapanov, "Derivation of Equations of Synthesis for a Linear Dynamic System with Restricted Excitation, Operating in the Transition Mode," in the collection Dinamika i prochnost' mashin [Dynamics and Strength of Machines], No. 12, 1971.

6. Vitkus, I.I. and K.M. Ragul'skis, Samosinkhronizatsiya mekhanicheskikh sistem [Autosynchronization of Mechanical Systems], Mintis Press, Vil'nyus, 1965.

7. Dikovskiy, B.L. and A.T. Poletskiy, "Calculation of a Pulser Cam on the Minsk-1 Digital Computer," Material vtorogo Vsesoyuznogo soveshchaniya po primeneniyu matematicheskikh mashin pri konstruirovanii i issledovanii avtomobiley i dvigateley [Materials of Second All-Union Conference on the Use of Mathematical Machines in Design and Study of Automobiles and Engines], Vol. 2, Minsk, 1965.

8. Ragul'skis, K.M. and I.K. Yaroslavskiy, "Dynamics of Mechanisms with Flexible Centrifugal-Inertial Connections," Nauchnyye trudy vuzov Lit. SSR, Vibrotekhnika 3(12) (1971).

SYNTHESIS OF VIBRATION SYSTEMS, HAVING GROUP SYMMETRY OR QUASI-SYMMETRY, ACCORDING TO THE FREQUENCY SPECTRUM

A.I. Andryushkevichyus and K.M. Ragul'skis
(Kaunas)

Torsional vibration systems, with finite numbers of degrees of freedom are investigated. In designing such systems, it is important to select parameters, so that the frequency spectrum of the natural vibrations is beyond the limits of the resonance danger region. In the case when the system has a large number of degrees of freedom, calculation of its natural frequencies, as well as tuning out the resonance danger zones is laborious. When the system being investigated has one group symmetry or another, solution of the problem mentioned above is facilitated, as a consequence of breaking down the frequency equations into several, which are smaller in size. In this article, an algorithm is given for tuning out the natural frequency spectrum from the forbidden region, by means of varying the rigidity of systems having group symmetries or group quasi-symmetries.

Let us assume that the vibrating system has some group sym- /241
metries. Then, using the theory of group representations, we convert the characteristic matrix of the system into block-diagonal form, i.e., $A = \begin{pmatrix} A_1 & & 0 \\ & \ddots & \\ & & A_i & \\ & & & \ddots \\ 0 & & & A_s \end{pmatrix}$, where A_i are quadratic matrices. Let

the resonance danger region consist of several nonintersecting intervals (α_j, β_j), where $j = 1, 2, \ldots, r$. We compile the

polynomial $P(\lambda) = = \prod_{j=1}^{r} (\lambda - \alpha_j)(\lambda - \beta_j)$ and the matrix $C = P(A)$. It is

easy to see that matrix C has a block-diagonal form:

$$C = \begin{pmatrix} C_1 & & 0 \\ & \ddots & \\ & & C_i & \\ & & & \ddots \\ 0 & & & C_s \end{pmatrix},$$

where $C_j = P(A_i)$. We construct the function $F_1(k, Z_j) = \dfrac{(C_1 Z_1, Z_1)}{(Z_1, Z_1)}$,

where z_i is a vector-column, the dimensions of which coincide with the dimensions of matrix C_1, and k is the vector of the varying rigidities.

By setting $k = k_0$, we find $\min\limits_{z_1} F_i(k_0, z_1)$, where $i = 1, 2, \ldots, s$, by the steepest descent method, and we select the smallest of them: $\min\limits_{z_1} F_1(k_0, z_1) = F_1(k_0, z_{10})$.

At point k_0, we find the gradient τ_0 of function $F_1(k, z_{1c})$, according to variable k and we assume that $k_1 = k_0 + f_c\sigma_0$.

At k_1, we find $\min\limits_{z_1} F_i(k_1, z_1)$ by the steepest descent method and we select the smallest of them: $\min\limits_{z_t} F_t(k_1, z_t) = F_1(k_1 z_{t1})$.

We find the gradient $F_t(k, z_{t1})\sigma_1$, according to variable k, and we assume that $k_2 = k_1 + \psi_1\sigma_1$, etc. The process is terminated upon satisfying the condition $\min\limits_{z_j} F_j > 0$, or upon going beyond the limits of the physically realizable variable rigidities, or upon reaching $\max\limits_{k} \min\limits_{z_j} F_j$.

When the system being investigated has group quasi-symmetries, i.e., the characteristic matrix of the system has the form $A = A_0 + \varepsilon B$ (where A_0 is a symmetric matrix, characterizing a system with group symmetries, εB is a symmetrically disturbing matrix and ε is a small parameter), it follows from the Vilant-Gorman theory that, with a sufficiently small εB, the natural values of matrices A and A_0 are close to one another. According to the algorithm set forth above, by varying the rigidities on which matrix A_0 depends, we tune out the spectrum of the natural values of matrix A_0 relative to the forbidden region. By varying the rigidities on which matrix εB depends, we find $\min \|\varepsilon B\|_E^2$. Since the natural values of matrix A_0 approximate the spectrum of the natural values of matrix A, at a sufficiently small $\min \|\varepsilon B\|_E^2$, it can be considered that the system being investigated has been tuned out relative to the resonance regions.

VIBRATION RESISTANCE OF THE WIRE-FEED
MECHANISM OF A MAGNETIC RECORDING APPARATUS

S.P. Kitra and R.-T.A. Tolochka
(Kaunas)

The necessity for ensuring the efficiency of magnetic record-
ing apparatus, under conditions of external mechanical and climatic
actions, introduces the problem of stability of the mechanisms which
pull through the record carrier.

By stability of the apparatus, we mean its ability to operate
normally under specific external influences. Stability charac-
terizes possible modes of operation.

The problems facing magnetic recording, as well as other
data transfer systems, can be reduced to two basic problems: the
problem of efficiency and the problem of reliability. By efficiency
of the system, we mean the ability to transfer the maximum amount
of data by the most economical means. System reliability is deter-
mined by its resistance to interference.

Efficiency and reliability of a circuit are determined by the
structural parameters and by the degree of perfection of methods
of production and treatment of individual elements of the trans-
port mechanism circuit. Determination of the extent of the effect
of these parameters on the circuit characteristics is one of the
basic problems of magnetic recording theory.

Devices for transporting magnetic record carriers are compara-
tively complicated dynamic systems, the theory of which is far /243
from worked out. Not only the processes taking place, but their
connection with external parameters, have been studied insuffi-
ciently.

Such a position frequently eliminates the possibility of the
optimum structure of a system and, in a number of cases, leads to
unjustified complication of it.

The absence of general methods of investigation of magnetic
recording systems hampers the search for ways of further development.

Magnetic recording apparatus with wire carriers are the most
stable, under conditions of climatic and mechanical influences.
They are practically stable towards climatic influences; however,
under mechanical influences, a whole series of factors, which are
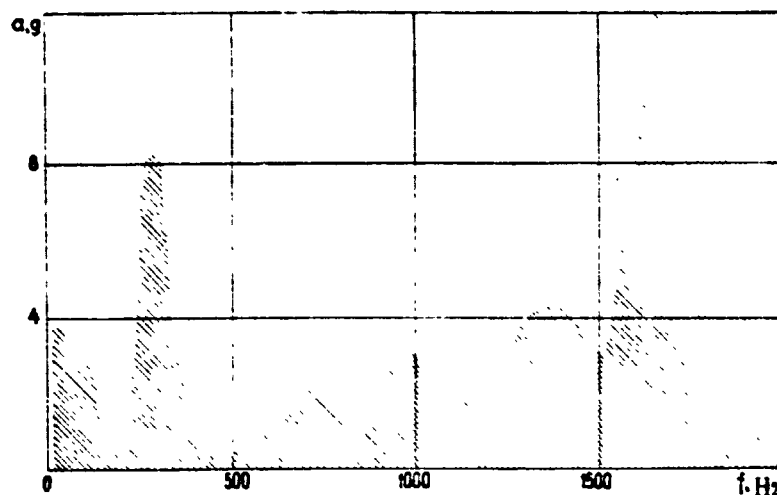uncharacteristic of normal operating conditions, appears.

Fig. 1. Amplitude modulation of signal reproduced with MPM [moving permanent magnet] vs. external vibration disturbance parameters; AM [amplitude modulation] exceeds 25% in the zone which is not cror -hatched.

Amplitude modulation of a signal reproduced with MPM vs. frequency and magnitude of acceleration of the active external disturbance is shown in Fig. 1. The mechanism remains comparatively efficient within a small range of change in vibration disturbance parameters.

The processes taking place in the mechanism and their connection with the vibration disturbance parameters must be determined for further development of the mechanism. It is interesting that /244 high-frequency disturbances (over 1.6 kHz) do not show a perceptible effect on the efficiency of the mechanism, even at considerable accelerations.

The resonance curves of the case and cover of the cassette mechanism are depicted in Fig. 2. A very sharply expressed resonance sets in at a frequency of 200 Hz. By comparison of this /245 curve with the amplitude modulation curve, it is clear that the mechanism has practically no vibration resistance at this frequency, even at low accelerations.

Self-starting and stable movement zones of a MPM distributing mechanism are presented in Fig. 3. It is easy to ascertain that these zones are identical, with a small frequency displacement, by more attentive analysis of the amplitude modulation and distributing mechanism movement zone curves. The cause of frequency displacement is the effect of removing the load from the distributing mechanism. The distributing mechanism is a dynamically complex assembly, with many degrees of freedom. Its resonance vibrations are one of the basic causes of amplitude modulation of the reprod·red signals.
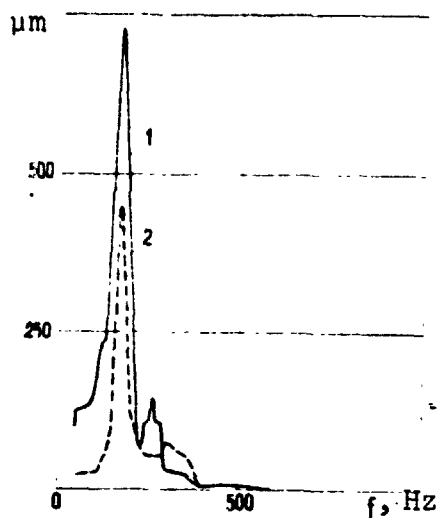
Fig. 2. Vibration amplitudes
of case (1) and cover (2) of
MPM cassette mechanism vs.
frequency of external vibra-
tion disturbance with an
acceleration a = 12 g.

Of course, what has been said
does not encompass all sources of
disturbance of uniform movement of
the wire carrier. Its disturbing
effect shows up to various degrees
in other assemblies and parts.
Spontaneous rotation of guide
rollers and other parts sets in
over wide frequency bands and
acceleration values. For example,
an oscillogram of the vibration
rate of the wire record carrier,
with an external mechanical shock
to the mechanism, is presented in
Fig. 4. Determination of the
dynamic characteristics of indi-
vidual assemblies and mechanisms
facilitates improvement and optimiza-
tion of the magnetic recording
apparatus as a whole.
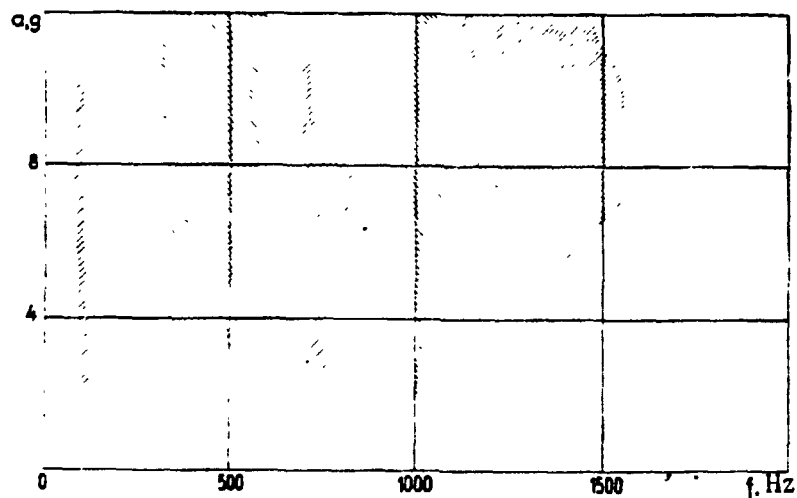

Fig. 3. Self-starting and stable movement zones of MPM
distributing mechanism vs. external vibration disturbance
parameters; change in direction of the cross-hatching
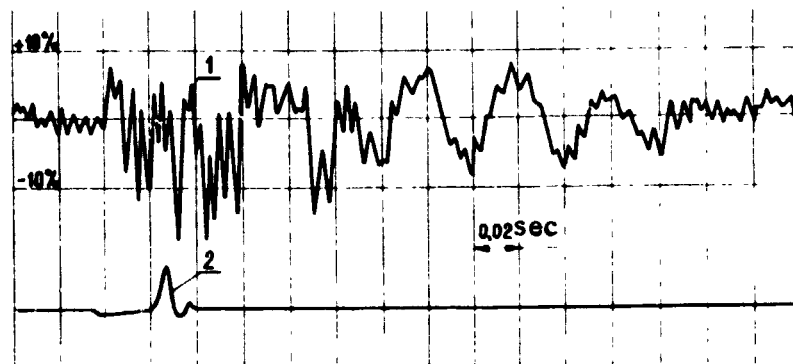corresponds to the direction of movement of the distributor.

273

Fig. 4. Oscillogram of vibration rate of wire record
carrier (1), with a single mechanical shock (2) on the
MPM, with acceleration a = 6 g; time mark 0.02 sec.

SPECTRAL COMPOSITION OF A MEASURING SIGNAL   /246
DURING MEASUREMENTS OF VIBRATION RATES OF A MOVING BODY

I.-A.I. Daynauskas and N.N. Slepov
(Kaunas-Moscow)

Since the spectral approach to a process being investigated
is one of the methods of cybernetic diagnostics of machines and
mechanisms in engineering, the problem arises of establishing the
accuracy of determination of its spectral composition. In systems
with rectilinear or rotary movement, the vibrations appear in the
form of movement rate vibrations, which are equivalent to frequency
modulation of the signal, in proportion to the mean movement rate
of the body.

Let us examine the case, in which a harmonic signal, which
reproduces and analyzes the characteristics of the frequency modu-
lated (FM) signal obtained, is recorded on a moving body (the case
of use of a magnetic carrier). The FM signal is converted to a
frequency-pulse modulated one (FPM), at phase Θ values, which are
multiples of 2 kΠ, i.e., the pulses are formed over the repetition
period of the FM signal. Let us consider that the carrier speed
vibrations (CSV) change harmonically. After standardization over
the length and amplitude of the pulse, we obtain a formula for the
FPM-1 spectrum (first kind) of the series from formula (4) in
work [1], in the form

$$F(t) = \sum_{m,n,q=-\infty}^{\infty} \frac{g(\omega_{mnq})\,\omega_{mnq}}{2\pi m} \cdot I_n(m\omega_0 t_d) \cdot I_q(\omega_{mn} t_{qc}) \times$$

$$\times \exp[j(\omega_{mnq} t + \Theta_{mnq})].$$

(1)

Here, ω_0 and t_0 are the FPM-1 series frequency and initial
phase; ω_{dr}, ψ_r and ω_{dp}, ψ_p are the frequency and initial phase of
the carrier speed vibration (CSV) during recording and reproduction
of the mark, respectively; d_r and d_p are the CSV coefficients
during recording and reproduction, respectively:

$$t_{dr} = \frac{d_r}{\omega_{dr}}; \quad t_{dp} = \frac{d_p}{\omega_{dp}}$$

is the equivalent CSV amplitude during recording and reproduction, /247
respectively; $g(\omega_{mnq})$ is the multiple spectral density of the FPM
pulse; I_n and I_q are Bessel functions of the first kind of the
integral index;

$$\omega_{mnq} = m\omega_0 + n\omega_{dr} + q\omega_{dp}$$

$$\Theta_{mnq} = n\tau_r + q\tau_p + (2n-1)\frac{\pi}{2} + \omega_m d_r \sin \tau_r -$$

$$- (m\omega_0 + n\omega_{dr} + q\omega_{dp}) t_{dp} \sin \tau_p$$

$$\omega_{mn} = m\omega_0 + n\omega_{dr}$$

Solving spectrum (1) and reducing it to the actual form, we obtain

$$F(t) = \frac{\tau_0}{T_0} + \frac{\tau_0 d_r \sin(\omega_{dr}\tau_0/2)}{T_0 \, \omega_{dr}\tau_0/2} \cdot I_0(\omega_{dr} t_{dp}) \cos(\omega_{dr} t - \Theta_n) +$$

$$+ \frac{\tau_0 d_p \sin(\omega_{dp}\tau_0/2)}{T_0 \, \omega_{dp}\tau_0/2} \cdot \cos(\omega_{dp} t + \Theta_q) +$$

$$+ \sum_{m,\,n=-\infty}^{\infty} \frac{g(\omega_{mn})}{\pi m} \frac{\omega_{mn}}{} \cdot I_n(m\omega_0 t_{dr}) \cdot I_0(\omega_{mn} t_{dp}) \times$$

$$\times \cos(\omega_{mn} t + \Theta_{mn}) + \sum_{\substack{m,\,q=-\infty \\ m,\,q\neq 0}}^{\infty} \frac{g(\omega_{mq})}{\pi m} \frac{\omega_{mq}}{} \times$$

$$\times I_0(m\omega_0 t_{dr}) \cdot I_q(m\omega_0 t_{dp}) \cos(\omega_{mq} t + \Theta_{nq}) +$$

$$+ \sum_{m=-\infty}^{\infty} \frac{g(m\omega_0)}{\pi} \frac{\omega_0}{} I_0(m\omega_0 t_{dr}) I_0(m\omega_0 t_{dp}) \cos(m\omega_0 t + \Theta_m) +$$

$$+ \sum_{q=-\infty}^{\infty} \frac{\tau_0 \omega_{1q} d_r \sin(\omega_{1q}\tau_0/2)}{T_0 \, \omega d_r \omega_{1q}\tau_0/2} \cdot I_q(\omega_{dr} t_{dp}) \cdot \cos(\omega_{1q} t + \Theta_{nq}) +$$

$$+ \sum_{\substack{m,\,n,\,q=-\infty \\ m,\,n,\,q\neq 0}}^{\infty} \frac{g(\omega_{mnq})}{\pi m} \frac{\omega_{mnq}}{} I_n(m\omega_0 t_{dr}) I_q(\omega_{mn} t_{dp}) \cos(\omega_{mnq} t + \Theta_{mnq}).$$

Here, $\omega_{1q} = \omega_{dr} + q\omega_{dp}$ and τ_0 is the duration of a normalized FPM pulse.

We introduce the designations

$$\varepsilon = \frac{\Delta\omega_0}{\omega_0}\,; \qquad \mu = \frac{\omega_0}{\omega_d}\,.$$

276

Here, ε is the relative frequency of the deviation, μ is the pulse series repetition coefficient, ω_d is the frequency modulating function, in our case the CSV frequency, and $\Delta\omega_0$ is the angular frequency of the deviation.

Let us consider that, in recording and reproducing the mark, the vibrations act with uniform frequencies and that the equivalent CSV amplitudes are equal during recording and reproduction. During demodulation of the FPM-1 series, we use a low frequency filter (LFF) and we restrict ourselves to examination of the frequency spectrum band $0-\omega_0$, proceeding from which, we assume m = 1. We designate $\alpha = \tau_0/T_0$. We express the . dule of the multiple pulse spectral density as

$$g(\omega) = \frac{2}{\omega}\sin\frac{\omega_0\tau_0}{2} = \tau_0\ \frac{\sin\frac{\omega\tau_0}{2}}{\frac{\omega\tau_0}{2}}.$$

Finally, after transformations, we obtain

$$F'(t) = \alpha + x\varepsilon\ \frac{\sin\frac{\pi x}{\mu}}{\frac{\pi x}{\mu}}\cdot I_0(\varepsilon)\cdot\cos(\omega_{dr}t+\Theta_n)+$$

$$+x\varepsilon\ \frac{\sin\frac{\pi x}{\mu}}{\frac{\pi x}{\mu}}\ \cos(\omega_{dp}t+\Theta_q)+$$

$$+\sum_{\substack{n=-1\\n\neq 0}}^{x}2x\left(1+\frac{n}{\mu}\right)\ \frac{\sin\pi x\left(1+\frac{n}{\mu}\right)}{\pi x\left(1-\frac{n}{\mu}\right)}\cdot I\ (\mu\varepsilon)\cdot I_0[\varepsilon(\mu+n)]\times$$

$$\times\cos[(\omega_0+n\omega_{dr})t+\Theta_{mn}]-\sum_{\substack{q=-x\\q\neq 0}}^{-x}\frac{2x}{\mu}(\mu+q)\ \frac{\sin\pi x\left(1+\frac{q}{\mu}\right)}{\pi x\left(1+\frac{q}{\mu}\right)}\times$$

$$\times I_0(\mu\varepsilon)\cdot I_q(\mu\varepsilon)\cdot\cos[(\omega_0-q\omega_{dp})t+\Theta_{mq}]+$$

$$+2x\ \frac{\sin\pi x}{\pi x}\cdot I_0(\mu\varepsilon)\cdot\cos(\omega_0 t+\Theta_m)+$$

$$+\sum_{\substack{q=-x\\q\neq 0}}^{x}x\varepsilon(q+1)\ \frac{\sin\frac{\pi x}{\mu}(1+q)}{\frac{\pi x}{\mu}(1+q)}\cdot I_q(\varepsilon)\cos[(\omega_{dr}+q\omega_{dp})t+\Theta_{n}]+$$

(3)

277

$$+ \sum_{\substack{n,\, q = -\ell \\ n,\, q \neq 0}}^{\ell} 2\varkappa \left(1 + \frac{n}{\mu} + \frac{q}{\mu} \right) \cdot \frac{\sin \pi \varkappa \left(1 + \frac{m}{\mu} + \frac{q}{\mu} \right)}{\pi \varkappa \left(1 + \frac{m}{\mu} + \frac{q}{\mu} \right)} \cdot I_n(\mu \varepsilon) \varkappa$$

$$\times I_q [\varepsilon (\mu + n)] \cos [(\omega_0 + n\omega_{dr} + q\omega_{dp}) t - \Theta_{mn}].$$

The structure of the spectrum obtained in the general case is represented in Fig. 1. Spectral components of the type $\omega_{dr} \pm q\omega_{dp}$, the amplitudes of which drop quickly with increase in q, are present in the spectrum, independently of the LFF transparency band selected. It is interesting to note that the amplitude components ω_{dr} and ω_{dp}, at identical CSV frequencies, appear with differences, defined by the Bessel functions $I_0(\varepsilon)$, which is a value of less than 10%, at values of ε up to 50%, in which the amplitude with ω_{dr} is less. Owing to the appearance of specular reflection at negative q,

Figure. Spectrum structure:
1 ω_{dr}, ω_{dp}; 1' $\omega_{dr} - q\omega_{dp}$;
1" $\omega_{dr} + q\omega_{dp}$; 2 ω_0; 2' $\omega_0 - n\omega_{dr}$;
2" $\omega_0 - n\omega_{dr} - q\omega_{dp}$; 2''' $\omega_0 + n\omega_{dr} + q\omega_{dp}$.

additional errors arise at identical ω_{dr} and ω_{dp}, at the frequencies $\omega_{dr} = \omega_{dp}$, because of the effect of the combined components $\omega_{dr} - q\omega_{dp}$.

REFERENCES

1. Slepov, N.N., "Interference Resistance of Magnetic FPM and FM Recording Systems," Pomekhi v tsifrovoy tekhnike-71 [Interferences in Digital Technology - 1971], Vil'nyus, 1971, pp. 129-133.

MEASUREMENT OF IRREGULARITIES IN ANGULAR VELOCITIES OF ROTATING ASSEMBLIES IN MEMORY DEVICES ON MAGNETIC CARRIERS

/250

G.I. Virakas, R.A. Matsyulevichyus, K.P. Minkevichyus,
Z.I. Potsyus, and B.D. Shirvinskas
(Kaunas)

Problems in measurement of irregularities in angular velocity of rotating assemblies in memory devices, with rigid and flexible magnetic data carriers, are discussed in the work.

In the Central Workshop, Scientific Research Laboratory of Vibration Engineering, Kaunas Polytechnic Institute, a device and method, allowing determination of change in angular velocities in the 0.01-1.0% range, at rotation rates of 0.5-3000 rpm, has been developed. The frequency range of the process being investigated is 0-300 Hz. The error in measurement is not more than ±5%.

Transformation of the parameter measured into an electrical signal is accomplished with the aid of a no-contact photoelectric sensor. A time-pulse modulated signal (TPM) from the sensor is converted into a frequency-pulse modulated (FPM) signal in the measuring device, with subsequent detection by means of a low-frequency filter.

A schematic diagram of a photoelectric sensor, the instantaneous signal pulse frequency of which is proportional to the instantaneous rotation rate, is shown in Fig. 1. The foundation of the sensor is two identical glass scanning disks 2 and 3. Disk 3, together with housing 4 of /251 the sensor, is fastened securely, and disk 2 is rigidly set onto shaft 1 and is rotated by the object measured. Black radial lines, the width of which equals the distance between them, are applied to the disks. The lines are applied to the insides of the disks, i.e., the disks are facing one another, and
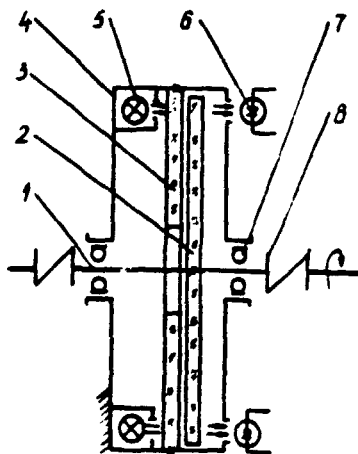

Fig. 1. Schematic diagram of photoelectric sensor: 1. shaft; 2, 3. scanning disks; 4. sensor housing; 5. light flux source; 6. photocell; 7. bearing; 8. flexible compensating coupling.

279

the distance between the disks is not more than 0.015 mm. When
the lines of both disks coincide, light from lamp 5 enters photo-
cell 6. During rotation of shaft 1, photocell 6 gives a periodic
signal, with a frequency proportional to the instantaneous angular
velocity, multiplied by the number of divisions (N = 7200). A
large number of divisions increases the sensitivity and accuracy
of measurement, and it expands the measurable frequency range, as
well. Special flexible compensating coupler 8 eliminates errors
in connection, when connected with the shaft of the measured object,
and it also eliminates errors in measurement, arising due to small
vibrations of the axis of the measuring object. The error of the
angular position signal can be reduced to 1 sec, owing to the high
accuracy of the disk divisions, accurate alignment of the disks,
and the integral method of obtaining the sensor signal.

It was revealed, by analysis of the results of the experiments
carried out, that misalignment of the raster poles, both between
themselves and with the center of rotation of the moving raster,
has a significant effect on the increase in accuracy of measure-
ment. Therefore, the effect of eccentricity in the raster dia-
phragm coupling on the transmission function was investigated.
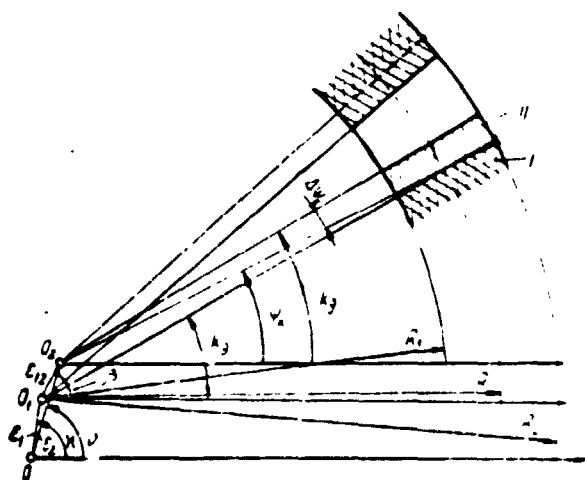
Fig. 2. Mutual location of raster
cells with eccentricity in both
rasters: I. fixed raster; II moving
raster.

The most characteristic /252
general case, when the poles
of both rasters O_1 and O_2 are
located eccentrically with
respect to the center of rota-
tion 0, in the amounts ε_1 and
ε_2, respectively, with 0 taken
as the center of the polar
coordinate system, is shown
in Fig. 2. We designate the
angles formed by the eccen-
tricities to the polar axis
by κ and ν. Angle ν is
variable and depends on the
angular displacement ψ of
the moving raster, i.e.,
$\nu = \nu_0 + \psi$, where ν_0 is the
initial angle (angle ν at
moment of time t = 0).

For the k-th cell, the
deflection of the phase angle
$\Delta\psi_k$ equals

$$\Delta\psi_k = \frac{\varepsilon_{12}}{R}\sin(\beta - kg),$$

(1)

280

where ε_{12} is the distance between poles O_1 and O_2, determined from the vector equation $\vec{\varepsilon}_{12} = \vec{\varepsilon}_2 - \vec{\varepsilon}_1$, R is the mean radius of the raster band and g is the angular spacing of the lines.

The quantity β is determined from the condition

$$\frac{\varepsilon_1}{\sin(\psi + \nu - \beta)} = \frac{\varepsilon_2}{\sin(\varkappa - \beta)}, \tag{2}$$

assuming $\varkappa = 0$ and $\nu = 0$ in the initial position,

$$\beta = \operatorname{arccot}(\cot\psi). \tag{3}$$

Substituting expression (3) in Eq. (1), we obtain

$$\Delta\gamma_k = \frac{\varepsilon_1}{R}\sin kg + \frac{\varepsilon_2}{R}\sin(\psi - kg). \tag{4}$$

The transmission function Π of the raster coupling is determined by the ratio of the light flux F passing through the coupling to the light flux F_0 incident on the coupling,

$$\Pi = \frac{F}{F_0}. \tag{5}$$

For the k-th cell, the transmission function Π_k, taking Eq. (4) into account, is expressed by the relationship

$$\Pi_k = \frac{1}{2} + \frac{4}{\pi}\sum_{m=0}^{\infty}\frac{1}{(2m+1)^2}\cos\Big\{(2m+1)N\Big[\psi +$$
$$- \frac{\varepsilon_1}{R}\sin kg + \frac{\varepsilon_2}{R}\sin(\psi - kg)\Big]\Big\}. \tag{6}$$

The instantaneous angular vibration frequency of the first harmonic of series (6) is determined from the expression

$$\Omega_{\varepsilon_{12}} = N\Big[\omega + \frac{\varepsilon_2\omega}{R}\cos(\psi - kg)\Big]. \tag{7}$$

281

The error in determination of the instantaneous rotation
rate of the moving raster can be represented by the function

$$\gamma = \frac{\iota_3}{R} \cos(\dot{\gamma} - kg).$$ (8)

A quantitative estimate of the effect of the magnitude of the
eccentricity in the raster diaphragm coupling on measurement of
irregularities in rotation rate can be determined from the relation-
ships obtained.

INVESTIGATION OF FLUCTUATIONS IN ANGULAR VELOCITY IN MAGNETIC MEMORY DEVICES

Yu.A. Meshkis and Z.Yu. Potsyus
(Kaunas)

An analytic study of fluctuations in the angular velocity of individual assemblies of a precision mechanical system, consisting of a: electric motor and a magnetic drum (MD), connected to it by a flexible coupling, was carried out.

A dynamic model was compiled, taking account of the absence of torsion in the absolutely rigid shafts of the electric motor drive rotor and the MD. The motion was described by Lagrange differential equations of the second kind

where

$$I_1\ddot{\beta}_1 + R_1(\dot{\beta}_1,\ \beta_1) + R_{12}(\dot{\beta}_1 - \dot{\beta}_2,\ \beta_1 - \beta_2) = M_1,$$

$$I_2\ddot{\beta}_2 - R_{12}(\dot{\beta}_1 - \dot{\beta}_2,\ \beta_1 - \beta_2) = M_2,$$

$$R_1 = h_1\dot{\beta}_1 + c_1\beta_1,$$

$$R_{12} = h_{12}(\dot{\beta}_1 - \dot{\beta}_2) + c_{12}(\beta_1 - \beta_2).$$

I_1 and I_2 are the summary moments of inertia of the rotating parts of the drive and MD, respectively, β_1 and β_2 are the instantaneous small deviations of the generalized coordinate from the angular position during uniform rotation, h_1 and h_{12} are the damping coefficients, c_1 and c_{12} are the rigidity coefficients, M_1 is the total driving force moment and the force of resistance on the motor shaft, and M_2 is the generalized moment of the external nonpotential forces.

For a steady mode of movement, with $M_1 = A\sin\omega t$ and $M_2 = 0$, where A is the variable component of the external moments and ω is the angular frequency of the forced vibrations, analytical expressions for the amplitude and phase shift angle of the forced /254 vibrations of the electric motor rotor and MD, respectively, were obtained:

$$\lambda_1 = A^* \tau_2^{\frac{1}{2}} \tau_4^{-\frac{1}{2}},$$

$$\lambda_2 = A^* [1 + (2\tau_{12}\tau)^2]^{\frac{1}{2}} \tau_4^{-\frac{1}{2}},$$

$$\alpha_1 = \arctan \frac{2[(1-r^2)\tau_{12}r^2 - q_{12}\tau_2 r^2 - \tau_3\tau_1]r}{(q_1^2-r^2)\tau_2 - \tau_3 r},$$

$$\alpha_2 = \arctan \frac{2[\tau_{12}r^2 - (q_1^2-r^2)\tau_2 r^2 - q_{12}\tau_2 r - \tau_3\tau_1]}{(q_1^2-r^2)\tau_3 - \tau_3 r^2 - (q_{12}^2 + 4\tau_1\tau_1)r^2}$$

283

Fig. 1. Nature of amplitude of
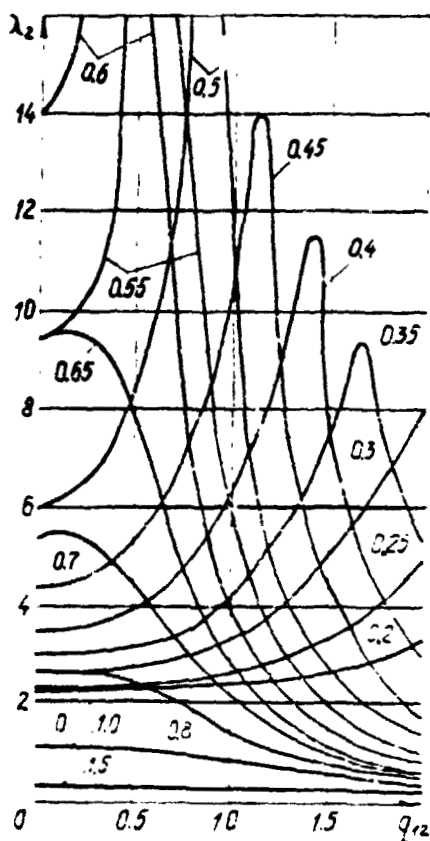fluctuation of MD angular
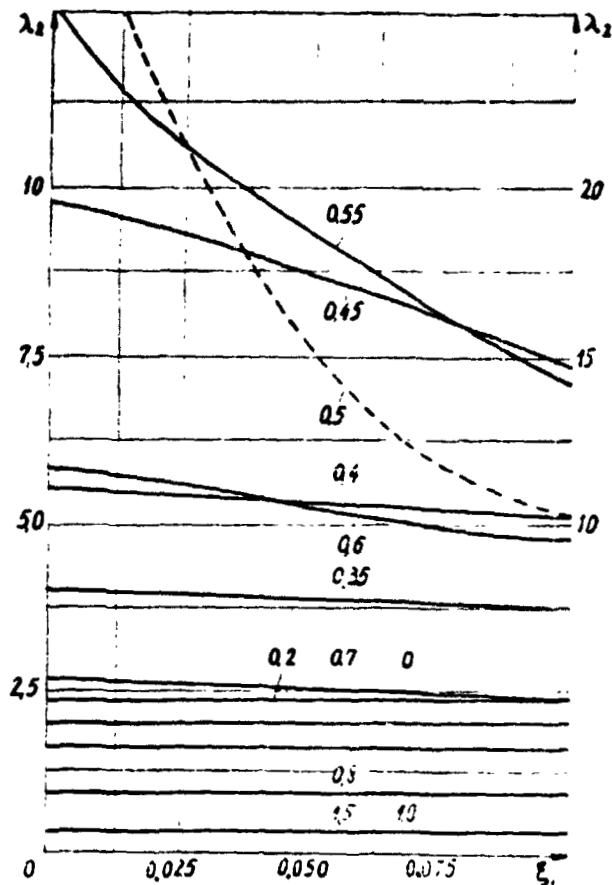velocity at a specific excita-
tion frequency r.

Fig. 2. Amplitudes of fluctua-
tion of MD angular velocity vs.
quantity of damping ξ_1 at
specific frequencies r.

The effect of individual parameters on the dynamics of the
entire system was determined with the aid of a digital computer.
Certain exemplary relationships are shown in the figures presented.

INVESTIGATION OF VIBRATION CHARACTERISTICS OF ELECTRIC MOTORS

A.K. Bakshis and Yu.K. Tamoshyunas
(Kaunas)

An electric motor propagates a complex spectrm of periodic, semiperiodic and random vibrations. Their causes and a decrease in the vibration level of both the entire spectrum and individual components of it, which is especially urgent for electric motors with increased vibroacoustical requirements, are being seriously investigated at the present time.

Investigations of the vibration characteristics of electric motors, using mathematical statistics methods, were carried out in this work.

A system for measurement of electric motor vibrations is shown in Fig. 1. To eliminate the effects of extraneous vibrations and to reduce the natural frequencies, a $P = 82$ electric motor ($\Pi = 1500$ rpm) was suspended on cable 7. Vibrations of the housing were measured by means of piezoelectric sensors 8 at two points: on lug I and lug II; vibration of the shaft relative to the housing, at one point, at the end of the shaft, by means of capacitance sensor 4. The electrical signal from the piezosensor went to SDM apparatus 1, and then to DISA apparatus 2, for recording on photofilm. The signal from the capacitance sensor went directly to the DISA apparatus. In parallel with the vibration signals, a pulse signal from photoelectric sensor 5, giving a "time mark," went to the recorder.

Calibration of the housing vibration measurement sensors was carried out with the SDM apparatus needle indicator. The following operation was carried out for calibration of the capacitance sensor: the sensor was installed in the operating position and a known static flexural deformation was set up in the electric motor shaft. The signal obtained from a given displacement was recorded on photofilm and subsequently served as a measurement scale of the true values of the shaft vibration. A visualization of the vibrations of the electric motor in the vertical direction is shown in Fig. 2.

Processing of the visualizations obtained was carried out by statistical methods, considering them as functions of a steady random process having ergodic properties. Determination of the statistical characteristics was carried out by one execution. The initial data for the digital computer was presented in the form of a table of values of the random process X_1, taken over equal intervals of time Δt, selected in such a manner that the process did not change within a single interval.
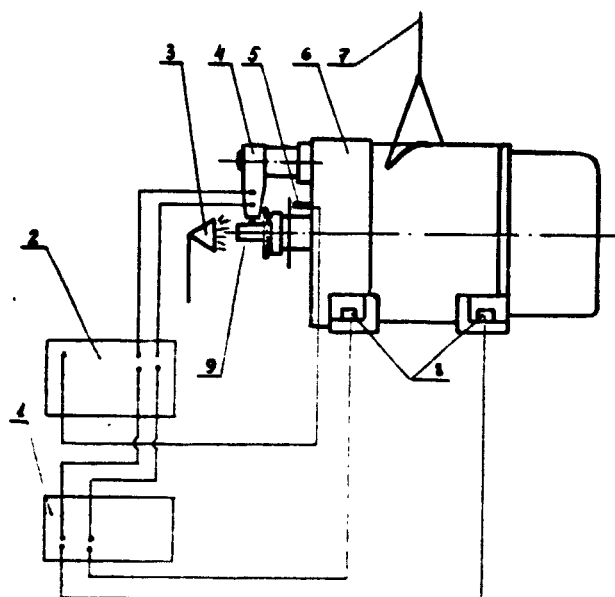
Fig. 1. Electric motor vibration measurement system.

Statistical evaluation of the random process was established by the following formulas:

-- evaluation by correlation function

$$K_x(\tau) = \frac{1}{N-\tau} \sum_{1}^{N-\tau} \overset{\circ}{x}_i \overset{\circ}{x}_i + \tau \qquad (1)$$

where N is the number of values of the random process; $\tau = 0, 1, 2, 3, \ldots, M$; $M \simeq N/10$ is the number of correlation function values; $\overset{\circ}{x}_1 = x_1 - m_x$ is the centered execution of the process;
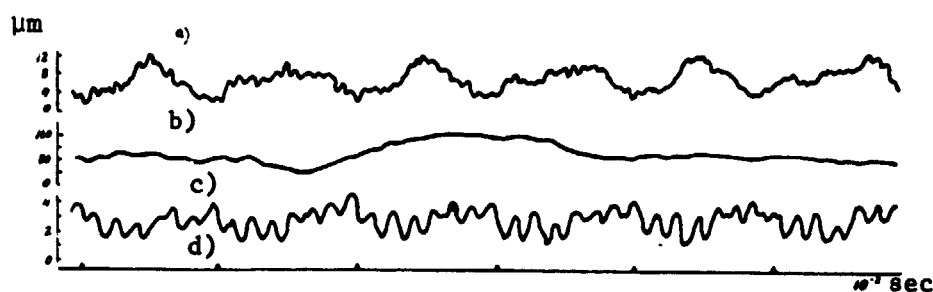
Fig. 2. Visualization of electric motor vibrations in the vertical direction: a) rotor vibration with respect to the housing; b) housing vibrations at the first lug; c) housing vibration at the second lug; d) electric motor shaft revolution signal.

m_x is the estimate of mathematical expectation; and the estimate /258 of the mutual correlation function

$$K_{xy}(\tau) = \frac{1}{N-\tau} \sum_{1}^{N-\tau} \overset{\circ}{x}_i \overset{\circ}{y}_i + \tau \qquad (2)$$

286

-- estimate by the spectral density

$$S_x(\omega) = \frac{k_\tau(0)}{2\pi} + \frac{1}{\pi} \sum_1^M \left(1 - \frac{\tau}{N}\right) \times$$

$$\times k_\tau(\tau) \left\{0.54 + 0.46 \cos \frac{\tau\tau}{M}\right\} \cos \omega\tau \qquad (3)$$

-- estimate by the mutual spectral density

$$S_{xy}(\omega) = \frac{1}{2\pi} \sum_{-M}^M \left(1 - \frac{\tau}{N}\right) k_{xy}(\tau) \left\{0.54 + 0.46 \cos \frac{\pi\tau}{M}\right\} e^{i\omega\tau} \qquad (4)$$

Knowing the basic statistical characteristics of the process of vibration of the rotor relative to the housing and of the housing itself, we can proceed to determination of the dynamic characteristics of the rotor-housing system.

Fig. 3. Amplitude-phase frequency characteristic of dynamic rotor-housing system at the first lug, in the vertical direction

An object with one input and two outputs was analyzed in finding the dynamic characteristics of this sytem. The vibrations of the rotating rotor relative to the housing x(t) were taken as the input of the object and the vibration of the housing itself

on one lug or the other $y_1(t)$ or $y_2(t)$ was taken as the output.

The transmission function of the dynamic rotor-housing system was determined from formula (5)

$$\Phi(j\omega) = \frac{S_{xy}(\omega)}{S_x(\omega)}.$$

(5)

All calculations were carried out with the aid of a Razdan type digital computer.

The amplitude-phase frequency characteristics of the dynamic rotor-housing system are presented in Figs. 3 and 4.

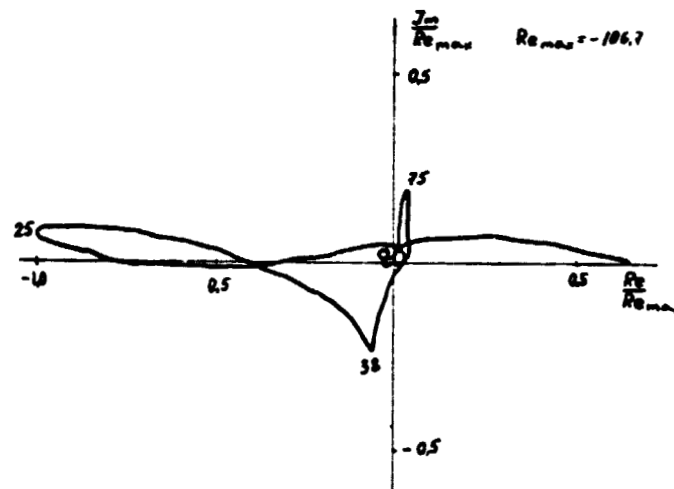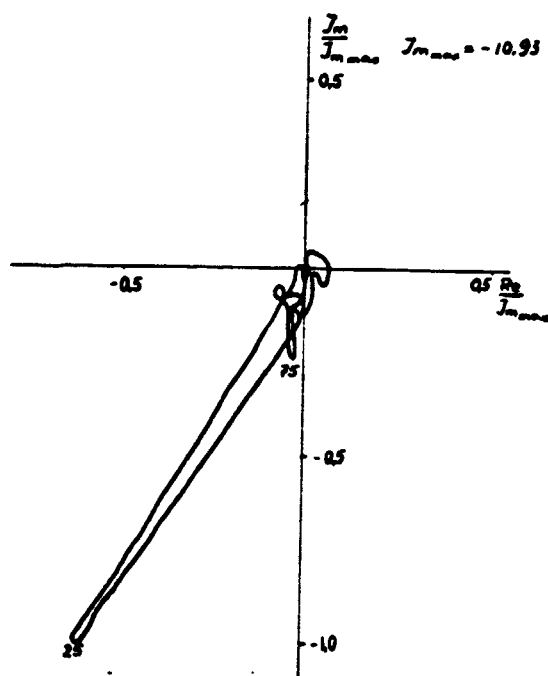Fig. 4. Amplitude-phase frequency characteristics of dynamic rotor-housing system at the second lug, in the vertical direction.

EXPERIMENTAL RESEARCH ON AEROSTATIC SUSPENSIONS

L.A. Bushma
(Kaunas)

Three types of suspension for carrying out experimental investigations, for the purpose of studying a number of problems in dynamics and stability of a suspended cylindrical body at various dynamic loads were investigated in the work.

The results of the experimental investigations served as a basis for building a stand with a variable resonator.

The experimental stand for suspension of a cylindrical object, with a comparatively high natural free vibration frequency in the vertical direction, coinciding with the axis of the suspended object, is distinguished by the possibility of regulating the size of the clearance and is intended for carrying out preliminary experimental studies, for the purpose of selection of optimum aerostatic suspension parameters.

The experimental studies showed that the first suspension has a comparatively high free oscillation frequency in the vertical plane (more than 20 Hz).

For reduction in the natural free vibration frequency of the object in an aerostatic layer, an improved suspension was developed, which is distinguished from the preceding one by diametric cavities, the volume of which can be regulated by a horizontally connected piston pair. The design changes introduced permitted the natural frequency of the suspension (12-15 Hz) to be reduced; however, at a specific mass of the object and thickness of the grease layer, autovibrations take place, the generation of which, in the first approximation, can be explained by the elasticity of the air and the turbulent flows in the working space.

A Helmholtz acoustical resonator usually is used for damping vibrations in aerostatic supports. In this case, this resonator has one basic defect, the damping can be carried out only in a narrow frequency range. With change in vibration frequency of the suspended object, the size of the resonator must be changed, which is impossible to accomplish with the resonator described above. Therefore, an aerostatic suspension with a variable volume resonator was developed.

The autovibration parameters (frequency, amplitude) of the
object are changed by a change in operating conditions (thickness of the grease layer, pressure, air flow rate). The volume of the resonator is changed and the autovibration damping range is extended by means of a piston pair. Experimental studies carried out showed that the presence of a variable volume resonator

ensures the lowest natural frequency (5-10 Hz) of free vertical vibrations of the suspended object.

The fundamental relationships between the individual parameters were introduced for calculation and design. A method of experimental investigation was introduced, and the apparatus and features of measurement of the individual parameters were described. The pattern of movement of the vibrating mass of the suspended object was determined with precision piezosensors, with subsequent double integration in the meter. Studies of the spectral components of the vibrations were carried out with the aid of spectrum analyzer.

The results of the experimental studies were presented. The static-rigidity characteristics of the aerostatic suspensions were investigated. Relationships of the lift of the object, radial displacement and angular rigidity to load, at various pressures, were obtained, and zones of unstable operation were revealed. The relationship of maximum rigidity to blowing pressure was determined.

Measurement of the free vibrations was accomplished by the impact loading method, in both the vertical and horizontal directions. The logarithmic decrement of attenuation of the vibrations, damping, as well as the effect of individual parameters on the operation of the system, were determined.

The relationship of the free oscillation frequencies and damping to blowing pressure was presented.

The suspension with a variable resonator has a very low natural frequency, which favorably affects the operation of the device installed on the object. An object on a suspension with a variable resonator has the greatest damping. An increase in input pressure leads to a decrease in damping. The dimensionless damping coefficient is small, on the order of several hundred. This demonstrates the presence of weak damping in aerostatic suspensions.

Dynamic loading of the experimental suspensions was carried out with the aid of a centrifugal vibrator. The vibration frequency was measured in the 5-150 Hz range. The relationship between swing of the suspended object and blowing pressure was determined at various loads.

The relationship of the spread of forced vibrations of the /262 suspended objects to the load was determined at various blowing pressures. An increase in load leads to a decrease in thickness of the grease layer. The rigidity is increased at lesser thicknesses, which entails a decrease in the spread of the forced vibrations.

The suspensions developed operate without autovibration at free vertical vibration frequencies of 5-35 Hz. They ensure suspension of the object, permitting free displacement of the suspended object relative to the air support and make it possible to rotate it without resistance.

SYNTHESIS OF A CORRECTING FILTER WITH PHASE STABILIZATION OF THE ANGULAR VELOCITY OF A SYNCHRONOUS MOTOR BY THE FEEDBACK SYSTEM METHOD

K.A. Kazlauskas and A.I. Kurlavichus
(Kaunas)

Synchronous motors are widely used to obtain stable rotation rates. The instantaneous speed of the engine is changed by the action of torque disturbances. A system of phase stabilization of the instantaneous angular velocity of rotation of a synchronous-reaction motor is shown in Fig. 1, where PM is a phase modulator, SM is a synchronous motor, S is a rotor angular position sensor, PD is a phase detector, F is a correcting filter, θ is the phase of the input electrical signal and M is the torque disturbance.
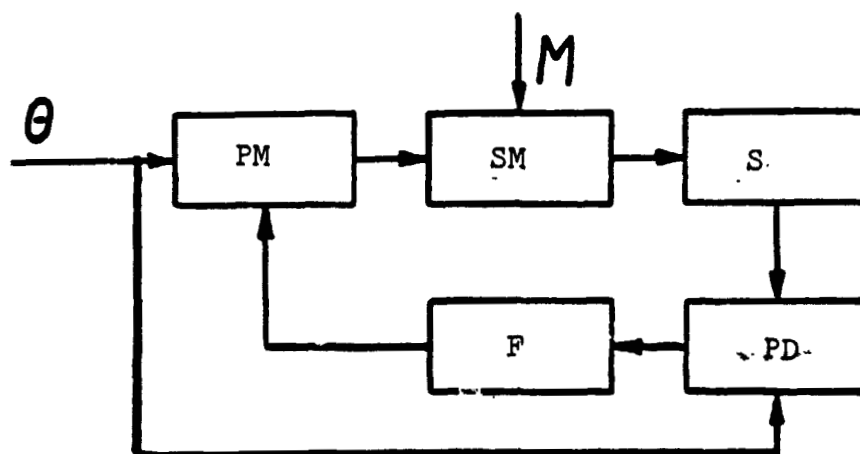
Fig. 1.

With small deviations of the input and output signals from their established values, the differential equation of a synchronous-reaction motor can be presented, for variable values, in the form

$$2\xi\omega_0 \frac{d\varphi}{dt} + \omega_0^2\varphi = \frac{d^2a}{dt^2} + 2\xi\omega_0 \frac{da}{dt} - \omega_0^2 a + \frac{M}{I} . \tag{1}$$

where ξ is the electric motor damping coefficient, ω_0 is the electric motor resonance frequency, I is the moment of inertia, calculated

292

on the motor shaft, ϕ is the change in phase of the electric motor supply voltage and a is the change in angular position of the rotor.

It has been shown that feedback system theory can be ⁓ ⁓ ⁓ calculation of the correcting filter. Thus, since there ⁓primar⁓ ⁓ is interest in the reaction of the system to interference, it was /263 assumed that $\Theta_{(p)} = 0$. Taking Eq. (1) into consideration, a structural diagram of the system is presented in the form of Fig. 2, where

$$W_1(p) = \frac{1}{I(p^2 + 2\xi\omega_0 p + \omega_0^2)} \ , \qquad W_2(p) = \frac{2\xi\omega_0 p + \omega_0^2}{p^2 + 2\xi\omega_0 p - \omega_0^2} \ .$$

$W(p)$ is the transmission function sought for the correcting filter, in operator form, and $\eta(p)$ is the interference introduced by the angular position sensor.
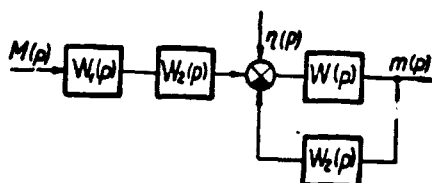

Fig. 2.

It is assumed in the first approximation that disturbances M and η are random functions of the "white noise" type. For a system which can be physically realized, the transmission function $W(p)$ is found from the conditions of minimum difference in the signals M and m, in root mean form.

STUDIES OF IRREGULARITIES IN MOTION
OF VIBROSHOCK TYPE MECHANISMS

S.Yu. Mateyshka
(Kaunas)

Reciprocating motion mechanisms, in which a mass with large gaps can be driven with almost uniform speed, are investigated. A single-mass system with dry friction, the motion of which is restricted by two stops, is examined. The system is put into motion by kinematic disturbances through a flexible link.

Periodic modes of movement, under conditions in which the disturbance arises from two impacts on the mass (from the right and left stops) are examined. Primary attention was given to irregularities in the course of the mass. The shock interaction of the mass with the stop was accounted for by the shock speed restoration coefficient R.

The shock-frequency characteristics of the free shock vibrations were determined. Expressions were obtained which define the transitional process. The phase and velocity of several succeeding shocks were determined. After taking account of the conditions of the steady mode of movement, velocities and phases in the steady mode of movement were obtained. Conditions for the existence of the steady shock modes of movement were presented, and their stability was investigated as well. For this, line   d equations were compiled, in variations ın the vicinities of t existing modes of motion, from which characteristic equations ʍₑᵣₑ obtained, the left side of which is a second degree polynomial relative to a characteristic number. Applying the Shur theorem to the characteristic equation, we reveal the zones of the steady, stable, shock modes of motion. Considering the regions indicated, practicable phase and velocity characteristics of the system were obtained.

The results of the investigations were tested by means of an analog computer.

The coefficient of irregularity in movement velocity was determined from the relationship

$$\delta = \frac{2(z'_{max} - z'_{min})}{z'_{max} - z'_{min}} \cdot 100\%$$

where z'_{max} and z'_{min} are the maximum and minimum movement velocities of the mass in the interval between two succeeding impacts.

It was established that the lowest value of the coefficient
of irregularity in motion was achieved at the maximum frequency
of operation and the greatest values of the coefficient of restora-
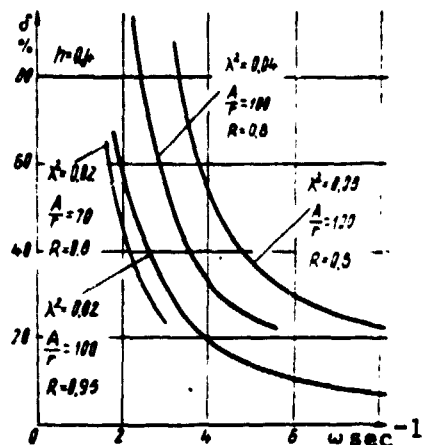tion of the impact velocity (Fig. 1).

As a consequence of
the generation of pulse
overloads of acoustical
noise and wave phenomena
caused by impacts in the
links of the mechanism,
arising in the system
during operation of a
mechanism with rigid
stops, a nonimpact action
system was investigated,
in which the rigid stops
are replaced by flexible
ones, and a comparison
of both systems was
carried out. It was
established that, in the
case of the system with
flexible stops, it is
easy to obtain a fictitious
impact velocity restoration
coefficient R_f, which is
close to unity, and that,
at $R = R_f$, both systems
are dynamically identical
(R_f is the ratio of the
velocity of exit of the
mass from the flexible stop
to the velocity achieved
by the latter).

Fig. 1. Coefficient of irregularity
in velocity vs. disturbance frequency:
A kinematic disturbance amplitude;
r half-space between stops; λ natural
vibration frequency; R impact velocity
restoration coefficient; $h = H/(mr\lambda^2)$
(H is the force of dry friction and m
is the mass.

The patterns of change in the coefficient δ are maintained.

In this manner, by calculation of the dynamic characteristics
of mechanisms with flexible stops, when the rigidity of the dis-
turbing flexible link is many times less than the rigidity of the
flexible stop, the interaction of the mass with the stop can be
assumed and taken into account with the impact velocity restora-
tion coefficient, and calculations can be carried out with $R = R_f$,
which considerably eases and simplifies the calculations.

STATISTICAL DETERMINATION OF THE ACCURACY OF RECORDING /266
OF A HIGH-SPEED ELECTROSTATIC RECORDER

A.-A.P. Laurutis and V.P. Laurutis
(Kaunas)

The accuracy of recording of rapidly changing processes with an electron beam electrostatic recorder, with high-speed mechanical scanning, depends on the precision of operation of all of its assemblies: linearity of the frequency and amplitude characteristics of the deflection amplifier, focusing quality and dynamic bias lighting as well as on the precision of feeding the data carrier. It should be noted that, at mechanical scanning speeds of up to 100-200 m/sec, which are necessary for recording data from a 0-50-100 kHz frequency spectrum, the accuracy of operation of the mechanical scanning assembly is a very complicated problem, especially if it is considered that the distance between the data carrier and the cathode ray tube line printing recorder should be held within the limits of 10-30 μm. The precision of feeding the data carrier is reduced, due to variability in its longitudinal speed and the appearance of transverse vibrations relative to the line writing tube, variability in the perpendicularity between the directions of the coordinates, and also due to change in the distance between the carrier and the line writer. This work is devoted to investigation of the data recording accuracy, as a function of all the factors enumerated, which cause vibrations of the data carrier and which affect the mechanical scanning precision. In particular, fluctuations in the linear velocity of the data carrier while recording cause a change in the time scale, according to the fluctuation pattern, i.e., a frequency modulation of the process recorded takes place. In the general case, the pattern of speed fluctuations, like other fluctuations of the carrier, are random processes. Therefore, the investigations were carried out by statistical methods.

Let a signal, with frequency f_{sign} be recorded and the speed of the carrier during recording be changed according to the pattern:

$$v_p(t) = v_{p_0}[1 + a_p \sigma_p(t)].$$

Then the execution period is

$$T_p(x) = \frac{v_p(t)}{f_{sign}} = v_p(t) T_{sign}$$

$$T_p(x) = T_{sign} v_{p_0}[1 + a_p \sigma_p(t)].$$

i.e., modulation of the execution period takes place. Subse-
quently, the realizations are sampled and the function entered
into the computer memory is frequency-modulated. Since the
sampling is carried out at a considerably slower speed, it can
be considered that the sampling intervals are constant and that
the principal errors appear during recording. The distribution
pattern of the recording function frequency, with a known dis-
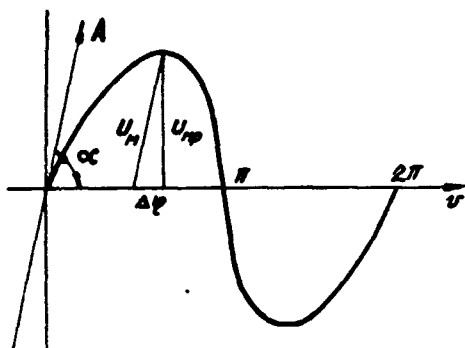tribution pattern of the scanning rate, is presented in the work.

Vibrations of the data carrier in the transverse direction
cause a displacement of the zero line, i.e., in case of absence
of the scanning beam on the screen of the recording tube, the
signal recorded will coincide with the carrier vibration signal.
Let $U_{sign}(t)$ be recorded, the carrier displacement be $\xi(t)$, and
then the recorded data takes the form

$$u_p(t) = u_{sign}(t) + \xi(t).$$

A simple summation of the two signals takes place and, with a
known distribution pattern of the data carrier vibrations in the
transverse direction, the distribution pattern of the execution
amplitude can be considered to be known also.

Fig. 1. Recording with perpen-
dicular scanning coordinates
$\alpha \neq 90°$.

Nonperpendicularity between
the data carrier velocity vector
and the line writing tube (Fig. 1)
causes amplitude and time dis-
tortions. Let there be recorded
a signal:

$$u_{sign}(t) = U_m \sin(\omega t + \varphi_0). \quad \text{then}$$

$$U_{m,s} = U_m \sin x$$

$$\Delta \varphi = U_m \cos x \sin(\omega t + \varphi_0)$$

The execution function will
have the form:

$$U_p(t) = U_m \sin x \sin [\omega t + U_m \cos x \sin(\omega t + \varphi_0) - \varphi_0].$$

In the case $\alpha = $ const, phase modulation takes place; in this
case, the modulated and modulating frequencies coincide.

Variability in angle $\alpha \neq$ const causes a fluctuation in amplitude and phase, and the phase modulation index is variable, in this case. It was assumed in this work that the pattern of change in the angle between the coordinates is a random function, with a normal distribution pattern, the mathematical expectation of which is α_0 and dispersion σ. The frequency and amplitude distribution patterns were written down and the corresponding conclusions were drawn. The distribution pattern of the harmonic amplitude and harmonic coefficient, as a function of the angle between the coordinates, during recording of a harmonic signal, can be presented as an example (Fig. 2).
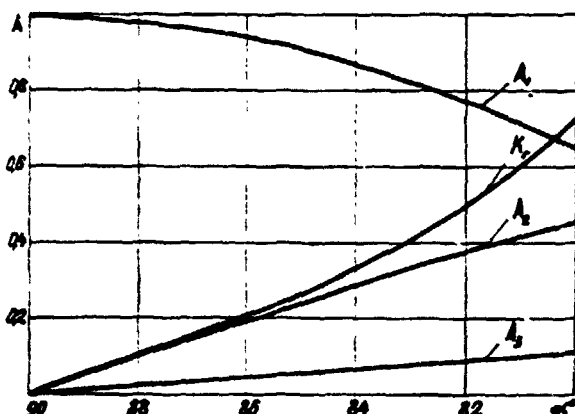
Fig. 2. Harmonic amplitude A_1 and distortion coefficient K_r vs. angle between scanning coordinates α.

The change in distance between the line writer tube and the data carrier causes a modulation in the brightness of the visual image. Since image brightness also changes, and as a consequence of change in the rate at which the process being investigated takes place, the use of brightness coordinates for transmission of analog data is undesirable, and additional modulation does not cause distortion of the data.

Extensive experimental data were presented in the work, a comparison of the accuracies of electrostatic and magnetic recording was made, and the results of the work are used for improving the recording accuracy and the quality of the visual image.

298

1. Gitlits, M.V., "The Dynamic Range of a Magnetic Recording
    Channel," Radiotekhnika 17(4) (1962).

2. Khar'kevich, A.A., Spektry i analiz [Spectra and Analysis],
    State Publishing House of Theoretical Literature, Moscow,
    1962.

3. Il'nitskiy, A.Ya., Radiotekhnika 18(6) (1963).

4. Venttsel', Ye.S., Teoriya veroyatnosti [Probability Theory],
    State Publishing House of Physical and Mathematical Litera-
    ture, Moscow, 1962.

INCREASING THE HIGH SPEED OF CENTRALIZED PHOTOSHUTTERS

D.Ch. Markshaytis and M.G. Tomilin
(Kaunas)

A major criterion for evaluating the quality of operation of a centralized photoshutter is the speed of operation of the mechanism, which depends to a considerable extent on an efficient drive system.

The work is devoted to dynamic optimization of various types of centralized photoshutters. The differential equation of the motion of the system being investigated has the form

where

$$M_p \ddot{x}_1 + \frac{1}{2} \frac{dM_p}{dx_1} \dot{x}_1^2 = F(x_1).$$

$$M_p = M_p(x_1, i_1, l_2, \ldots, l_n, m_1, m_2, \ldots, m_n).$$

$\ddot{x}_1$ is displacement of the drive link, l_1, l_2, ..., l_n are the geometric parameters of individual links of the kinematic system; m_1, m_2, ..., m_n are the masses of the individual links, and $F(x_1)$ is the driving force.

The optimum high-speed structural parameters of a number of typical kinematic systems of drive mechanisms were determined by use of a computer.

Investigations were carried out to determine the transfer ratios and engine characteristics for given speeds and accelerations of the driven units. A series of characteristic types of transfer function, expressed by trigonometric and exponential polynomials, were studied, and the best, in the sense of high spec, expressions of the transfer ratio were developed.

The investigations carried out permit the conclusion to be /270 drawn that, by selection of an efficient drive mechanism, the high speed of a photoshutter can be considerably increased and the shock load on the operating link can be minimized. Thus, by appropriate selection of the kinematic parameters of the mechanism, an increase in the high speed of a photoshutter of 40-60% is achieved.

ANALYSIS OF THE DYNAMICS AND FREQUENCY SPECTRUM SYNTHESIS OF AN OPTICAL-MECHANICAL SCANNING DEVICE

A.I. Andryushkyavichyus, A.L. Kumpikas, and K.L. Kumpikas
(Kaunas)

A two-coordinate optical-mechanical scanning device (OMSD), the operating unit of which is a scanning aisk, with directional and focusing optics and a board, on which the data carrier is placed, is examined. The disk and board are kinematically connected by a transmission mechanism, consisting of a worm and complex gear drive and a tightening screw-nut with correcting device, and it is run by a synchronous type motor.

The dynamic errors in the system depend, first, on irregularities in rotation of the disk, fluctuations in its axis and vibrations of the table in the plane parallel to the plane of the disk. The basic sources of the fluctuations referred to above are residual disbalance of the rotor and other rotating masses, the periodic component of the driving torque of the synchronous motor, variability in the resistance, kinematic errors in the drive and other things.

The fluctuations can be transmitted to the operating units through the kinematic link as a flexural-torsional system, as well as through vibrations of the housing of the device. The latter is not discussed in the work, i.e., it is assumed that the motor has an individual base and that the vibrations of its housing are not transmitted to the device. In view of the fact that the masses of the shafts, in comparison with the concentrated masses (disks, gears) and their partial frequencies are not of the same order, in which the partial frequency of the former is far from the high excitation frequency itself, the problem is reduced to investigation of the torsional vibrations of the system.

For dynamic calculations, it is expedient to represent the system in the form of a chain arrangement, with inertial masses, rigidities and damping values, referred to a single element. /271

The dynamic analysis of the system is considerably complicated by the self-stopping worm gear, and taking account of the kinematic errors and the clearances in the kinematic pairs, as well.

Conditions for opening the clearances and the operating conditions for stopping the worm gear were obtained. It was established that, under normal conditions of operation of the device, the clearances between the teeth are not opened up and that the worm gear operates in the traction mode.

The general case of dynamics of the device was resolved by mathematical modeling on a continuous action analog computer.

The case of the normal conditions of operations of the device, taking account of the kinematic errors, was examined analytically by the small parameter method. It was shown that the dynamic accuracy of the system depends mainly on the mutual locations of the excitation frequency spectrum and the natural vibration frequency spectrum. The excitation frequency spectrum depends on the type and angular velocity of the motor, as well as on the kinematic circuit parameters. It is assumed to be unchanging in solution of the problem. In view of the fact that there is the possibility of varying certain rigidities and moments of inertia (and the natural vibration spectrum, thereby), we formulate the following problem.

Let the forbidden region be the set of intervals $(\alpha_i \beta_i)$, where $i = 1, 2, \ldots, r$, u be the vector of the variable parameters and λ_s the squares of the natural frequencies ($s = 1, 2, \ldots, n$). The requirement is to find the vector u*, under which the following conditions are satisfied:

1) All λ_s must be located outside the forbidden spaces;

2) The distance between the forbidden spaces closest to the edges is the squares of the natural frequencies, on the one hand, and the boundaries mentioned above, on the other hand, must have maximum values;

3) The vector of the variable parameters after detuning must deviate the least from the vector before the detuning. To satisfy each of the conditions enumerated, target functions $f_j(u)$ are constructed, where $j = 1, 2, \ldots, t$ and a global functional $F(u)$ must be selected. The vector u*, minimizing the functional $F(u)$, is a compromise solution of the problem set out, i.e., a solution in which each of the criteria $f_j(u)$ does not take its extreme value, but is the most acceptable for satisfying all the conditions raised. The target function for the first requirement has the form /272

$$f_1(u) = \frac{(B(u) X, X)}{(X, X)} .$$

where B(u) is a matrix of the type

$$\prod_{i=1}^{r} (A - x)(A - \beta_i);$$

302

A is a symmetrical matrix of the coefficients of the system being studied; X is the vector-column, the number of coordinates of which coincides with the dimensions of matrix B. The target function for the second requirement has the form $f_{2p}(u) = (\alpha_k - \lambda_{m2p})$ and $f_{2p+1}(u) = (\lambda_{m2p+1} - \beta_k)$, where p = 1, 2, ..., (t-1)/2; m_{2p} is the number of the square of the natural frequency closest to the end of the forbidden interval α_k. The target function for the third requirement has a quadratic form $f_t(u) = ((u^{(0)} - u), (u^{(0)} - u))$, where $u^{(0)}$ is the vector of the variable parameters before detuning.

Since it is not known how accomplishment of optimality by each criterion is reflected on the others, all functions $f_1(u)$ are not comparable among themselves. A portion of the target functions enumerated is maximized, and the other portion is minimized. Besides, they do not have identical dimensions. In view of the three reasons enumerated, the global optimality criterion is assumed to be the dimensionless target function

$$F(u) = \sum_{j=1}^{t-1} \frac{f_j^{(0)} - f_j}{f_j^{(0)}} + \frac{f_t - f_t^{(0)}}{f_t^{(0)}} .$$

where $f_j^{(0)}$ is the optimum value of the j-th function.

The problem set up is solved with the aid of the following algorithm:

1. By the method set forth in Eq. (2), we find

$$\max_u \min_X \frac{(B(u) X, X)}{(X, X)} = f_1^{(0)}(u').$$

If $f_1^{(0)} > 0$, then we find the spectrum of the squares of the natural frequencies λ_s at u' and we select the closest ones to the ends of the forbidden spaces λ_2.

2. By the method set forth in work [2], we find

$$\max_u (\alpha_k - \lambda_{m_{2p}}) = f_{2p}^{(0)} \quad \text{and} \quad \max_u (\lambda_{m_{2p+1}} - \beta_k) = f_{2p+1}^{(0)} .$$

as well as

$$\min_u \left((u^{(0)} - u), \ (u^{(0)}) \right) = f_i^{(i)}$$

under the conditions

$$\min_X \frac{(BX, \ X)}{(X, \ X)} > 0, \ \lambda_{m_{2p}} < z_k, \ \lambda_{m_{2p+1}} > \beta_k.$$

3. By the same method as in the second stage, we find

$$\min_u F(u), \quad \text{under conditions} \quad \min_X \frac{(BX, \ X)}{(X, \ X)} > 0, \ \lambda_{m_{2p}} < z_k, \ \lambda_{m_{2p+1}} > \beta_k.$$

The vector u* obtained is a compromise solution of the problem set up.

The effect of the algorithm presented above is illustrated by the example of a branched vibrating chain, having eight degrees of freedom.

304

REFERENCES

1. Glazman, I.M. and L.I. Shteynvol'f, "Elimination of Resonance-Danger Zones from the Natural Frequencies of a Vibrating System by Varying Its Parameters," Izv. AN SSSR ser. mekhanika i mashinostroyeniye 126(4) (1964).

2. Grinkevich, V.K., I.M. Sobol', and R.B. Statnikov, "A Method of Search for Optimum Parameters of a Vibrating System," AN SSR, Mashinovedeniye [sic] (1) (1971).

305

ACOUSTICAL DIAGNOSTICS OF IMPACT PROCESSES
OF SOLID BODIES

M.E. Akelis, A.T. Brazdzhionis, Yu.D. Valanchauskas,
V.K. Naynis, and V.L. Ragul'skene
(Kaunas)

The investigation of impact processes of two solid bodies was carried out on two test stands.

Longitudinal vibrations were measured on a vertical stand (Fig. 1, where 1 is the object being studied, 2 is the vibration acceleration sensor, 3 is the sound pickup, 4 is the impact force sensor, 5 is the dynamic resistance recorder and 6 are strain gauges). Study of transverse vibrations was carried out on the horizontal stand (Fig. 2, where sensors were used for recording the dynamic processes, as in the stand shown in Fig. 1).
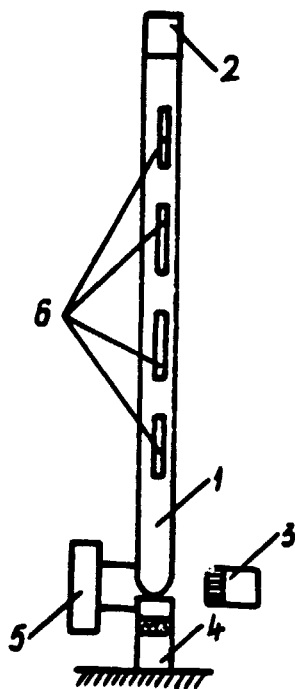
The results of the experi- /274 mental investigations were processed with the aid of the Minsk-22 digital computer. The spectral and statistical characteristics, as well as the transfer functions /275 between the individual processes, were determined by means of analysis. A logarithmic amplitude-frequency characteristic (1) and its approximate curve (2) of sound vs. vibration of the object being investigated are shown in Fig. 3.

The results of the investigations can be used for study of vibroshock systems, namely, in determination of the spectral and statistical characteristics, transfer functions, system parameters and sources of disturbance.
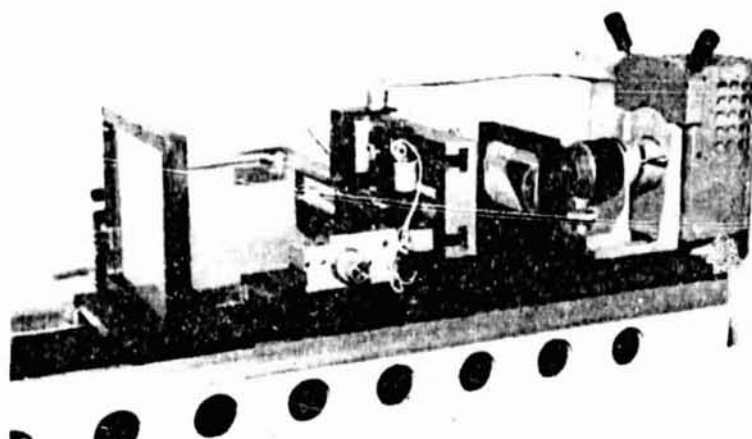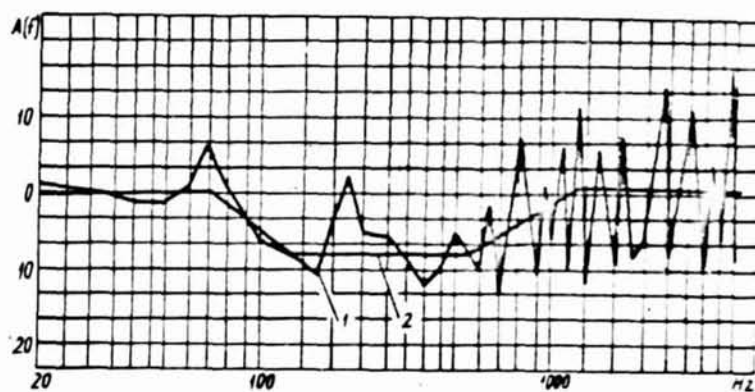

Fig. 1.

Fig. 2.

Fig. 3.

NEW METHODS OF FRAGMENTARY APPROXIMATION
OF A FUNCTION

S.G. Kolesnichenko and A.A. Maslov
(Moscow)

The overwhelming majority of problems in science and technology, in particular, problems of cybernetic diagnostics of machines, require the use of computing devices, an inherent part of which is nonlinear function converters, for their solution.

In the report, certain special methods of fragmentary approximation of a function are examined and the prop⁻ ⁱᵉs of the most widespread elementary functions for such appr⁻ ⁻tion methods are investigated, for the purpose of developi⁻ ⁻eful characteristics and properties for practical realization, ⁻ ⁻articular, for their reproduction by analog functional converters, with a significantly smaller number of controlable or adjustable parameters than in known ones.

The following conditions are proposed as new criteria, defin- /278
ing the pattern of partition of the approximating functions:

1. Constancy of the product of the approximation interval length and the increment of the derivatives of the approximating functions within these intervals:

$$\Delta f_i'(x) \cdot \Delta x_i = \text{const.} \tag{1}$$

2. Constancy of the product of the length of the approximation intervals and the integral of the slopes of the linear-broken approximating curves in adjacent sections of the partition of these functions:

$$\Delta K_i \, \Delta x_i = \text{const.} \tag{2}$$

$$\Delta K_i \cdot \Delta x_{i-1} = \text{const.} \tag{3}$$

where $\Delta K_i = K_i - K_{i-1}$, K_i is the slope of the approximating line in the i-th section of the linear approximation; and $\Delta x_i = x_i - x_{i-1}$.

The optimum partition pattern is determined by uniform distribution of the maximum methodical error between sections of the approximation:

$$\max \varepsilon(x) = \max_{x \in [r_{i-1}, r_i]} |f(x) - \varphi_n(x)| \leqslant \Delta = \text{const,} \qquad (4)$$

where Δ is the given methodical error and $\phi_n(x)$ is the approximating function.

The class of the functions investigated is determined by proceeding from the following practical considerations:

1. The possibility of expansion of the function (or its continuous sections) in a Taylor series, which is provided by the existence of continuous and limited derivatives to the n-th order everywhere, with the exception, perhaps, of a finite number of discontinuity points of the first kind.

2. The possibility of using the approximation of polynomials of finite degrees, which is provided by decrease in the absolute values of the superior products, beginning with a certain one.

3. The possibility of presenting the function in the form of the sum of elementary curves with the second derivative of unchanged sign.

Taking these conditions into account and being limited to functions of the polynomial type, not higher than the fifth degree, using dimensionless and relative values, the polynomials

$$\bar{y} = f(\bar{x}) = \sum_{i=0}^{5} a_i x^i$$

were analyzed in segment [0, 1], with the restrictions

$$a_0 = a_1 = 0; \quad \sum_{i=0}^{5} a_i = 1; \quad a_i \leqslant 1; \quad a_2 \geqslant 0; \quad a_3 \geqslant 0. \qquad (6)$$

Replacement of polynomial (5) by segment [0, 1] of the linear function $\bar{y} = \bar{x}$ introduces a methodical error:

$$\varepsilon(\bar{x}) = f(\bar{x}) - \bar{x} .$$

The experimental properties of the relation

312

$$z = \frac{\bar{z}(\bar{x})}{\Delta f'(x) \cdot \Delta x} = z(\bar{x},\ a_2,\ a_1,\ a_1,\ a_3) \tag{7}$$

were studied in region (6), with the exception of one of the variables converging on a closed region of three-dimensional space, let us say, by a_2, a_3, a_5. A test of the necessary conditions for existence of an extreme in the closed region permits it to be concluded that, with the limitations introduced on coefficients a_i, relation (7), for the class of functions being examined, changes within relatively narrow limits and is limited by the inequalities

$$7.52 \leqslant \frac{\Delta f'(x) \cdot \Delta x}{z(x)} \leqslant 10.27.$$

This permits use, with an accuracy adequate for engineering calculations, of the condition

$$\Delta f'(x) \cdot \Delta x = \text{const}$$

as a partition pattern, which is close to the optimum.

Similar limitations for criteria (2) and (3) are demonstrated in a similar manner.

The functional converter constructed on the base of the partition pattern generated by conditions (2) or (3) provides the possibility of use of one and the same controlable parameter, for example, a potentiometer or digitally controlled conductivity, for simultaneous adjustment of the function in two sections of the approximation at once.

The use of nonlinear functions $\phi_{r_\lambda}(x)$ for the approximations maintains the magnitudes of the relations examined (1)-(3) within sufficiently narrow limits and generates a partition pattern which is close to the optimum.

INVESTIGATION OF A VIBRATION-DAMPING UNIT
FOR REDUCTION IN LOW-FREQUENCY VIBRATIONS OF ELECTRIC MOTORS

/280

N.V. Grigor'yev and M.A. Fedorovich

Investigation of the vibroacoustical characteristics of different types of electric motors has shown that the basic source of vibrations at low frequencies is rotor disbalance.

Reduction in vibration at the rotation frequency in an electric motor is complicated by the fact that its disbalance component of the vibration changes in the process of operation and in different modes of operation.

We use a flexible damping support, with antivibrator, to obtain the vibroacoustical effect of reduction in the basic harmonic of the rotor in an electric motor.

A simplified model diagram of an electric motor is represented in Fig. 1. In the low frequency region, we consider the electric motor as a system with concentrated masses and noninertial flexible couplings. We examine only vibrations of the machine caused by the disbalance of the rotor. The designations on the diagram are: m_p is the corrected rotor mass; K_p is the rigidity of the rotor at the point of attachment of the mass; K_s is the rigidity of the /281 support; m_m is the mass of the motor; K_{sa} is the rigidity of the external shock absorption and C_{sa} is the damping coefficient of the external shock absorption.
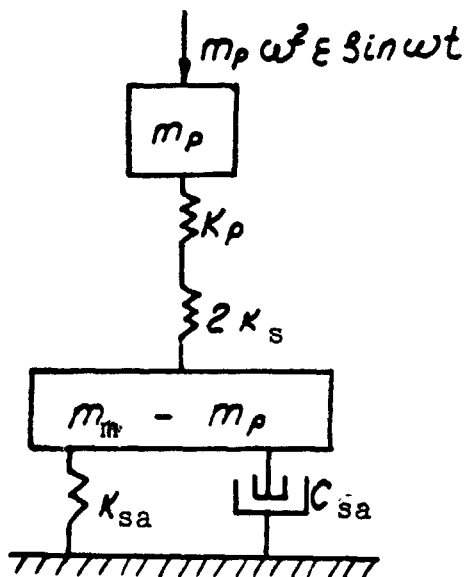
Fig. 1.

For reduction of the low-frequency vibrations transmitted from the rotor to the motor housing, we introduce an additional mass in the bearing assembly and we flexibly connect an antivibrator, adjusted to the frequency of rotation of the rotor.

As a result, we obtain a four-mass model, which permits the behavior of the system to be studied in a relatively simple way, at various values of the masses of the intermediate body m_2 and antivibrators m_4 and at various values of the

rigidities of the first k_1 and second k_2 shock absorbing cascades and flexible antivibrator-intermediate body k_4 connection (Fig. 2). For investigation of the effect of damping on the efficiency of operation of the antivibrator, damping coefficient c_4 was introduced into the system.

Movement of the four- /282 mass system produced is described by the following system of differential equations:

$$\begin{cases} m_1\ddot{x}_1 + k_1(x_1 - x_2) = m\varepsilon\omega^2 \sin \omega t \\ m_2\ddot{x}_2 + c_4(\dot{x}_2 - \dot{x}_4) + k_1(x_2 - x_1) + k_2(x_2 - x_3) + k_4(x_2 - x_4) = 0 \\ m_3\ddot{x}_3 + c_3\dot{x}_3 + k_2 x_3 = 0 \\ m_4\ddot{x}_4 + c_4(\dot{x}_4 - \dot{x}_2) + k_4(x_4 - x_2) = 0 \end{cases}$$

where x_1 is the displacement of the rotor mass m_1 from the equilibrium position; x_2 is the displacement of intermediate mass m_2 from the equilibrium position; x_3 is the displacement of the housing mass m_3 from the equilibrium position; and x_4 is the displacement of the antivibrator mass m_4 from the equilibrium position.
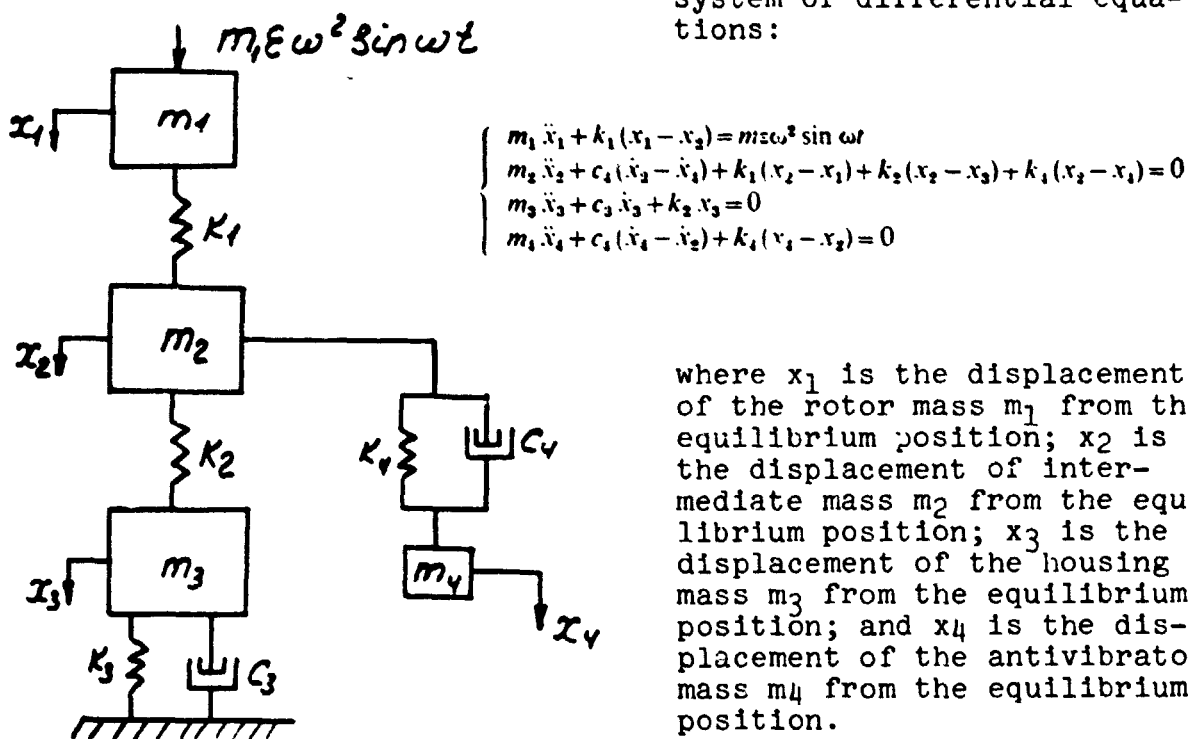
Fig. 2.

For determination of the effectiveness of the vibration quenching, we determine the value of the amplitude of vibration of the motor housing (mass m_3), according to the Fig. 2 calculation model, at various system parameters m_2, m_4, k_1, k_2 and k_4. All calculations were carried out on a digital computer.

For an approximate estimate of the effectiveness of the vibration protection, a still simpler model can be used, which is an individual vibration conductor, by which the vibrations are transmitted from the rotor to the housing (Fig. 3). The basic idea of constructing such a calculation model is the simultaneous replacement of the exciting force created by the rotor disbalance and its inertial-rigidity characteristics by a limiting kinematic disturbance.
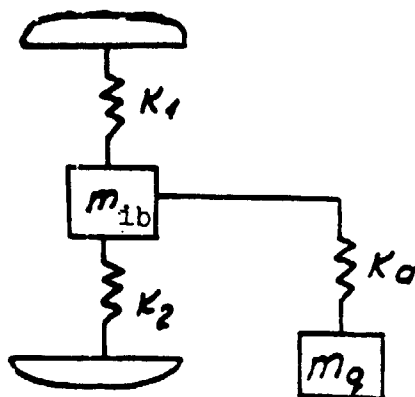
315

Fig. 3.

The effectiveness of the vibration isolation by this system is determined by the expression:

$$L_{eff} = 20\log\left|\frac{(k_1+k_2+k_4-m_2\,\omega^2)(k_4-m_4\,{}^2)-k_4^2}{2k_1(k_4-m_4\,\omega^2)}\right|$$

$m_2 = m_{1b}$ is the mass of the intermediate body; $m_4 = m_a$ is the anti-vibrator mass; and $k_4 = k_a$ is the rigidity of the flexible "anti-vibrator-intermediate body" connection.

It should be noted that, by introduction of only two cascades of flexible elements, with a total pliability $(1/k_1) + (1/k_2) = \lambda$, a certain reduction in the vibration level can be obtained, if the rotor is transferred to the supercritical mode of operation, in this case.

Calculations carried out by the simplified scheme indicated above show that the effectiveness of the vibration isolation is increased with decrease in rigidity of the first and second shock absorbing cascades.

The effectiveness is increased with increase in antivibrator mass, i.e., the larger the total mass of the antivibrators of the two-cascade shock absorption, the higher the effectiveness of this vibration damping unit.

316

INVESTIGATION OF THE POSSIBILITY OF USE
OF VIBROACOUSTICAL SIGNALS FOR PURPOSES OF DIAGNOSTICS
IN AERONAUTICAL ENGINEERING

A.R. Pres
(Minsk)

The methods and means for diagnostics of aircraft engines existing in operation do not always permit timely exposure of a number of defects in them.

Among these defects are:

-- breaking away of compressor and turbine blades;
-- decrease in efficiency of the fuel atomizers;
-- defects in the engine transmission bearings.

An experiment was carried out under field conditions, which permitted identification of defects introduced by the nature of change in the amplitude-frequency characteristic of the noises and vibrations of an aircraft jet engine:

-- compressor blade breakaway,   /284
-- breakdown of one fuel atomizer,
-- breakdown of the engine lubrication system.

Simulation of these defects was accomplished by:

-- cutting off the fuel supply to one atomizer,
-- cutting the blade of one stage of the compressor for 1/3
   of its length,
-- draining the oil from the engine and recording the vibro-
   acoustical signals after 40 minutes of operation without
   oil.

The following apparatus was used for the experiment:

a) Signal receiver:
   -- 4145 measuring microphone, with Bruel and Kjaer Company
      2803 power source,
   -- KD-12 seismic sensor;

b) Analyzing apparatus:
   -- Bruel and Kjaer Company 2107 acoustical frequency analyzer;

c) Recording apparatus:
   -- Bruel and Kjaer Company 2305 automatic level recorder.

The investigation consisted of determination of the amplitude-frequency characteristics of the noise and vibrations of the engine in good working order, with defects introduced.

For the purpose of determination of the most informative operating conditions, the amplitude-frequency characteristics were obtained in three modes of operation of the engine.

For the purpose of determination of the most informative signal recording points, the vibration AFC [amplitude-frequency characteristics] were measured at six points on the engine and the noise AFC were measured at three points.

Analysis of the AFC obtained shows:

-- The frequency bands corresponding to the working and blade frequencies are the most characteristic in the noise and vibration spectra;

-- The clearest information on the nature of the engine vibration was obtained from the engine compressor housing, in the case of compressor blade breakaway and simulation of lubrication deficiency and from points on the combustion chamber housing in the case of cutoff of its atomizers;

-- The clearest information on the nature of noise was obtained by installation of a microphone in the air scoop area;

-- Most informative for diagnostic purposes is its stable mode of operation with the minimum possible rotation rate;

-- A discrepancy in one fuel atomizer causes an increase in vibration amplitude in the working frequency band at 14 dB.

There are no significant changes in the rest of the frequency /285 range.

We observe an extension of the frequency band in the working frequency zone, upon analysis of the noise AFC, the amplitude of which reaches 110 dB.

The amplitude is increased by 10 dB in the frequency band 10-20 Hz higher than the working band:

-- Compressor blade breakaway causes an increase in vibration amplitude in the working frequency by 20 dB and by 10 dB in the blade frequency band;

There is a similar picture upon analysis of the noise AFC:

318

-- Simulation of the engine lubrication system breakdown
was carried out in the presence of a broken-off compressor
blade.

In this case, a 15 dB increase in vibration and noise amplitude
is observed in the frequency band 30 Hz above the working bands.